Ciesielski, P. F., Kristoffersen, Y., et al., 1988
Proceedings of the Ocean Drilling Program, Scientific Results, Vol. 114

7. SITE 700[1]

Shipboard Scientific Party[2]

HOLE 700A

Date occupied: 26 March 1987

Date departed: 27 March 1987

Time on hole: 1 day

Position: 51°31.992′S, 30°16.697′W

Bottom felt (rig floor; m; drill-pipe measurement): 3611.5

Distance between rig floor and sea level (m): 10.50

Water depth (drill-pipe measurement from sea level; corrected m): 3601.0

Total depth (rig floor; corrected m): 3621.0

Penetration (m): 9.6

Number of cores: 2

Total length of cored section (m): 9.6

Total core recovered (m): 0.19

Core recovery (%): 1.0

Oldest sediment cored:
Depth sub-bottom (m): 0.25
Nature: diatom ooze
Age: Pliocene
Measured velocity (km/s): —

HOLE 700B

Date occupied: 28 March 1987

Date departed: 3 April 1987

Time on hole: 5 days, 14 hr

Position: 51°31.977′S, 30°16.688′W

Bottom felt (rig floor; m; drill-pipe measurement): 3611.5

Distance between rig floor and sea level (m): 10.50

Water depth (drill-pipe measurement from sea level; corrected m): 3601.0

Total depth (rig floor; corrected m): 4100.50

Penetration (m): 489.0

Number of cores: 54

Total length of cored section (m): 489.0

Total core recovered (m): 245.40

Core recovery (%): 50.2

Oldest sediment cored:
Depth sub-bottom (m): 489.0
Nature: limestone
Age: Late Cretaceous, Coniacian
Measured velocity (km/s): 2.98

Principal results: Site 700 is in the western region of the East Georgia Basin (51°31.992′S, 30°16.697′W; water depth of 3601 m) on the northeastern slope of the Northeast Georgia Rise. Site 700 is a companion site to Site 699, which was prematurely terminated at 518 m below seafloor (mbsf) in upper Paleocene strata about 250 m above basement. To reach the deeper objectives not achieved at Site 699, Site 700 was located 21 km east of the preceding site where post-Eocene sediments are greatly attenuated (<50 m thick), allowing for rapid penetration of the Upper Cretaceous–Paleogene. The objectives for Site 700 were complementary to those reported for Site 699. Foremost of these was to obtain an Upper Cretaceous–Paleogene section recording the possible role of the Georgia Basin as an avenue for deep-water communication between the Weddell Sea and the South Atlantic. An additional objective was to obtain an older Cretaceous section than that recovered at Site 698, which might further constrain the nature, age, and subsidence history of the Northeast Georgia Rise.

Site 700 consists of two rotary drilled holes: Hole 700A with only two cores, penetrating to 9.6 mbsf with a recovery of 0.19 m, and Hole 700B with 54 cores, penetrating to 489 mbsf with a recovery of 245.4 m (50.2%). Both holes were terminated as a result of premature bit release. Hole 700B was drilled to within 100 m of basement and was logged using standard Schlumberger stratigraphic and geochemical tools. The site was occupied between 26 March and 3 April 1987 in moderate to rough seas.

The stratigraphic section at Hole 700B consists of a thin unit of carbonate ooze above a thick section of chalks and limestones. The pelagic carbonates of Hole 700B show progressive lithification with depth from ooze, to friable chalk, to indurated chalk, and finally, to limestone. The dominant lithologies and ages of the stratigraphic sequence are as follows:

0–0.29 mbsf: diatom ooze of Quaternary to late Pliocene age
0.29–26.4 mbsf: no recovery
26.4–45.4 mbsf: nannofossil ooze of late middle Eocene age
45.4–168.9 mbsf: nannofossil chalk of late early Eocene to middle Eocene age
168.9–228.5 mbsf: micritic nannofossil chalk of earliest Eocene to late early Eocene age
228.5–319.0 mbsf: indurated micritic nannofossil chalk of early Paleocene to earliest Eocene age
319.0–359.0 mbsf: micritic nannofossil-bearing limestone of Maestrichtian to early Paleocene age
359.0–441.5 mbsf: micritic limestone alternating with clay-bearing/clayey limestone of Campanian to Maestrichtian age
441.5–489.0 mbsf: micritic limestone alternating with clay-bearing/clayey micritic limestone with dispersed, discrete ash layers, early Campanian to Coniacian age.

A thin (<26.4 m) diatom ooze of late Pliocene–Quaternary age disconformably overlies a thick sequence of Upper Cretaceous to upper middle Eocene oozes, chalks, and limestones. Between 26.4 and 228.5 mbsf, Hole 700B recovery repeats the lower to upper middle Eocene section recovered at Site 699, thus providing better stratigraphic representation of an interval that was poorly recovered at both sites (55.2% at Site 699 and 40.2% at Site 700). A 260.5-m-thick Paleocene to Coniacian section provides a greatly expanded section for a 32-m.y. interval that was only sparsely represented at Sites 698 and 699. Site 700 and companion Site 699 provide a Late Cretaceous–Paleogene pelagic record spanning 66 m.y. within a combined stratigraphic thickness of 640 m. These two sites provide the most continuous record of this period obtained from the Southern Ocean.

[1] Ciesielski, P. F., Kristoffersen, Y., et al., 1988. *Proc. ODP, Init. Repts.*, 114: College Station, TX (Ocean Drilling Program).

[2] Shipboard Scientific Party is as given in the list of Participants preceding the contents.

A clear succession of magnetic polarity zones was identified in Upper Cretaceous to lower Paleocene chalks and limestones below 270 mbsf. Good recovery (69%) and relatively little core disturbance in this interval resulted in identification of latest Campanian to early Paleocene Chrons C33N to C26R. This section will allow the first calibration of high-latitude siliceous and calcareous microfossil assemblages to the geomagnetic polarity time scale (GPTS) and will provide a temporal framework for interpretation of Late Cretaceous–Paleocene Southern Ocean oceanography.

Sedimentation rates were not more than 10 m/m.y. during the Coniacian-Santonian and 26 m/m.y. during the Campanian, decreasing to 5 m/m.y. during the Maestrichtian. Average sedimentation rates during the Paleogene were 13 m/m.y. The only recognized hiatuses occur within the upper Santonian to Maestrichtian, at the Cretaceous/Tertiary boundary (Chron C29R, 330.7 and 331.0 mbsf), and the upper middle Eocene to upper Pliocene.

Siliceous microfossils are abundant and well preserved in the Paleocene and upper Pliocene–Quaternary. Abundant and well-preserved radiolarians occur from the lower Maestrichtian to the base of the hole. All calcareous microfossil groups are represented throughout the Upper Cretaceous and Paleogene, although there is evidence for secondary calcite overgrowths and recrystallization below the lowermost Eocene.

Faunal and floral assemblages provide a detailed record of the paleoenvironmental evolution of this region. Late Cretaceous assemblages are distinct from those of the low latitudes but have some low-latitude affinities. Variations in Late Cretaceous climate are represented by fluctuations in the abundance of globotruncanids and radiolarians. Maximum climatic warmth in the Paleogene occurred during the early Eocene, enabling the introduction of low-latitude fauna and flora. As at Site 699, the middle Eocene represents a period of transition from the warmer water assemblages of the Paleocene–early Eocene to late Eocene assemblages with a more definite high-latitude affinity.

There is no evidence for major erosional events at Sites 699 and 700, which predate the Eocene opening of the Islas Orcadas Rise–Meteor Rise gateway. Therefore, if the East Georgia Basin served as a deep-water passage between the Weddell Sea and South Atlantic, thermohaline convection in the antarctic was too weak to cause significant erosion during the early Paleogene.

Post-early Oligocene to pre-Quaternary faulting vertically displaced corresponding stratigraphic levels at Sites 699 downward by about 500 m relative to Site 700. Adjacent scarps form major north-trending lineaments that may be related to the same tectonic episode. This faulting left Site 700 as an isolated bathymetric high more susceptible to deep-cutting erosion (Neogene?) that is estimated to have removed 300–500 m of sediments of post-late middle Eocene age at Site 700.

BACKGROUND AND OBJECTIVES

Site 700 is in the western region of the East Georgia Basin (51°31.977′S, 30°16.688′W) on the northeastern slope of Northeast Georgia Rise in a water depth of 3601 m (Fig. 1). The site position is only 21 km due east of Site 699, where drilling was prematurely terminated at 518 mbsf in upper Paleocene strata, about 250 m above basement. To obtain, as rapidly as possible, the deeper and older objectives not reached at Site 699 (see "Background and Objectives" section, "Site 699" chapter, this volume), Site 700 was located where the post-Eocene sediments appeared to be only 50 m thick.

The particular objectives of Site 700 were complementary to those previously outlined for Site 699. Broadly summarized, these objectives were to obtain a Upper Cretaceous to Paleogene section that (1) records the early history of deep-water communication between the Weddell and Georgia basins with the South Atlantic Basin and (2) documents the paleoenvironmental evolution of the subantarctic region during the initiation and early expansion of the antarctic ice sheet (see "Background and Objectives" section, "Site 699" chapter, for a more detailed discussion of the objectives).

A new, additional objective for Site 700 resulted from our discovery of nonpelagic lithologies at Site 699, which strongly suggests that basement forming the structural framework of the Northeast Georgia Rise may have continental as well as oceanic components. This is a possibility not considered by the current model for the origin of the rise (LaBrecque and Hayes, 1979). A continental origin for parts of Northeast Georgia Rise also has significance for its role as a topographic element constraining Late Cretaceous oceanic circulation. Therefore, an attempt to penetrate and obtain basement became an important objective at Site 700.

Single-channel seismic-reflection data show a 540-m-thick section, based on two-way traveltime (TWT), at Site 700 with an acoustic character similar to the lower part of the section at Site 699 (Fig. 2). Site 700 is on a horst where Miocene and younger sediments (with a maximum thickness of 40 m) were expected to unconformably overlie Eocene and older sediments. The Eocene section has a thickness comparable to that observed at Site 699 (Fig. 2). Below the Eocene nannofossil chalk, a transition to Paleocene limestone was expected. Late Cretaceous and older sediments were thought to include claystone above a basal transgressive sand.

Site 700 lies on the northeastern slope of Northeast Georgia Rise on crust that structurally must be considered to be part of the rise itself (Fig. 1). Basement at Site 698 was Campanian (or older), weakly differentiated, iron-rich oceanic basalt that had been subjected to subaerial weathering. In a plate tectonic framework, the rise lies between oceanic crust older than Campanian (Chron 34) to the east and younger than Aptian to the west (LaBrecque and Hayes, 1979). The origin of the rise is considered to have been the result of intra-plate deformation in response to rotation of the Malvinas plate against the Falkland block during the Campanian-Eocene. The depositional environment at Site 698 during this time interval does not reflect any tectonic activity, although the appearance of zeolites in the upper Paleocene section at Site 699 suggests a higher terrigenous input. Any incipient subduction to form a fossil island arc must be, therefore, of pre-Turonian age. By completing the deep objectives of Site 699 at Site 700, the potential existed for obtaining further constraints on the nature, age, and subsidence history of Northeast Georgia Rise.

The drilling plan for Site 700 was to rotary drill to basement and to obtain 50 m of basement or to drill up to the original maximum time allotment for Site 699. Two standard Schlumberger logging runs were planned using the stratigraphic and geochemical tools.

OPERATIONS

Site 700 Operations Summary

The transit to Site 700 was quick because this site is only 12 nmi from Site 699. We decided to attempt reaching basement at this site rather than respudding at Site 699 for two reasons. First, fairly abundant sand/gravel layers created recovery problems at Hole 699A and led directly to its loss. Therefore, we felt that the chances of reaching basement and having a stable, loggable hole were greater at Site 700. Second, basement was thought to be shallower at this site and could be reached in less time. The geology at the basement high was projected to be nearly identical to that at the original Site 699 hole except that the upper, younger material was missing. This was acceptable to the shipboard scientific party because this part of the section had been successfully cored already and the older section (not recovered at Site 699) could be rapidly penetrated.

En route to the site, the rig crew continued to work feverishly at removing the sanded-up core barrel from the seal bore outer

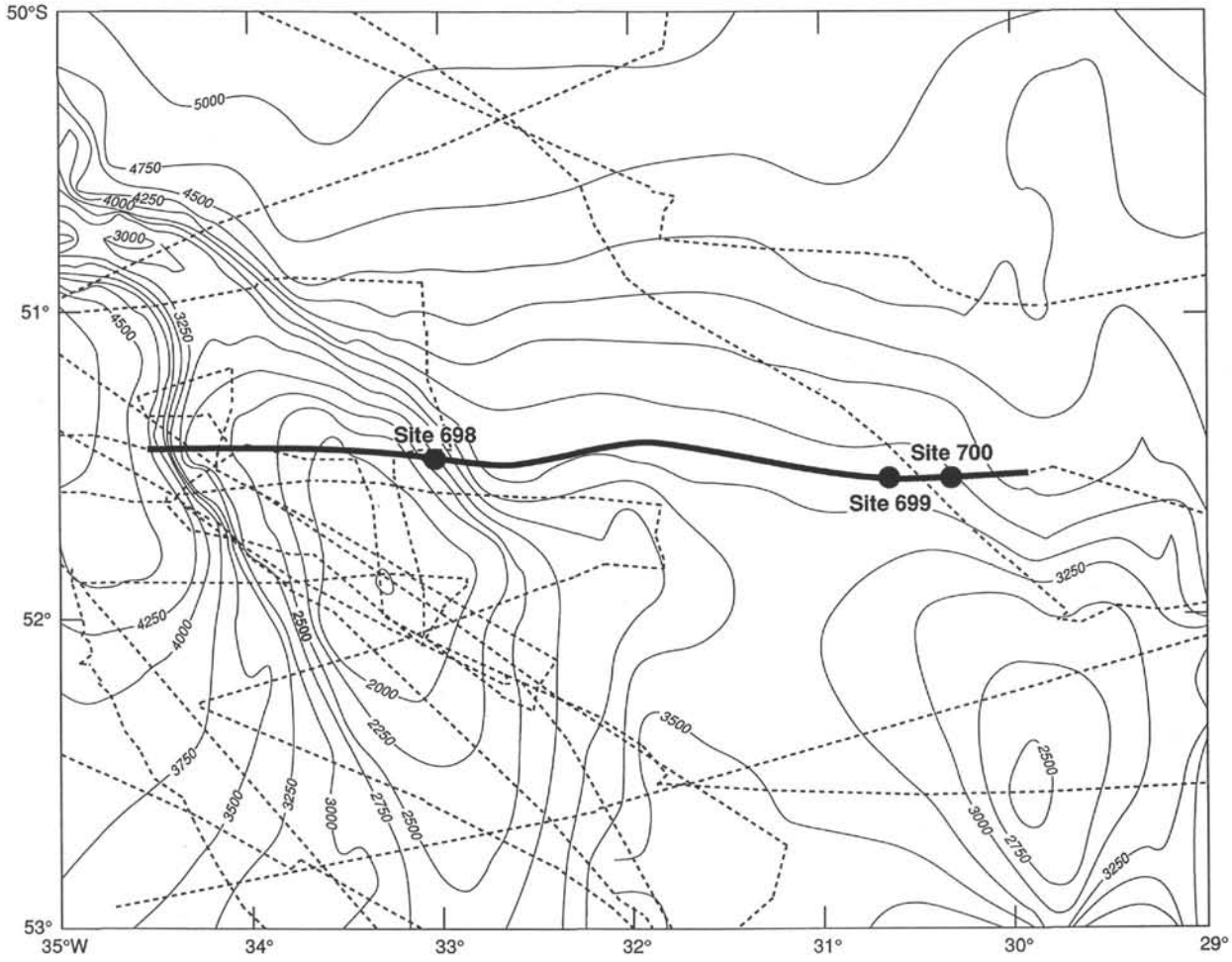

Figure 1. Location map showing positions of Site 700 and other sites drilled during Leg 114 on the Northeast Georgia Rise. The bold ship track is the single-channel seismic-reflection profile of *Islas Orcadas* cruise 0775 (Fig. 2). Isobaths in meters.

core barrel. A scant 3.25 hr later, at 2315 hr on 26 March 1987, a beacon was dropped to initiate Site 700.

Hole 700A

Immediately upon deploying the positioning beacon, the profiling gear was retrieved and the vessel returned to the site. By 0115 hr the vessel was stabilized over the hole location, and the rig crew began preparing to run in the hole. Because the upper, softer sediments had already been successfully cored at Hole 699A, basement and the Cretaceous to Paleocene sequence were the primary objectives at this site. The rotary core barrel (RCB) system was used for coring to ensure penetration of the expected limestones and basement. We anticipated that the total penetration of the hole would be in excess of 400 mbsf, so a hydraulic bit-release (HBR) system was deployed, allowing the hole to be logged upon completion of coring operations.

At 1000 hr on 27 March 1987, Hole 700A was spudded (Table 1). Two cores were recovered before it became evident that something was wrong downhole. The assistant driller reported difficulty in engaging the core barrel for Core 114-700A-3R. After the second wireline run came up without the barrel, the overshot was changed in the hope that it was only a problem with the pulling neck engagement. About this time, the driller reported that his pump pressures were reading much lower than earlier, and we suspected that the pipe was now open-ended. Because all of the string weight was accounted for, it appeared that the HBR had prematurely released the core bit. In an effort to salvage the core barrel, the drill string was slacked off and another unsuccessful attempt was made to engage the core barrel. The sand line was retrieved and the drill string was tripped out of the hole. At 1600 hr the pipe was pulled clear of the mud line and by 2245 hr the working end arrived at the rotary table, minus the bit. Early indications are that the HBR dogs were never fully engaged in the bit disconnect. After repeated blows with the core-barrel assembly, the bit simply fell off. Components are being modified in compliance with design modifications so that engagement of the dogs is verified prior to future deployment.

Hole 700B

Weather conditions were deteriorating as the new bit and release assembly were made up. Because we did not know at the time why the HBR prereleased (three successful deployments had been made during Leg 113 operations), a mechanical bit-release (MBR) assembly was used. The bottom-hole assembly was run in the hole along with a partial string of drill pipe before operations were halted to cut and slip the drilling line. With the weather continuing to deteriorate, the pipe was run to bottom, but the spudding of Hole 700B was delayed until more favorable operating conditions were at hand. A stand of wear-knotted drill pipe was put in the string immediately below the two (20- plus 30-ft) drilling joints that are normally used. Waiting on weather began on the second consecutive site after having successfully completed the first Leg 114 site (698) without experiencing any lost time because of weather. This storm, although

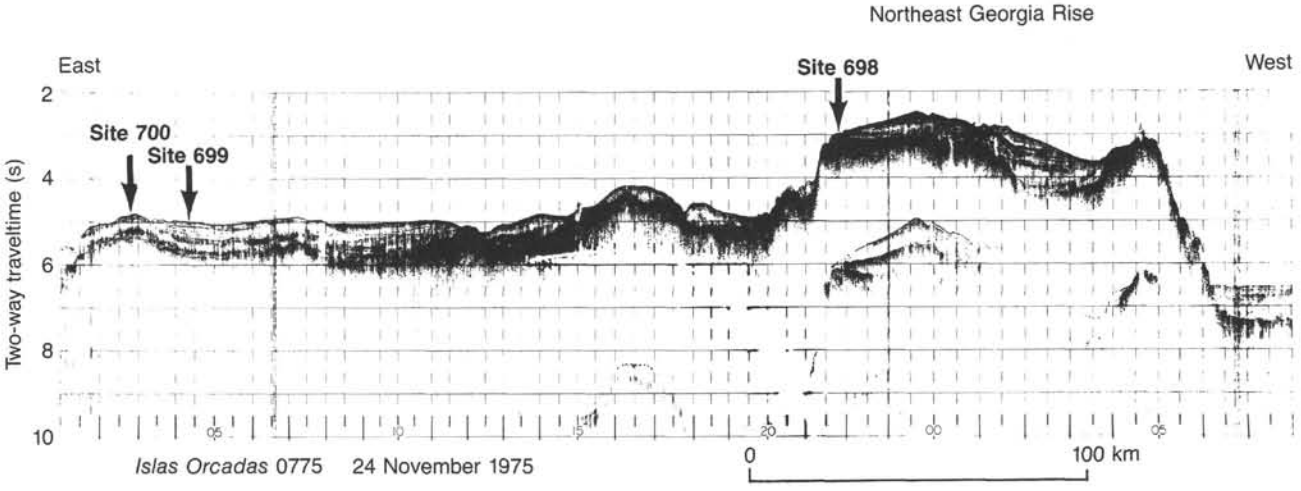

Figure 2. *Islas Orcadas* cruise 0775 single-channel seismic-reflection profile showing position of Site 700 in relation to other Leg 114 sites drilled on Northeast Georgia Rise. Location of profile shown in Figure 1.

milder than the one experienced at Site 699, still packed winds gusting to 54 kt and was associated with several swells that caused the vessel to roll 8°–12°.

After a 3-hr delay the pipe trip was resumed, and Hole 700B was spudded at 1430 hr on 28 March 1987. Coring continued, with the driller watchful for a potentially dangerous sand layer as was experienced in Hole 699A, where a sudden influx of sand/gravel from this zone led to the loss of that hole. At approximately the same stratigraphic level in the formation, the driller noticed a sharp increase in pump pressure associated with a loss of circulation. He responded by ceasing coring operations and immediately picking up off bottom with the drill string. We decided to go ahead and pull the core barrel and then proceed with pumping a high-viscosity mud pill in an attempt to clean and stabilize the hole. An overpull of 3000 lb was experienced while unseating the core barrel, but to everyone's relief the core barrel was freed and the loss of another hole was avoided.

Continuous coring operations continued through Core 114-700B-23R. While attempting to retrieve Core 114-700B-24R the adapter-sub crossover from the sinker bars to the wireline swivel backed off, forcing us to fish for the tool. Three attempts with a fishing tool fabricated aboard ship were required before the tool was successfully recovered. The first attempt did not engage the tool. The second attempt engaged the tool, but it fell off while being retrieved from the hole. Modifications were made to the tool, and on the third try, the fish was both engaged and recovered from the string, allowing coring to resume. An inspection of the sinker-bar string indicated that the connection had been baker-locked, as is standard practice; however, it apparently did not cure properly, which allowed the connection to back off during retrieval. The condition was aggravated by a wireline swivel that had locked. The swivel had just been greased and checked prior to the core run. Upon inspection in the tool room, we found that the snap ring retaining the grease seal had come out of its groove, creating a metal to metal contact and virtually locking the swivel. This condition was duplicated in the shop by regreasing the swivel and again unseating the snap ring. Design modifications are being developed to prevent this from happening in the future.

On 29 March at 2300 hr, *Maersk Master* returned from South Georgia Island with the second and final load of fuel for *JOIDES Resolution*. By 1300 hr on 30 March, an additional load of 196,218 gal. of fuel was taken aboard the vessel, and *Maersk Master* was underway for her third rendezvous with the tanker *Sunny Trader*, waiting at anchor in King Edwards Cove, South Georgia Island. This third load of fuel was for *Maersk Master* and not for transfer to *JOIDES Resolution*.

Continuous coring continued through Core 114-700B-38R, with signs of hole problems beginning with Core 114-700B-35R. At that time a 20-bbl pill of viscous mud was pumped. Upon tagging bottom for Core 114-700B-36R nearly 5.5 m of fill was encountered. The formation showed signs of intruding the borehole while this core was being cut so another 30-bbl pill was circulated to the mudline before retrieving the core. Another pill was circulated while coring on Core 114-700B-37R, and the hole showed signs of stabilizing because it was clean of fill at the start of Core 114-700B-38R. Normal coring operations continued until 1030 hr on 1 April 1987. At that time severe hole problems again began to occur. Apparently the previously stabilized zone was deteriorating or another bad zone had been penetrated. The pipe began torquing and pump pressures were again elevated. A high-viscosity pill was circulated while we considered making a short wiper trip in an attempt to clean and stabilize the hole. We felt that this should be done before attempting to make any additional hole or resuming coring operations. An approximately 200-m wiper trip took 3 hr to make. The hole was circulated continuously and swept periodically with mud to condition it as much as possible. The wiper trip appeared to be successful because there were no additional torquing problems or bridges encountered except in the lowermost 9 m of the hole. After cleaning out the hole to bottom, we found that the wash barrel could not be retrieved and was apparently stuck downhole. After three wireline attempts the barrel came free. A conventional core barrel was deployed, and while cleaning the hole to bottom, the driller again noticed drill pipe torquing. This time the torquing was associated with pump pressures significantly lower than normal. The wash barrel, upon breaking off the bit deplugger, was found to be filled with medium to coarse sand. Several runs with the sand line were made to no avail. The core barrel could not be located. It appeared that the sleeve in the MBR had shifted while pulling the stuck wash barrel.

One additional wireline run was made to verify that the bit disconnect was indeed gone and that the pipe was free of any obstructions. The pipe was then tripped to 3750 m with one additional knobby joint added to the string. The logging sheaves were rigged and after one missed run, two successful suites of logging tools were run. All logging operations were completed by 0215 hr on 3 April 1987. The hole was displaced with heavy mud and abandoned. The pipe cleared the rotary table at 1245 hr after an arduous trip in very rough weather.

Table 1. Site 700 coring summary.

Core no.	Date (1987)	Local time (hr)	Depths (mbsf)	Cored (m)	Recovered (m)	Recovery (%)
Hole 700A:						
1R	Mar 27	1100	0.0–0.1	0.1	0.04	40.0
2R	27	1200	0.1–9.6	9.5	0.15	1.6
				9.6	0.19	
Hole 700B:						
1W	28	1515	0.0–16.9	16.9	0.21	1.2
2R	28	1615	16.9–26.4	9.5	0.00	0.0
3R	28	1715	26.4–35.9	9.5	1.60	16.8
4R	28	1812	35.9–45.4	9.5	1.80	18.9
5R	28	1925	45.4–54.9	9.5	6.25	65.8
6R	28	2025	54.9–64.4	9.5	9.15	96.3
7R	28	2120	64.4–73.9	9.5	9.51	100.0
8R	28	2225	73.9–83.4	9.5	7.22	76.0
9R	28	2325	83.4–92.9	9.5	8.31	87.5
10R	29	0025	92.9–102.4	9.5	3.96	41.7
11R	29	0120	102.4–111.9	9.5	0.54	5.7
12R	29	0210	111.9–121.4	9.5	0.22	2.3
13R	29	0255	121.4–130.9	9.5	7.78	81.9
14R	29	0345	130.9–140.4	9.5	0.43	4.5
15R	29	0435	140.4–149.9	9.5	0.14	1.5
16R	29	0515	149.9–159.4	9.5	9.09	95.7
17R	29	0610	159.4–168.9	9.5	0.05	0.5
18R	29	0730	168.9–178.4	9.5	6.20	65.2
19R	29	0830	178.4–187.9	9.5	0.02	0.2
20R	29	1120	187.9–192.9	5.0	3.87	77.4
21R	29	1305	192.9–200.0	7.1	5.19	73.1
22R	29	1500	200.0–209.5	9.5	0.43	4.5
23R	29	1640	209.5–219.0	9.5	0.00	0.0
24R	30	0010	219.0–228.5	9.5	0.28	3.0
25R	30	0225	228.5–238.0	9.5	0.42	4.4
26R	30	0400	238.0–247.5	9.5	4.44	46.7
27R	30	0515	247.5–257.0	9.5	1.96	20.6
28R	30	0615	257.0–266.5	9.5	6.38	67.1
29R	30	0730	266.5–276.0	9.5	3.07	32.3
30R	30	0840	276.0–285.5	9.5	8.17	86.0
31R	30	0950	285.5–295.0	9.5	9.80	103.0
32R	30	1110	295.0–304.5	9.5	8.30	87.3
33R	30	1330	304.5–314.0	9.5	1.40	14.7
34R	30	1500	314.0–319.0	5.0	4.32	86.4
35R	30	1640	319.0–326.0	7.0	3.16	45.1
36R	30	1720	326.0–330.7	4.7	3.81	81.0
37R	30	2205	330.7–335.5	4.8	3.48	72.5
38R	31	0010	335.5–345.0	9.5	7.83	82.4
39R	31	0155	345.0–354.5	9.5	5.66	59.6
40R	31	0320	354.5–364.0	9.5	7.67	80.7
41R	31	0445	364.0–373.5	9.5	6.00	63.1
42R	31	0630	373.5–383.0	9.5	4.84	50.9
43R	31	0840	383.0–392.5	9.5	9.94	104.0
44R	31	1050	392.5–397.0	4.5	1.71	38.0
45R	31	1355	397.0–403.5	6.5	3.34	51.4
46R	31	1600	403.5–413.0	9.5	4.70	49.5
47R	31	1802	413.0–422.5	9.5	7.08	74.5
48R	31	2045	422.5–432.0	9.5	9.02	94.9
49R	31	2310	432.0–441.5	9.5	7.21	75.9
50R	Apr 1	0140	441.5–451.0	9.5	4.20	44.2
51R	1	0345	451.0–460.5	9.5	9.36	98.5
52R	1	0550	460.5–470.0	9.5	5.19	54.6
53R	1	0815	470.0–479.5	9.5	6.73	70.8
54R	1	1010	479.5–489.0	9.5	3.96	41.7
				489.0	245.40	

LITHOSTRATIGRAPHY

Hole 700A (Core 114-700A-1R and Section 114-700A-2R, CC) reached 9.6 mbsf and recovered Quaternary and upper Pliocene olive-colored (5Y 5/4) diatom ooze. The recovery in this hole was very poor and, because of a premature bit release, this first attempt was abandoned and a second hole was drilled nearby.

Hole 700B is in a water depth of 3601 m and was rotary drilled to a total depth of 489 mbsf. A total of 245.40 m of sediments was recovered in 54 cores, with an average core recovery of 50%.

Below a surficial layer of Quaternary diatom ooze, Hole 700B exhibits a pelagic carbonate record extending from the middle Eocene down to the Coniacian(?) and Campanian, at which depth the hole was discontinued because the drill bit was lost. The sediments consist primarily of pelagic carbonates showing a progressive lithification with depth, from soft ooze to friable chalk, indurated chalk, and finally, to limestone. The carbonates are composed essentially of foraminifers and nannofossils; locally, reworked pelecypods and shallow-water microfauna indicate gravity processes (Core 114-700B-40R, see "Biostratigraphy" section, this chapter). Some sparse fragments of *Inoceramus* shells were also observed in the Upper Cretaceous section (Cores 114-700B-43R, 114-700B-47R, and 114-700B-52R).

Although there are no marked lithologic changes within the section cored, five main lithostratigraphic units can be distinguished on the basis of diagenetic evolution and sedimentology (Figs. 3 and 4).

Unit I: Quaternary–upper Pliocene diatom ooze
Unit II: middle Eocene nannofossil ooze
Unit III: middle to lower Eocene nannofossil chalk (Subunit IIIA) overlying micritic nannofossil chalk (Subunit IIIB)
Unit IV: upper Paleocene to lower Paleocene micritic, indurated nannofossil chalk
Unit V: lower Paleocene to Santonian and Turonian(?) micrite-nannofossil-bearing limestone (Subunit VA) overlying micritic limestone alternating with clay-bearing or clayey micritic limestones (Subunit VB), with ash layers at the base (Subunit VC).

Unit I: Cores 114-700A-1R through 114-700A-2R and Sections 114-700B-1R, CC, through 114-700B-2R, CC; Depth: 0–26 mbsf; Age: late Pliocene–Quaternary.

Despite poor recovery of this interval it is apparent that the upper Pliocene–Quaternary deposits at this site must be very thin. The exact thickness and precise stratigraphic limits of the unit cannot be determined, but the unit must extend at least from 1 to 26.4 mbsf. The recovered sediment consists of olive (5Y 5/4, 5Y 5/3) muddy diatom ooze and diatom ooze (Section 114-700B-1R, CC, and Core 114-700B-2R).

Unit II: Cores 114-700B-3R and 114-700B-4R; Depth: 26.4–45.4 mbsf; Age: middle Eocene.

The upper part of the middle Eocene sequence is composed of white (5Y 8/1) to very pale brown (10YR 6/4) micritic nannofossil ooze. Carbonate contents in the white parts of the ooze are high (73%) compared with the more clay-rich pale brown horizons (46%). Sediments exhibit a mottled appearance because of minor bioturbation. *Zoophycos* was observed in Sample 114-700B-3R-1, 63 cm.

As for Unit I, the exact thickness of Unit II cannot be determined precisely because of poor recovery. However, the boundaries of Unit II are between 3.35 and 19 mbsf.

Unit III: Cores 114-700B-5R through 114-700B-24R; Depth 45.4–228.5 mbsf; Age: middle Eocene to early Eocene.

This unit consists of white nannofossil chalk (Subunit IIIA), resting above very pale brown micritic nannofossil chalk (Subunit IIIB).

Subunit IIIA: Cores 114-700B-5R through 114-700B-17R; Depth: 45.4–168.9 mbsf; Age: middle to early Eocene.

This unit includes middle early Eocene deposits of white (no code) nannofossil chalk. Very pale brown (10YR 6/3) clay-rich

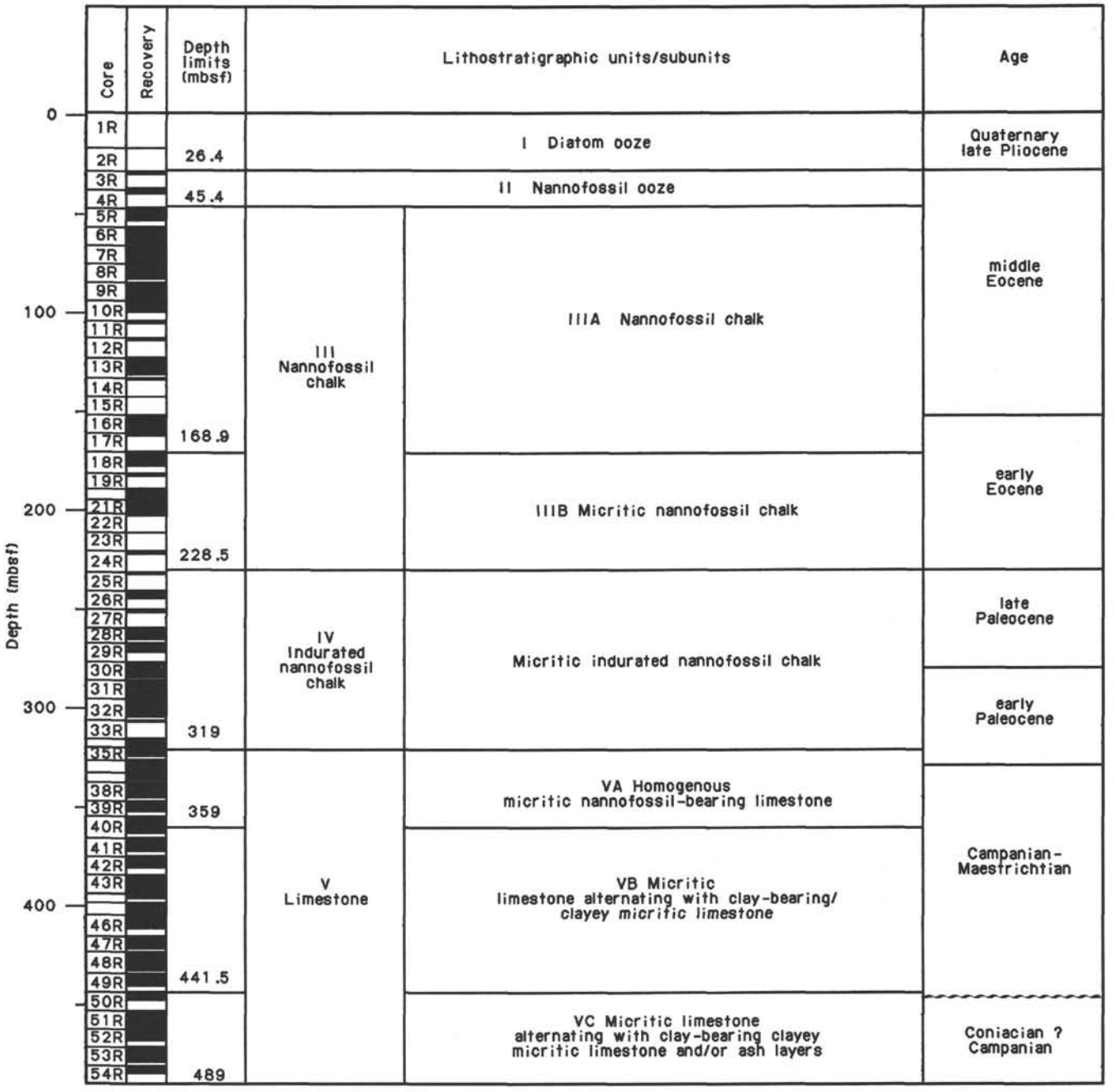

Figure 3. Lithostratigraphic units in Hole 700B.

horizons occur in the upper part (Cores 114-700B-5R–114-700B-9R) whereas the lower part, below Core 114-700B-9R, is homogenous. Carbonate contents correlate well with the lithology (Figs. 4 and 5). Fluctuations occur in the upper part as a result of lower $CaCO_3$ contents in the clay-rich horizons. There is an overall increase in carbonate from 41% to 91% with depth in this unit. Abundant clinoptilolite was observed (Fig. 6).

Manganese nodules occur in Cores 114-700B-7R and 114-700B-10R, although a few may be displaced. Mn-stained filaments or impregnations are also observed (Core 114-700B-10R).

The sediments are faintly to moderately bioturbated, with the ichnofauna consisting of *Zoophycos, Planolites*, and some *Chondrites*, which is usually in association with *Planolites* as "composite traces."

Subunit IIIB: Cores 114-700B-18R through 114-700B-24R; Depth: 168.9–228.5 mbsf; Age: early Eocene.

Subunit IIIB consists of micritic nannofossil chalk of a generally darker hue—very pale brown (10YR 8/3) to pale brown (10YR, 7/3) and pale yellow (2.5Y 7/4)—than the overlying Subunit IIIA. Color changes are gradational. Carbonate contents remain high (77%–86%), with lower values occurring in the white horizons (Fig. 3). Micrite increases downhole (Fig. 4). As in Subunit IIIA, clinoptilolite is abundant (Fig. 6).

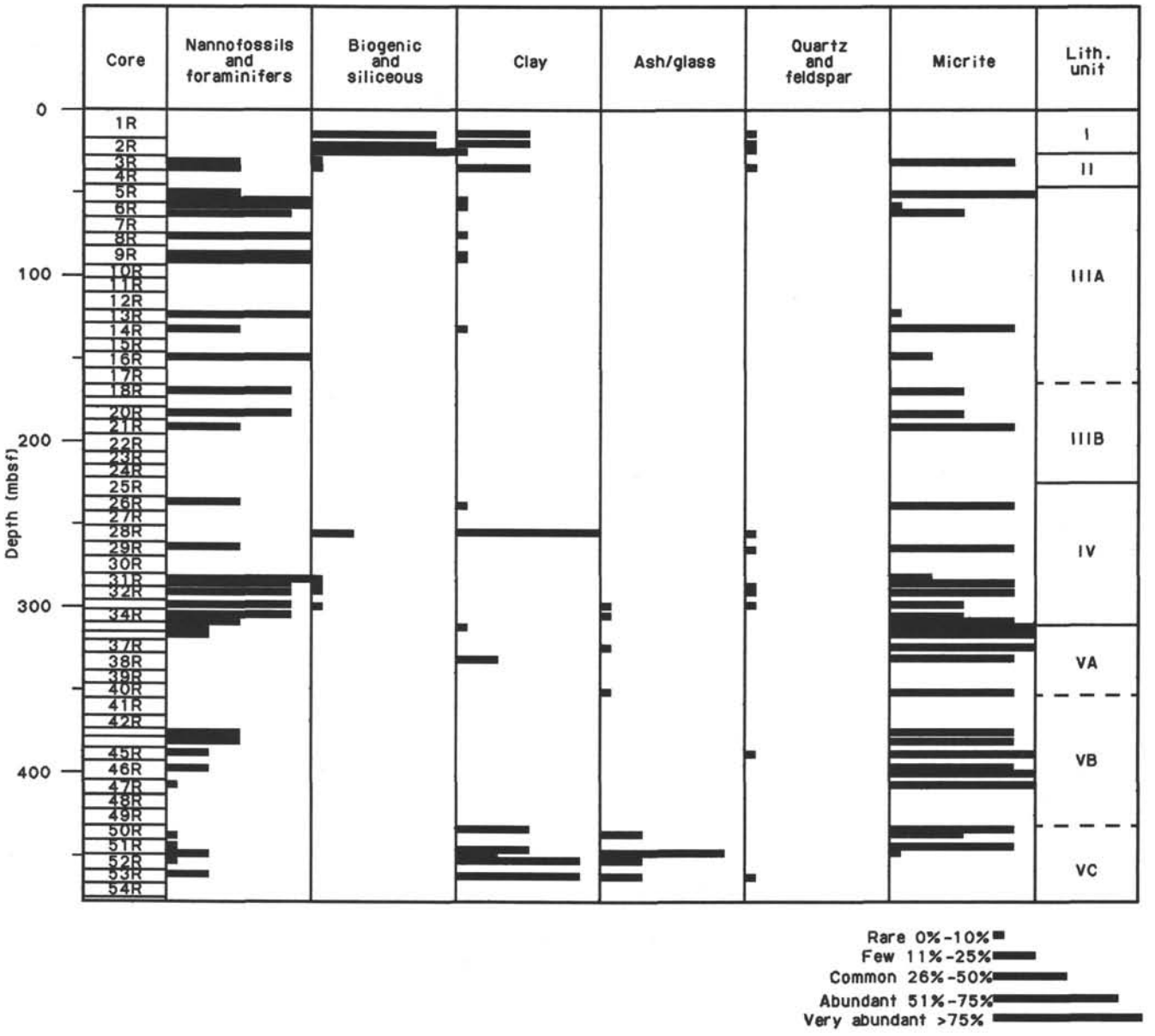

Figure 4. Relative abundance of smear slide components, Hole 700B.

Bioturbation is moderate to strong throughout Subunit IIIB and consists of the same ichnofauna as in Subunit IIIA.

Unit IV: Cores 114-700B-25R through 114-700B-34R; Depth: 228.5–319 mbsf; Age: late Paleocene to early Paleocene.

We use the term "indurated chalk" here to refer to this transitional diagenetic step between the friable chalk of Unit II and the limestone of Unit IV.

This homogeneous unit is composed of indurated micritic nannofossil chalk, either white (no code) or uniform light gray (5Y 7/1) in color. Biosiliceous components are present but uncommon (Figs. 4 and 6) and could contribute to the highly fluctuating carbonate content (Fig. 5). The carbonate value of almost zero at a depth of 200 mbsf comes from a siliceous-bearing claystone interval (Core 114-700B-28R). Chert and limestone nodules were observed in Core 114-700-26R.

Bioturbation is moderate to strong and consists of *Zoophycos* (Fig. 7), *Planolites, Thalassinoides*, and *Chondrites*, which generally occurs in a composite trace association with *Planolites*.

Unit V: Cores 114-700B-35R through 114-700B-54R; Depth: 319–489 mbsf; Age: early Paleocene to Santonian and Turonian(?).

This unit is composed of limestone and can be subdivided into three subunits on the basis of changes in lithology: homogeneous limestone (Subunit VA); alternating clay-bearing limestone, clayey limestones, and limestone (Subunit VB); and ash-bearing limestone alternating with limestone (Subunit VC).

Subunit VA: Core 114-700B-35R to Section 114-700B-40R-3; Depth: 319–359 mbsf; Age: early Paleocene to Maestrichtian.

This subunit consists of homogeneous nannofossil-bearing micritic to micritic limestone ranging in color from light gray

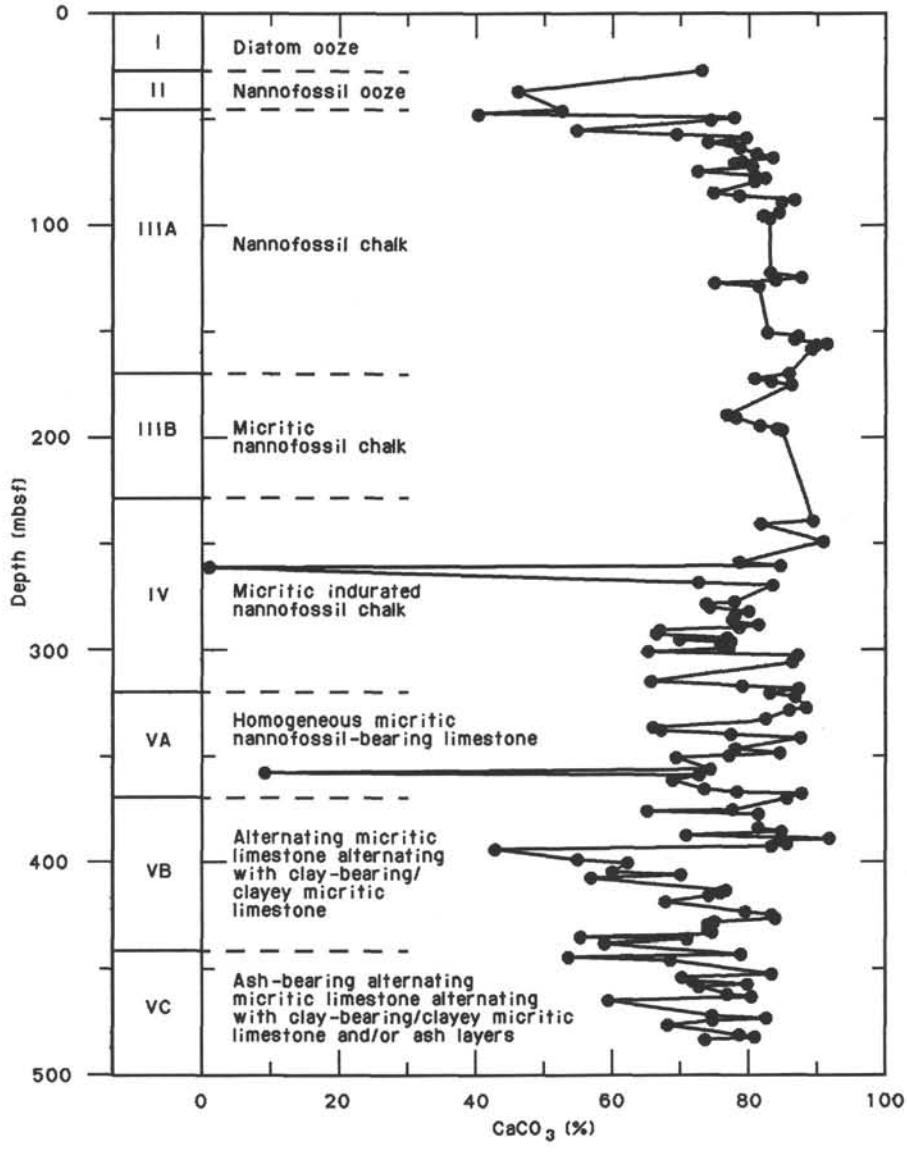

Figure 5. Calcium carbonate, Hole 700B.

(5Y 7/1) to white (no code) or light gray (10YR 7/2), respectively. Clay-bearing micritic limestone horizons are gray to light gray (5Y 6/1, 7/1), and toward the bottom of the unit, alternating colors in the micritic limestone become progressively darker (white with light gray, 10YR 7/2, light gray, 2.5Y 5/2, to light grayish brown, 2.5Y 4/2, or dark grayish brown, 2.5Y 4/2).

The increasingly darker color changes correlate with clay content and with increasing micrite contents at the expense of biocarbonate (Fig. 4). The carbonate content (Figs. 4 and 6) remains high, although variable (65%–88%), with a decreasing downward overall trend. The very low value at 357 m reflects a claystone interval (Core 114-700B-40R). A few chert nodules occur in Cores 114-700B-36R and 114-700B-38R.

Subunit VA is strongly bioturbated. The ichnocommunities are similar to those noted in the overlying units.

Subunit VB: Section 114-700B-40R-4 to Core 114-700B-49R; Depth: 359 to 441.5 mbsf; Age: Maestrichtian to Campanian.

This subunit is characterized by alternating white (10YR 7/1), light greenish gray (5GY 7/1), and light gray (2.5Y 7/2) homogeneous micritic limestone and white (no code), light greenish gray (5Y 7/1, 7/2), and greenish gray (5GY 6/1) clay-bearing limestone to greenish gray (5G 7/1) and light greenish gray (5G 7/2) clayey limestone. Clay-rich horizons have a generally darker hue and also occur as thinner intervals (Fig. 8 and 9). A hiatus (see "Biostratigraphy" and "Paleomagnetics" sections, this chapter) separates Subunit VB (Core 114-700B-49R) and Subunit VC (Core 114-700B-50R).

The carbonate content fluctuates (Fig. 6) as a result of changes in the clay content and an increase in silica in the limestone. Chert nodules appear at the base of the subunit where the carbonate content is low, from 55% to 59% in Cores 114-700B-47R to 114-700B-50R (Fig. 5).

The same ichnocommunities are observed in Subunit VB as in the sediments above. However, the unusual occurrence of *Zoophycos* raphe (the vertical axis from which the feeding traces start) was noted in several cores (Figs. 10 and 11).

Synsedimentary faulting cutting through a *Planolites* burrow but not through a *Zoophycos* trace only a few centimeters above it was also noted in this section.

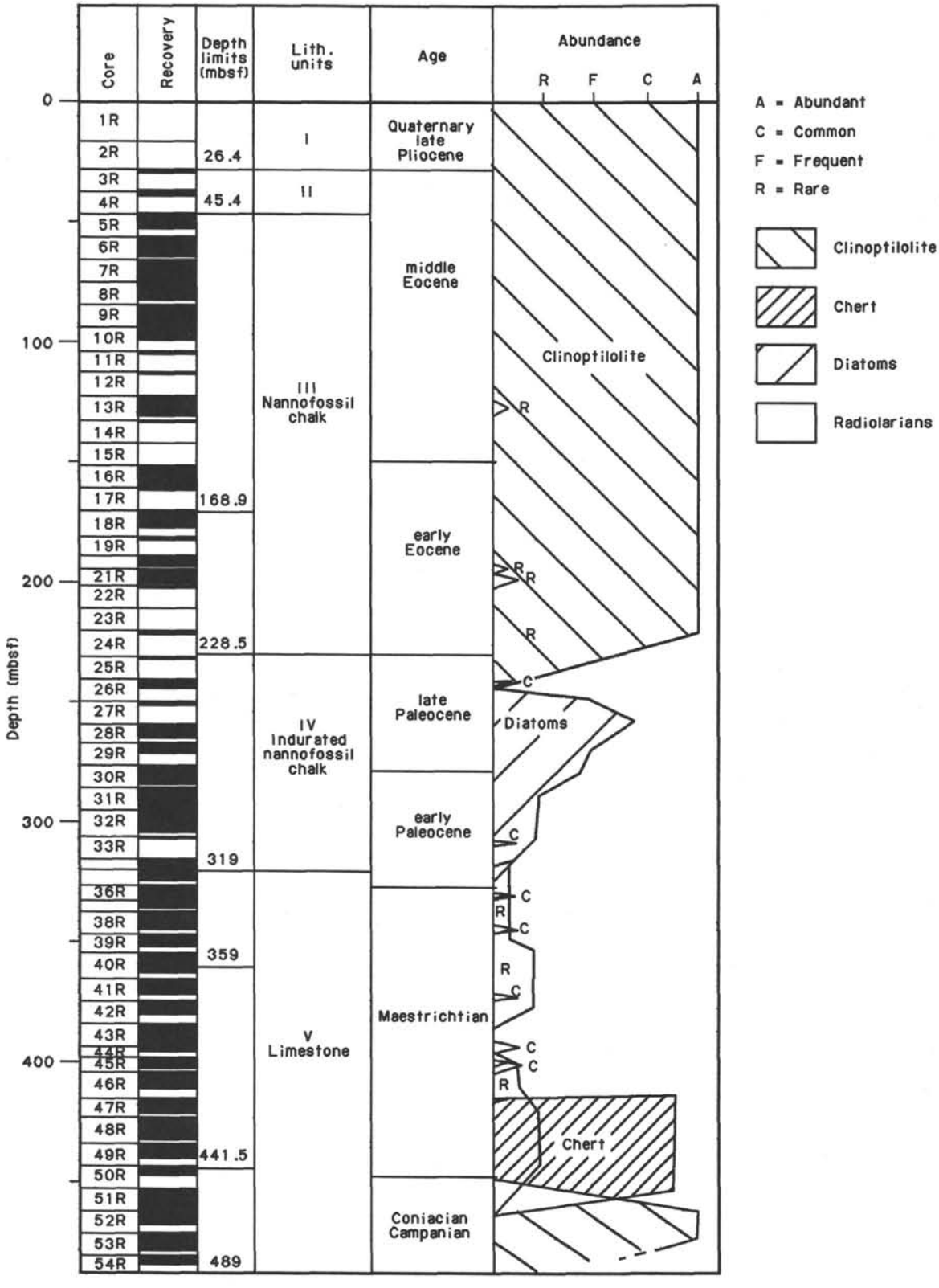

Figure 6. Occurrence of radiolarians, diatoms, clinoptilolite, and chert in the different lithostratigraphic units at Hole 700B.

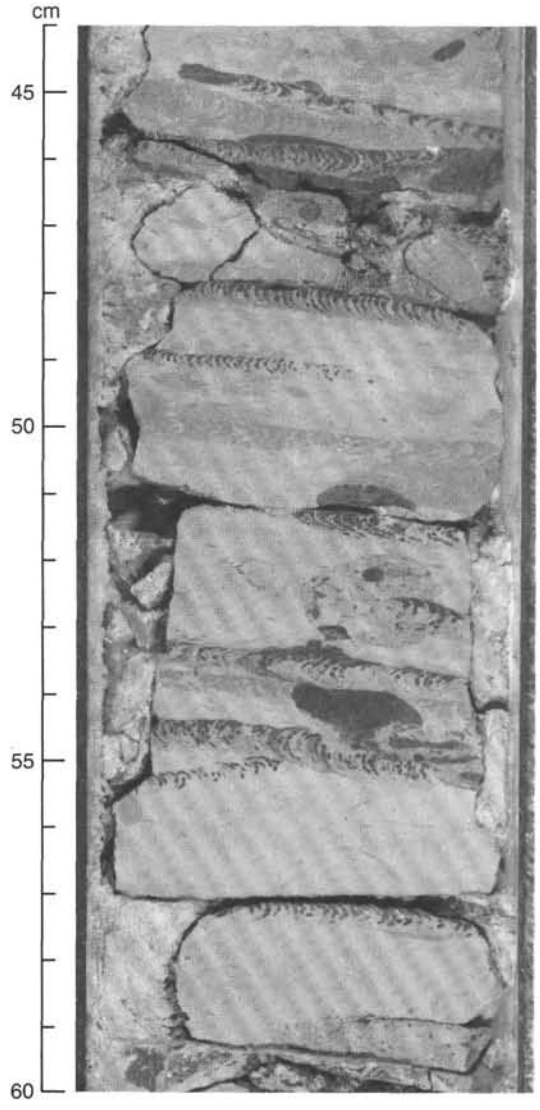

Figure 7. Large *Zoophycos* with internal pellets in Unit IV (Sample 114-700B-28R-3, 44–60 cm).

Subunit VC: Cores 114-700B-50R to 114-700B-54R; Depth: 441.5–489 mbsf; Age: Campanian, Santonian, and Turonian.

This subunit shows the same lithologic characteristics as Subunit VB (i.e, micritic limestone alternating with clay-bearing to clayey micritic limestones) but contains ash-bearing zeolitic clay horizons (Figs. 4 and 11) ranging in color from greenish gray (5GY 6/1) in Core 114-700B-51R to dark brown (7.5YR 4/6, 5/4) in Cores 114-700B-52R and 114-700B-53R.

There is a gradual increase in the volcanic ash component downhole, and discrete ash layers appear in Cores 114-700B-51R (Fig. 12), 114-700B-53R, and 114-700B-54R.

The fluctuating carbonate content (50%–83%; Fig. 6) reflects the alternating lithology. Clinoptilolite is also abundant in this subunit (Fig. 5).

Inoceramus shell fragments occur in Cores 114-700B-47R, 114-700B-50R, and 114-700B-54R (Fig. 13).

Synsedimentary deformation is also observed in this subunit (Figs. 14 and 15). Disturbance of the sediment in Sample 114-700-53R-2, 50–67 cm, (Figs. 14 and 15) was caused by a sudden event that resulted in a thixotropic reaction of the sediment. Undeformed sediments above and below this structure support the contemporaneous nature of the deformation.

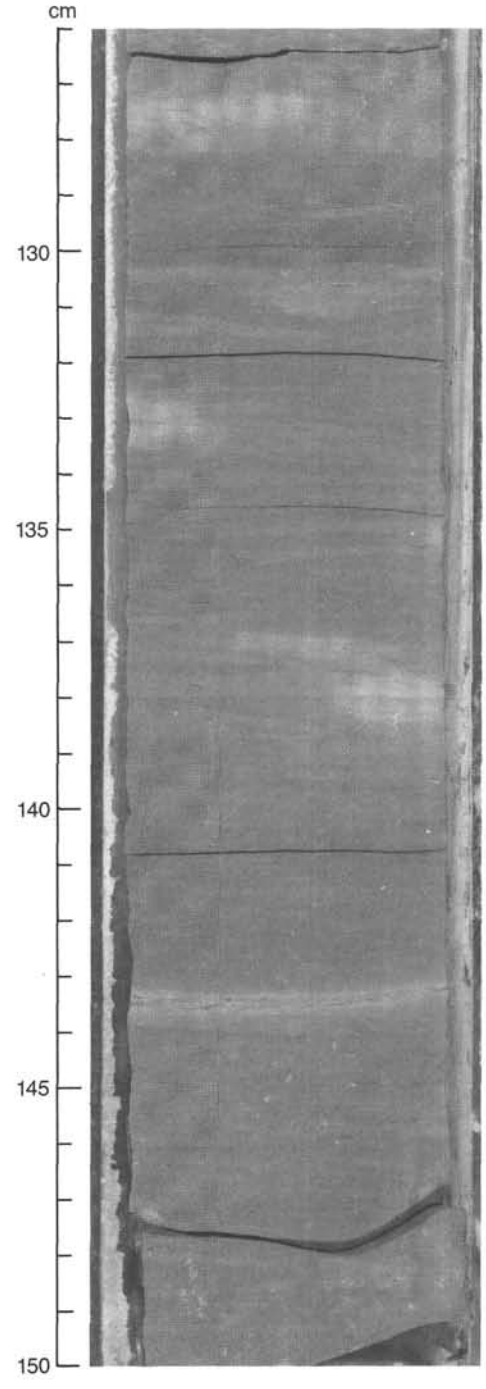

Figure 8. Detail of the alternating hues in Subunit VB limestone (Sample 114-700B-40R-4, 126–150 cm).

Diagenesis

The pelagic carbonate sediments at Hole 700B show a progressive lithification with depth from soft ooze (Unit I) to friable chalk (Unit II) to indurated chalk (Unit III) to limestone (Unit IV). Site 700, in conjunction with Site 699, offers a particularly good opportunity to study the diagenesis of deep-sea carbonates.

The boundaries between the diagenetic units are shown in Table 2. The boundary between the ooze/chalk transition at 45.4 mbsf in Hole 700B is sharp. In contrast, the contact between chalk and limestone is gradational, and we denote the in-

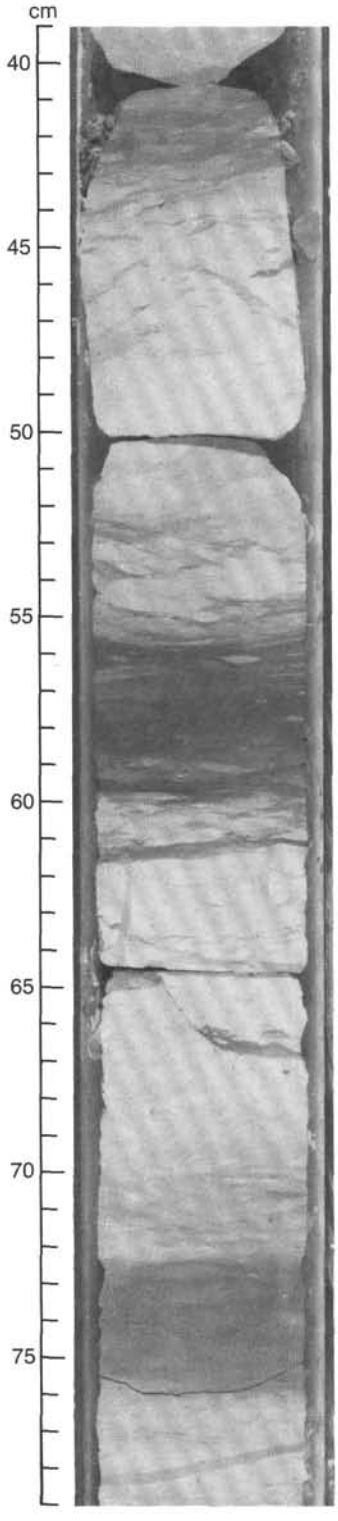

Figure 9. White micritic limestone alternating with thinner clay-bearing/clayey limestone in Subunit VB (Sample 114-700B-42R-2, 39–79 cm). Vertical bioturbation develops from the clayey interval (62–64 cm).

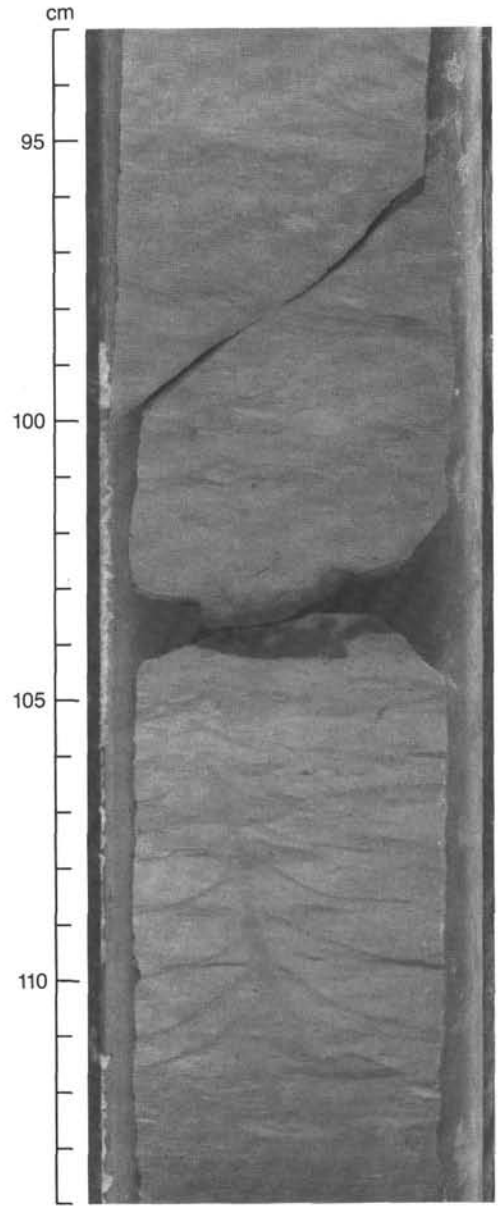

Figure 10. Vertical axis of a complete *Zoophycos* showing the helicoidal development of feeding traces from the axis, or raphe, in Subunit VB (Sample 114-700B-48R-1, 93–114 cm).

termediate degrees of lithification as indurated chalk. Texturally, the transition from chalk to indurated chalk to limestone is characterized by a progressive increase in the importance of microcrystalline carbonate, which fills interstitial voids. The physical properties (porosity, density, and sonic velocity; see "Physical Properties" section, this chapter) show a gradual change throughout the chalk/indurated chalk interval, indicating a smooth diagenetic continuum.

The carbonate content is relatively high throughout the section (see "Geochemistry" section, this chapter). Unit III (chalk) is marked by high $CaCO_3$ content (over 80%) with low variability. The variability in the $CaCO_3$ percentage begins to increase in Unit IV at about 262 mbsf (Core 114-700B-28R, upper Paleocene), probably reflecting the increase in clay content (Fig. 4). Carbonate variability remains high throughout the Cretaceous limestone (Unit V) because of clay-bearing and clayey limestone interbeds.

The diagenetic histories of Holes 699A and 700B appear to be comparable. A comparison of the two sites in Table 2 shows, however, that the chalk/ooze transition in Hole 700B occurs in older sediments than in Hole 699A. This could be because of the removal of 200–350 m of overburden from the Hole 700B section (see "Physical Properties" and "Seismic Stratigraphy"

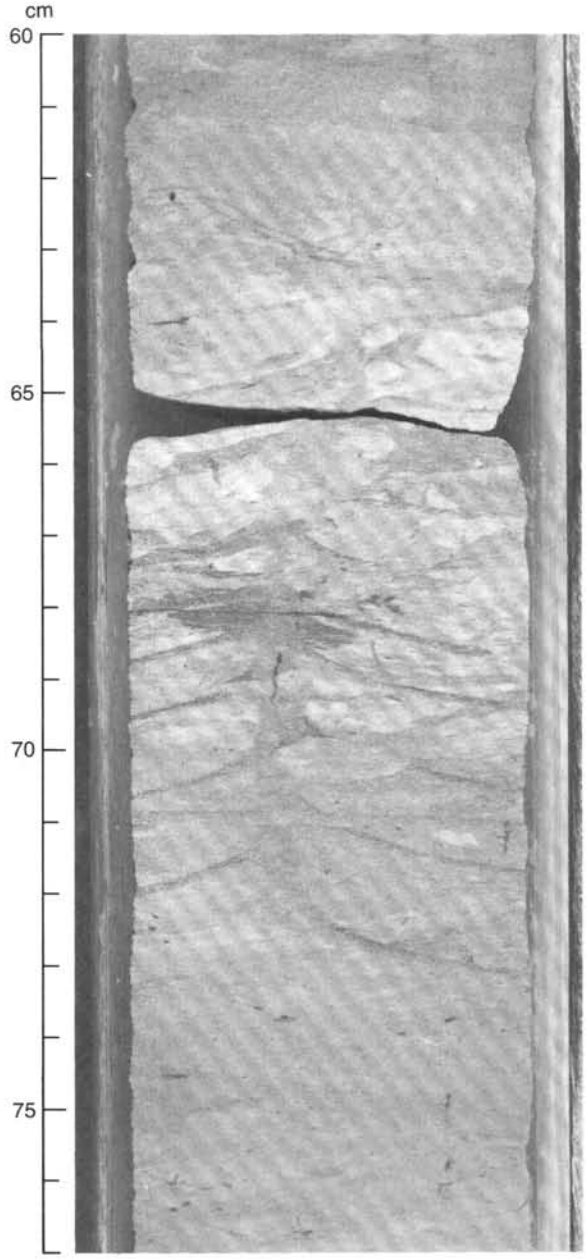

Figure 11. A typical raphe of *Zoophycos*, Subunit VB (Sample 114-700B-48R-1, 60–77 cm).

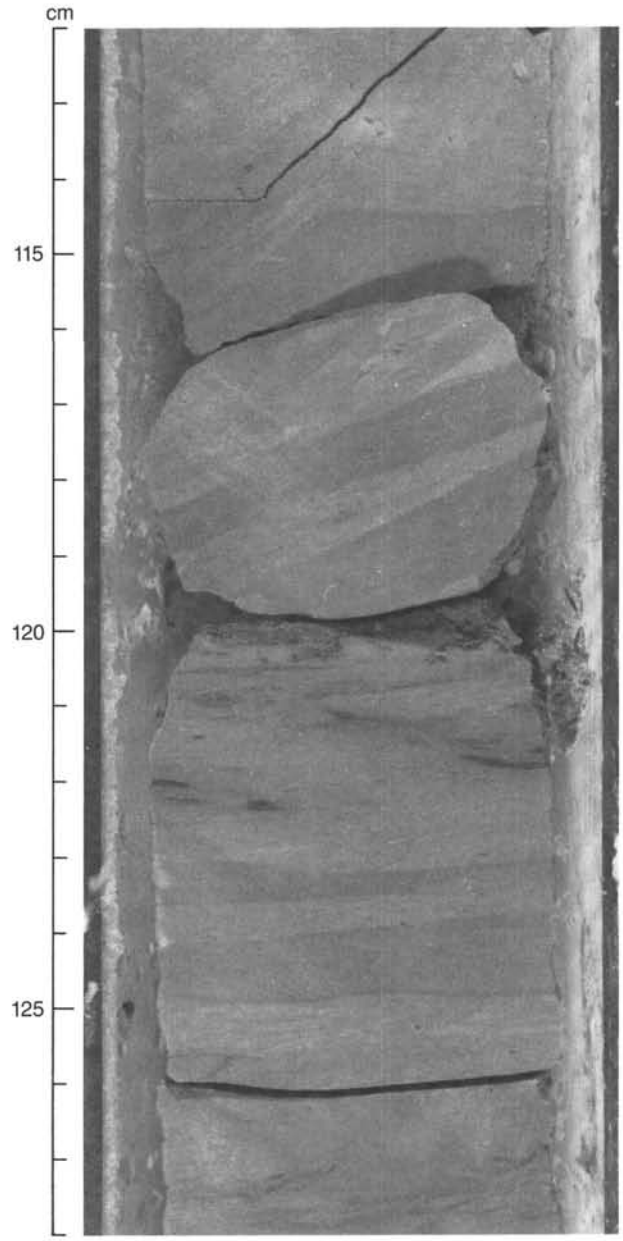

Figure 12. Alternating limestone with ash layer at 120 cm in Sample 114-700B-51R-3, 112–128 cm, Subunit VC.

sections, this chapter). Post-middle Eocene block faulting resulted in a 500-m difference in elevation between the two sites. Removal of 200–350 m of the overlying sediments could have resulted from subsequent erosion caused by strong bottom currents or other processes related to enhanced bottom relief. Diagenesis, meanwhile, continued uninterrupted in Hole 699A.

Chert nodules and layers in Hole 700B occur in the Cretaceous section, where they are abundant in the lower half of Subunit VB and the top of Subunit VC (Fig. 5; Cores 114-700B-47R (Fig. 16) to 114-700B-50R). The chert is invariably found in the purer pale brown (10YR 6/3) micritic limestone horizons, rather than those containing clay, and it does not occur in the ash-bearing limestones at the base of the sequence.

It is now generally accepted that the formation of chert nodules and lenses in marine sediments is related to the dissolution and reprecipitation of biogenic silica (Wise and Weaver, 1974; Kastner, 1981). In the sequence cored at Hole 700B, the sediments of Units III and IV could be a source of silica. Radiolarians found in these carbonate sediments (Fig. 6) suggest that diatoms were also originally present but have been completely removed by dissolution. This hypothesis is supported to a certain extent by the fact that the nodules do not occur in either the clay-rich or the ash-bearing sediments and by the presence of clinoptilolite (see "Geochemistry" section).

Ichnology

The sedimentary succession in Hole 700B shows remarkably pervasive, continuous, and consistent ichnocommunities consisting of *Zoophycos, Planolites, Thalassinoides*, and *Chondrites*, which is generally observed in association with other burrows to form a composite trace.

The occurrence of *Chondrites* is generally considered to indicate poorly oxygenated interstitial waters. However, *Chondrites* is usually found in association with *Planolites* in these sedi-

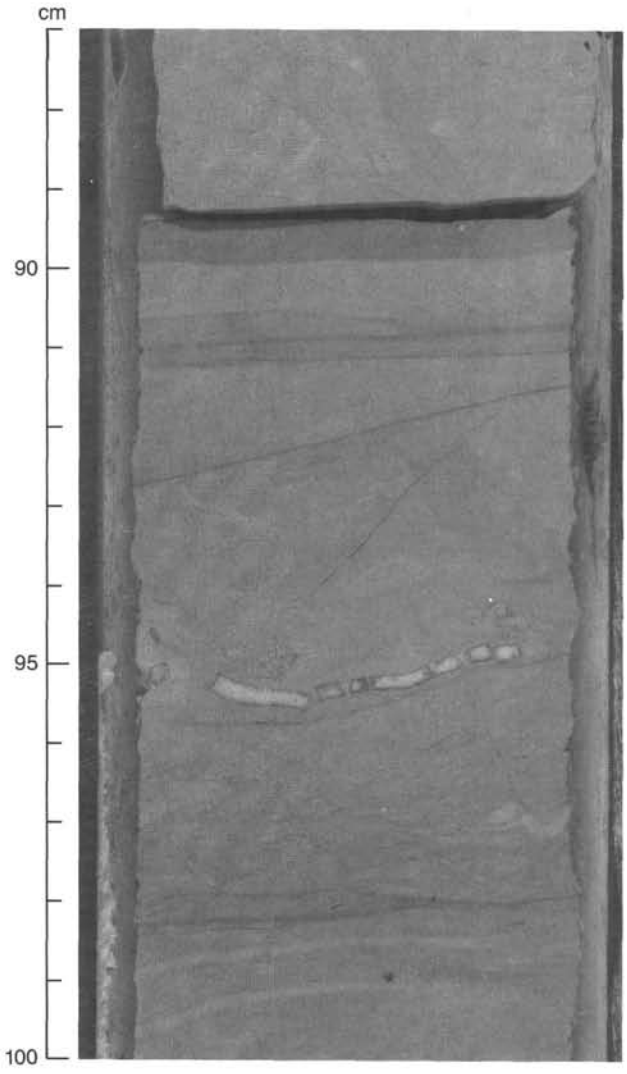

Figure 13. *Inoceramus* shell fragments, Subunit VC (Sample 114-700B-51R-5, 87–100 cm).

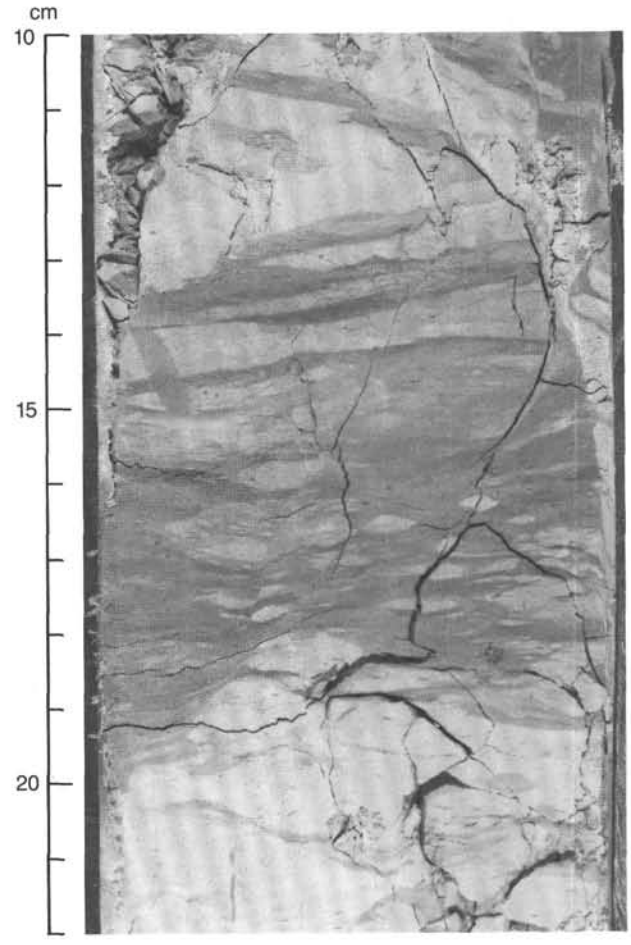

Figure 14. Synsedimentary distensional faulting in Subunit VC (Sample 114-700-43R-7, 10–22 cm). The synsedimentary fault is rotational and cuts several *Planolites* burrows but not the horizontal *Zoophycos* burrow at 15 cm. Note the principal and satellite faults.

ments and therefore, may not be indicative of a particular interstitial environment. However, one explanation for these composite traces is that there may have been a relatively high oxygen content near the seafloor or within the sediment. In such a situation, the organism producing *Chondrites* would be restricted to previously made, less-oxygenated traces.

Another interesting observation of these sediments is the occurrence of central parts of *Zoophycos* system (Figs. 10 and 11), which show the raphe (vertical axis) and the formation of helicoidal feeding traces from the raphe. The presence of a number of *Zoophycos* raphe in several cores indicates a particular abundance of *Zoophycos*.

Paleoenvironmental Interpretation and Conclusions

The sediment sequence from Hole 700B provides information concerning recent oceanography and, in particular, an extremely well-preserved middle Eocene to Coniacian(?) and Turonian(?) pelagic carbonate series.

1. Middle Eocene to Santonian and Turonian(?) sediments display a progressive downhole lithologic change from ooze through chalk, homogeneous indurated chalk, homogeneous limestones, alternating limestones, and clayey limestones, which contain ash horizons at the base. The carbonates at this site contain an excellent record of progressive diagenesis, terminated by post-middle Eocene block faulting, that overlaps with the record from Hole 699A.

2. Comparison of Holes 700A and 700B reveals the existence of a major unconformity between the Quaternary–upper Pliocene and the middle Eocene.

3. Ichnocommunities are continuous throughout the succession, probably reflecting a stable environment of regular subsidence in the area.

4. Paleodepths for Hole 700B show a steady increase from 1500–2000 m during the Cretaceous to more than 3000 m by middle Eocene (see "Biostratigraphy" section).

Paleocirculation during this period appears to have been quiet, and there are no indications of strong bottom-current activity from the sediments. A minor hiatus occurring in the Campanian (Fig. 3) and covering 4 m.y. ± 2 m.y (see "Biostratigraphy" section) may have resulted from bottom-current erosion or other processes associated with tectonism.

Post-middle Eocene (and probably late Oligocene) block faulting produced a 500 m offset of Site 700 relative to Site 699, which resulted in increased elevation and susceptibility to possible erosion by deep currents or other processes related to enhanced bottom relief. Erosion of 200–350 m of post-middle Eocene sediments (see "Physical Properties" and "Seismic Stratigraphy" sections) occurred after the block faulting.

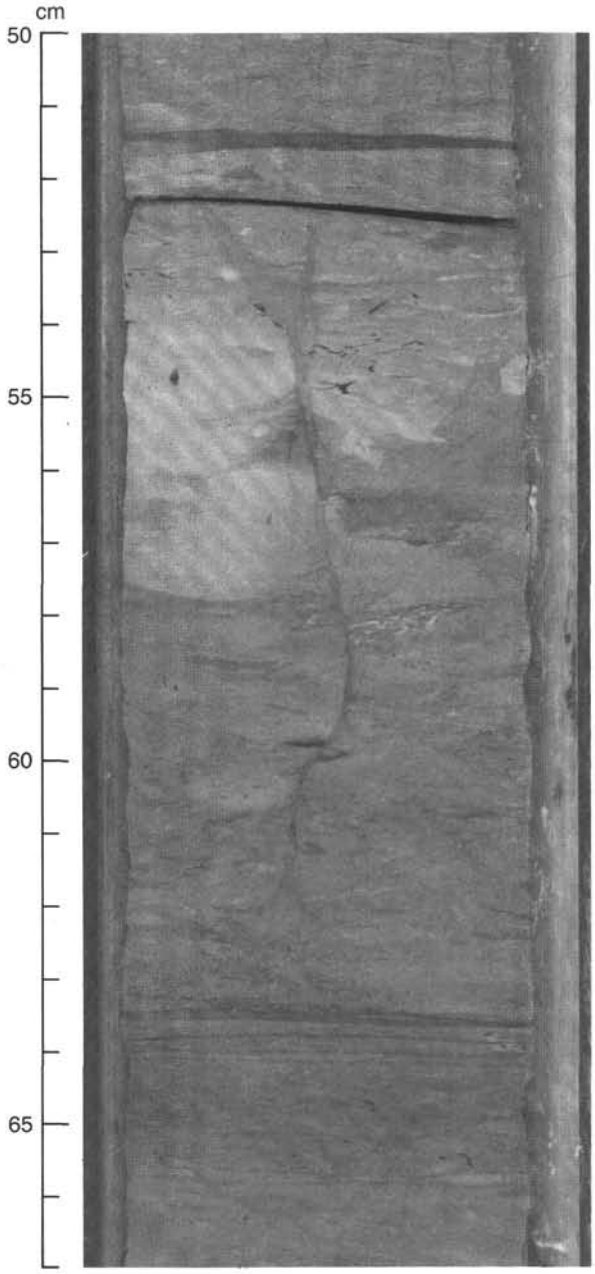

Figure 15. Deformation in Subunit VC that could be related to a seismic event, introducing a quick differential (thixotropic) deformation and compaction in the soft sediment (Sample 114-700B-53R-2, 50–67 cm).

5. A short review of the sedimentology of the drilled section shows:

Active volcanism in the area during the deposition of the Upper Cretaceous sediments, as recorded by the presence of tephra in Santonian and Turonian(?) alternating micritic, clayey, and ash-bearing limestones.

Local evidence of gravity sedimentation is shown by reworked pelecypods and shallow-water microfauna (see "Biostratigraphy" section). The alternating clay-rich and -poor sediments in the Upper Cretaceous (Fig. 9) may be due to fluctuations in biogenic productivity related to changes in climate or to tectonic events (Fig. 8), provoking synsedimentary instability. Processes conducive to the formation of synsedimentary deformation such as microfaulting and the formation of local thixotropic structures in the sediments (Figs. 15 and 16) can perhaps also be related to tectonic movements during the Late Cretaceous.

Table 2. Limits of diagenetic stages in the carbonate sedimentology sequences in Hole 699A and 700B.

	Hole 699A		Hole 700B	
Transition	Depth (mbsf)	Age	Depth (mbsf)	Age
Ooze/chalk	325.6–335.1	NP18, late Eocene	45.4	NP16, middle Eocene
Chalk/indurated chalk	382.6–392.1	NP16–14, middle Eocene	228.5	NP10, early Eocene
Chalk/limestone	—Not recovered—		319	NP4, early Paleocene

BIOSTRATIGRAPHY

Site 700 was rotary drilled in a water depth of 3601 m. Two cores were recovered from Hole 700A, and 54 cores were recovered from Hole 700B. The core catchers have been examined for microfossils.

Planktonic foraminifer preservation is variable at Hole 700B, showing moderate to strong dissolution in certain intervals. Benthic foraminifers are well preserved in the Eocene section. In the lowermost Eocene to Upper Cretaceous (Sections 114-700B-24R, CC, to 114-700B-49R, CC), foraminifers show evidence of recrystallization, but despite this, morphology is well preserved. Below this level, foraminifers are severely recrystallized with overgrowths.

Calcareous nannofossil preservation decreases from the middle Eocene to the Paleocene. Preservation is highly variable in the Cretaceous section, where dissolution removed many of the more delicate nannofossil species.

Abundant and well-preserved radiolarians, silicoflagellates, and diatoms were recovered from the first two core-catcher samples of Holes 700A and 700B. Siliceous microfossils are absent from the Eocene at Hole 700B. Moderately well-preserved radiolarians and silicoflagellates and poorly to moderately preserved diatoms were found in the Paleocene from Sections 114-700B-26R, CC, through 114-700B-32R, CC. Below another barren interval, well-preserved radiolarians were observed between Cretaceous Sections 114-700B-43R, CC, and 114-700B-50R, CC.

Biostratigraphy

Zonal assignments for the two cores recovered from Hole 700A are shown in Figure 17.

The Hole 700B zonal assignments by each microfossil group are illustrated in Figure 18. The extensive Maestrichtian section is supported by paleomagnetic evidence that shows many normal and reversed polarity intervals in this section. Nannofossil evidence indicates a hiatus between Sample 114-700B-50R-2, 26–27 cm, and Section 114-700B-50R, CC. The age/depth relationships of zonal and paleomagnetic boundaries are shown in Figure 19 and given in Table 3.

Paleoenvironment

Benthic foraminifers indicate a Cretaceous depth range of 1500–2000 m. The Paleocene depth range was 2000–2500 m. The early Eocene depth was 2500–3000 m and 2750–3000 m by the middle Eocene.

Peak abundances of the Cretaceous warm-water planktonic foraminifer group Globotruncanids are inversely correlated with peaks of siliceous microfossil preservation (Fig. 20). This suggests either that there may have been warm/cold surface-water fluctuations during the Cretaceous or that the Globotruncanids were not preserved during possible instances of stronger dissolution.

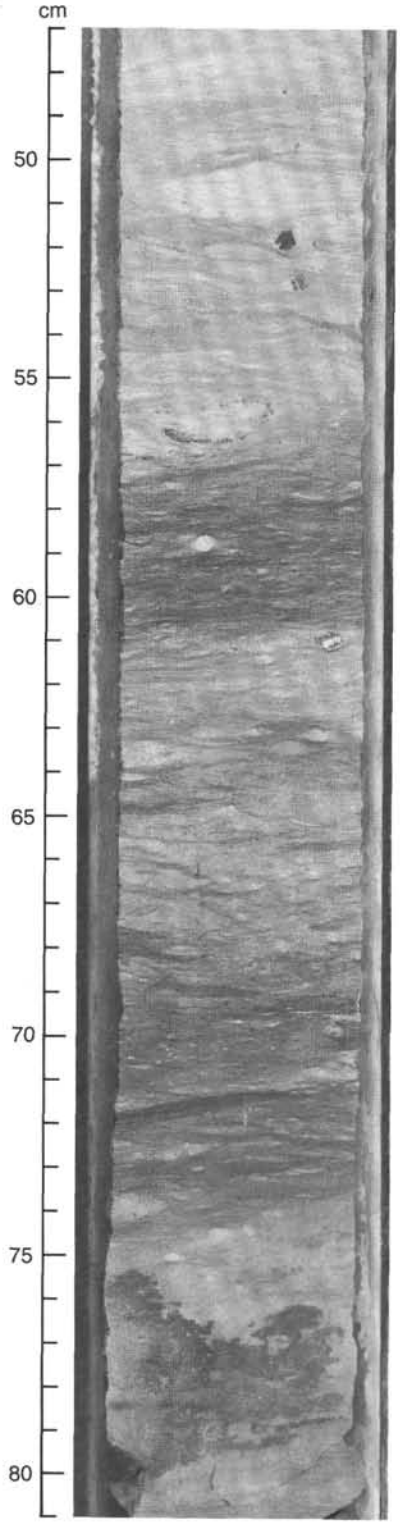

Figure 16. Alternating limestone showing the development of chertification, 76–80 cm (Sample 114-700B-47R-1, 47–81 cm).

Preliminary investigations assign the Paleocene planktonic foraminifer fauna to a temperate province. Planktonic foraminifer species diversity is highest in the uppermost Paleocene to the lower Eocene, including highly abundant warm-water Acarininids and a few strongly keeled Morozovellids. The first downhole co-occurrence of Sphenoliths and the common nannofossil *Zygrhablithus bijugatus* indicate relatively warm surface waters

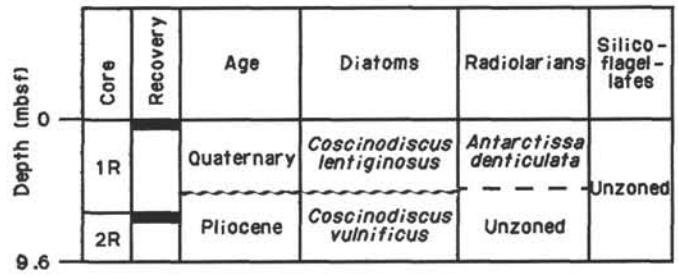

Figure 17. Hole 700A chronostratigraphic summary.

in the early Eocene. Middle Eocene nannofossil floras at Hole 700B are similar to those found at Hole 699A. They are transitional between Paleocene–lower Eocene warmer water assemblages and Oligocene colder water assemblages. By the middle Eocene, the planktonic foraminifers are less diversified and only cold-water and dissolution-resistant species are present.

The Cenozoic sedimentation rate was calculated to be 15 m/m.y. based on microfossil datum levels (Table 3) and the time scale of Berggren et al. (1985) (Fig. 19).

Calcareous Nannofossils

Thirty-two core samples and all the core-catcher samples from Hole 700B were examined for calcareous nannofossils. Most of the samples studied contain rich nannofossil floras that were assigned to the zonation schemes of Martini (1971) and Sissingh (1977) (see "Explanatory Notes" chapter, this volume).

Biostratigraphy

The sample from Section 114-701B-1R, CC, is barren of *in-situ* nannofossils; isolated reworked Paleogene species were recorded.

The nannofossil floras from between Sample 114-700B-3R-1, 59–60 cm, and Section 114-700B-4R, CC, are assigned to NP16 (middle Eocene). The presence of this zone is indicated by the co-occurrence of *Chiasmolithus solitus* and *Reticulofenestra bisecta*. The base of NP16 cannot be defined in most areas outside northwest Europe because of the absence of *Rhabdosphaera gladius*. In this study, the first appearance datum (FAD) of *R. bisecta* is used to define the base of definite NP16. The underlying interval between Sample 114-700B-5R-2, 70–71 cm, and Section 114-700B-8R, CC, is assigned to NP16–15 (middle Eocene). Supporting evidence for this zonal assignment is provided by the occurrence of *Nannotetrina fulgens* between Sample 114-700B-7R-2, 33–34 cm, and Section 114-700B-8R, CC.

Sample 114-700B-9R-6, 28–29 cm, to Section 114-700B-14R, CC, are assigned to NP15?–14 (middle lower Eocene) by virtue of their stratigraphic position between NP16–15 and NP14 strata. The presence of NP14 is inferred from the first downhole occurrence of *Discoaster lodoensis* in Section 114-700B-15R, CC. The base of NP14 is defined by the FAD of *Discoaster sublodoensis* recorded in Section 114-700B-16R, CC.

Sample 114-700B-18R-1, 80–81 cm, to Section 114-700B-18R, CC, are assigned to NP13 (lower Eocene). The interval between Sample 114-700B-20R-2, 106–107 cm, and Section 114-700B-22R, CC, is assigned to NP12–10 (lower Eocene) on the basis of the presence of *Tribrachiatus orthostylus*. The top of NP12 is defined by the last appearance datum (LAD) of *T. Orthostylus*, and its base is defined by the FAD of *D. lodoensis*. The latter species is rare or absent in the samples from this interval, as is *Tribrachiatus contortus*, the LAD of which defines the base of NP11; therefore, NP12–10 are grouped together. Section 114-700B-24R, CC, is tentatively assigned to NP10 (lower Eocene) by virtue of its stratigraphic position between NP12–10 and NP9 strata. The taxa that define the top and bottom of NP10 were not recorded in Hole 700B.

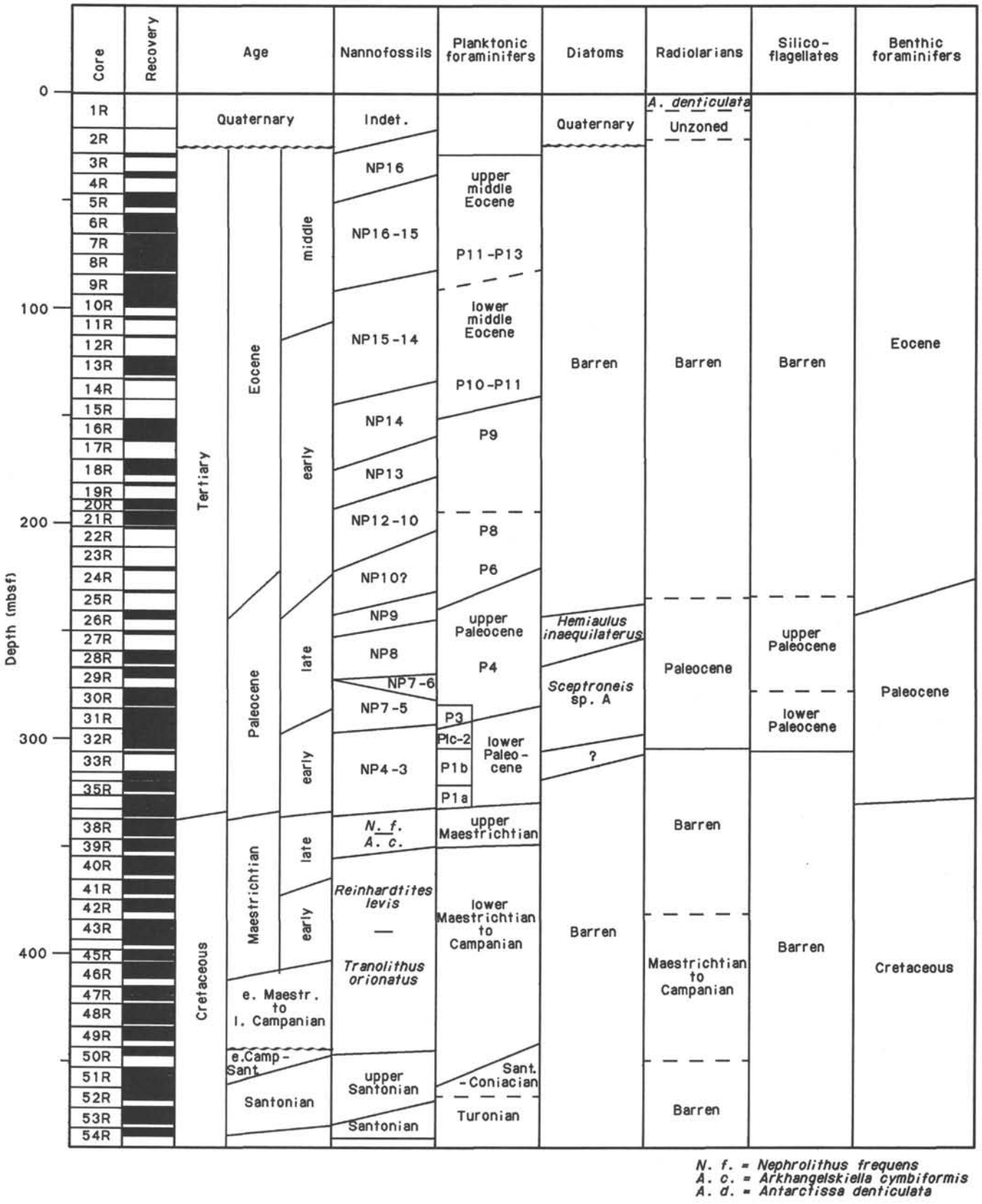

Figure 18. Hole 700B chronostratigraphic summary.

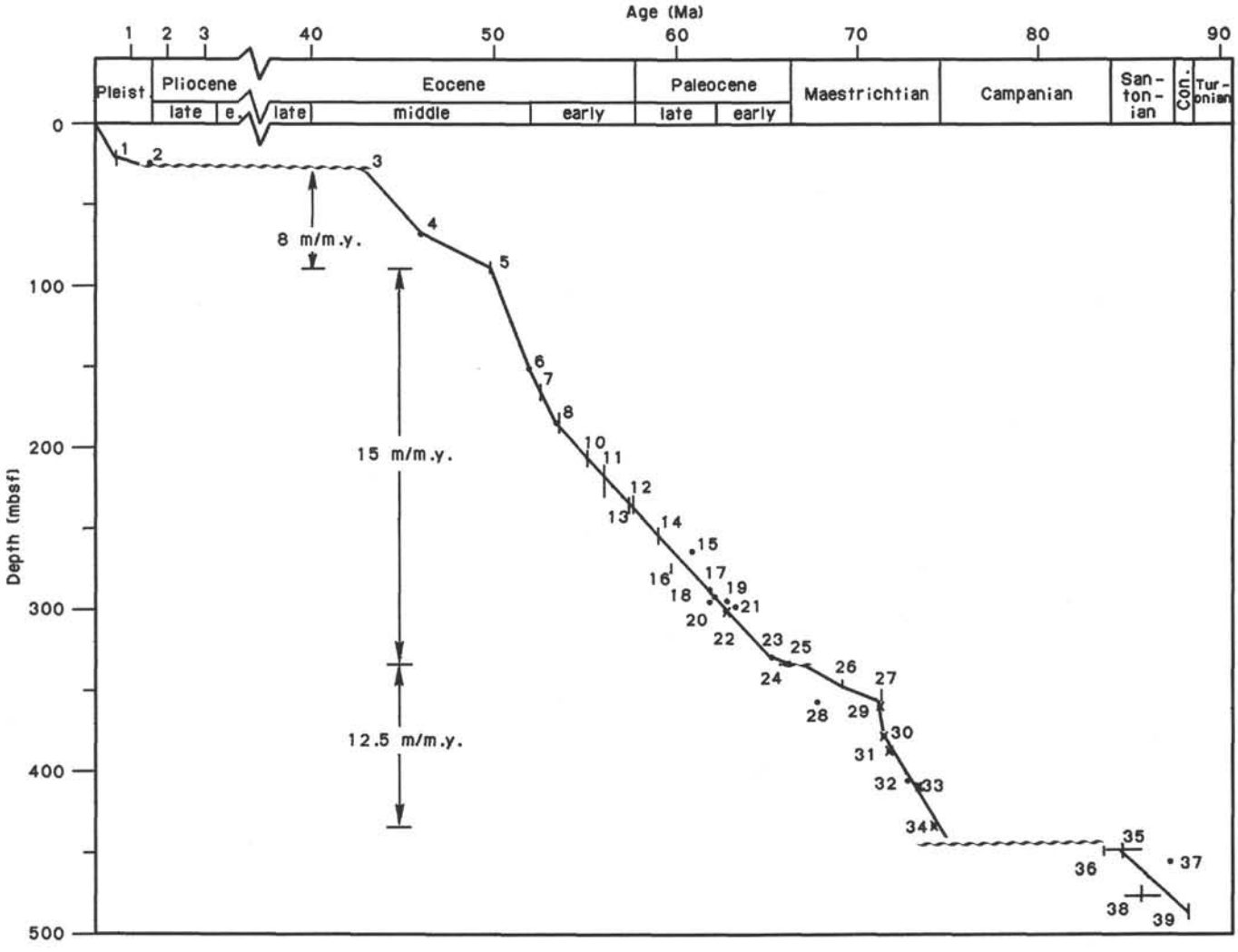

Figure 19. Age vs. depth relationship at Hole 700B.

The co-occurrence of *Fasciculithus tympaniformis* and *Discoaster multiradiatus* in Sample 114-700B-26R-1, 40–41 cm, to Section 114-700B-26R, CC, is taken here to indicate the presence of NP9 (upper Paleocene). The absence of *D. multiradiatus* and the occurrence of *Heliolithus riedelii* in Section 114-700B-27R, CC, and Sample 114-700B-29R-2, 122–124 cm, indicate the presence of NP8 (upper Paleocene).

Section 114-700B-29R, CC, contains *Heliolithus kleinpellii*, the FAD of which defines the base of NP6. Thus, this sample is assigned to NP7–6 (upper Paleocene). The FAD of *Discoaster mohleri* defines the NP7/6 contact, but *D. mohleri* is absent from Hole 700B.

Samples 114-700B-30R-2, 120–121 cm, to 114-700B-31R-5, 115–116 cm, continue to contain *F. tympaniformis* and are thus assigned to NP7–5 (upper Paleocene). The FAD of *F. tympaniformis* defines the base of NP5.

Sections 114-700B-31R, CC, to 114-700B-36R, CC, yielded *Hornibrookina teuriensis, Cruciplacolithus edwardsii*, and *Prinsius martinii*. These species probably indicate the presence of NP4–3 (upper lower Paleocene) but do not define these zones.

A stratigraphic break possibly occurs between Section 114-700B-36R, CC, and Sample 114-700B-37R-2, 31–32 cm. This break separates the lower Paleocene from the uppermost Maestrichtian strata. The presence of *Nephrolithus frequens* between Sample 114-700B-37R-2, 31–32 cm, and Section 114-700B-40R, CC, indicates the presence of the *N. frequens* Zone (upper Maestrichtian); however, in this area, the stratigraphic range of *N. frequens* overlaps with that of *Reinhardtites levis*. Sissingh (1977) considered the two species to be mutually exclusive and defined the *Arkhangelskiella cymbiformis* Zone as an interval between the LAD of *R. levis* and the FAD of *N. frequens*. No such interval exists at this high latitude, probably because *N. frequens* has an earlier FAD here. This species is known to have a preference for the colder water areas. Thus, the interval from Samples 114-700B-37R-2, 31–32 cm, to 114-700B-39R-2, 32–33 cm, is assigned to the *N. frequens/A. cymbiformis* Zones (upper Maestrichtian), and the interval from Section 114-700B-39R, CC, to Sample 114-700B-50R-2, 26–27 cm, is assigned to the *R. levis/Tranolithus orionatus* Zones (middle Maestrichtian to upper Campanian). The top of the last zone is defined by the LAD of *Tranolithus orionatus* (*Tranolithus phacelosus*). This species is present in Hole 700B, and its occurrence is irregular and not reliable. The LADs of *Broinsonia parca, Eiffellithus eximius, Staurolithites ellipticus* (*sensu* Crux, 1982) and *Orastrum campanensis* are also recorded in this interval, thus confirming its age as middle Maestrichtian to late Campanian.

A stratigraphic break representing most of the Campanian and some of the Santonian separates Sample 114-700B-50R-2, 26–27 cm, and Section 114-700B-50R, CC.

The presence of *Serbiscutum primitivum* in Section 114-700B-50R, CC, indicates the penetration of upper Santonian or older strata. In Section 114-700B-53R, CC, the first downhole occur-

Table 3. Microfossil datums in Hole 700B.

Microfossil and paleomagnetic datums[a]	Age (Ma)	Reference[b]	Interval in Hole 700B	Depth (mbsf)	Mean position (mbsf)
1. LAD *Actinocyclus ingens* (D)	+0.62	10	1R, CC to 2R, CC	16.90–26.40	21.65
*2. Base *A. ingens* Zone (D)	+1.50	10	2R, CC	26.40	
Hiatus (Minimum duration = 41.1 m.y.; 42.6 to 1.5 Ma)				26.46–26.40	26.43
*3. Top P13 Zone (F)	42.60	7	3R-1, 44 cm	26.46–26.84	26.65
4. Base P12 Zone (F)	46.00	7	7R-2, 29 cm, to 7R-3, 27 cm	67.67–66.19	66.93
5. Base NP15 Zone (N)	49.80	4	8R, CC, to 9R-6, 28 cm	83.90–91.18	87.54
6. Base P10 Zone (F)	52.00	4, 6	15R, CC, to 16R-1, 40 cm	149.90–150.30	150.10
7. Base NP14 Zone (N)	52.60	4	16R, CC, to 18R-1, 80 cm	159.40–169.70	164.55
8. Top NP12 Zone (N)	53.70	4	18R, CC, to 20R-2, 106 cm	178.40–190.46	184.30
9. Base P9 Zone (F)	53.40	4, 6	20R, CC, to 21R-1, 26 cm	192.90–193.16	193.03
10. Base P8 Zone (F)	55.20	4	21R, CC, to 22R, CC	200.00–209.50	204.75
11. Base P7 Zone (F)	56.10	4	22R, CC, to 24R, CC	209.50–228.50	219.00
12. LAD *Fasciculithus* (N)	57.60	4	24R, CC, to 26R-1, 40 cm	228.50–238.40	233.45
13. Base P6 Zone (F)	57.80	4	24R, CC, to 26R-1, 130 cm	228.50–239.30	233.90
14. Base NP9 Zone (N)	59.20	4	26R, CC, to 27R, CC	247.50–257.00	252.25
15. Base P4 Zone (F)	61.00	4	28R-3, 104 cm, to 28R-4, 102 cm	261.04–262.52	261.78
16. Base NP8 Zone (N)	59.90	4	29R-2, 124 cm, to 29R, CC	269.24–276.00	272.62
17. Base P3b Zone (F)	62.00	4	30R, CC, to 31R-1, 141 cm	285.50–286.91	286.21
18. Base P3a Zone (F)	62.30	4	31R-4, 143 cm, to 31R-5, 140 cm	286.93–292.90	289.92
19. Base P2 Zone (F)	63.00	4	31R-5, 142 cm, to 31R-6, 140 cm	292.92–294.90	293.91
20. Base NP5 Zone (N)	62.00	4	31R-5, 116 cm, to 31R, CC	292.66–295.00	293.83
21. Base P1c Zone (F)	64.50	4	32R-1, 32 cm, to 32R-2, 30 cm	295.32–296.80	296.06
22. Chron C26R/C27N boundary	63.03	4	32R-3, 104 cm, to 32R-3, 125 cm	299.04–299.25	299.15
23. Chron C28R/C29N boundary	65.50	4	36R-1, 115 cm, to 36R-1, 125 cm	327.15–327.25	327.20
24. Base P1b Zone (F)	66.20	4	36R, CC, to 37R-1, 100 cm	330.70–331.70	331.20
Hiatus Cretaceous/Tertiary boundary Maximum duration = ~3.0 m.y. (65.5–68.5 Ma) Minimum duration = ~0.2 m.y. (66.2–66.5 Ma)				332.51–330.70	
25. Top *Nephrolithus frequens* Zone (N)	66.40	5	36R, CC, to 37R-2, 31 cm	330.70–332.51	331.61
26. Chron C30N/C30R boundary	69.40	4	38R-5, 80 cm, to 39R-2, 5 cm	342.30–346.56	344.43
27. Top *Reinhardtites levis* Zone (N)	71.50	5	39R-2, 32 cm, to 39R, CC	346.82–354.50	350.66
28. Base *Abathomphalus mayaroensis* Zone (F)	68.00	5	40R-1, 27 cm, to 40R-2, 25 cm	354.77–356.25	355.51
29. Chron C30R/C31N boundary	71.37	4, 5	40R-3, 25 cm, to 40R-3, 35 cm	357.75–357.85	357.80
30. Chron C31N/C31R boundary	71.65	4, 5	42R-2, 145 cm, to 42R-3, 5 cm	376.45–376.55	376.50
31. Chron C31R/C33N boundary	71.91	4, 5	43R-2, 25 cm, to 43R-2, 35 cm	384.75–384.85	384.80
32. *Globotruncana contusa* to *Globotruncana gansseri* Zones (F)	73.00	5	45R, CC, to 46R-1, 20 cm	403.50–403.70	403.60
33. Chron C32N/C32R boundary	73.55	4, 5	46R-3, 85 cm, to 46R-3, 95 cm	407.35–407.45	407.40
34. Chron C32R/C33N boundary	74.30	4, 5	48R-6, 85 cm, to 48R-6, 104 cm	430.85–431.04	430.92
Hiatus Most of Campanian missing Maximum duration = ~9 m.y. (75–84 Ma)				443.27–451.00	
35. Top *Serbiscutum primitivum* (N)	84.0–86.0	3, 5	50R-2, 27 cm, to 50R, CC	443.27–451.00	447.14
36. Campanian/Santonian (F)	84.00	5	50R-3, 53 cm, to 50R, CC	445.03–451.00	448.02
37. Santonian/Coniacian (F)	87.50	5	51R-3, 89 cm, to 51R-4, 89 cm	454.89–456.39	455.64
38. Top *Lithastrinus floralis* (N)	85.0–87.0	3, 5	52R, CC, to 53R, CC	470.00–479.50	474.75
39. Top Turonian? (F)	88.50	5	53R, CC, to 54R, CC	479.50–489.00	484.25

[a] + = direct correlation to paleomagnetic stratigraphy; # = absolute age data; * = probable truncation of datum by hiatus; D = diatom; F = planktonic foraminifer; N = calcareous nannofossil.
[b] 3. Perch-Nielsen (1985); 4. Berggren et al. (1985); 5. Kent and Gradstein (1985); 6. Jenkins (1985); 7. McGowran (1986); 10. Ciesielski (1983).

rence of *Lithastrinus floralis* and the continued occurrence of *A. cymbiformis* confirms the presence of Santonian strata. The lowest sample examined, in Section 114-700B-54R, CC, contains *A. cymbiformis*, which indicates an age no older than Santonian.

Paleoenvironment

The nannofossil floras of the middle Eocene interval of Hole 700B are similar to those recorded in Hole 699A. They are transitional between the warmer water assemblages of the lower Eocene and the colder waters of the Oligocene (Hole 699A only). Like the nannofossil floras of Hole 699A, the floras of this hole contain increasing numbers of discoasters and sphenoliths downhole through the middle Eocene.

The common occurrence of *Zygrhablithus bijugatus* in the lower Eocene and its absence from the middle Eocene section possibly indicate a shallower water depth (less than 1000 m) for this interval. The Cretaceous nannofossil floras are typical of high-latitude assemblages, with the geographically restricted species *N. frequens, Biscutum dissimilis, Monomarginatus quaternarius, S. ellipticus* (sensu Crux, 1982), and *O. campanensis* present in the Maestrichtian to Campanian interval. The high-latitude species *S. primitivum* is common in the underlying Santonian.

Preservation

The nannofossil floras recovered from Hole 700B are moderately to poorly preserved, with overgrowth of secondary calcite increasing downhole.

Planktonic Foraminifers

Biostratigraphy

Section 114-700B-1R, CC, does not contain any planktonic foraminifers. The interval between Samples 114-700B-3R-1, 44–46 cm, and 114-700B-7R-5, 27–29 cm, can be assigned to upper

middle Eocene *Globigerinatheka index* Zone, P13–11 (upper part). The FAD of *G. index* divides the middle Eocene into the upper middle Eocene above and the lower middle Eocene below. The upper boundary of the *G. index* Zone is marked by the extinction of *Acarinina primitiva* and the base of the LAD of *Planorotalites* taxon, which is calibrated to fall in the lower part of P11 Zone. The interval between Sections 114-700B-10R, CC, and 114-700B-15R, CC, belongs to the lower middle Eocene *A. primitiva* Zone, P11 (lower part)–P10.

Morozovella crater Zone, considered equivalent to P9 by Pujol and Sigal (1979), represents the interval between Samples 114-700B-16R-1, 40–42 cm, and 114-700B-21R-1, 26–28 cm, which can be considered upper lower Eocene. The interval from Sample 114-700B-21R-2, 18–20 cm, to Section 114-700B-21R, CC, belongs to the lower Eocene *Pseudohastigerina wilcoxensis* Zone, P8. *Acarinina pentacamerata*, the marker species of this zone, has been found associated with *Globigerinatheka senni*, the LAD of which is considered to indicate the base of the P8 Zone.

The age of Sections 114-700B-22, CC, to 114-700B-24, CC, is assigned to the lower Eocene *P. wilcoxensis* Zone, P7–6. *Morozovella marginodentata* occurs within this interval, and this species' range is within P7–6. The age of Section 114-700B-25, CC, is uncertain because of strong dissolution of planktonic foraminifers; radiolarians are more abundant than foraminifers in this core-catcher sample.

The interval from Samples 114-700R-26R-1, 130–132 cm, to 114-700B-28R-3, 102–104 cm, can be assigned to upper Paleocene P4 Zone because of the occurrence of *Subbotina pseudobulloides* and *Subbotina triloculinoides* and the abundance of large *Planorotalites*, such as *Planorotalites australiformis*.

The presence of abundant radiolarians prevents placement of the P4/3 contact, but Section 114-700B-30R, CC, represents the base of P3b Zone because of the presence of *Planorotalites pusillus pusillus*. The interval from Samples 114-700B-31R-1, 141–143 cm, to 114-700B-31R-4, 140–142 cm, can be assigned to the P3a Zone by the presence of the marker species *Morozovella angulata*. The P2 Zone is probably represented in Sample 114-700B-31R-5, 140–142 cm.

The P1c–1b zones can be identified between Sample 114-700B-31R-6, 140–142 cm, and Section 114-700B-36R, CC. The basal Tertiary at this site is represented by the P1b Zone because of the occurrence of *S. pseudobulloides* just above the Upper Cretaceous.

The interval from Samples 114-700B-37R-1, 100–102 cm, to 114-700B-40R-1, 25–27 cm, is assigned to the *Abathomphalus mayaroensis* Zone of the upper Maestrichtian, which corresponds to the total range of the marker species.

Sample 114-700B-40R-1, 25–27 cm, to Section 114-700B-45R, CC, are middle Maestrichtian, considering that the base of middle Maestrichtian is equated to the base of *Cansserina gansseri* Zone, because of the first occurrence (FO) of *Globotruncanella pschade* in the latter core-catcher sample. Below this interval to Core 114-700B-48R there are no indicative species, and it is not possible to define the Maestrichtian/Campanian boundary or to evaluate the continuity of the sequence.

The interval from Sample 114-700B-49R-2, 75–77 cm, to Section 114-700B-49R, CC, contains *Heterohelix glabrons* and some *Marginotruncana*, and therefore can be assigned to lower Campanian.

Pithonella krasheninnikovi is abundant from the uppermost Maestrichtian to Section 114-700B-49R, CC.

Section 114-700B-50R, CC, contains abundant *Marginotruncana marginata* and cannot be younger than Santonian, at the top of which the species has its LAD. There is no evidence for differentiating the Santonian from Coniacian; however, Sample 114-700B-52R-1, 89–91 cm, falls at the base of the Coniacian *Dicarinella concavata* Zone. This sample and Sample 114-700B-52R-2, 89–91 cm, are attributed to *Marginotruncana schneegauri* Zone of Coniacian age.

The interval between Sample 114-700B-52R-3, 89–91 cm, and Section 114-700B-54R, CC, can be assigned to the Turonian based on an acme of *Marginotruncana marianosi*, which has a stratigraphic range that does not extend above the Turonian/Coniacian contact. The FOs of *Hedbergella flaudrini* and *Archaeoglobigerina* occur within Cores 114-700B-53R and 114-700B-54R. Moreover, *Praeglobotruncana aumalensis* is probably present in Section 114-700B-54R, CC, but the occurrence of this species is not certain because it it has been observed only in thin section.

Paleoenvironment

Globotruncanids occur in several samples in the Cretaceous stratigraphic interval in Hole 700B, and their disappearance probably corresponds to stratigraphic intervals of strong dissolution. It is possible that the environment was cool, as represented primarily by assemblages of *Hedbergella, Globigerinelloides, Whiteinella*, and *Heterohelix*, with warm influences from an oceanic circulation system that brought in the warm species of globotruncanids.

According to the method of investigation applied by Boersma and Premoli Silva (1983), combined faunal and isotopic analyses may provide detailed descriptions of biogeographic provinces within the Paleocene. From the shipboard preliminary observations, we infer that this area can be assigned to a temperate province in the Paleocene.

This site confirms that the maximum species diversity of warm-water Acarininids and the presence of few strongly keeled Morozovellids occurred through the early Eocene, although deep- and intermediate-water Subbotininids were dominant. In the uppermost part of the lower Eocene, the *M. crater* acme horizon was found between 156.30 and 157.80 mbsf and can be correlated to the same horizon found in Hole 699A.

In the middle Eocene the planktonic foraminifers become less and less diversified and oligotypic, and only cold-water and dissolution-resistant forms, such as *G. index, Subbotina angiporoides, Subbotina linaperta*, and *Catapsydrax* are present in the sediments.

Preservation

Planktonic foraminifers are present continuously and are generally abundant from Sample 114-700B-3R-1, 44–46 cm, downhole. Their preservation is moderate in the Tertiary section and is moderate to poor in the Cretaceous interval. They were deposited above the carbonate compensation depth (CCD) from Coniacian to middle Eocene but show strong dissolution in three stratigraphic intervals, with deposition below the planktonic foraminifer lysocline: (1) 364–373 mbsf (Sections 114-700B-40R, CC, to 114-700B-41R, CC—middle Maestrichtian); (2) 228–285 mbsf (Sections 114-700B-24R, CC, to 114-700B-30R, CC—lower Eocene–upper Paleocene); and (3) 35–54 mbsf (Sections 114-700B-3R, CC, to 114-700B-5R, CC—upper middle Eocene). In intervals (1) and (3) the strong dissolution of foraminifers seems to be associated with the presence of shallow-water organisms. In stratigraphic interval (3) there is a decrease in abundance of planktonic foraminifers upward through the sequence, and there are only few stout and compact forms belonging to dissolution-resistant species in Section 114-700B-5R, CC. The biostratigraphic data from Holes 698A, 699A, and 700B are complementary because at each site the dissolution horizons and intervals of poor recovery occur at different stratigraphic levels.

Benthic Foraminifers

Generally good preservation of Eocene to Cretaceous benthic foraminifers at Hole 700B yielded primarily diverse and

abundant assemblages. The only exception is Section 114-700B-1R, CC, which contains a single specimen of *Cyclammina* sp. In the lowermost Eocene core-catcher sample (Section 114-700B-24R, CC), Paleocene and Cretaceous foraminifers show evidence of recrystallization; however, morphology is well preserved.

The Eocene fauna is dominated throughout by *Nuttallides truempyi, Cibicidoides praemundulus, Cibicidoides eocaenus, Cibicidoides grimsdalei, Cibicidoides havanensis, Alabamina dissonata*, and *Nonion havanensis*, with common occurrences of *Anomalinoides capitatus, Hanzawaia ammophila, Pullenia eocenica*, and *Pullenia quinqueloba*. The buliminids are common in and below Section 114-700B-6R, CC, dominated by *Bulimina semicostata* and including *Bulimina thanetensis, Bulimina trinitatensis, Bulimina tuxpomensis*, and *Buliminella grata*. Three common taxa not observed below the middle Eocene at Hole 700B are *Anomalinoides semicribratus, Cibicidoides bradyi*, and *Cibicidoides micrus*. Common taxa with LADs in the lower Eocene are *Aragonia aragonensis, Osangularia mexicana, Tappanina selmensis*, and *Turrilina alsatica*. Agglutinated taxa include *Eggerella* sp., *Gaudryina pyramidata, Karreriella chapapotensis, Plectina* sp., *Spiroplectammina spectabilis, Textularia* spp., and *Vulvulina spinosa*. Common undifferentiated taxa are *Anomalinoides, Dentalina, Gyroidinoides, Lenticulina, Oridorsalis, Pleurostomella*, pleurostomellids, polymorphinids, and *Stilostomella*.

A major change in the benthic foraminifer fauna occurred near the end of the Paleocene. A rich Paleocene benthic foraminifer assemblage disappears between Sections 114-700B-29R, CC, and 114-700B-26R, CC. Taxa that do not continue into the Eocene include *Angulogavelinella avnimelechi, Aragonia velascoensis, Bulimina velascoensis, Cibicidoides velascoensis, Osangularia velascoensis, Cibicidoides hyphalus, Cibicidoides* cf. *pseudoperlucidus, Bolivinoides delicatula, Buliminella beaumonti, Neoeponides hildebrandti, Neoeponides lunata, Neoflabellina semireticulata, Quadratobuliminella pyramidalis, Stensioina beccariiformis*, and *Tritaxia paleocenica*. The most abundant Paleocene taxa in Hole 700B are *N. truempyi* and *S. beccariiformis*. *C. hyphalus* is also present in every sample, but it is not as abundant. *A. capitatus* first appears in Section 114-700B-29R, CC, and becomes common in the Eocene. Common taxa in addition to those above include *B. trinitatensis* and *Pullenia bulloides*. Common to frequent, undifferentiated taxa are *Anomalinoides, Dentalina, Gyroidinoides, Lenticulina, Nonion, Oridorsalis, Pleurostomella*, pleurostomellids, polymorphinids, and *Stilostomella*. Section 114-700B-33R, CC, contains the notable occurrence of *Alabamina creta*, which has been found exclusively in the Caribbean and the Falkland Plateau in Zones P1–5 (Tjalsma and Lohmann, 1983).

The Cretaceous benthic foraminifer assemblage is similar to the Paleocene fauna with new taxa observed sporadically with increasing depth. These new taxa include *Globorotalites michelinianus, Spirobolivina australis, Allomorphina minuta, Bulimina limbata, Valvulineria* spp., *Bolivina incrassata, Gavelinella stephonsi*, and *Bolivinoides laevigata*. The most interesting trend is the decreasing abundance of *N. truempyi* with depth until its FO in Section 114-700B-47R, CC (which coincides with this taxon's Campanian FO at other sites). Simultaneously, the abundance of *S. beccariiformis* increases downhole. Section 114-700B-40R, CC, contains large nodosarids and agglutinants common in outer neritic–upper bathyal Cretaceous environments (Sliter and Baker, 1972), suggesting that there is a displaced component in this sample. There is a change in fauna in and below Sections 114-700B-49R, CC, and 114-700B-50R, CC. This is also the level below which diversity is low and preservation is poor, with foraminifers showing severe recrystallization with overgrowths. Genera observed in Sections 114-700B-52R, CC, and 114-700B-53R, CC, include *Gavelinella, Gyroidinoides, Lenticulina, Osangularia, Pullenia, Tritaxia*, and *Valvulineria*.

The general Campanian-Maestrichtian assemblages found in Hole 700B are similar to those at Deep Sea Drilling Project (DSDP) Site 327 on the Falkland Plateau, as identified in rapid shipboard analysis as *Allomorphina, Gavelinella, Gyroidinoides, Osangularia, Pleurostomella*, and *Pullenia*. This assemblage suggests a paleodepth of 1500–2500 m (Sliter, 1977). Comparison of the Paleocene fauna with Tjalsma and Lohmann (1983) and van Morkhoven et al. (1986) indicates a Paleocene paleobathymetric depth range at Hole 700B of 2000–2500 m, based upon equal abundances of *S. beccariiformis* and *N. truempyi* and supported by moderate abundances of *Aragonia* spp., *Lenticulina* spp., *Tritaxia* spp., and buliminids. The early Eocene depth at Hole 700B was 2500–3000 m, based upon moderate to high abundances of buliminids, *Clinapertina* spp., *A. dissonata*, and *Abyssamina poagi* and low abundances of *Lenticulina* spp. The disappearance of a buliminid assemblage in the Eocene above the interval between Sections 114-700B-6R, CC, and 114-700B-8R, CC, suggests that the site subsided below about 2750–3000 m by the middle Eocene (Tjalsma and Lohmann, 1983; Miller and Katz, in press).

Diatoms

Hole 700A was terminated after the second core. It recovered a diatomaceous ooze of Quaternary *Coscinodiscus lentiginosus* Zone McCollum (1975) in the first core (Section 114-700A-1R, CC). Section 114-700A-2R, CC, was placed into the upper Pliocene *Coscinodiscus vulnificus* Zone Ciesielski (1983) because of the presence of the marker species *C. vulnificus, C. elliptipora, Thalassiosira lentiginosa*, and *Actinocyclus ingens*.

Hole 700B recovered 483.5 m of highly calcareous sediment, which shows a regular, gradual compaction and increasing diagenetic alteration of the carbonate with depth. Silica diagenesis is strong in the Paleogene and Cretaceous sections, with clinoptilolite dominating the silt fraction in the Eocene and Santonian sediments and chert layers present in Cores 114-700-47R to 114-700B-50R.

Only the two first cores (Quaternary) and Cores 114-700B-26R to 114-700B-33R (Paleocene) contained diatoms. The abundance of diatoms in the sediments of this hole is given in Figures 20 and 23 ("Geochemistry" section).

No reworking of older species was observed at this site.

The Quaternary sediment is a diatom ooze underlying a layer of dropstones. Section 114-700B-1R, CC, belongs in the *C. lentiginosus* Zone McCollum (1975) with *T. lentiginosa* and *Thalassiosira gracilis* present. In Section 114-700B-2R, CC, *T. lentiginosa* is accompanied by *C. elliptipora* and *A. ingens*, placing this sample in the *C. elliptipora/A. ingens* Zone McCollum (1975).

The whole Eocene section is characterized by intensive silica dissolution, with only a few archaeomonads and sporadic radiolarian fragments remaining.

Poorly to moderately preserved diatom assemblages are found in the Paleocene sediments.

Sections 114-700B-26R, CC, and 114-700B-27R, CC, fall into the *Hemiaulus inaequilaterus* Zone Gombos (1977), because of the presence of the name-giving species. Further characteristic species present are *Hemiaulus incurvus, Triceratium gracillium* sensu Gombos (1977), *Triceratium planum*, and *Sceptroneis* sp. A of Gombos (1977). According to Gombos (1984) this zone ranges from within calcareous nannofossil Zone NP9 possibly down into NP8 or deeper, with his underlying *Sceptroneis* sp. A Zone and *Odontotropis klavsenii* Zone being older, but not older than NP5. The diatomaceous clayey chalk examined from Sections 114-700B-28R, CC, to 114-700B-31R, CC, lacks the marker species *H. inaequilaterus* and *O. klavsenii* but has *Sceptroneis* sp. A Gombos (1977) present. Therefore, this interval was assigned to the *Sceptroneis* sp. A Zone Gombos (1977).

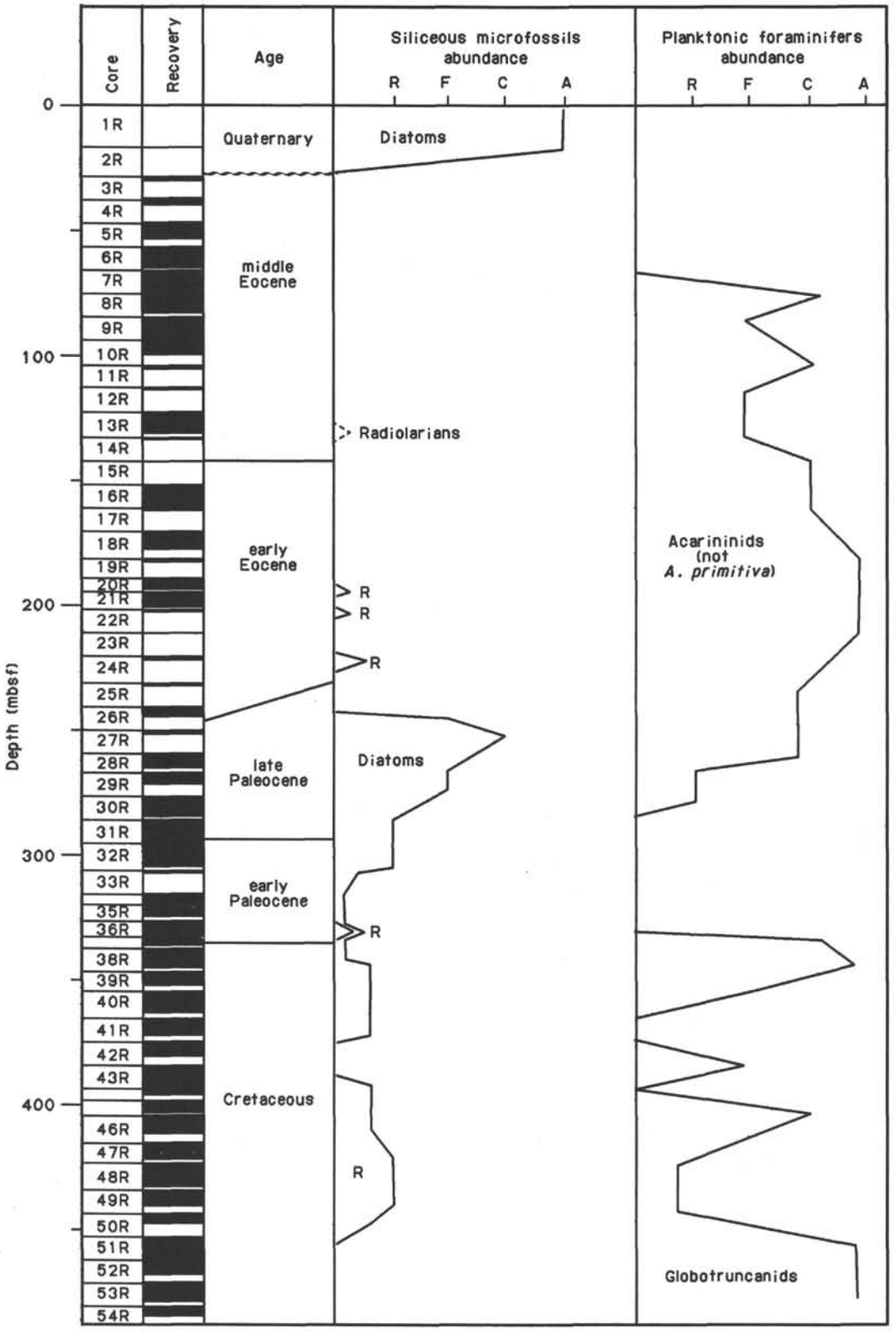

Figure 20. Comparison of occurrences of siliceous microfossils with those of planktonic foraminifer species at Hole 700B.

As the calcareous nannofossils indicated an age equivalent to somewhere within NP9 to NP5 for these samples, this age assignment agrees with that of Gombos (1977). A more accurate age determination can be obtained for Cores 114-700B-30R and 114-700B-31R from the paleomagnetic record. Correlation of the paleomagnetic record with the calcareous nannofossil stratigraphy suggests an age range of 61.5 to 62.5 m.y. for these two cores, which would be the latest early Paleocene.

The diatom valves recovered from Sections 114-700B-32R, CC, and 114-700B-33R, CC, were too poorly preserved to allow stratigraphic zonal assignment. The few species occurring can be related to the paleomagnetic record, which suggests an age of 62.5 to 64.2 m.y.

In all samples below Core 114-700B-33R diatoms were dissolved, although in some intervals in the Upper Cretaceous radiolarians remained relatively well preserved.

Radiolarians

Abundant and well-preserved radiolarians were recovered from two core-catcher samples from Hole 700A; Section 114-700A-1R, CC, is assigned to *Antarctissa denticulata* Zone; whereas Section 114-700A-2R, CC, apparently belongs to the lower Pliocene, but zonal assignment was not possible because index forms are absent.

In Hole 700B, radiolarians are absent between Sections 114-700B-3R, CC, and 114-700B-25R, CC, but from Sections 114-700B-26R, CC, through 114-700B-32R, CC, abundant and moderately well-preserved radiolarians of late to early Paleocene age are observed. The presence of several species belonging to genus *Buryella*, including *Buryella tetradica*, and the absence of *Bekoma bidartensis*, suggest that the section can be assigned to an "unzoned" interval for the tropical zonal scheme of Sanfilippo et al. (1985). The absence of *Phormocyrtis striata exquisita* from this interval, whereas it is present in Site 698 samples, suggests that the Paleocene radiolarian-bearing section of this hole is older than that of Site 698.

Radiolarians are absent from Sections 114-700B-33R, CC, through 114-700B-42R, CC, but well-preserved, abundant, and taxonomically diversified Mesozoic radiolarians were recovered from between Sections 114-700B-43R, CC, and 114-700B-50R, CC. From the presence of some characteristic forms, such as "*Amphipyndax tylotus*," *Theocapsomma comys* group, and *Archaeodictyomitra* species, this interval was tentatively assigned to the "*Amphipyndax tylotus*" Zone of Sanfilippo and Riedel (1985), which encompasses the Maestrichtian and upper Campanian. In retrospect, Section 114-698A-16R, CC, may be correlative with this interval because of the presence of the same species, "*Amphipyndax tylotus*." The occurrence of radiolarians of Late Cretaceous age and older from the mid- to high-latitude Southern Ocean has only been reported from Site 275 of DSDP Leg 29 (Pessagno, 1975), Site 323 of DSDP Leg 35 (Weaver, 1976), and a few sites from Leg 113 (Barker, Kennett, et al., 1988). Among them, only the assemblages from Site 275 were examined in detail (Pessagno, 1975), resulting in the assignment of a Maestrichtian to late Campanian age. Unfortunately, Pessagno's (1975) identification of taxa was based entirely on scanning electron microscope observations, and this was not practical for our shipboard analysis. However, with the good shipboard paleomagnetic record from this hole, detailed analysis of radiolarians from the thick radiolarian-bearing section should provide a good opportunity for establishing a new Upper Cretaceous zonation for this part of the Southern Ocean.

Radiolarians were completely absent in core-catcher samples from Sections 114-700B-51R, CC, through 114-700B-54R, CC.

Silicoflagellates

Sections 114-700A-1R, CC, and 114-700A-2R, CC, contain a hitherto unzoned Quaternary–lower Pliocene silicoflagellate assemblage from antarctic waters. The interval from Sections 114-700B-3R, CC, through 114-700B-25R, CC, was barren, but well-preserved, common to abundant, upper Paleocene silicoflagellate assemblages were recovered between Sections 114-700B-26R, CC, and 114-700B-32R, CC. Within this interval, no zonal assignment was possible, but the following four-fold division was recognized:

Sections 114-700B-26R, CC–114-700B-28R, CC: last occurrence (LO) of *Naviculopsis contricta*; Section 114-700B-29R, CC: LO of *Corbisema inermis inermis*; Sections 114-700B-30R, CC, and 114-700B-31R, CC: LO of *Corbisema disymmetrica disymmetrica*; Section 114-700B-32R, CC: LO of *Corbisema inermis crenulata*.

It should be noted that the latter two taxa were originally observed at Site 208 by Dumitrica (1973) and subsequently at Site 327 by Bukry (1976) and Busen and Wise (1977). It seems, therefore, that their paleogeographical distribution was limited to the middle to high latitudes of the Southern Ocean.

Silicoflagellates are absent below Sections 114-700B-33R, CC, through 114-700B-54R, CC.

Ebridians

Throughout samples from Site 700, only *Ammodochium rectangulare* and possibly a new species of genus *Ammodochium* were observed from the upper Paleocene (Sections 114-700B-26R, CC, through 114-700B-28R, CC). However, their presence in upper Paleocene samples may signal the earliest stratigraphic occurrence for species *A. rectangulare* as well as for genus *Ammodochium*.

GEOCHEMISTRY

Pore waters were squeezed from seven 5- or 10-cm whole-round samples taken at about 30-m intervals. The results of the pore-water chemical analyses are reported in Table 4 and Figure 21.

Headspace samples were analyzed for volatile hydrocarbon gases (Table 5). Organic carbon and calcium carbonate were determined throughout the section (Table 6).

Pore-water samples were recovered from only seven cores in the upper 250 m of Hole 700B because of insufficient pore-water volume recovery in the indurated chalks and limestones at greater depths. Pore-water chemistry in Hole 700B is similar to that at Hole 699A. The chemistry of interstitial waters in Hole 700B reflects reactions with basalt basement (Ca and Mg gradients) and reactions within the sediment column involving silica diagenesis (diatom dissolution and zeolite formation).

Calcium and Magnesium

Calcium concentrations increase downhole from a bottom-water concentration of 10 mmol/L to about 29 mmol/L by 241 mbsf. Magnesium, on the other hand, decreases from a bottom-water concentration of 55 mmol/L to about 40 mmol/L at this depth. These signatures reflect reactions either deeper in the sediment column (below the recovered interval) or, more likely, reactions with basalt. The magnesium/calcium ratio decreases downhole from the seawater value (5.2) to almost 1.0. A calcium vs. magnesium plot for both Holes 699A and 700B (Fig. 22) demonstrates that the relative changes in calcium and magnesium concentrations at both holes lie on virtually the same straight line, implying conservative behavior for both ions over the recovered section. The slope of this line is $\Delta Mg/\Delta Ca$ =

Table 4. Interstitial-water chemistry, Hole 700B.

Core, section, sample (cm)	Depth (mbsf)	Volume (mL)	pH	Alkalinity (mM)	Salinity (g/kg)	Magnesium (mM)	Calcium (mM)	Chloride (mM)	Sulfate (mM)	Fluoride (μM)	Silica (μM)	Mg/Ca
3R-1, 145–150	27.85	40	7.76	3.70	34.6	51.57	12.02	553.2	26.72	76.1	761	4.29
6R-5, 145–150	62.35	60	7.55	4.01	34.8	48.91	14.52	548.3	25.32	60.2	418	3.37
9R-5, 145–150	90.85	34	7.20	4.06	35.2	48.07	17.02	555.1	24.74	58.3	379	2.82
13R-4, 140–150	127.30	60	7.55	3.95	35.0	46.28	19.37	556.1	25.16	58.7	605	2.39
16R-5, 140–150	157.30	45	7.35	5.12	35.2	44.50	22.96	561.9	23.98	60.6	465	1.94
20R-2, 140–150	190.80	24	7.63	4.35	35.0	43.50	23.49	555.1	24.04	61.9	569	1.85
26R-2, 140–150	240.90	24	7.45	4.26	35.0	39.98	28.51	549.3	22.82	54.2	1131	1.40

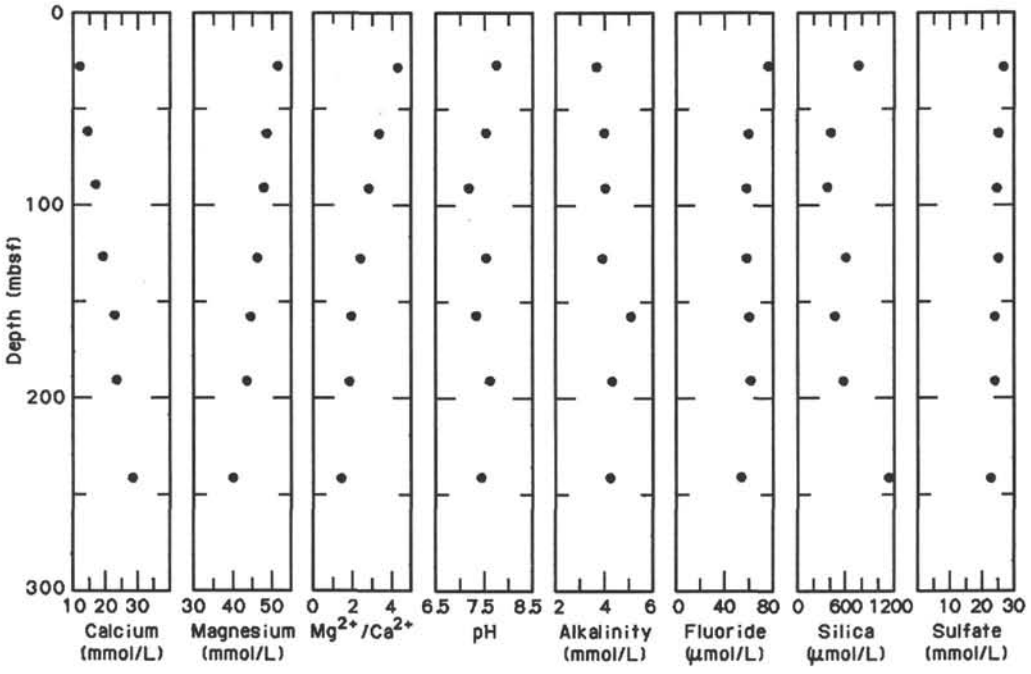

Figure 21. Pore-water calcium, magnesium, Mg/Ca ratio, pH, titration alkalinity, fluoride, silica, and sulfate profiles, Hole 700B.

−0.5, fairly typical of basalt basement reaction signatures (Gieskes, 1983; Baker, 1986). This would suggest that basement at Sites 699 and 700 (and also at 698) is basaltic—the Northeast Georgia Rise and East Georgia Basin are composed of oceanic (not sialic) crust.

That pore-water chemistry for Ca and Mg in Hole 700B should display virtually the same behavior as in Hole 699A is not surprising; the sites are close together in the East Georgia Basin (about 16 km apart) and presumably lie on the same basement structure that was downfaulted at Site 699 in post-early Oligocene time. The identical slopes of the pore-water Mg vs. Ca plots for both holes demonstrate that the reactions controlling the diffusive exchange of calcium and magnesium between basalt basement and the overlying seawater are identical at both sites. As at Hole 699A, there are apparently no chemical reactions within the sediment column affecting the concentration gradients of the two ions. These arguments, as reviewed in the "Site 699" chapter ("Geochemistry" section), do not absolutely rule out the possibility of unforseen sedimentary reactions in the basal unrecovered section that might mimic basalt Mg/Ca reaction signatures. Absence of dolomite in the recovered Upper Cretaceous limestones would seem to rule out at least one major possibility.

Assuming that the measured gradient of Mg in Hole 700B continues linearly to basement (see "Geochemistry" section, "Site 699" chapter), then the depth at which Mg approaches zero (maximum depth of inferred basement) is about 800 mbsf at this site. The difference between pore-water-inferred basement depths in Holes 699A (>1000 mbsf) and 700B (800 mbsf) is roughly equal to the missing time interval in Hole 700B compared to that recovered in Hole 699A (Pliocene + Miocene + Oligocene = 270 m). This is consistent with a diffusive/basement reaction model.

Acoustic basement was anticipated at 600 mbsf in Hole 700B, shallower than that predicted by the pore-water model. Either (1) the magnesium gradient becomes steeper near basement, which results in the basement depth determined by extrapolating pore-water gradients to be too deep and/or (2) vertical sonic velocities increase below the recovered section, which causes acoustic basement as observed in the seismic record to be too shallow.

Alkalinity

Alkalinity increases downhole from bottom-water concentrations (2.5 mmol/L) to a maximum of less than 5 mmol/L (more likely about 4.2 mmol/L, ignoring one high value). These pro-

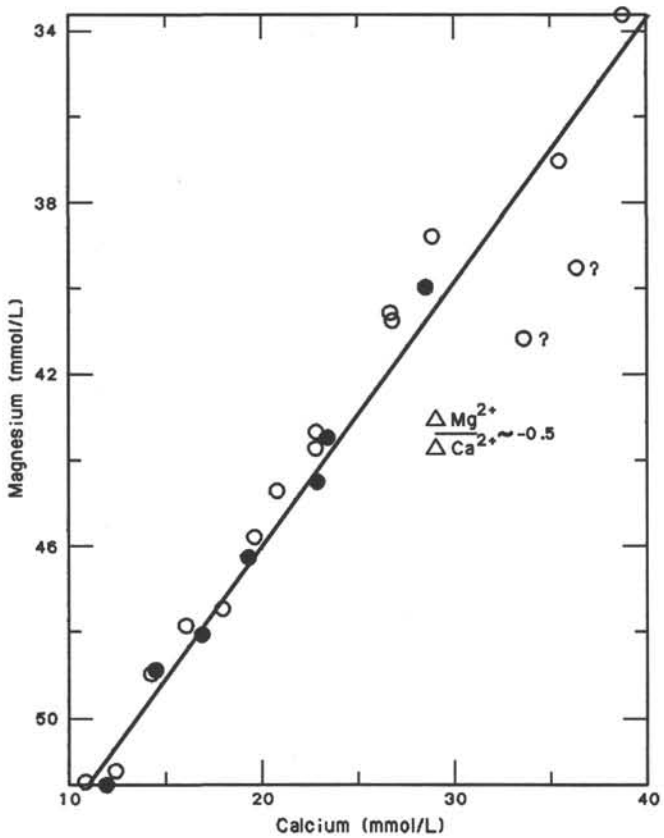

Figure 22. Pore-water calcium vs. magnesium in Holes 699A and 700B. Open data points are from Hole 699A, and solid data points are from Hole 700B. The line is a linear least-squares regression, with a slope of about $\Delta Mg/\Delta Ca = -0.5$, through all the data points.

files are consistent with the virtual absence of presently occurring organic matter diagenesis or carbonate dissolution/reprecipitation in the upper 250 m of the section at this site.

Fluoride, Silica, and Sulfate

Fluoride decreases downhole from bottom-water concentrations of 70 μmol/L to about 54 μmol/L at 240 mbsf. This gradual decrease is probably related to both uptake by clays and/or to the disseminated precipitation of extremely small quantities of phosphorite.

Dissolved silica displays a maximum value in the uppermost sample (28 mbsf) of 761 μmol/L and decreases downhole to a broad minimum between 50 and 200 mbsf, displaying concentrations of 400–600 μmol/L. Below 200 mbsf silica increases again to over 1100 μmol/L in the bottom sample (240 mbsf). Although these data are sparse, they display roughly the same relationships with diatom dissolution and zeolite formation as that observed for Hole 699A. Dissolved silica concentrations are high in the lithologic units containing biogenic opal (Units I and III) (Fig. 23). This confirms the supposition deduced from the Hole 699A profiles that diatoms are dissolving and providing a diffusive flux of dissolved silica downward from Unit I into Unit II and upward from Unit III into Unit II. This silica appears to be precipitating into the zeolites in Unit II.

Clinoptilolite occurs abundantly in the Eocene section of Hole 700B, and may thus have initially originated from prior dissolution of diatoms no longer present as fossils in the sediments or from dissolution of volcanic glass. As pointed out by Kastner (1981), several sources of dissolved silica are possible for the formation of authigenic clinoptilolite in the sediments. Comparison of Figure 23 with Figure 18 in the "Site 699" chapter demonstrates that dissolved silica profiles are related to lithostratigraphy of these sections, a common observation in pelagic sections (Gieskes, 1983).

Sulfate decreases slightly from bottom-water concentrations (28 mmol/L) to about 23 mmol/L at 240 mbsf. Thus, the sediment column is suboxic. Manganese staining of burrows is common throughout the recovered section, confirming that the sediment column has never been anoxic.

Volatile Hydrocarbon Gases

Methane concentrations are below 5 ppm in headspace samples, demonstrating the absence of methanogenesis. Ethane was generally below detection.

Sedimentary Organic Carbon and Calcium Carbonate

As in Hole 699A, organic matter contents of these sediments are essentially zero, with all of the organic carbon having been oxidized when the sediments were at or near the sediment/water interface.

The relationships between calcium carbonate, lithostratigraphy, logging stratigraphy, and physical properties are discussed in these respective sections of this site chapter.

PALEOMAGNETICS

A major objective of drilling at Site 700 was to investigate the nature of the basement and the overlying Cretaceous sediments, which had not been reached at nearby Site 699 because the drill bit was lost. It was necessary to use rotary drilling to achieve this objective, which resulted in a higher degree of drilling disturbance in the upper part of the cored section than that expected with the advanced hydraulic piston corer or extended core barrel systems. The most common form of drilling disturbance in these cores was biscuiting (breaking of the core into small disk-shaped pieces, usually only a few centimeters in length). Downhole contamination was also a problem (see "Operations" section, this chapter). Contamination restricted paleomagnetic sampling from cores above about 270 mbsf, but good paleomagnetic data were obtained below this level.

Two holes were drilled at Site 700. Only two cores, with little sediment recovery, were obtained from Hole 700A. Consequently, paleomagnetic investigations for this site have focused on Hole 700B, which penetrated 489 m of predominantly nannofossil chalk and limestone of Late Cretaceous to middle Eocene age. The lithostratigraphic units for this hole (see "Lithostratigraphy" section, this chapter) represent a sequence of progressively increasing diagenesis with depth. There is little overall change in sediment composition over the entire interval sampled, except for the appearance of some clay and volcanic ash within the lowest lithostratigraphic unit (Subunit VC).

Intensity of Magnetization

The variation of natural remanent magnetization (NRM) intensity with depth is shown in Figure 24, together with the lithostratigraphic unit boundaries. The intensity remains low (typically less than 0.3 mA/m) throughout the upper 400 m, with the exception of a few localized intervals of higher intensity within Subunit VA. Below 450 mbsf there is a significant increase in NRM intensity, which appears to relate to the presence of disseminated volcanic ash and discrete ash layers within Subunit VC.

Directions of Magnetization and Magnetic Stability

Downhole contamination, particularly in the upper 270 m of the cored section, caused a continuing problem in the acquisition of meaningful paleomagnetic data using the pass-through cryogenic magnetometer. Above this depth, concentrations of

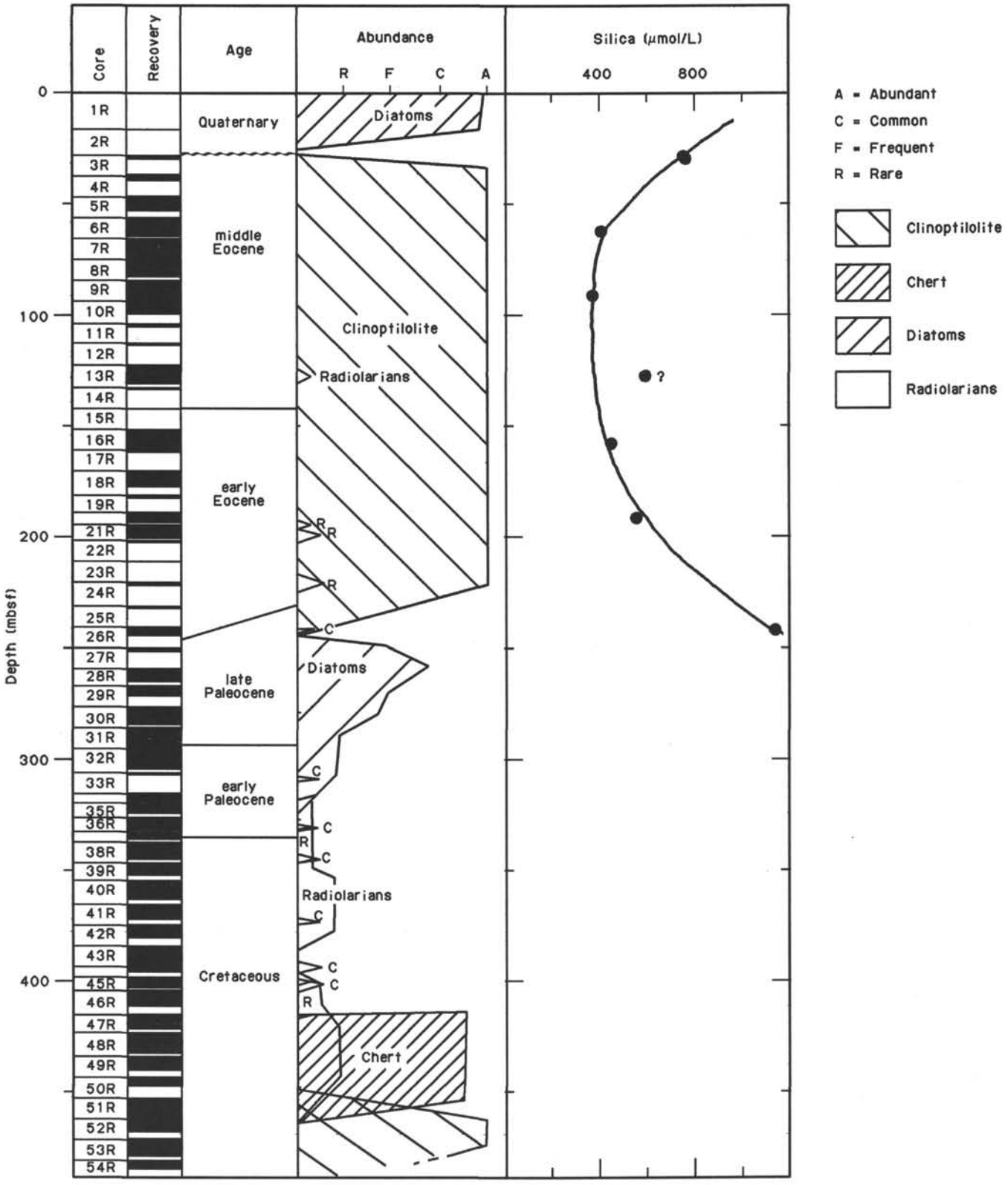

Figure 23. Relative abundances of diatoms, zeolites (clinoptilolite), radiolarians, and chert in comparison to the silica profile for Hole 700B.

Table 5. Volatile hydrocarbon gases (methane and ethane) from headspace samples, Hole 700B.

Core, section, sample (cm)	Depth (mbsf)	C_1 (ppm)	C_2 (ppm)
3R-1, 115–120	27.55	2.7	0.0
5R-3, 145–150	49.85	3.8	0.0
6R-5, 115–120	62.05	1.3	0.0
7R-5, 145–150	71.85	3.2	0.0
9R-5, 115–120	90.55	4.0	0.0
13R-3, 145–150	125.85	3.7	0.3
16R-4, 145–150	155.85	1.6	0.0
18R-4, 145–150	174.85	3.9	0.0
20R-2, 145–150	190.85	5.5	0.0
26R-1, 145–150	239.45	3.4	0.0
28R-2, 145–150	259.95	3.5	0.3
30R-3, 145–150	280.45	1.9	0.0
32R-3, 145–150	299.45	0.5	0.0
35R-2, 149–150	321.99	3.1	0.4
38R-3, 145–150	339.95	2.6	0.3
40R-3, 145–150	358.95	3.2	0.4
42R-2, 145–150	376.45	5.0	0.4
45R-1, 149–150	398.49	4.8	0.4
47R-1, 149–150	414.49	3.6	0.0
49R-2, 149–150	434.99	2.7	0.0
50R-2, 145–150	444.45	2.5	0.0
51R-3, 145–150	455.45	2.7	0.0

ferromanganese concretions and pebbles, mostly of basaltic composition, occurred in the upper 10 to 20 cm of each core. These pebbles typically range up to several centimeters or more in diameter and appear to have been derived from the seafloor in the immediate vicinity of the drill hole. They represent a combination of glacial dropstones and manganese nodules. In addition to the larger pebbles at the top of each core, finer black particles, typically ~1 mm in diameter and believed to have originated from the same source, occur along the outside of most of the core sections in this depth interval (between the core and the liner). The intensity of magnetization of these particles is considerably stronger than that of the sediments, so that they consistently obscure the paleomagnetic signal of interest. For this reason it was not possible to acquire meaningful paleomagnetic data from the upper 270 m (Cores 114-700B-1R to 114-700B-29R). However, discrete samples free from downhole contamination were obtained from various cores in this interval, and post-cruise paleomagnetic investigations of these samples may yield useful results. In this section the shipboard results from Cores 114-700B-30R to 114-700B-54R are described.

Archive halves of all cores in this interval were subjected to partial alternating field (AF) demagnetization. Routine demagnetization was conducted at 5 mT, but where the polarity was not established clearly by this treatment, a field of 9 mT was used. Biscuiting was fairly common in Cores 114-700B-30R to 114-700B-34R, but was relatively rare in deeper cores because of the increasing degree of lithification. Despite this fragmentation of the cores as a result of rotary drilling, the inclination of remanent magnetization shows a consistent pattern of variation with depth (Fig. 25). This figure is a plot of the results after three-axis demagnetization at 5 mT and measurement with the pass-through magnetometer. A succession of clearly defined polarity reversals is evident from these data.

A total of 50 discrete samples from this section were subjected to shipboard paleomagnetic analysis. Approximately 10% of these samples were incrementally demagnetized at 5- or 10-mT intervals up to a maximum field in the range 30 to 50 mT. Vector-end-point plots for three representative samples are illustrated in Figure 26. The results show the presence of a low coercivity component of magnetization, which is removed by treatment at about 5 to 10 mT to reveal a more stable component. This indicates that AF demagnetization of the archive halves of the cores at 5 to 9 mT is likely to be effective in defining the stable characteristic magnetization of these sediments. The remaining discrete samples were AF demagnetized at 5 and/or 10 mT, and the directions of magnetization after this treatment are plotted as solid circles in Figure 25. There is excellent agreement between the discrete sample and pass-through data shown on this diagram.

Polarity Stratigraphy

The succession of polarity reversals defined by the AF demagnetized pass-through paleomagnetic data, supplemented by the discrete sample data, is shown in Figure 25 and in the vertical column of Figure 27. Available nannofossil and foraminifers zonations for this hole (see "Biostratigraphy" section) indicate an early Paleocene age for Cores 114-700B-31R and 114-700B-32R and that a hiatus exists at the Cretaceous/Tertiary contact between Cores 114-700B-36R and 114-700B-37R. Therefore, the long reverse polarity magnetozone in Cores 114-700B-30R to 114-700B-32R can be correlated with the distinctive long reverse polarity Chron C26R, which extends from upper NP6 to middle NP4 (Berggren et al., 1985). The base of this magnetozone in Core 114-700B-32R can be correlated with the C26R/C27N Chron boundary and assigned a numerical age of 63 Ma, using the GPTS of Berggren et al. (1985).

It is now well established that the Cretaceous/Tertiary boundary lies within reverse polarity Chron C29R. The apparent absence of a reverse polarity magnetozone in Hole 700B at the Cretaceous/Tertiary hiatus between Cores 114-700B-36R and 114-700B-37R indicates that this hiatus and/or the recovery gap between the two cores must represent a minimum time span of 0.57 Ma (the duration of Chron C29R).

The reverse polarity magnetozone in Core 114-700B-35R can be correlated with Chron C28R, and its upper and lower boundaries, in Cores 114-700B-35R and 114-700B-36R, respectively, can be assigned calibration ages of 65.12 and 65.50 Ma on the Berggren et al. (1985) time scale. The age/depth calibration lines through these two points and the Chron C26R/C27N boundary calibration point indicate a mean sedimentation rate of about 10 m/m.y. at this site through the early Paleocene (Fig. 27). Biostratigraphy data for Cores 114-700B-38R to 114-700B-54R are currently sparse, but available nannofossil and foraminifer determinations indicate that the upper part of this sequence is late Maestrichtian and the lower part is Santonian to Coniacian in age. It is tempting to correlate the distinctive reverse polarity magnetozone in Cores 114-700B-46R to 114-700B-48R with the early Campanian Chron C33R (Kent and Gradstein, 1985). However, preliminary nannofossil data suggest that these cores are unlikely to be older than late Campanian, so a correlation with Chron C32R may be more valid. The overlying succession of reverse and normal polarity magnetozones in Cores 114-700B-43R to 114-700B-38R thus provides a good match with Chrons C31R to C30N. The resulting set of six age/depth calibration points indicates high and variable sedimentation rates throughout the Late Cretaceous at Site 700B, with a mean value of about 26 m/m.y. in the early Maestrichtian, decreasing to about 7 m/m.y. in the late Maestrichtian.

In summary, a clear succession of magnetic polarity zones has been identified in the Upper Cretaceous to lower Paleogene sediments recovered from Hole 700B. These provide a good correlation with late Campanian to early Paleocene Chrons C33N to C26R. This preliminary magnetostratigraphy will be refined through post-cruise paleomagnetic and biostratigraphic investi-

Table 6. Sedimentary calcium carbonate and organic carbon, Hole 700B.

Core, section sample (cm)	Depth (mbsf)	C_{org} (%)	$CaCO_3$ (%)
3R-1, 98–100	27.38	−0.04	73.31
4R-1, 98–100	36.88	0.04	46.54
5R-1, 81–83	46.21	0.07	52.88
5R-2, 100–102	47.90		40.87
5R-3, 100–102	49.40		77.98
5R-4, 100–102	50.90		74.64
6R-1, 98–100	55.88	0.06	55.13
6R-2, 100–102	57.40		69.64
6R-3, 100–102	58.90		79.65
6R-4, 100–102	60.40		77.65
6R-5, 100–102	61.90		74.23
6R-6, 100–102	63.40		78.81
7R-2, 100–102	66.90	−0.07	81.23
7R-3, 100–102	68.40		83.56
7R-4, 100–102	69.90		79.06
7R-5, 100–102	71.40		78.15
7R-6, 100–102	72.90		80.56
8R-1, 100–102	74.90	0.04	72.72
8R-2, 100–102	76.40		80.73
8R-3, 100–102	77.90		82.48
8R-4, 100–102	79.40		80.81
9R-1, 100–102	84.40		74.98
9R-2, 100–102	85.90		78.81
9R-3, 100–102	87.40		86.82
9R-4, 100–102	88.90		84.98
10R-1, 100–102	93.90	−0.01	84.57
10R-2, 100–102	95.40		82.15
10R-3, 80–82	96.70		83.15
13R-1, 99–101	122.39	0.35	83.32
13R-2, 109–111	123.99		87.90
13R-3, 99–101	125.39		83.98
13R-4, 103–104	126.93		75.31
13R-5, 99–101	128.39		81.48
16R-1, 102–104	150.92	−0.02	82.82
16R-2, 99–101	152.39		87.40
16R-3, 99–101	153.89		86.97
16R-4, 101–103	155.41		91.57
16R-5, 101–103	156.91		89.91
16R-6, 98–100	158.38		89.40
18R-1, 101–103	169.91	−0.24	86.07
18R-2, 101–103	171.41		81.06
18R-3, 80–82	172.70		83.40
18R-4, 100–102	174.40		86.49
20R-1, 98–100	188.88	−0.08	77.06
20R-2, 99–101	190.39		78.31
21R-1, 100–102	193.90	−0.15	81.82
21R-2, 100–102	195.40		84.32
21R-3, 100–102	196.90		85.15
26R-1, 100–102	239.00	−0.02	89.65
26R-2, 104–106	240.54		81.82
27R-1, 104–106	248.54	−0.01	91.07
28R-1, 121–123	258.21	−0.16	78.81
28R-2, 102–104	259.52		84.73
28R-3, 40–42	260.40		1.25
29R-1, 101–103	267.51	−0.03	72.97
29R-2, 101–103	269.01		83.57
30R-1, 92–94	276.92	−0.29	78.06
30R-2, 100–102	278.50		74.06
30R-3, 103–105	280.03		74.73
30R-4, 100–102	281.50		80.06
30R-5, 104–106	283.04		78.23
31R-1, 100–102	286.50	0.02	77.98
31R-2, 103–105	288.03		81.57
31R-3, 100–102	289.50		78.81
31R-4, 82–84	290.82		67.30
31R-5, 101–103	292.51		66.89
31R-6, 100–102	294.00		77.14
31R-7, 30–32	294.80		70.14
32R-1, 102–103	296.02	−0.68	77.56
32R-2, 102–103	297.52		76.14
32R-3, 101–103	299.01		77.31
32R-4, 100–102	300.50		65.80
32R-5, 104–106	302.04		87.32
33R-1, 99–101	305.49	−0.26	86.74

Table 6 (continued).

Core, section sample (cm)	Depth (mbsf)	C_{org} (%)	$CaCO_3$ (%)
34R-1, 65–67	314.65	0.08	66.14
34R-2, 92–94	316.42		79.31
34R-3, 95–97	317.95		87.49
35R-1, 100–102	320.00	−0.23	83.32
35R-2, 100–102	321.50		87.07
36R-1, 110–112	327.10	−0.22	88.65
36R-2, 84–86	328.34		86.15
37R-1, 124–125	331.94	−0.03	82.65
37R-2, 119–120	333.39		80.40
38R-1, 103–105	336.53		66.30
38R-2, 88–90	337.88		67.39
38R-3, 103–105	339.53		77.65
38R-4, 98–99	340.98		87.65
39R-1, 114–116	346.14	0.14	78.31
39R-2, 126–128	347.76		84.65
39R-3, 110–112	349.10		77.23
39R-4, 53–55	350.03		69.56
40R-1, 100–102	355.50	−0.20	74.73
40R-2, 100–102	357.00		9.67
40R-3, 100–102	358.50		73.06
40R-4, 100–102	360.00		69.22
41R-1, 100–102	365.00	0.00	73.81
41R-2, 100–102	366.50		78.56
41R-3, 100–102	368.00		87.74
41R-4, 100–102	369.50		85.82
42R-1, 100–102	374.50	−0.02	77.81
42R-2, 100–102	376.00		65.64
42R-3, 100–102	377.50		81.65
43R-1, 99–101	383.99	−0.07	81.57
43R-2, 99–101	385.49		84.98
43R-3, 99–101	386.99		71.22
43R-4, 103–105	388.53		91.74
43R-5, 99–101	389.99		84.73
43R-6, 102–104	391.52		85.65
43R-7, 38–40	392.38		83.48
44R-1, 101–103	393.51	−0.10	43.28
45R-1, 111–113	398.11	−0.04	55.29
45R-2, 112–113	399.62		62.63
46R-1, 103–105	404.53	−0.07	60.21
46R-2, 101–103	406.01		70.39
46R-3, 102–104	407.52		57.30
47R-1, 22–24	413.22		76.81
47R-1, 101–103	414.01		75.98
47R-2, 97–99	415.47		74.39
47R-3, 98–100	416.98		74.48
47R-4, 102–104	418.52		68.22
48R-1, 96–98	423.46	0.00	79.65
48R-2, 107–109	425.07		83.48
48R-3, 108–110	426.58		84.07
48R-4, 113–115	428.13		75.31
48R-5, 108–110	429.58		74.14
48R-6, 104–106	431.04		74.23
49R-1, 112–114	433.12	−0.02	74.98
49R-2, 122–124	434.72		55.54
49R-3, 102–104	436.02		71.39
49R-4, 128–130	437.78		59.21
50R-1, 96–98	442.46	−0.06	79.06
50R-2, 87–89	443.87		54.13
50R-3, 58–60	445.08		68.89
51R-1, 126–128	452.26	−0.05	83.40
51R-2, 136–138	453.86		70.46
51R-3, 142–144	455.42		72.14
51R-4, 125–127	456.75		79.98
51R-5, 129–131	458.29		72.98
52R-1, 112–114	461.62	0.00	77.06
52R-2, 92–94	462.92		80.48
52R-3, 116–118	464.66		59.71
53R-1, 129–131	471.29	−0.03	74.98
53R-2, 129–131	472.79		82.65
53R-3, 131–133	474.31		75.06
53R-4, 131–133	475.81		68.39
54R-1, 87–89	480.37	−0.02	78.65
54R-2, 90–92	481.90		81.06
54R-3, 37–39	482.87		73.89

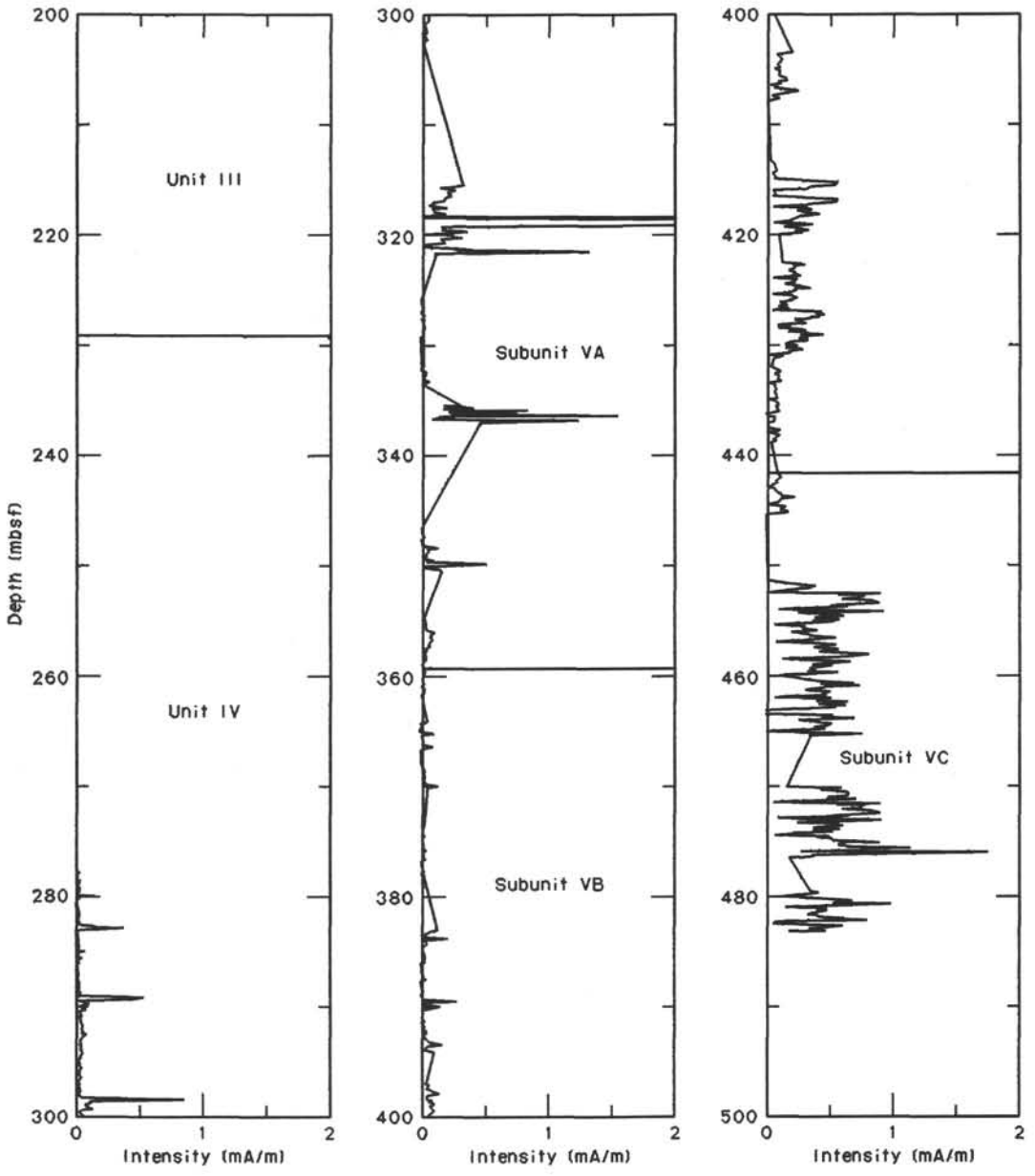

Figure 24. Magnetization (NRM) intensities measured using the three-axis pass-through cryogenic magnetometer for Hole 700B. Also shown are the boundaries of the lithostratigraphic units.

gations, which will provide an important basis for the calibration of high-latitude calcareous nannofossil, planktonic foraminifer, and radiolarian zonations in these cores and also a temporal framework for the interpretation of Cretaceous–Early Cenozoic oceanographic data from Hole 700B.

PHYSICAL PROPERTIES

The aim of physical-property measurements at Site 700 was to study the link between changes in the physical properties and changes in the diagenetic alteration of pelagic sediments with depth. For this purpose, we investigated the physical properties of a complete nannofossil ooze-chalk-limestone sequence recovered at Site 700 (see "Lithostratigraphy" section). This sequence has been correlated with the lithostratigraphic units (i.e., chalk) of Site 699 for a composite depth section of physical properties from the Upper Cretaceous to the Paleogene. The composite depth section provides a physical-property model for a detailed interpretation of seismic-reflector sequences within the context of the diagenetic sequences in this particular area of the Southern Ocean.

The methodology for physical-property measurements is described in the "Explanatory Notes" chapter. Four sets of measurements were obtained on selected samples of undisturbed rotary-cored sediment sections:

1. Index properties (wet-bulk density, dry-bulk density, porosity, water content, and grain density)
2. Compressional-wave (*P*-wave) velocity
3. Vane shear strength
4. Thermal conductivity.

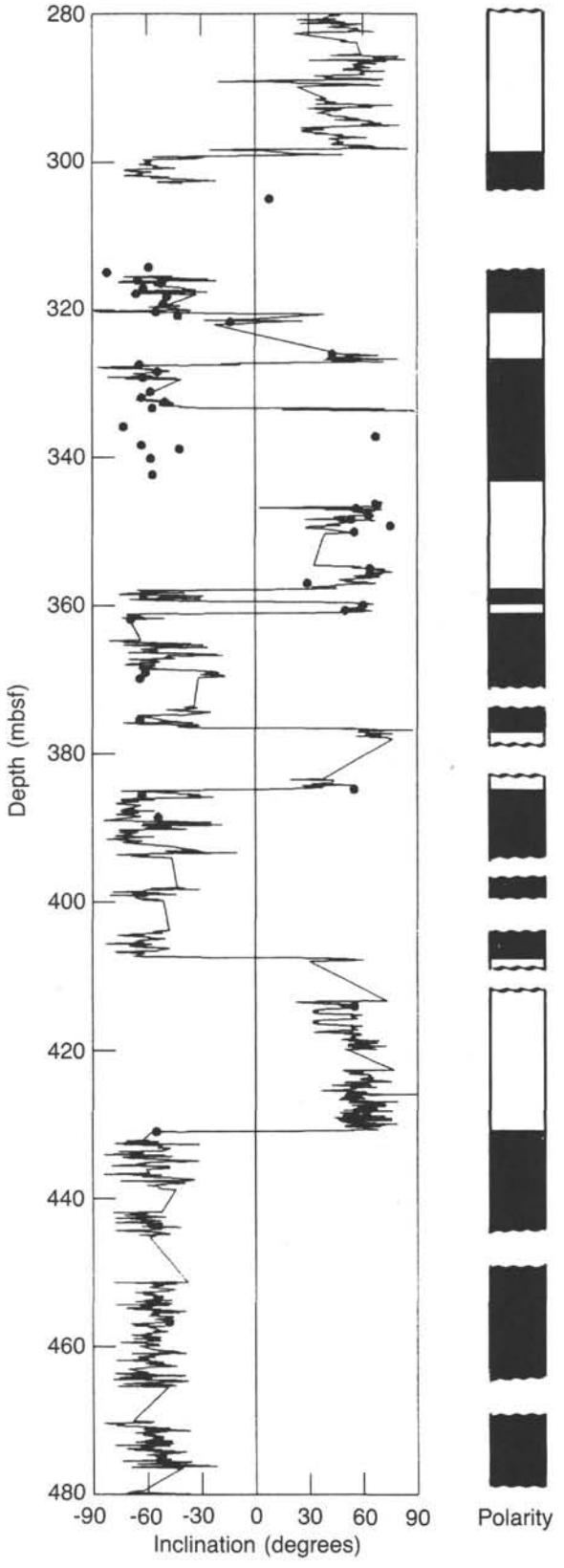

Figure 25. Results of pass-through measurements of the archive halves (solid lines) and discrete sample measurements using the Molspin magnetometer (solid circles) on cores from Hole 700A. Both sets of data are after AF demagnetization at 5 mT. Because of the randomization of core azimuths by rotary drilling, the magnetic declinations have no significance; therefore, the polarity is interpreted on the basis of the inclination record.

The carbonate content (see "Geochemistry" section) is shown for comparison with the physical-property data. All the data presented are unfiltered for any bad data points, except for one obviously anomalous result.

Physical-Property Summary and Lithostratigraphic Correlation

Index properties, carbonate content, *P*-wave velocity, thermal conductivity, and shear strength data are listed in Tables 7 through 11. Downcore profiles of wet-bulk density, porosity, water content, grain density, carbonate content, *P*-wave velocity, thermal conductivity, and shear strength are illustrated in Figure 28. The changes shown by these properties illustrate the interaction between consolidation and the diagenetic alteration of sediments with depth of burial. For example, the effect of consolidation can be seen in a steady increase of wet-bulk density and a steady decrease of porosity with depth (Fig. 28). To illustrate this progression, we summarize the physical properties for four lithostratigraphic units of nannofossil ooze, nannofossil chalk, indurated nannofossil chalk, and limestone (see "Lithostratigraphy" section) as follows:

Lithostratigraphic Unit II, a nannofossil ooze (26.4–45.4 mbsf), is characterized by high fluctuations in carbonate content (Fig. 28) that gradually disappear across the transition zone from nannofossil ooze to nannofossil chalk (Unit III). However, the ooze/chalk contact (45.4 mbsf) is sharp and marked by a distinct change in wet bulk-density, grain density, and porosity (Table 7) over the depth interval from 36.88 to 49.40 mbsf. In the nannofossil ooze, distinct changes in porosity, water content, and wet-bulk density clearly correspond to changes in the carbonate content (Fig. 28). A decrease in carbonate content (from 73.13% to 46.54%) between 27.38 and 36.88 mbsf, for example, corresponds to an increase in water content (from 44.66% to 50.76%), an increase in porosity (from 69.39% to 74.86%), and a decrease in wet-bulk density (from 1.59 to 1.51 g/cm^3) (Table 7).

Unit II (26.40–45.4 mbsf, middle Eocene)

		Mean	Minimum	Maximum
Wet-bulk density	(g/cm^3)	1.55	1.51	1.59
Dry-bulk density	(g/cm^3)	0.81	0.74	0.88
Grain density	(g/cm^3)	2.66	2.66	2.67
Porosity	(%)	72.15	69.39	74.86
Water content	(%)	47.71	44.66	50.76
Carbonate content	(%)	59.93	46.54	73.31
Thermal conductivity	(W/m/K)	1.132	1.016	1.248
Shear strength	(kPa)	31.40	30.70	32.10
P-wave velocity	(m/s)		?1439	

Lithostratigraphic Unit III (45.4–228.5 mbsf) is subdivided into two subunits, nannofossil chalk (Subunit IIIA, 45.4–168.9 mbsf) and micritic nannofossil chalk (Subunit IIIB, 168.9–228.5 mbsf). High concentrations of carbonate (greater than 70%) with low variability (approximately 10%) dominate throughout these subunits, and distinct grain density peaks of about 3.0 g/cm^3 mark the top of each subunit (Fig. 28). The overall pattern of Unit III, however, shows a consistent decrease in water content and porosity with depth and a corresponding increase in wet-bulk density and *P*-wave velocity (Fig. 28). The steep gradients reflect consolidated sediments of nannofossil chalk, which contrast with the nannofossil ooze of Unit I for which the changes in the physical properties appear to correspond to changes in the carbonate content only.

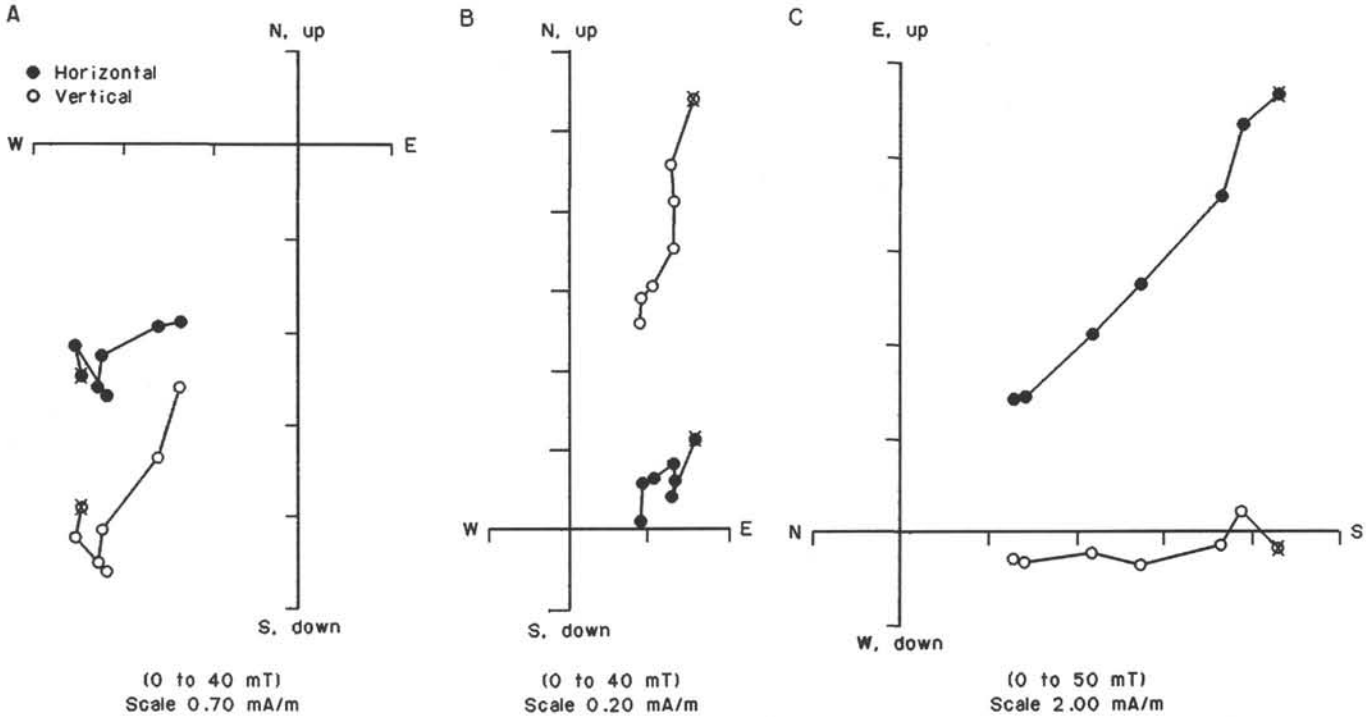

Figure 26. Examples of response to AF demagnetization of three discrete samples from Hole 700B, plotted on vector-end-point diagrams. **A.** Sample 114-700B-47R-4, 93 cm. **B.** Sample 114-700B-38R-1, 38 cm. **C.** Sample 114-700B-51R-4, 125 cm.

Subunit IIIA (45.4–168.9 mbsf, lower to middle Eocene)

		Mean	Minimum	Maximum
Wet-bulk density	(g/cm^3)	1.82	1.60	2.00
Dry-bulk density	(g/cm^3)	1.22	0.82	1.44
Grain density	(g/cm^3)	2.74	2.62	2.97
Porosity	(%)	58.48	49.29	75.37
Water content	(%)	33.13	26.10	48.40
Carbonate content	(%)	78.82	40.87	91.57
Thermal conductivity	(W/m/K)	1.4681	0.5260	2.2970
Shear strength	(kPa)	68.76	41.90	93.10
P-wave velocity	(m/s)	1764	1569	1979

Subunit IIIB (168.9–228.5 mbsf, lower Eocene)

		Mean	Minimum	Maximum
Wet-bulk density	(g/cm^3)	2.01	1.91	2.07
Dry-bulk density	(g/cm^3)	1.51	1.37	1.61
Grain density	(g/cm^3)	2.81	2.73	3.02
Porosity	(%)	48.69	43.00	53.15
Water content	(%)	24.82	21.53	28.14
Carbonate content	(%)	82.63	77.06	86.49
P-wave velocity	(m/s)	1876	1736	1948

Lithostratigraphic Unit IV (228.5–319 mbsf) consists of a micritic indurated nannofossil chalk in which the carbonate content and the physical properties (wet-bulk density, porosity, grain density, and *P*-wave velocity) start to become highly variable below 260 mbsf (Fig. 28). An extremely low carbonate content of about 1% at 260 mbsf indicates the onset of these dramatic changes, which may also represent a distinct sequence of reflectors in the seismic records. Whether the highly fluctuating values are fingerprints of the observed diagenetic alteration of the sediments or simply changes in the dilution of carbonate sediments by noncarbonate material (for example, clay) during sedimentation will be investigated in a more detailed onshore study.

Unit IV (228.5–319 mbsf, lower Eocene to lower Paleocene)

		Mean	Minimum	Maximum
Wet-bulk density	(g/cm^3)	2.18	1.72	2.36
Dry-bulk density	(g/cm^3)	1.78	0.94	2.06
Grain density	(g/cm^3)	2.75	2.63	3.02
Porosity	(%)	39.54	28.61	76.85
Water content	(%)	18.84	12.43	45.65
Carbonate content	(%)	74.93	1.25	91.07
P-wave velocity	(m/s)	2182	1855	2538

Lithostratigraphic Unit V (319–489 mbsf) is subdivided into three subunits. The tops of Subunits VA (homogenous nannofossil-bearing micritic to micrite-bearing limestone, 319–359 mbsf) and VC (micritic alternating with clay-bearing to clayey micritic limestone with some ash-bearing zeolitic clay horizons, 441.5–489 mbsf) are delineated by distinct peaks in grain density (Fig. 28), which have been observed also in the nannofossil chalk at the top of Subunits IIIA and IIIB. This downcore pattern appears to correspond to the diagenetic alteration of sediments across lithologic boundaries. Highly variable physical properties in the lower part of the nannofossil chalk-limestone sequence and the presence of chert between 400 and 450 mbsf in Subunit VB (see "Lithostratigraphy" section) may confirm this observation. Subunit VB (359–441.5 mbsf), in contrast with the other subunits, is characterized by distinctly higher wet-bulk density, *P*-wave velocity, and grain density values (Fig. 28). The abrupt increases in *P*-wave velocity (500 to 1000 m/s) and wet-bulk density (0.3–0.8 g/cm^3) may give rise to impedance contrasts large enough to create a distinct sequence of seismic reflectors.

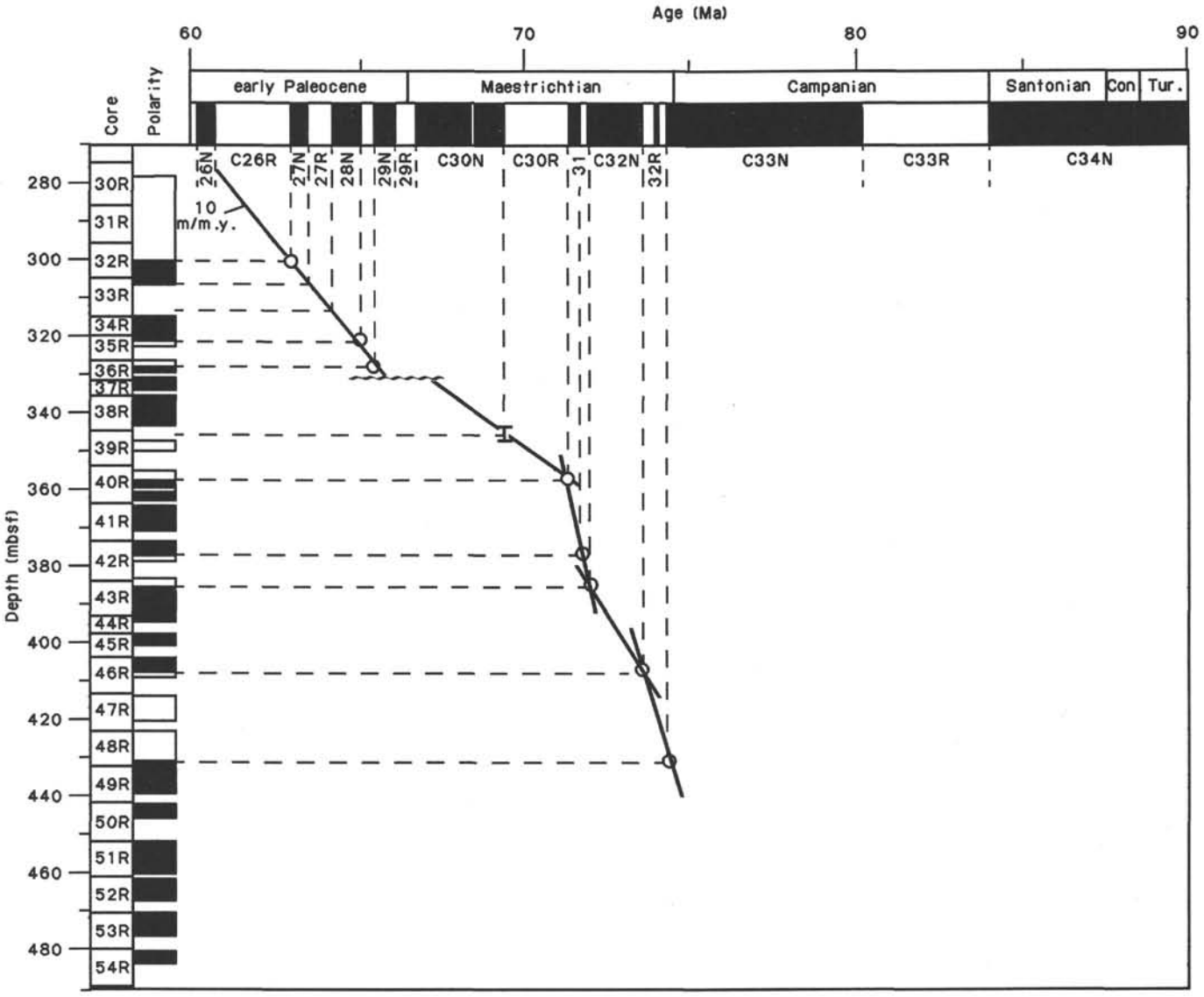

Figure 27. Tentative correlation of magnetic polarity zones in Hole 700B (vertical axis) with the GPTS of Berggren et al. (1985) (horizontal axis). Normal polarity black; reverse polarity white. This correlation is based on preliminary shipboard biostratigraphic data. Specific correlation points corresponding to chron boundaries are indicated by open circles, and lines through these points represent provisional age/depth calibration lines.

Subunit VA (319–359 mbsf, Maestrichtian to lower Paleocene)

		Mean	Minimum	Maximum
Wet-bulk density	(g/cm^3)	2.27	2.01	2.51
Dry-bulk density	(g/cm^3)	1.91	1.40	2.22
Grain density	(g/cm^3)	2.77	2.54	3.05
Porosity	(%)	35.44	27.79	59.34
Water content	(%)	16.23	11.36	30.29
Carbonate content	(%)	79.78	66.30	88.65
P-wave velocity	(m/s)	2408	1975	2737

Subunit VB (359–441.5 mbsf, Campanian to Maestrichtian)

		Mean	Minimum	Maximum
Wet-bulk density	(g/cm^3)	2.40	2.14	2.76
Dry-bulk density	(g/cm^3)	2.10	1.76	2.51
Grain density	(g/cm^3)	2.76	2.59	3.17
Porosity	(%)	29.42	18.88	46.48
Water content	(%)	12.67	7.53	20.48
Carbonate content	(%)	69.70	43.28	89.57
P-wave velocity	(m/s)	2774	2241	3586

Subunit VC (441.5–489 mbsf, Santonian-Turonian(?) to Campanian)

		Mean	Minimum	Maximum
Wet-bulk density	(g/cm^3)	2.37	2.21	2.54
Dry-bulk density	(g/cm^3)	2.07	1.83	2.25
Grain density	(g/cm^3)	2.78	2.67	2.91
Porosity	(%)	29.42	24.34	36.85
Water content	(%)	12.79	10.38	17.08
Carbonate content	(%)	74.05	54.13	83.40
P-wave velocity	(m/s)	2683	2363	2981

Comparison of Sites 700 and 699

Figures 29 and 30 illustrate the composite sections for porosity and velocity, which are based on correlation of the biostratigraphic records (see "Biostratigraphy" sections) of Sites 700 and 699 as follows:

	Site 700	Site 699
Core:	114-700B-3H	114-699A-38X
Age:	middle Eocene (NP16–15)	late Eocene (NP18–19)

Table 7. Index properties, Hole 700B.

Core, section, sample (cm)	Depth (mbsf)	Water content (%)	Porosity (%)	Densities: Wet bulk (g/cm^3)	Densities: Grain (g/cm^3)	Densities: Dry bulk (g/cm^3)
3R-1, 98–100	27.38	44.66	69.39	1.59	0.88	2.67
4R-1, 98–100	36.88	50.76	74.86	1.51	0.74	2.66
5R-1, 81–83	46.21	42.47	68.54	1.65	0.95	2.74
5R-2, 100–102	47.90	48.40	75.37	1.60	0.82	2.97
5R-3, 100–102	49.40	34.44	58.61	1.74	1.14	2.75
5R-4, 100–102	50.90	37.46	63.99	1.75	1.09	2.80
6R-1, 98–100	55.88	41.02	67.16	1.68	0.99	2.70
6R-2, 100–102	57.40	36.82	63.77	1.77	1.12	2.77
6R-3, 100–102	58.90	37.40	64.30	1.76	1.10	2.83
6R-4, 100–102	60.40	33.70	59.24	1.80	1.19	2.72
6R-5, 100–102	61.90	36.85	63.50	1.77	1.11	2.73
6R-6, 100–102	63.40	37.43	64.14	1.76	1.10	2.62
7R-2, 100–102	66.90	37.25	63.51	1.75	1.10	2.75
7R-3, 100–102	68.40	37.03	63.71	1.76	1.11	2.71
7R-4, 100–102	69.90	35.07	59.84	1.75	1.14	2.74
7R-5, 100–102	71.40	36.19	62.76	1.78	1.13	2.71
7R-6, 100–102	72.90	33.73	59.52	1.81	1.20	2.72
8R-1, 100–102	74.90	33.70	59.40	1.81	1.20	2.73
8R-2, 100–102	76.40	33.34	58.11	1.79	1.19	2.80
8R-3, 100–102	77.90	32.60	56.93	1.79	1.21	2.73
8R-4, 100–102	79.40	34.75	61.72	1.82	1.19	2.72
9R-1, 100–102	84.40	32.18	57.82	1.84	1.25	2.74
9R-2, 108–110	85.98	31.31	55.51	1.82	1.25	2.75
9R-3, 100–102	87.40	33.94	60.02	1.81	1.20	2.80
9R-4, 100–102	88.90	30.11	54.28	1.85	1.29	2.66
10R-1, 100–102	93.90	30.32	55.21	1.87	1.30	2.73
10R-2, 100–102	95.40	28.57	53.49	1.92	1.37	2.74
10R-3, 80–82	96.70	29.21	53.44	1.87	1.33	2.73
13R-1, 99–101	122.39	29.15	54.09	1.90	1.35	2.77
13R-2, 109–111	123.99	31.23	55.45	1.82	1.25	2.74
13R-3, 99–101	125.39	28.69	52.52	1.88	1.34	2.62
13R-4, 101–103	126.91	29.64	54.44	1.88	1.32	2.70
13R-5, 99–101	128.39	28.20	52.01	1.89	1.36	2.73
16R-1, 102–104	150.92	26.10	49.29	1.93	1.43	2.74
16R-2, 99–101	152.39	26.92	49.98	1.90	1.39	2.66
16R-3, 99–101	153.89	27.24	51.68	1.94	1.41	2.77
16R-4, 101–103	155.41	27.62	53.81	2.00	1.44	2.62
16R-5, 101–103	156.91	27.46	53.00	1.98	1.43	2.74
16R-6, 98–100	158.38	28.22	53.45	1.94	1.39	2.83
18R-1, 101–103	169.91	24.43	47.89	2.01	1.52	2.76
18R-2, 101–103	171.41	25.32	49.70	2.01	1.50	2.95
18R-3, 80–82	172.70	28.14	52.50	1.91	1.37	2.74
18R-4, 100–102	174.40	25.39	51.24	2.07	1.54	3.02
20R-1, 98–100	188.88	24.26	48.30	2.04	1.55	2.74
20R-2, 99–101	190.39	21.53	43.00	2.05	1.61	2.78
21R-1, 100–102	193.90	24.24	48.35	2.04	1.55	2.77
21R-2, 100–102	195.40	22.53	44.06	2.00	1.55	2.73
21R-3, 100–102	196.90	27.54	53.15	1.98	1.43	2.78
26R-1, 103–105	239.03	13.52	30.78	2.33	2.02	2.66
26R-2, 104–106	240.54	14.15	30.80	2.23	1.91	2.71
27R-1, 84–86	248.34	15.75	35.66	2.32	1.96	2.71
28R-1, 121–123	258.21	20.04	41.99	2.15	1.72	2.80
28R-2, 102–104	259.52	17.01	38.86	2.34	1.94	2.93
28R-3, 40–42	260.40	45.65	76.85	1.72	0.94	2.70
29R-1, 101–103	267.51	23.51	48.09	2.10	1.60	2.83
29R-2, 101–103	269.01	17.99	37.08	2.11	1.73	2.67
30R-1, 92–94	276.92	19.80	41.28	2.14	1.71	2.72
30R-2, 100–102	278.50	20.60	42.60	2.12	1.68	2.88
30R-3, 103–105	280.03	20.23	40.79	2.07	1.65	2.64
30R-4, 100–102	281.50	18.29	37.94	2.12	1.74	2.63
30R-5, 104–106	283.04	20.41	41.53	2.08	1.66	2.69
31R-1, 100–102	286.50	19.04	41.99	2.26	1.83	2.84
31R-2, 103–105	288.03	14.63	32.64	2.29	1.95	2.85
31R-3, 100–102	289.50	18.13	39.64	2.24	1.83	2.79
31R-4, 82–84	290.82	20.93	45.81	2.24	1.77	2.65
31R-5, 101–103	292.51	19.72	40.46	2.10	1.69	2.66
31R-6, 100–102	294.00	17.09	35.86	2.15	1.78	2.70
31R-7, 30–32	294.80	17.23	36.25	2.16	1.78	2.70
32R-1, 102–104	296.02	19.14	39.03	2.09	1.69	2.69
32R-2, 102–104	297.52	17.71	36.82	2.13	1.75	2.70
32R-3, 101–103	299.01	19.79	41.03	2.12	1.70	2.77
32R-4, 100–102	300.50	19.42	42.94	2.27	1.83	3.02
32R-5, 104–106	302.04	15.21	34.17	2.30	1.95	2.78
33R-1, 99–101	305.49	17.35	38.29	2.26	1.87	2.84
34R-1, 65–67	314.65	18.81	40.17	2.19	1.78	2.80

Table 7 (continued).

Core, section, sample (cm)	Depth (mbsf)	Water content (%)	Porosity (%)	Densities: Wet bulk (g/cm^3)	Densities: Grain (g/cm^3)	Densities: Dry bulk (g/cm^3)
34R-2, 90–92	316.40	12.75	28.65	2.30	2.01	2.78
34R-3, 95–97	317.95	12.43	28.61	2.36	2.06	2.74
35R-1, 100–102	320.00	11.36	27.79	2.51	2.22	3.05
35R-2, 100–102	321.50	12.33	28.34	2.36	2.07	2.77
36R-1, 110–112	327.10	11.79	28.49	2.48	2.18	2.69
36R-2, 84–86	328.34	12.66	29.60	2.40	2.09	2.87
37R-1, 124–125	331.94	16.76	36.09	2.21	1.84	2.72
37R-2, 118–119	333.38	16.35	35.80	2.24	1.88	2.78
38R-1, 103–105	336.53	20.89	42.46	2.08	1.65	2.82
38R-2, 88–90	337.88	13.39	29.93	2.29	1.98	2.66
38R-3, 103–105	339.53	17.67	37.60	2.18	1.79	2.91
38R-4, 98–99	340.98	14.92	33.91	2.33	1.98	2.64
39R-1, 114–116	346.14	15.62	34.96	2.29	1.94	2.74
39R-2, 126–128	347.76	12.47	30.57	2.51	2.20	2.90
39R-3, 110–112	349.10	17.86	36.98	2.12	1.74	2.65
39R-4, 53–55	350.03	17.34	37.77	2.23	1.84	2.73
40R-1, 100–102	355.50	14.76	31.13	2.16	1.84	2.54
40R-2, 100–102	357.00	30.29	59.34	2.01	1.40	2.88
40R-3, 100–102	358.50	19.53	41.77	2.19	1.76	2.76
40R-4, 100–102	360.00	15.57	35.33	2.32	1.96	2.81
41R-1, 100–102	365.00	13.92	30.88	2.27	1.96	2.62
41R-2, 100–102	366.50	17.58	36.73	2.14	1.76	2.62
41R-3, 100–102	368.00	12.42	29.20	2.41	2.11	2.80
41R-4, 100–102	369.50	13.43	30.03	2.29	1.98	2.69
42R-1, 100–102	374.50	13.89	31.87	2.35	2.02	2.73
42R-2, 100–102	376.00	13.89	31.87	2.35	2.02	2.73
42R-3, 100–102	377.50	13.70	31.81	2.38	2.05	2.68
43R-1, 99–101	383.99	12.98	28.95	2.29	1.99	2.73
43R-2, 99–101	385.49	10.61	25.08	2.42	2.17	2.74
43R-3, 99–101	386.99	15.52	33.98	2.24	1.90	2.80
43R-4, 103–105	388.53	13.94	30.41	2.23	1.92	2.67
43R-5, 99–101	389.99	11.46	27.98	2.50	2.22	2.70
43R-6, 102–104	391.52	13.52	30.06	2.28	1.97	2.59
43R-7, 38–40	392.38	12.62	29.12	2.36	2.07	2.77
44R-1, 101–103	393.51	15.21	33.44	2.25	1.91	2.70
45R-1, 111–113	398.11	13.57	30.44	2.30	1.99	2.60
45R-2, 112–114	399.62	14.10	32.13	2.34	2.01	2.75
46R-2, 101–103	406.01	20.48	46.48	2.33	1.85	2.68
46R-3, 102–104	407.52	15.33	34.12	2.28	1.93	2.74
47R-1, 22–24	413.22	9.77	23.28	2.44	2.20	2.79
47R-1, 101–103	414.01	10.68	25.97	2.49	2.22	2.84
47R-2, 97–99	415.47	13.05	30.97	2.43	2.11	2.80
47R-3, 98–100	416.98	11.80	27.76	2.41	2.13	2.91
47R-4, 102–104	418.52	11.28	27.30	2.48	2.20	2.90
48R-1, 96–98	423.46	9.63	23.18	2.47	2.23	2.76
48R-2, 107–109	425.07	7.91	20.78	2.69	2.48	2.82
48R-3, 108–110	426.58	7.53	18.88	2.57	2.38	2.89
48R-4, 113–115	428.13	9.07	24.42	2.76	2.51	2.86
48R-5, 108–110	429.58	9.84	24.19	2.52	2.27	2.81
48R-6, 104–106	431.04	11.28	26.91	2.44	2.17	2.75
49R-1, 112–114	433.12	9.71	23.64	2.49	2.25	2.72
49R-2, 122–124	434.72	12.27	29.23	2.44	2.14	2.75
49R-3, 102–104	436.02	13.58	31.11	2.35	2.03	2.83
49R-4, 128–130	437.78	12.30	32.25	2.69	2.36	3.17
50R-2, 87–89	443.87	15.64	34.40	2.25	1.90	2.72
50R-3, 58–60	445.08	13.56	30.77	2.32	2.01	2.74
51R-1, 126–128	452.26	12.54	28.91	2.36	2.06	2.78
51R-2, 136–138	453.86	16.22	35.81	2.25	1.89	2.84
51R-3, 142–144	455.42	11.22	26.32	2.40	2.13	2.77
51R-4, 125–127	456.75	10.46	25.62	2.51	2.25	2.88
51R-5, 129–131	458.29	14.44	32.36	2.30	1.97	2.80
52R-1, 112–114	461.62	11.85	26.78	2.32	2.04	2.68
52R-2, 92–94	462.92	10.80	25.95	2.46	2.20	2.91
52R-3, 116–118	464.66	17.08	36.85	2.21	1.83	2.67
53R-1, 129–131	471.29	15.78	34.12	2.21	1.86	2.74
53R-2, 131–133	472.81	11.45	27.75	2.48	2.20	2.88
53R-3, 131–133	474.31	10.38	24.34	2.40	2.15	2.80
53R-4, 131–133	475.81	11.12	27.00	2.49	2.21	2.74
54R-1, 87–89	480.37	12.54	29.78	2.43	2.12	2.83
54R-2, 90–92	481.90	11.66	26.74	2.35	2.07	2.74
54R-3, 37–39	482.87	10.75	26.63	2.54	2.27	2.75

Table 8. Carbonate content, Hole 700B.

Core, section sample (cm)	Depth (mbsf)	$CaCO_3$ (%)
3R-1, 98–100	27.38	73.31
4R-1, 98–100	36.88	46.54
5R-1, 81–83	46.21	52.88
5R-2, 100–102	47.90	40.87
5R-3, 100–102	49.40	77.98
5R-4, 100–102	50.90	74.64
6R-1, 98–100	55.88	55.13
6R-2, 100–102	57.40	69.64
6R-3, 100–102	58.90	79.65
6R-4, 100–102	60.40	77.65
6R-5, 100–102	61.90	74.23
6R-6, 100–102	63.40	78.81
7R-2, 100–102	66.90	81.23
7R-3, 100–102	68.40	83.56
7R-4, 100–102	69.90	79.06
7R-5, 100–102	71.40	78.15
7R-6, 100–102	72.90	80.56
8R-1, 100–102	74.90	72.72
8R-2, 100–102	76.40	80.73
8R-3, 100–102	77.90	82.48
8R-4, 100–102	79.40	80.81
9R-1, 100–102	84.40	74.98
9R-2, 100–102	85.90	78.81
9R-3, 100–102	87.40	86.82
9R-4, 100–102	88.90	84.98
10R-1, 100–102	93.90	84.57
10R-2, 100–102	95.40	82.15
10R-3, 80–82	96.70	83.15
13R-1, 99–101	122.39	83.32
13R-2, 109–111	123.99	87.90
13R-3, 99–101	125.39	83.98
13R-4, 103–104	126.93	75.31
13R-5, 99–101	128.39	81.48
16R-1, 102–104	150.92	82.82
16R-2, 99–101	152.39	87.40
16R-3, 99–101	153.89	86.97
16R-4, 101–103	155.41	91.57
16R-5, 101–103	156.91	89.91
16R-6, 98–100	158.38	89.40
18R-1, 101–103	169.91	86.07
18R-2, 101–103	171.41	81.06
18R-3, 80–82	172.70	83.40
18R-4, 100–102	174.40	86.49
20R-1, 98–100	188.88	77.06
20R-2, 99–101	190.39	78.31
21R-1, 100–102	193.90	81.82
21R-2, 100–102	195.40	84.32
21R-3, 100–102	196.90	85.15
26R-1, 100–102	239.00	89.65
26R-1, 104–106	240.54	81.82
27R-1, 104–106	248.54	91.07
28R-1, 121–123	258.21	78.81
28R-2, 102–104	259.52	84.73
28R-3, 40–42	260.40	1.25
29R-1, 101–103	267.51	72.97
29R-2, 101–103	269.01	83.57
30R-1, 92–94	276.92	78.06
30R-2, 100–102	278.50	54.29
30R-3, 103–105	280.03	74.73
30R-4, 100–102	281.50	80.06
30R-5, 104–106	283.04	78.23
31R-1, 100–102	286.50	77.98
31R-2, 103–105	288.03	81.57
31R-3, 100–102	289.50	78.81
31R-4, 82–84	290.82	67.30
31R-5, 101–103	292.51	66.89
31R-6, 100–102	294.00	77.14
31R-7, 30–32	294.80	70.14
32R-1, 102–103	296.02	77.56
32R-2, 102–103	297.52	76.14
32R-3, 101–103	299.01	77.31
32R-4, 100–102	300.50	65.80
32R-5, 104–106	302.04	87.32
33R-1, 99–101	305.49	86.74
34R-1, 65–67	314.65	66.14
34R-2, 92–94	316.42	79.31

Table 8 (continued).

Core, section sample (cm)	Depth (mbsf)	$CaCO_3$ (%)
34R-3, 95–97	317.95	87.49
35R-1, 100–102	320.00	83.32
35R-2, 100–102	321.50	87.07
36R-1, 110–112	327.10	88.65
36R-2, 84–86	328.34	86.15
37R-1, 124–125	331.94	82.65
37R-2, 119–120	333.39	80.40
38R-1, 103–105	336.53	66.30
38R-2, 88–90	337.88	67.39
38R-3, 103–105	339.53	77.65
38R-4, 98–99	340.98	87.65
39R-1, 114–116	346.14	78.31
39R-2, 126–128	347.76	84.65
39R-3, 110–112	349.10	77.23
39R-4, 53–55	350.03	69.56
44R-1, 101–103	393.51	43.28
45R-1, 111–113	398.11	55.29
45R-2, 112–113	399.62	62.63
46R-1, 103–105	404.53	60.21
46R-2, 101–103	406.01	70.39
46R-3, 102–104	407.52	57.30
47R-1, 22–24	413.22	89.57
47R-1, 101–103	414.01	75.98
47R-2, 97–99	415.47	74.39
47R-3, 98–100	416.98	74.48
47R-4, 102–104	418.52	68.22
48R-1, 96–98	423.46	79.65
48R-2, 107–109	425.07	83.48
48R-3, 108–110	426.58	84.07
48R-4, 113–115	428.13	75.31
48R-5, 108–110	429.58	74.14
48R-6, 104–106	431.04	74.23
49R-1, 112–114	433.12	74.98
49R-2, 122–124	434.72	55.54
49R-3, 102–104	436.02	71.39
49R-4, 128–130	437.78	59.21
50R-1, 96–98	442.46	79.06
50R-2, 87–89	443.87	54.13
50R-3, 58–60	445.08	68.89
51R-1, 126–128	452.26	83.40
51R-2, 136–138	453.86	70.46
51R-3, 142–144	455.42	72.14
51R-4, 125–127	456.75	79.98
51R-5, 129–131	458.29	72.98
52R-1, 112–114	461.62	77.06
52R-2, 92–94	462.92	80.48
52R-3, 116–118	464.66	59.71
53R-1, 129–131	471.29	74.98
53R-2, 129–131	472.79	82.65
53R-3, 131–133	474.31	75.06
53R-4, 131–133	475.81	68.39
54R-1, 87–89	480.37	78.65
54R-2, 90–92	481.90	81.06
54R-3, 37–39	482.87	73.89

	Site 700	Site 699
Core:	114-700B-25X to 114-700B-26X	114-699A-53X to 114-699A-54X
Age:	late Paleocene–early Eocene (NP10–9)	late Paleocene–early Eocene (NP12–9)

The biostratigraphy is from core-catcher samples and is based on an average sample interval of about 9.5 m.

A composite of the velocity (Fig. 29) and porosity records (Fig. 30) and of the diagenetic sequences from Sites 700 and 699 illustrates a remarkable fit, in both physical properties and diagenetic boundaries. This suggests a strong similarity in the diagenetic and burial history of Eocene and older sediments at Sites 700 and 699.

Table 9. *P*-wave velocity, Hole 700B.

Core, section sample (cm)	Depth (mbsf)	Direction[a]	Velocity (m/s)
3R-1, 99-101	27.39	C	1439.0
6R-1, 80-82	55.70	C	1568.7
10R-1, 98-100	93.88	C	1738.1
10R-3, 48-50	96.38	C	1645.9
13R-1, 98-100	122.38	C	1667.4
13R-2, 108-110	123.98	C	1829.0
13R-3, 98-100	125.38	C	1831.9
16R-1, 102-104	150.92	C	1690.3
16R-2, 98-100	152.38	C	1734.1
16R-4, 98-100	155.38	C	1954.7
16R-6, 98-100	158.38	C	1978.6
18R-1, 100-102	169.90	C	1895.6
18R-3, 80-82	172.70	C	1842.4
18R-4, 100-102	174.40	C	1867.7
20R-1, 100-102	188.90	C	1735.5
20R-2, 100-102	190.40	C	1906.3
21R-1, 100-102	193.90	C	1892.0
21R-2, 100-102	195.40	C	1948.0
21R-3, 100-102	196.90	C	1920.6
26R-2, 100-102	240.50	C	2072.4
27R-1, 100-102	248.50	C	2444.8
28R-1, 100-102	258.00	C	2354.7
28R-2, 100-102	259.50	C	2315.4
29R-1, 100-102	267.50	C	1867.6
30R-2, 100-102	278.50	C	2052.9
30R-4, 100-102	281.50	C	2265.6
31R-1, 100-102	286.50	C	2107.4
31R-3, 100-102	289.50	C	2153.8
31R-5, 100-102	292.50	C	2214.6
31R-7, 30-32	294.80	C	2276.7
32R-2, 100-102	297.50	C	2085.7
32R-4, 100-102	300.50	C	2292.0
33R-1, 100-102	305.50	C	1855.0
34R-1, 65-67	314.65	C	2014.0
34R-2, 90-92	316.40	C	2537.5
35R-1, 100-102	320.00	C	2591.3
35R-2, 100-102	321.50	C	2425.5
36R-1, 100-102	327.00	C	2737.0
36R-2, 100-102	328.50	C	2650.5
37R-1, 124-125	331.94	A	2531.6
37R-1, 125-127	331.95	C	2632.1
37R-2, 100-102	333.20	C	2171.4
37R-2, 118-119	333.38	A	2506.0
37R-2, 119-121	333.39	C	2475.9
38R-1, 100-102	336.50	C	1975.0
38R-2, 108-110	338.08	C	2518.2
38R-5, 95-97	342.45	C	2235.9
39R-2, 100-102	347.50	C	2581.7
39R-3, 100-102	349.00	C	2366.1
40R-1, 100-102	355.50	C	2427.5
40R-2, 100-102	357.00	C	2042.7
40R-3, 100-102	358.50	C	2066.7
40R-4, 100-102	360.00	C	2489.2
41R-1, 110-112	365.10	C	2886.0
41R-3, 100-102	368.00	C	2997.0
41R-4, 100-102	369.50	C	2857.0
42R-2, 100-102	376.00	C	2629.1
42R-3, 100-102	377.50	C	2697.1
43R-1, 100-102	384.00	C	2265.3
43R-3, 100-102	387.00	C	2498.2
43R-5, 100-102	390.00	C	2849.0
43R-6, 122-124	391.72	A	2574.2
43R-7, 38-40	392.38	C	2240.8
45R-1, 111-112	398.11	A	2488.3
45R-2, 112-114	399.62	A	2273.7
46R-1, 103-105	404.53	A	3264.0
46R-2, 101-103	406.01	A	2858.8
46R-3, 101-103	407.51	A	2369.3
47R-1, 22-24	413.22	A	2673.0

Table 9 (continued).

Core, section sample (cm)	Depth (mbsf)	Direction[a]	Velocity (m/s)
47R-1, 101-103	414.01	A	2861.5
47R-2, 97-99	415.47	A	2695.0
47R-3, 98-100	416.98	A	2586.3
47R-4, 102-104	418.52	A	2564.1
48R-1, 96-98	423.46	C	2981.8
48R-2, 107-109	425.07	C	3153.6
48R-3, 108-110	426.58	C	3169.6
48R-4, 113-115	428.13	C	2866.7
48R-5, 108-110	429.58	C	2914.6
48R-6, 104-106	431.04	C	2651.6
49R-1, 112-114	433.12	C	3036.6
49R-2, 122-124	434.72	C	2995.7
49R-3, 102-104	436.02	C	2652.2
49R-4, 128-130	437.78	C	2777.8
50R-1, 96-98	442.46	C	2966.7
50R-2, 87-89	443.87	C	2676.5
50R-3, 58-60	445.08	C	2527.3
51R-1, 126-128	452.26	C	2790.7
51R-2, 136-138	453.86	C	2519.0
51R-3, 142-144	455.42	C	2363.6
51R-4, 125-127	456.75	C	2738.5
51R-5, 129-131	458.29	C	2487.5
52R-1, 112-114	461.62	C	2888.0
52R-2, 92-94	462.92	C	2856.5
52R-3, 116-118	464.66	C	2707.5
53R-1, 129-131	471.29	C	2572.1
53R-2, 129-131	472.79	C	2639.4
53R-3, 131-133	474.31	C	2712.8
53R-4, 131-133	475.81	C	2595.1
54R-1, 87-89	480.37	A	2557.9
54R-2, 90-92	481.90	A	2790.9
54R-3, 37-39	482.87	A	2669.1

[a] A = perpendicular to split-core surface; B = parallel to split-core surface; C = axial.

A comparison of the diagenetic boundaries and the porosity record (Fig. 29) allows us to estimate the time and the amount of removed sediments. Based on the composite section, a minimum of 350 and a maximum of 550 m of sediments have been removed from the top of Site 700. The stiffness of the sediments, resulting from diagenesis, in lithostratigraphic Units II and IV of Site 699 lends credence to a tectonically influenced sediment removal from Site 700. However, intense bottom-water current activity can not be ruled out at this time as another possible means for the removal of the upper sedimentary sequences at Site 700. The maximum value of sediment removal includes the missing sediment thicknesses resulting from hiatuses at Site 699, as discussed previously in the "Physical Properties" section of the "Site 699" chapter.

The porosity curves for the overlapping sequences of Sites 700 and 699 are parallel but offset (Fig. 29), which is indicative of sediment rebound after overburden removal. Extrapolation of the Site 699 porosity curve to greater depths leads us to suggest that the deeper sections of Site 700 have also undergone some rebound. The increase in the porosity is estimated to be between 5% and 15% in the overlapping section and probably less in the deeper sections, although specific values can not be assigned without further shore-based work.

The parallel porosity curves and the similarity of the diagenesis in the overlapping sections of Sites 700 and 699 lead us to conclude that the uplift and removal of 350 to 550 m of sediments from Site 700 occurred after the diagenesis of the sediments. After this erosional event, the sediments rebounded as the overburden pressure was relieved, giving rise to a porosity increase of approximately 5% to 15%.

SEISMIC STRATIGRAPHY

Single-channel seismic-reflection data show that the upper part of the section drilled at Site 699 is not present over a basement culmination about 10 nmi east of the site.

Leaving Site 699, *JOIDES Resolution* looped westward and started recording seismic-reflection data about 2 nmi west of Site 699 on a course of 90° underway to Site 700 (Fig. 31). A single 80-in.^{3} water gun was used as the sound source.

Table 10. Thermal conductivity, Hole 700B.

Core, section, sample (cm)	Depth (mbsf)	Thermal conductivity (W/m/K)
3R-1, 100	27.40	1.2480
4R-1, 100	36.90	1.0160
5R-1, 100	46.40	0.8430
5R-3, 100	49.40	1.4250
5R-4, 100	50.90	1.3520
6R-1, 100	55.90	1.2490
6R-2, 100	57.40	1.3100
6R-3, 100	58.90	1.3370
6R-4, 100	60.40	1.4940
7R-3, 100	68.40	1.3010
7R-4, 100	69.90	1.3860
7R-5, 100	71.40	1.3630
7R-6, 100	72.90	1.5670
8R-2, 100	76.40	1.5980
8R-3, 100	77.90	1.5310
8R-4, 100	79.40	1.5290
8R-5, 90	80.80	1.3770
9R-1, 100	84.40	1.5490
9R-2, 100	85.90	1.3010
9R-3, 100	87.40	1.6170
9R-4, 100	88.90	1.6700
10R-1, 100	93.90	1.6390
10R-2, 100	95.40	1.5170
13R-1, 100	122.40	1.6180
13R-2, 100	123.90	1.7440
13R-3, 100	125.40	1.9030
13R-4, 100	126.90	1.5180
13R-5, 100	128.40	1.2870
16R-1, 100	150.90	2.2970
16R-2, 100	152.40	1.6590
16R-3, 100	153.90	1.7020
16R-4, 100	155.40	0.5260
16R-5, 100	156.90	1.1520
16R-6, 100	158.40	1.6170

Table 11. Shear strength, Hole 700B.

Core, section, sample (cm)	Depth (mbsf)	Shear strength (kPa)
3R-1, 100–102	27.40	32.1
4R-1, 100–102	36.90	30.7
5R-1, 83–85	46.23	65.2
5R-2, 100–102	47.90	48.9
5R-3, 100–102	49.40	76.8
5R-4, 100–102	50.90	51.2
6R-1, 100–102	55.90	48.9
6R-2, 100–102	57.40	83.8
6R-5, 100–102	61.90	88.4
6R-6, 90–92	63.30	93.1
7R-2, 102–104	66.92	41.9
7R-5, 100–102	71.40	88.4
8R-3, 108–110	77.98	69.8

The seismic stratigraphy at Site 700 shows a reflection pattern very similar to that of the deep section at Site 699 (Fig. 32). At Site 700, we therefore expected to find Eocene chalk below an upper 40-m-thick unit of Miocene to Recent diatomaceous ooze. This stratigraphic level would correspond to a depth of 250–300 mbsf at Site 699.

At Site 700, *P*-wave velocities show a generally linear increase with depth, as do the wet-bulk densities (Fig. 32). This pattern compares well with that of the corresponding stratigraphic interval at Site 699. However, the *P*-wave velocities also show considerable downhole fluctuations where changes in character broadly correspond to lithostratigraphic boundaries. Low-velocity zones are present in the indurated micritic nannofossil chalk and within the homogeneous micritic nannofossil-bearing limestone. Another weak low-velocity zone is present in the lower micritic limestone, where alternating intervals of clay-bearing limestone and/or ash layers occur. The porosity of the calcareous sediments shows a linear decrease with depth, with small variations superimposed.

The transition from nannofossil ooze to chalk at 45 mbsf is associated with an increase in wet-bulk density that generates an impedance contrast and a strong reflection (Fig. 32). The seismic response of the nannofossil chalk is characterized by numerous short, randomly distributed reflection segments and associated diffraction patterns, which result in a generally reflection-free appearance. Although variation of *P*-wave velocity with depth shows stepwise changes of 0.3 km/s within this unit, similar lateral velocity variations must exist to generate an essentially random velocity distribution superimposed on the general linear increase with depth (Fig. 32). The velocity of carbonate rocks is largely a function of their diagenetic states, but lithification is not a simple function of burial depth or time (Garrison, 1981; Schlanger and Douglas, 1974). The acoustic image of the transition between the micritic nannofossil chalk and the micritic indurated nannofossil chalk seen in Figure 32 is a semi-chaotic reflection pattern that probably is the most dramatic expression of the degree of anisotropy of the diagenetic process. This reflection pattern could also be interpreted as a contorted upper surface of the underlying reflective unit for which there is no evidence in the recovered samples. Therefore, we infer that the degree of lithification can, at least in some cases, show variations along a depositional surface, as well as a complex variation with depth (Garrison, 1981).

The most continuous acoustic stratification is observed in the homogeneous micritic nannofossil-bearing limestone and the underlying subunit in which alternating clay-bearing limestone intervals appear. It is not readily apparent, however, from the observed downhole variation in physical properties why this would be so, and the most likely explanation is greater lateral uniformity in the impedance contrast. The lowermost subunit, a micritic limestone alternating with more clay-rich intervals and/or ash layers, has a weak velocity inversion that gives rise to a low-amplitude reflection at its upper surface. Basement is anticipated about 100 m below the 489 mbsf base of Hole 700B.

The stratigraphic control and the seismic correlation between Sites 699 and 700 clearly demonstrate that corresponding stratigraphic levels were vertically displaced along two major faults, with a total throw of about 500 m (Fig. 33). This faulting involved basement. Two major scarps farther east form north-trending topographic lineaments and are probably also generated by faulting. The older depositional units immediately east of Site 699 are conformable with the substratum up through the lower Oligocene, where onlap on a westward-tilting surface becomes apparent (Fig. 33). The major hiatus at Site 700 is between the uppermost Quaternary diatom ooze and the middle Eocene nannofossil ooze. The fault movement was therefore post-early Oligocene and pre-Quaternary. Based on a comparison of the variation of physical properties with depth for the two sites, an estimated sediment thickness of about 350 m has been removed from the top of the middle Eocene chalk at Site 700 (see "Physical Properties" section). This is reasonable in view of the observed 200 m thickness of the upper middle Eocene to lower upper Oligocene sediments at Site 699. Thus, post-early Oligocene block faulting led to erosion of the elevated block until a change in the local current regime during the Quaternary allowed renewed deposition of ooze.

LOGGING

The three major objectives of the downhole geophysical and geochemical measurements carried out at Site 700 were (1) to

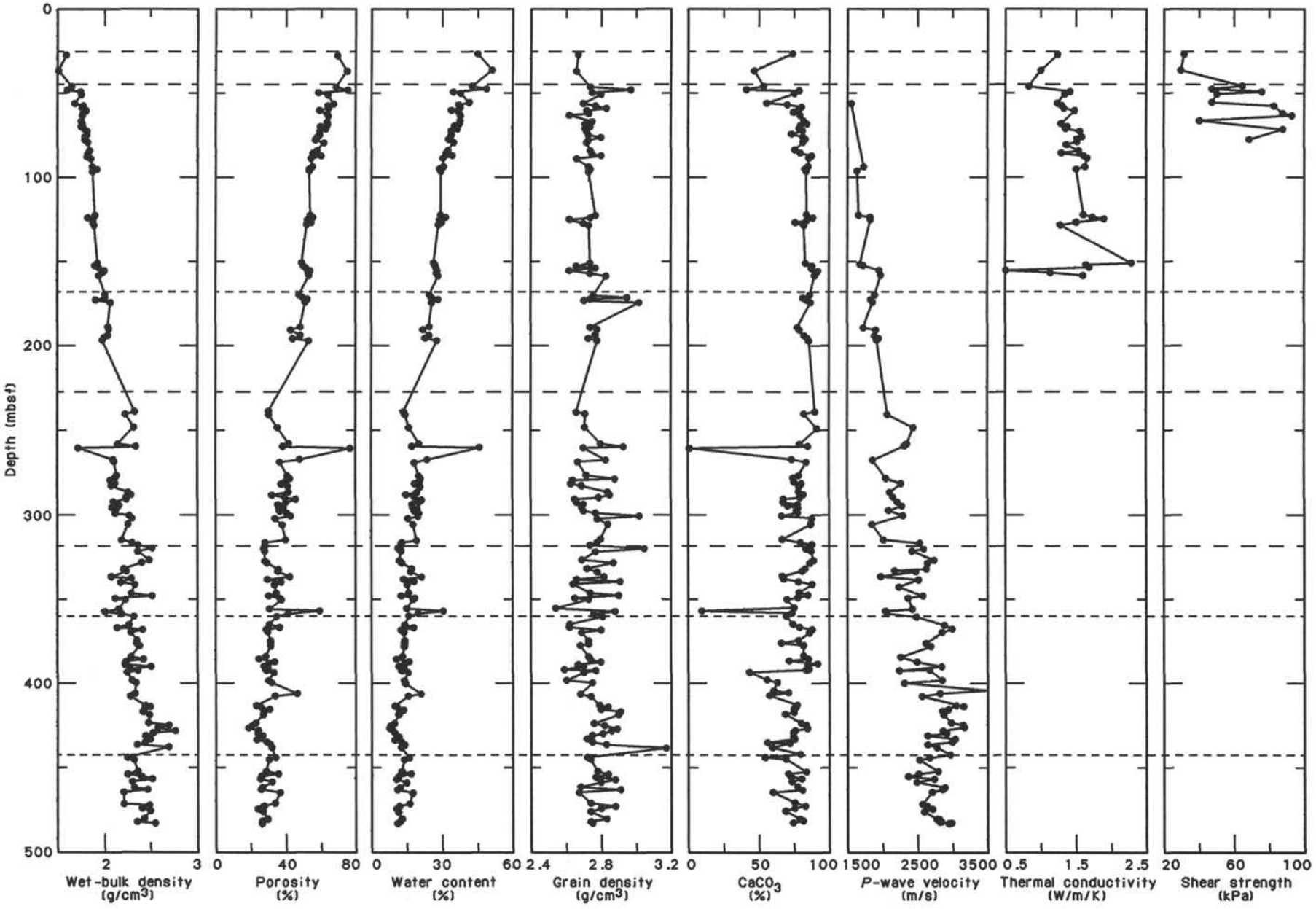

Figure 28. Wet-bulk density, porosity, water content, grain density, carbonate content (from "Geochemistry" section), *P*-wave velocity, thermal conductivity, and shear strength profiles, Hole 700B.

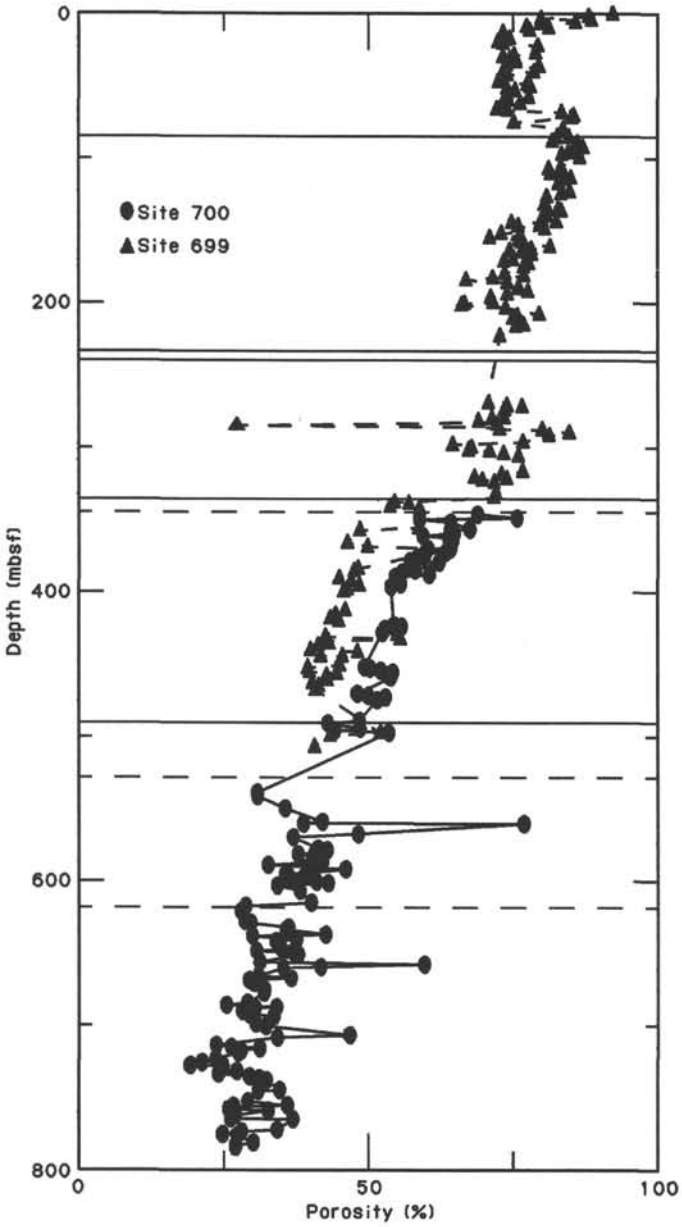

Figure 29. Composite section of porosity from Site 700 (dots) and Site 699 (triangles). Diagenetic boundaries of Site 700 are shown by dashed lines and diagenetic boundaries of Site 699 by solid lines.

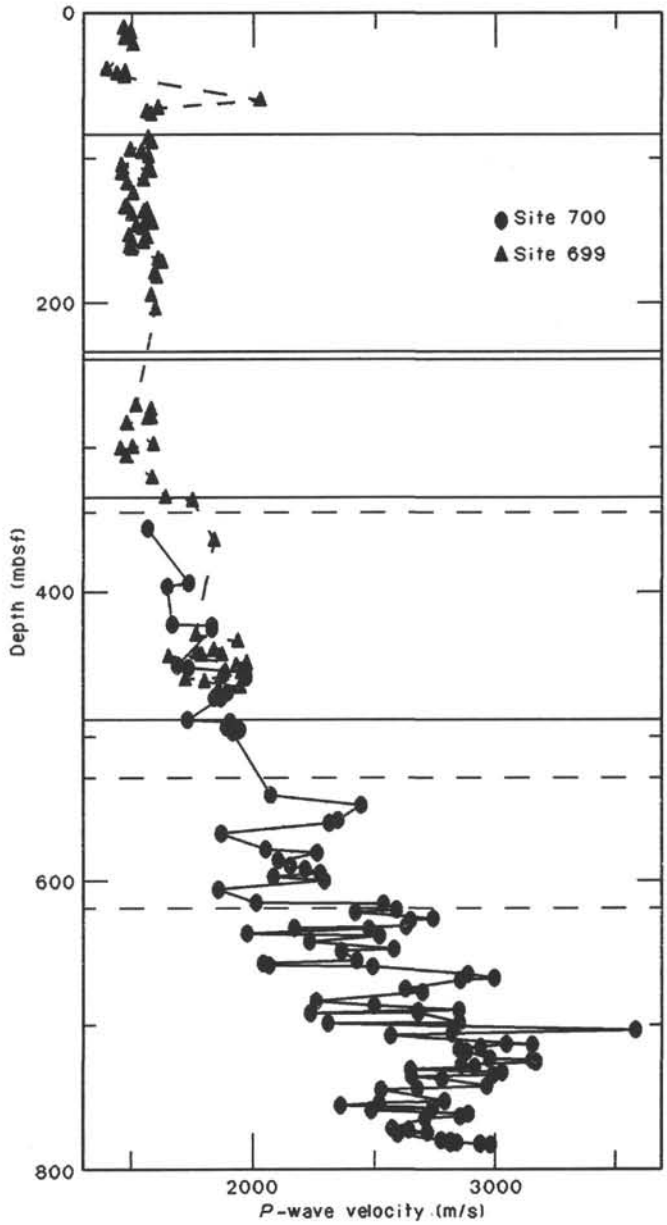

Figure 30. Composite section of *P*-wave velocity from Site 700 (dots) and Site 699 (triangles). Diagenetic boundaries of Site 700 are shown by dashed lines and diagenetic boundaries of Site 699 by solid lines.

provide a continuous record of geophysical and geochemical data to tie in with the lithostratigraphy and interpret sections with poor core recovery, (2) to provide insight into the depositional environment and diagenetic processes in carbonate sediments, and (3) to acquire *in-situ* sonic velocity data for interpreting the nature of seismic reflectors observed from surface seismic records. Two logging runs, the seismic-stratigraphic combination (sonic velocity, resistivity, gamma ray, and caliper; SDT/DIPH/GR/CALI) and the geochemical combination (induced gamma-ray spectroscopy, aluminum clay tool, and natural gamma-ray spectrometry; GST/ACT/NGT) (see "Explanatory Notes" chapter) were made, and the parameters measured are presented in Table 12. The 8-channel digital sonic tool (SDT) malfunctioned during the logging operations; however, excellent data were acquired with the rest of the logging parameters in the seismic-stratigraphic combination string. All the logging tools were provided by Schlumberger Well Logging Services.

Logging Operations

The conditions of Hole 700B were good, and there was no need to use the side entry sub as was originally planned because of previous bridging problems encountered after drilling through soft sediments. The drill pipe terminated at 138.5 mbsf, and all logging measurements were acquired in open hole below this depth. The hole was drilled to 489 mbsf, but because of some bridging problems and a lost core barrel at the bottom, the measurements were acquired only up to a depth of 450 mbsf.

The first logging run was the SDT/DIPH/GR/CALI seismic-stratigraphic combination, which was run uphole from 450 to 132.5 mbsf at a logging speed of 4 m/min (800 ft/hr). All the

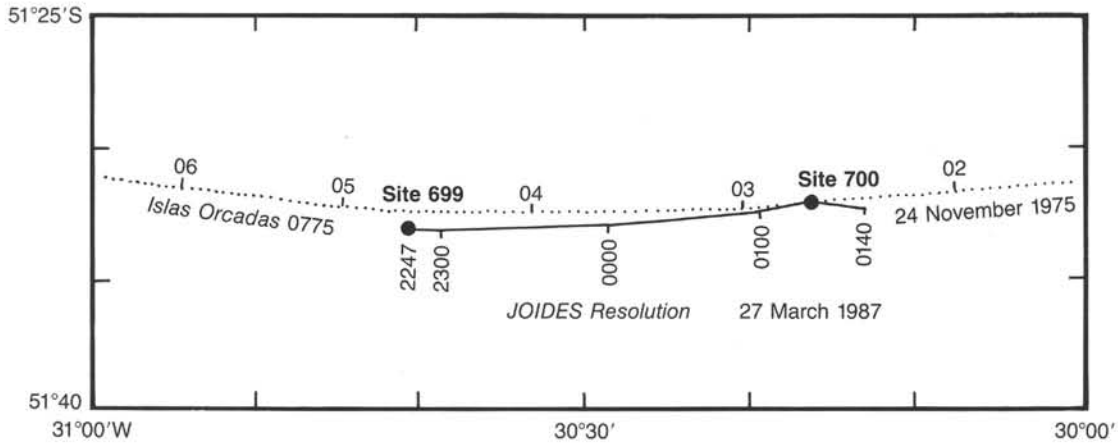

Figure 31. Track of *JOIDES Resolution* in transit between Sites 699 and 700, recording single-channel seismic-reflection data. Survey speed about 6 kt.

measurements were acquired at a sample depth interval of approximately 15 cm. The second logging run, the GST/ACT/NGT geochemical combination, started from 415 mbsf because of a bridging problem at that depth and reached 126 mbsf. The logging speed for this run was 1.5 m/min (300 ft/hr), and measurements were sampled at 15-cm intervals.

Discussion of Results

A description of the logging tools used at Site 700 is given in the "Explanatory Notes" chapter. Table 12 gives a summary of the measured and computed parameters from the two logging runs carried out at this site. All of the logs in the preceding discussion are referenced to zero depth at the seafloor. This depth was determined from the drilling information and should coincide with the core depths. The water depth at Hole 700B is 3601 m.

Figure 34 shows the natural gamma-ray spectral (NGT) logs (total count, K, U, and Th). The application of NGT logs in formation evaluation is mainly in lithologic identification (total count, K, U, and Th), clay typing and content determination (K, U, and Th), and evaluation of depositional environment (U). Thorium and potassium concentrations indicate the presence of micaceous clay minerals and can be used in clay typing (Hassan, 1976) and estimating the clay content.

Within the logged depth interval, three major lithologies are recognized from the variations in the natural radioactivity. Log Unit 1 from 138 to 235 mbsf has fairly low levels of radioactivity with an increase at its base (219–235 mbsf). The radioactivity is mainly derived from potassium and thorium (see K and Th logs, Fig. 34) and is therefore an indication of the presence of clay minerals. Log Unit 2, from 235 to 330 mbsf, has even lower radioactivity than log Unit 1. There is an anomalous increase in radioactivity between 259.0 and 261 mbsf. The radioactivity increase in this zone is mainly derived from uranium (see U log, Fig. 34). Uranium is very mobile in nature, and in carbonate rocks it tends to concentrate in reducing environments associated with phosphatization and/or organic materials. We infer from this data that the depositional environment changed at this point in time. Log Unit 3, from 330 to 428 mbsf (the lowest depth logged with the NGT), has relatively higher levels of radioactivity compared to both log Units 1 and 2. Radioactivity results mainly from an increase in the concentration of thorium and potassium. This unit may be divided into subunits according to the varying levels of radioactivity or clay content. Between 330 and 361 mbsf there are two zones of increased clay content at around 340 and 359 mbsf. The other subunits are observed from 361 to 390 and 390 to 428 mbsf (Fig. 35). There are a number of high-frequency variations in radioactivity that reflect the variation in the clay content within these sections. An attempt will be made later to relate these variations with the alternating clay and micritic limestone bands.

The three phasor induction resistivity logs (spherically focused log, medium induction log, and deep induction log; SFL, IMPH, and IDPH, respectively) are shown in Figure 35 together with the total count gamma-ray (SGR) log and porosity log derived from resistivity. Resistivity variations within carbonate sediments are primarily a function of temperature, porosity, and salinity of the pore fluids. Because resistivities mainly reflect changes in porosity within the formation, apparent porosities were determined from the resistivity logs using Archie's (1942) law (Serra, 1984). The porosities are only approximate because variations in borehole diameter and clay content affect the apparent resistivities. The resistivities were not corrected for the borehole effects. There is little departure between the three resistivities (SFL, IMPH, and IDPH logs), indicating that borehole effects are minimal. The porosity log shown is derived from the deep induction resistivity log for two cementation factors (m = 1.7 and m = 2.0). Four major lithologic units are apparent from the resistivity data: log lithologic Unit 1, 142–237 mbsf; log lithologic Unit 2, 237–330 mbsf; log lithologic Unit 3, 330–392 mbsf; and log lithologic Unit 4, 392 mbsf to the bottom of the log. There is a gradual increase in the resistivities within the first log lithologic unit that reflects changes in porosity caused by diagenesis, mainly by dewatering of sediments resulting from compaction. Log lithologic Unit 2 has relatively higher resistivities, between 2 to 4 ohm-m. The lower and upper parts of this unit have resistivities higher than average and may constitute subunits. There are fairly uniform resistivities in log lithologic unit 3 around 3 ohm-m, except for the low-resistivity clay layer at 358 mbsf. The lowermost log lithologic unit shows a gradual increase in resistivities. These log lithologic units correlate very well with the units defined from the natural gamma-ray logs. The porosity log shows a general decrease in porosity with depth. The high porosity encountered around 358 mbsf is probably fictitious, reflecting an abnormally high clay content within this zone.

The interpretation of the induced gamma-ray spectroscopy (GST) data consists of using the elemental yield ratios for lithologic identification, porosity estimates, and determinations of

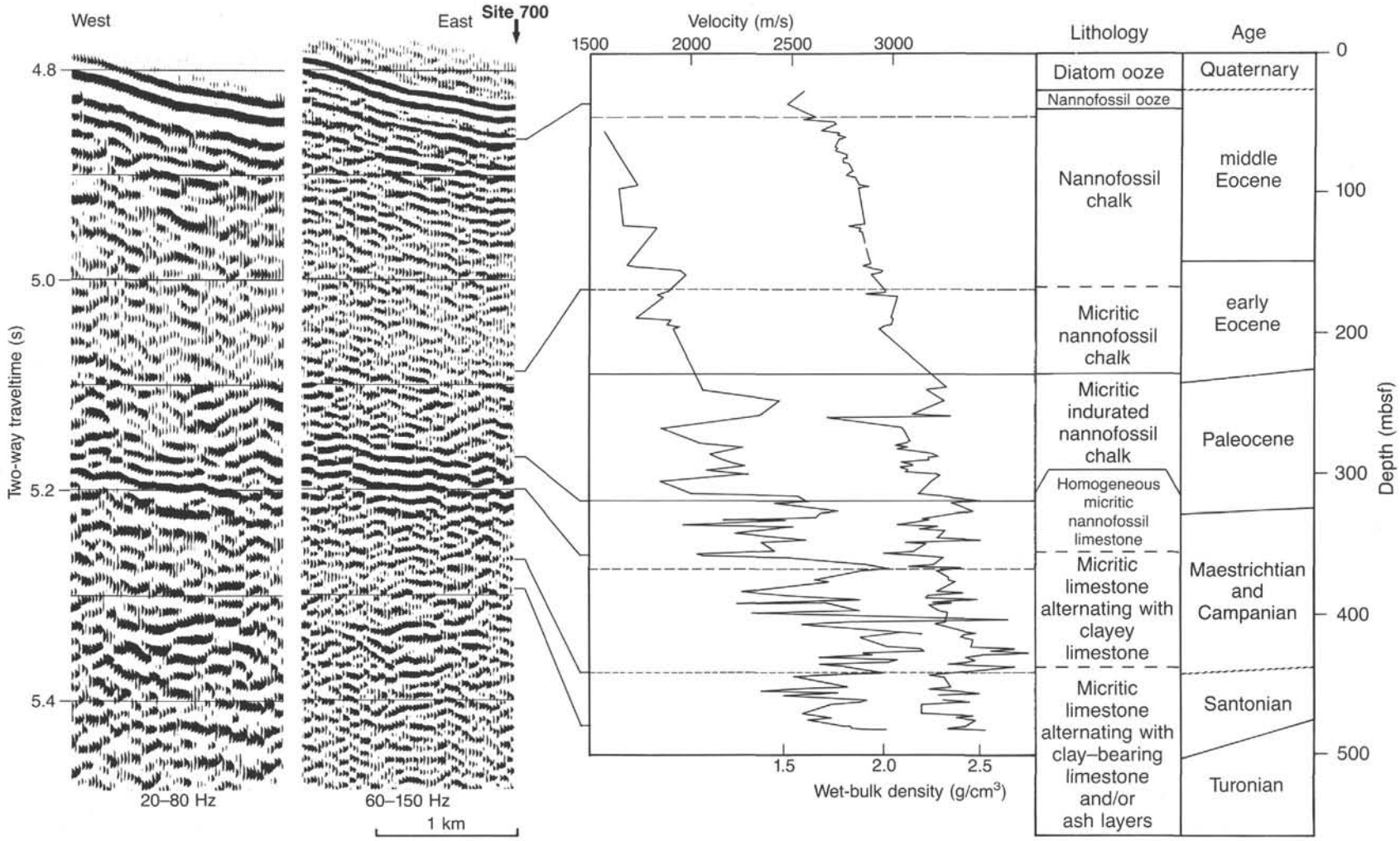

Figure 32. *JOIDES Resolution* analog single-channel seismic-reflection profile acquired on approach to Site 700. Survey speed 6 kt. Seismic source is a single 80-in.^{3} water gun. Downhole variation of *P*-wave velocity and wet-bulk density from "Physical Properties" section, and lithology and stratigraphic age from "Lithostratigraphy" and "Biostratigraphy" sections, respectively.

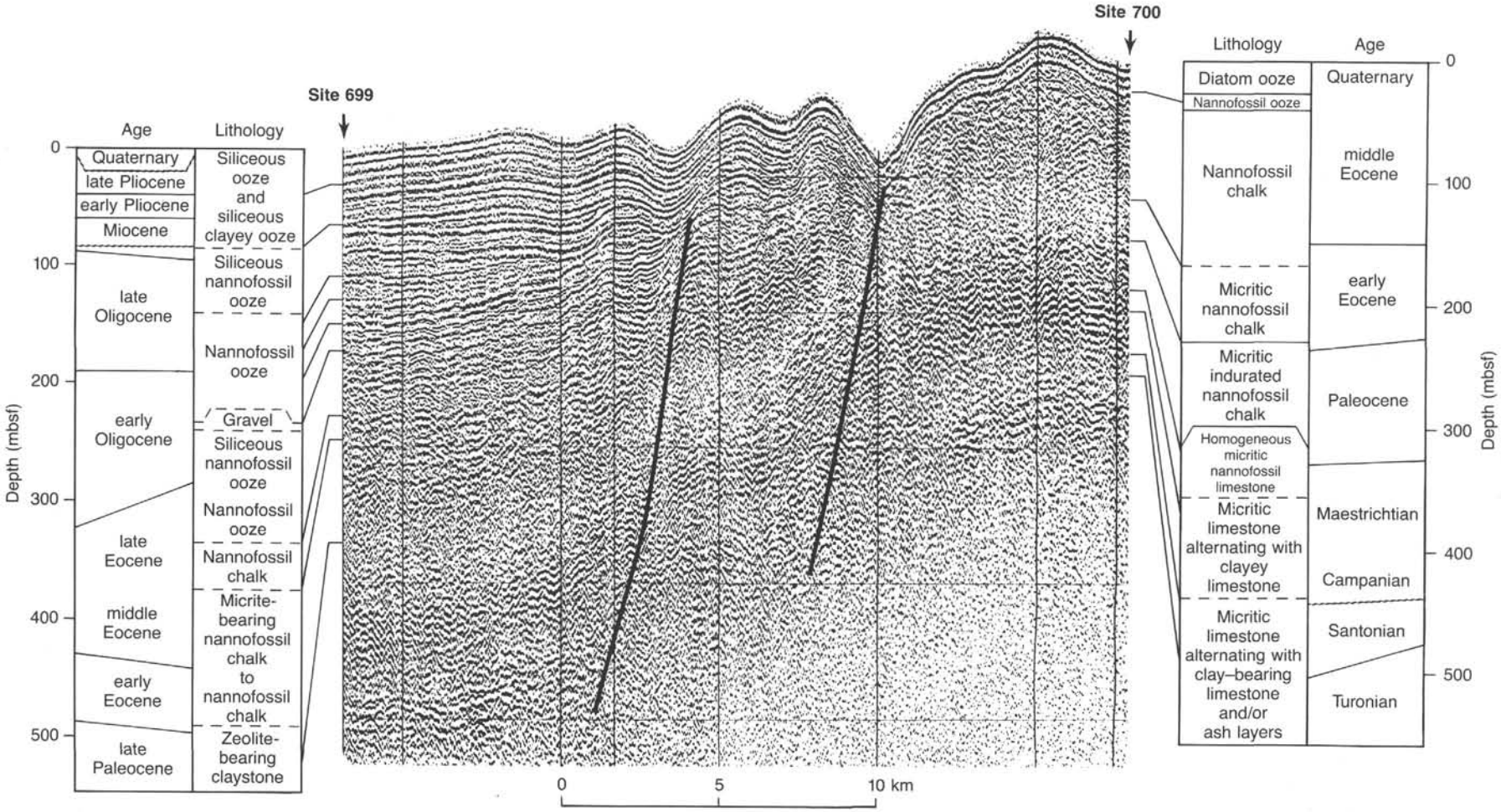

Figure 33. *JOIDES Resolution* single-channel seismic-reflection profile between Sites 699 and 700, with summary of lithostratigraphy and stratigraphic ages.

Table 12. Logging parameters, Site 700.

Run 1: Seismic-stratigraphic combination (SDT/DIPH/NGT/CALI)

Mnemonic	Tool	Measurement	Unit
CALI	Caliper	Hole size	in.
DIPH	Phasor dual induction	Deep, medium, and focused resistivity	ohm-m
SDT	Digital sonic	Sonic transit time	μs/ft
		Compressional-wave velocity	km/s
NGT	Natural gamma-ray spectrometry	Total count (K, U, and Th)	API
		Uranium and thorium	ppm
		Potassium	wt%

Run 2: Geochemical combination (GST/ACT/NGT)

Mnemonic	Tool	Measurement	Unit
GST	Induced gamma-ray spectrometry	Elemental yields (Ca, Cl, H, Fe, S, and Si)	
		Elemental yield ratios:	
		LIR = lithology indicator	Si/(Ca + Si)
		PIR = porosity indicator	H/(Ca + Si)
		IIR = iron indicator	Fe/(Ca + Si)
		SIR = salinity indicator	Cl/H
		GIP = anhydrite/gypsum	S/(Ca + Si)
ACT	Aluminum clay tool	Al and Mn	wt%
NGT	Natural gamma-ray spectrometry	Total count (K, U, and Th)	API
		Uranium and thorium	ppm
		Potassium	wt%

the salinity of the formation fluid. These ratios are given in Table 12. In addition to the GST we also ran the aluminum clay tool (ACT), which provides absolute elemental concentrations of aluminum (Al in wt% if the tool is calibrated) and relative variations in manganese. Figure 36 shows three elemental yield ratios (lithology, iron, and porosity indicator ratios; LIR, IIR, and PIR, respectively) and the SGR log. Three major units are easily distinguishable from the ratios. These units correlate well with those derived from the gamma-ray and induction resistivity data. Log Unit 1 has a fairly constant lithology and iron ratios. The porosity ratio, however, shows a gradual decrease reflecting change in diagenesis (mainly compaction). The iron and porosity ratios may be used to subdivide log Unit 2 into three subunits, with the upper and lower subunits defined by lower ratios. The middle subunit indicates slight increases in the iron content and porosity. The lithology ratio is again fairly constant but a little lower than that in log Unit 1, indicating lower silica content. Log Unit 3 is characterized by an increase in the gamma-ray, iron, and silica content. There is a steady decrease in the porosity ratio with depth.

Figure 37 shows a comparison of the gamma-ray, induction conductivity, and the GST porosity and calcium yield data. The region between 237 to 330 mbsf shows a high degree of correlation between conductivity, porosity, and calcium yield data. High calcium content at the top and the bottom of log Unit 2 correlates with a decrease in conductivity. The lower conductivities suggest that the porosity is lower and may be interpreted as resulting from diagenetic changes of compaction and/or recrystallization (calcite cementation). There seems to be no change in the silica content (see LIR log) that could reflect silicification and hence an increase in resistivities. The fine-scale variations in the calcium yield log do not correlate well with the $\%CaCO_3$ data ("Physical Properties" section) because of the very coarse sample interval of this data set (one sample per 1.5-m core section). Some of the lows in the calcium log correlate with the $\%CaCO_3$ data (between 350 to 360 and between 390 and 400 mbsf). The general trend in the porosity indicator ratio and conductivity is that of a gradual decrease with increasing depth of burial. Within log lithologic Unit 2, the porosity indicator ratio correlates fairly well with the porosities determined from the resistivity data. The central part shows higher than average porosities than the top and bottom of the unit.

Correlation of Logging Data with Lithostratigraphy

The following is a summary of the lithology of Site 700 ("Lithostratigraphy" section).

Lithostratigraphic unit/subunit	Depth interval (mbsf)	Description
I	0.0–26.4	Diatom ooze
II	26.4–45.4	Nannofossil ooze
IIIA	45.4–168.9	Nannofossil chalk
IIIB	168.9–228.5	Micritic nannofossil chalk
IV	228.5–319.0	Micritic indurated nannofossil chalk
VA	319.0–359.0	Homogeneous micritic nannofossil-bearing limestone
VB	359.0–441.5	Micritic limestone alternating with clay-bearing/clayey limestone
VC	441.5–489.0	Micritic limestone alternating with clay bearing/clayey micritic limestone and/or ash layers

Core recovery was poor in a number of sections, especially in zones with high clay content. The downhole measurements were tied in to the core depths by the gamma-ray anomalies between 259 and 261 mbsf (Core 114-700B-28R), 335 and 340 mbsf (clay-bearing micritic limestone, Core 114-700B-38R), and 358 and 360 mbsf (clay-rich section in Core 114-700B-40R). Discrepancies in depth are of the order of 1 m in these sections.

Lithostratigraphic Subunit IIIB is described as a pale brown, micritic limestone. The change in the color from the white nannofossil chalk of Subunit IIIA may reflect changes in clay content. There appears to be an increase in the clay content toward the bottom of this unit (see K and Th logs, Fig. 34). The contact between lithostratigraphic Units III and IV is at 228.5 mbsf at the top of Core 114-700B-25R. Only 40 cm of sediments were recovered in this core. This implies that there is an uncertainty of approximately 9 m in the placement of this core. The convention for establishing the depth of the recovered core in the case of poor core recovery is to place it at the top of the drilled section. There is no way of determining whether the 40-cm recovered core was from the bottom or the top of Core 114-700B-25R. The uncertainty in the contact location is a function of the core recovered. In the case of the contact between lithostratigraphic Units III and IV, the uncertainty in its location is therefore 9 m. The lithologic contact determined from the geophysical and geochemical logs is at 237 mbsf. There is a prominent change in the response characteristics of the logs at this point. If the recovered 40 cm of the core is placed at the bottom of Core 114-700B-25R, this location coincides with the lithologic contact determined from the geophysical and geochemical logs. Figure 38 is an expanded section of the total count gamma-ray (GR) log

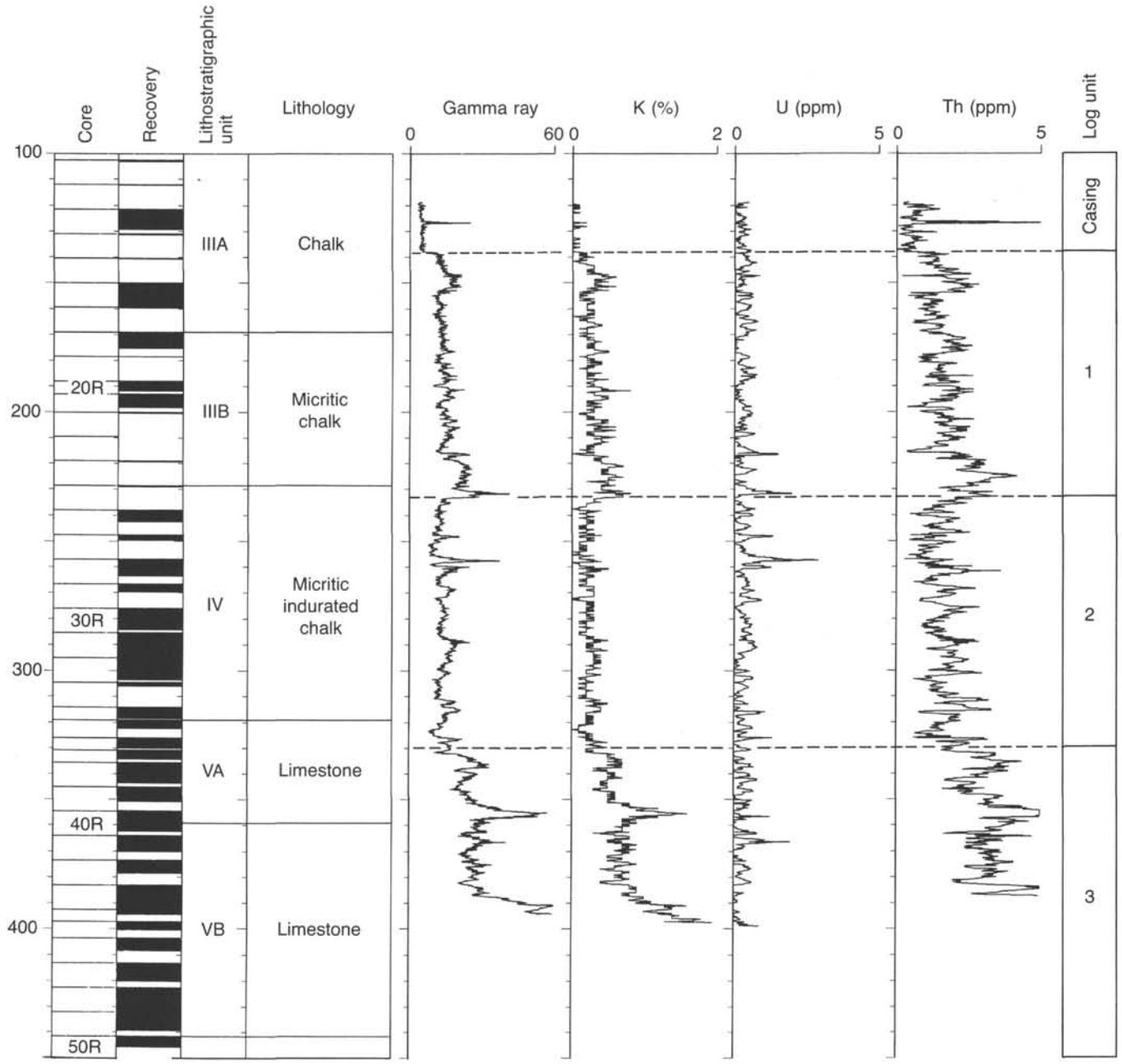

Figure 34. Natural gamma-ray spectral logs recorded in Hole 700B.

and the three conductivities (reciprocal of the deep, medium, and focused resistivities). The figure illustrates the problem in lithologic contact definition when there is poor core recovery and the discrepancy that results between the log-derived and the lithologic unit contact.

Most of the logs show lithostratigraphic Unit IV as being fairly uniform, except for the resistivity and the calcium yield logs that suggest that the upper and lower parts are different. These parts have higher resistivities and calcium than the rest of the unit. The caliper log indicates very good hole conditions and this is also reflected by the three resistivity logs having no significant departures.

The Cretaceous/Tertiary contact is at 319 mbsf at the top of Core 114-700B-35R (lithostratigraphic Units IV/V). Core recovery was 3.15 m out of 9.5 m of section drilled; hence, the uncertainty in the location of the contact is 6.35 m. Most of the downhole logs indicate a lithologic contact by a prominent change in the physical and the geochemical signature at approximately 330 mbsf, which could well be the Cretaceous/Tertiary boundary. However, the boundary between the Cretaceous and Tertiary is defined on the basis of biostratigraphy and may not reflect a change in the physical and geochemical characteristics of the formations on either side.

At least two of the subunits in lithostratigraphic Unit V are delineated by the downhole measurements. The homogeneous nannofossil-bearing limestone of Subunit VA does not appear to be homogeneous (see K, Th, and calcium logs). The NGT logs indicate that Subunit VB may be further subdivided into three sections (360–392, 392–411, and 411 mbsf to the bottom of the logs; Fig. 35). The development of diagenetic chert at the

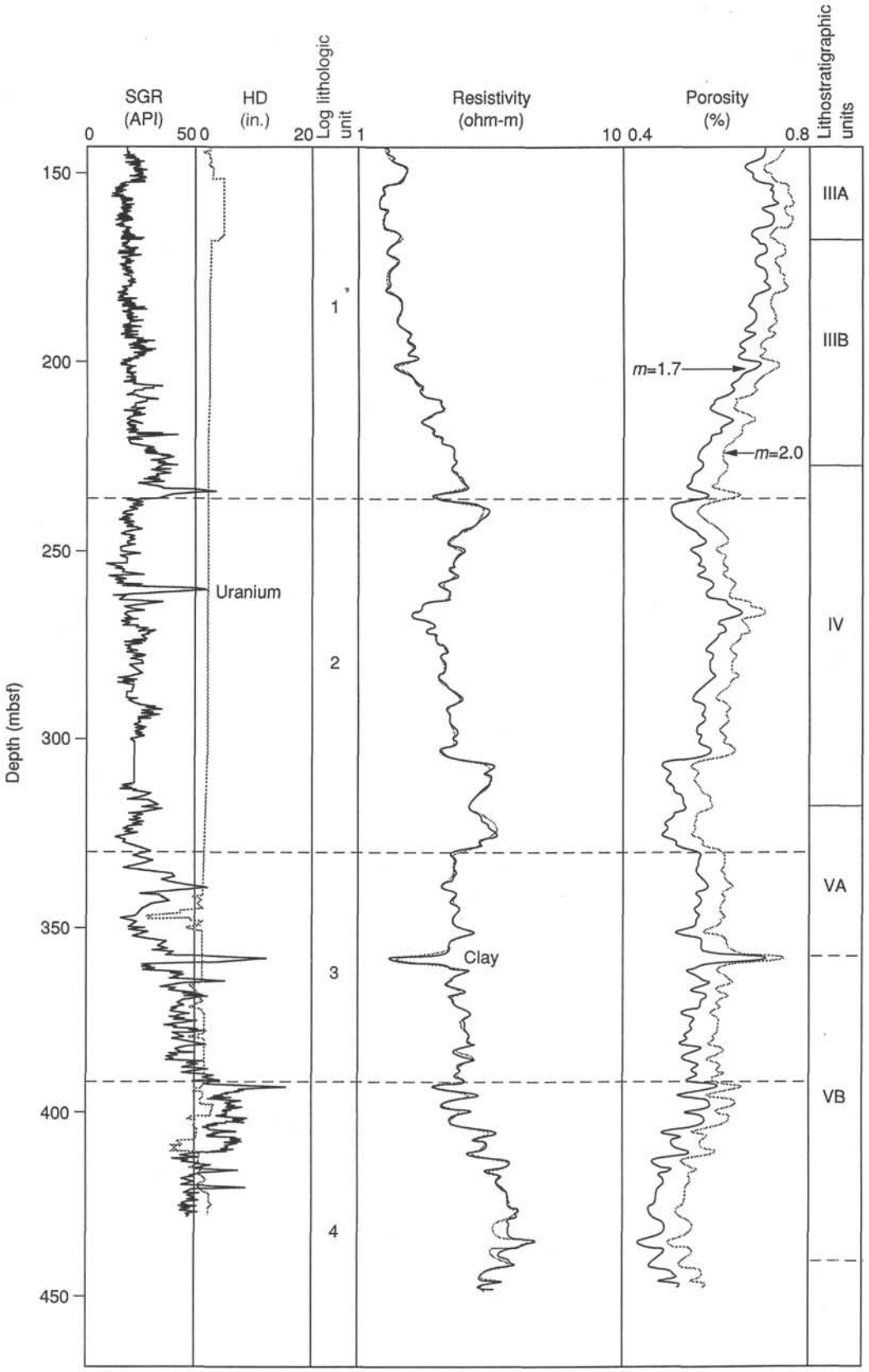

Figure 35. Total count gamma ray (SGR), caliper log hole diameter (HD), phasor dual induction resistivity logs (IMPH and IDPH), and porosity recorded in Hole 700B. The porosity logs are computed from the deep resistivity log for two cementation factors, $m = 1.7$ and $m = 2.0$.

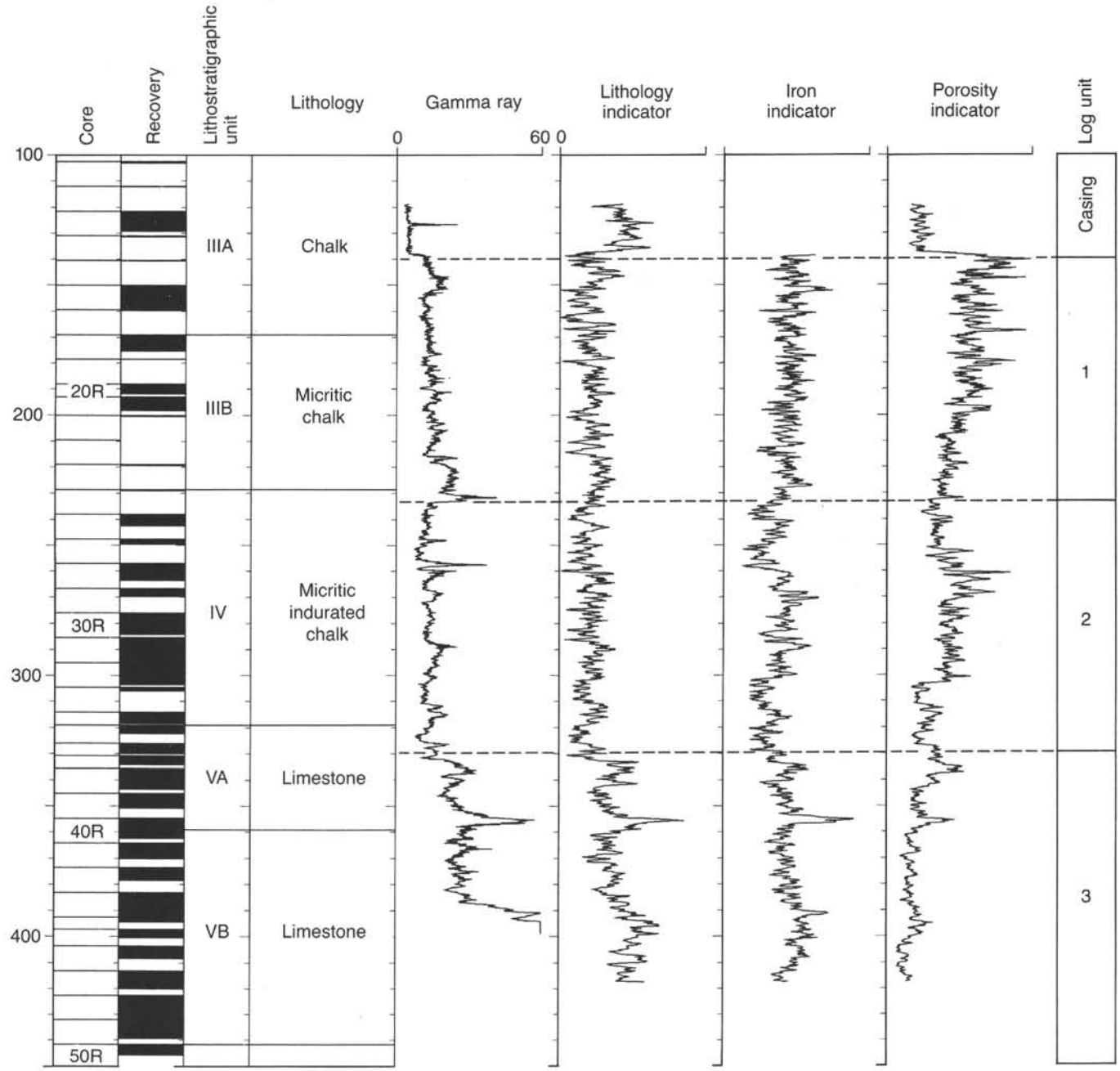

Figure 36. Elemental yield ratios from the induced gamma-ray spectrometry tool recorded in Hole 700B. Shown are the total count gamma-ray, lithology indicator ratio, iron indicator ratio, and porosity indicator ratio.

bottom of Subunit VB is reflected in an increase in resistivities. The alternating micritic limestone and clay-bearing limestone is clearly indicated in most of the measurements. The interpretations of their significance in terms of depositional environment and diagenesis will not be speculated on at this time and will await a more detailed, shore-based study of the lithologic descriptions.

Figure 37 shows the major subdivisions of the lithology as determined from the total count gamma-ray, calcium yield, and porosity indicator ratio logs. These subdivisions are compared to the lithostratigraphic units.

Conclusions

The high-resolution, continuous downhole geophysical, and geochemical measurements have shown that a better definition of lithologic boundaries can be attained with these measurements. Porosity data show a general trend that decreases with depth, reflecting normal diagenetic changes along the sedimentary column. Clay typing and a quantitative estimate of the clay content within the carbonates may provide some clues into the depositional environments.

SUMMARY AND CONCLUSIONS

Summary

Site 700 is in the western region of the East Georgia Basin (51°31.992′S, 30°16.697′W) on the northeastern slope of the Northeast Georgia Rise. The water depth is 3601 m. Site 700 is a companion site to Site 699, which was prematurely terminated at 518 mbsf in upper Paleocene strata about 250 m above base-

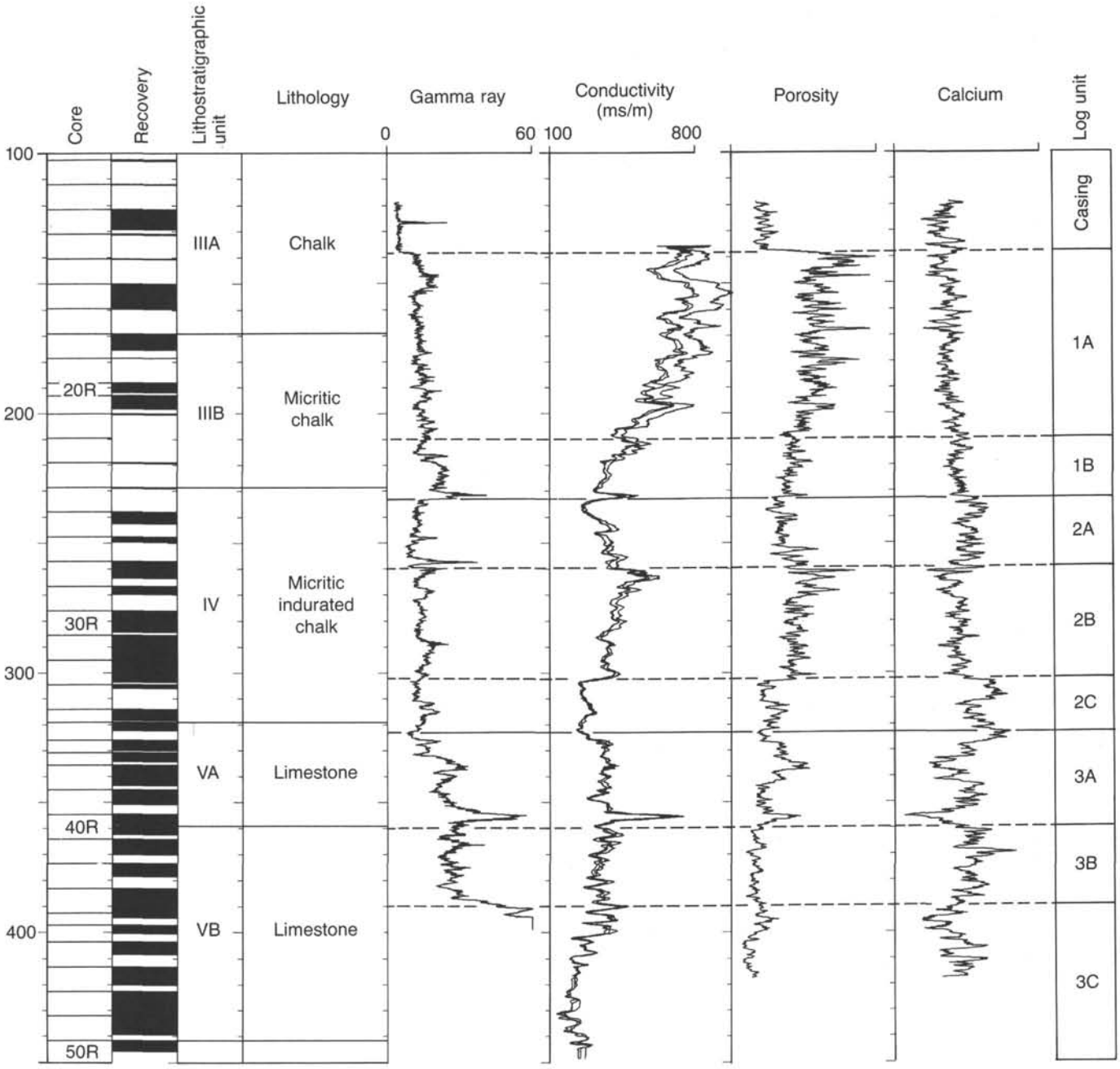

Figure 37. Stratigraphic units determined from total count natural gamma-ray radioactivity, induction conductivity, porosity, and calcium logs compared to lithostratigraphic and log units.

ment. In order to obtain the deeper objectives not reached at Site 699, Site 700 was occupied at a location 21 km east of the previous site (Fig. 1), where post-Eocene sediments are greatly attenuated (<50 m thick; Fig. 32), allowing for rapid penetration of the Upper Cretaceous–Paleogene sequence. The objectives for Site 700 were complementary to those reported previously for Site 699 (see "Background and Objectives" section, "Site 699" chapter). Foremost of these was to obtain an Upper Cretaceous–Paleogene section recording the possible role of the Georgia Basin in deep-water communication between the Weddell Sea and the South Atlantic (Fig. 39). An additional objective was to obtain an older Cretaceous section than recovered at Site 698, which might further constrain the nature, age, and subsidence history of the Northeast Georgia Rise.

The seismic stratigraphy of the 540 m-thick (TWT) section of sediments above basement at Site 700 (Fig. 32) is very similar to that of the deep section at Site 699 (Fig. 33). At Site 700, we therefore expected to find Eocene chalk below a 40-m-thick unit of Miocene to Recent diatomaceous ooze. This stratigraphic level corresponds to a depth of 250–300 mbsf at Site 699.

Site 700 consists of two rotary-drilled holes: Hole 700A with only two cores penetrating to 9.6 mbsf, with a recovery of 0.19 m, and Hole 700B with 54 cores penetrating to 489 mbsf, with a recovery of 245.4 m (50.2%). Both holes were terminated

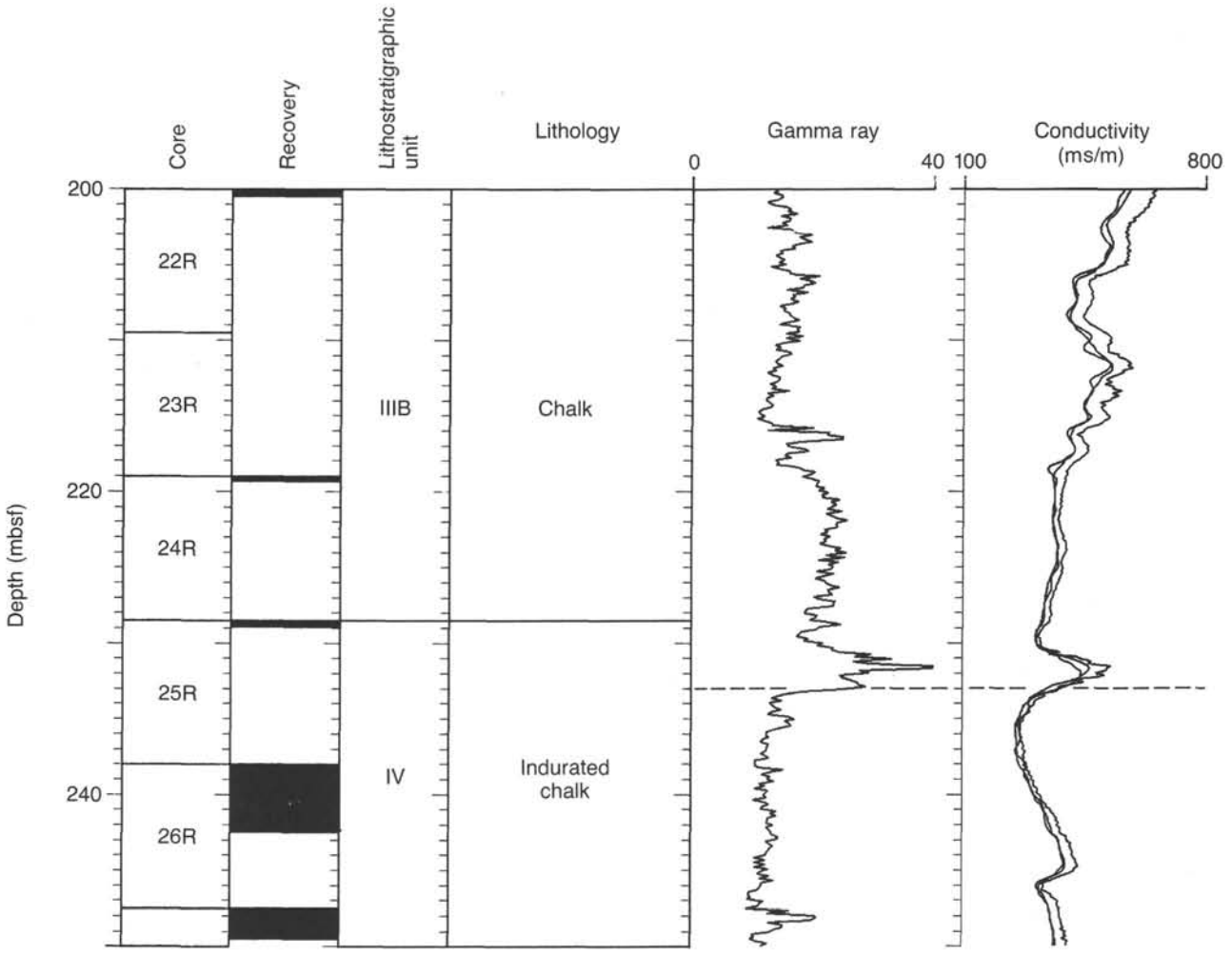

Figure 38. Expanded section of the total count gamma-ray log and induction conductivity log illustrating the problem of defining lithostratigraphic boundaries when there is poor core recovery. Downhole logging measurements are used to resolve this problem.

as a result of premature bit release. Hole 700B reached to within 100 m of basement and was logged using the standard Schlumberger stratigraphic and geochemical tools. The site was occupied between 26 March and 3 April 1987 in moderate to rough seas.

The stratigraphic section at Site 700 consists of a thin unit of upper Pliocene to Recent siliceous ooze overlying a thick section of Upper Cretaceous and Paleogene carbonates (Fig. 40). The carbonates show progressive lithification with depth from ooze through chalk, indurated chalk, and finally, limestone. The section may be divided into five lithostratigraphic units (Fig. 3).

Unit I is a diatom ooze of late Pliocene to Quaternary age of which only 0.29 m was recovered. Although no sediments were recovered between 0.29 and 26.4 mbsf, a major hiatus must be present between Unit I and older sediments.

Unit II is a micritic nannofossil ooze of middle Eocene age that extends from 26.4 to 45.4 mbsf. It constitutes the upper part of the Paleogene carbonate sequence at the site. Significant variations occur in the carbonate content, with lower carbonate intervals having a higher clay content.

Unit III (45.4–228.5 mbsf) is divided into two subunits, a nannofossil chalk of early to middle Eocene age (Subunit IIIA, 45.4–168.9 mbsf) and an underlying micritic nannofossil chalk (Subunit IIIB, 168.9–228.5 mbsf) of early Eocene age. Subunit IIIA exhibits a downward increase in carbonate content (41% to 91%), with increased clay in low-carbonate intervals. Manganese filaments, impregnations, and a few nodules are present. Subunit IIIB has a high carbonate content (77%–86%) and increased micrite with depth. Clinoptilolite is abundant throughout the unit.

Unit IV is an indurated nannofossil chalk of early to late Paleocene age, extending from 228.5 to 319 mbsf. Scattered chert/limestone nodules are present in addition to some siliceous horizons, which may be responsible for the highly fluctuating carbonate content. The unit contains chert and limestone nodules, as well as a thin, siliceous-bearing claystone.

Unit V (319–489 mbsf) consists of an Upper Cretaceous to lower Paleocene micritic limestone with a significant clay and ash component that increases with depth, which is the basis for its subdivision into three subunits. Clinoptilolite is abundant throughout the unit. Subunit VA is a 40-m-thick (359–319 mbsf) homogeneous, nannofossil-bearing micritic limestone to micritic limestone of Maestrichtian to early Paleocene age. The carbonate content is high (65%–88%) but decreases toward the base. A few chert nodules occur in the middle of the subunit, and a claystone interval is prominent toward the base. Subunit VB (359–441.5 mbsf) is characterized by alternating homogeneous micritic limestone and clay-bearing to clayey limestone of Campanian to Maestrichtian age. Clay- and silica-rich horizons generally occur as thinner intervals, and chert nodules are present at the base of the subunit. Subunit VC (441.5–489 mbsf) has the same lithological characteristics as the overlying subunit but also con-

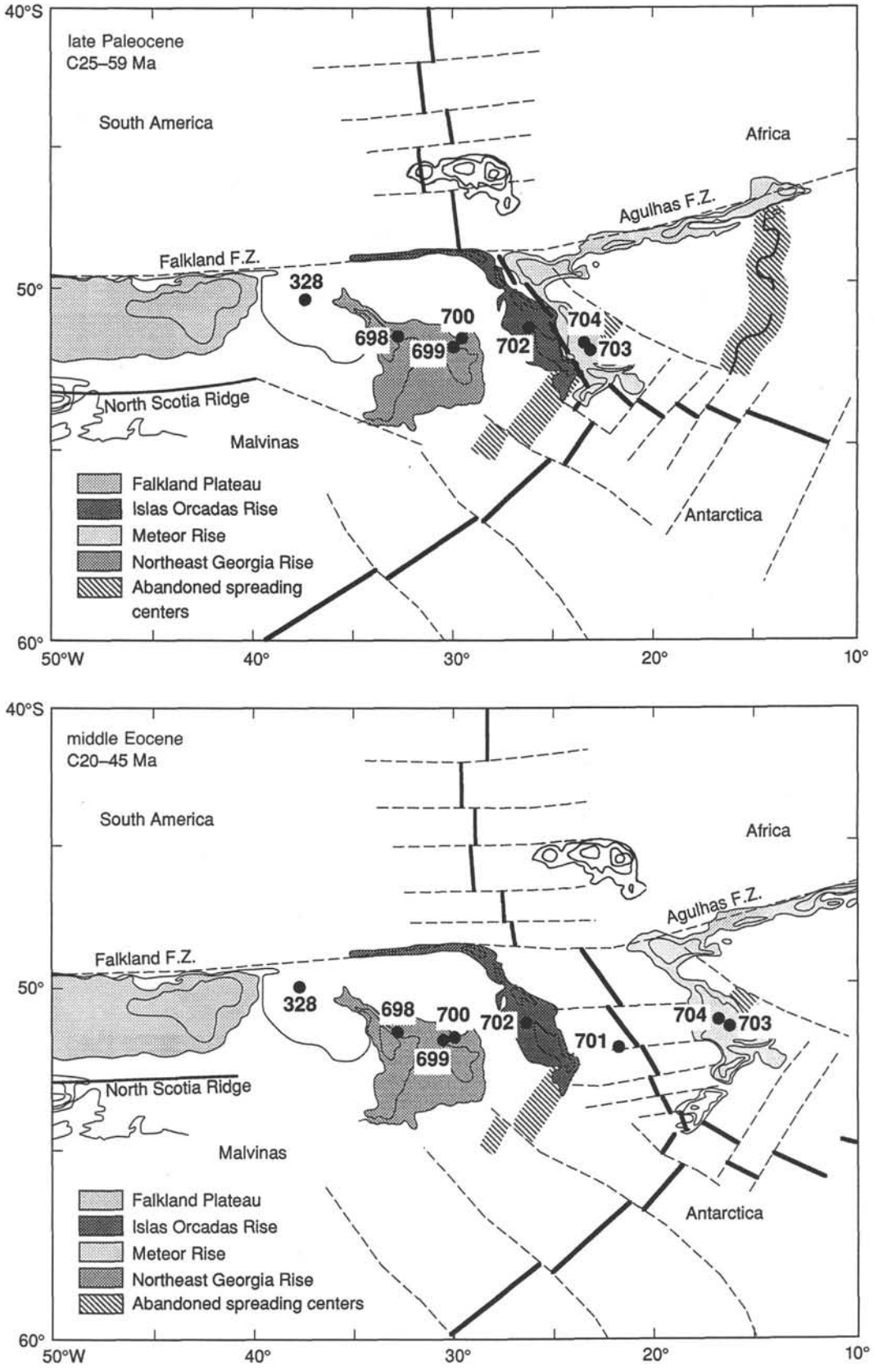

Figure 39. Tectonic reconstructions of the late Paleocene and middle Eocene positions of Site 700. A major objective at this site was to evaluate the nature of deep circulation through the Georgia Basin prior to and following formation of the deep-water gateway between the Islas Orcadas Rise and Meteor Rise.

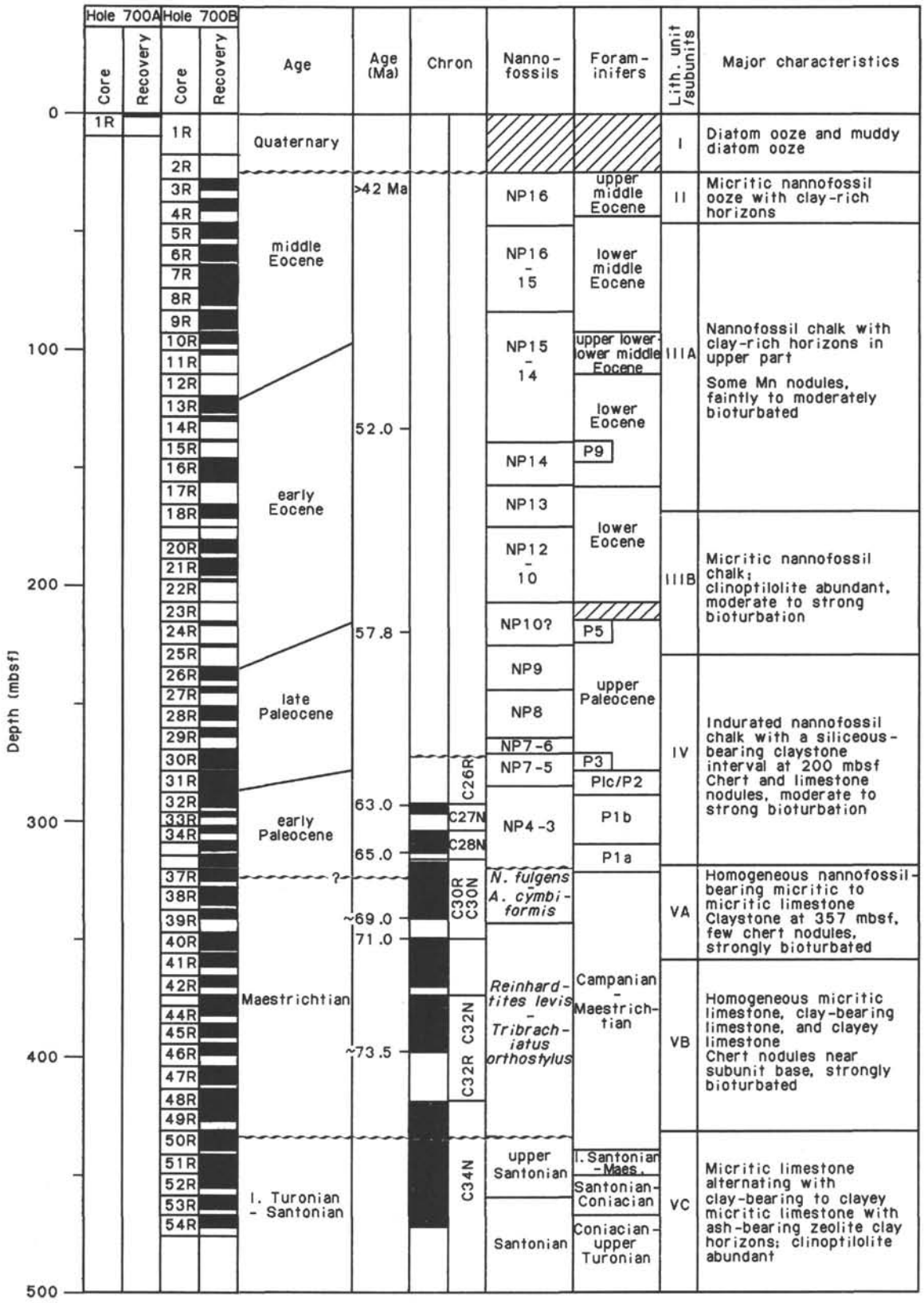

Figure 40. Summary of selected findings from Site 700, including depth (mbsf), sediment recovery, age, paleomagnetic polarity zones and their correlation to the GPTS, calcareous nannofossil and foraminifer zones, lithostratigraphic units and subunits with a description of their major characteristics, variations in sediment composition, percent carbonate, and porosity.

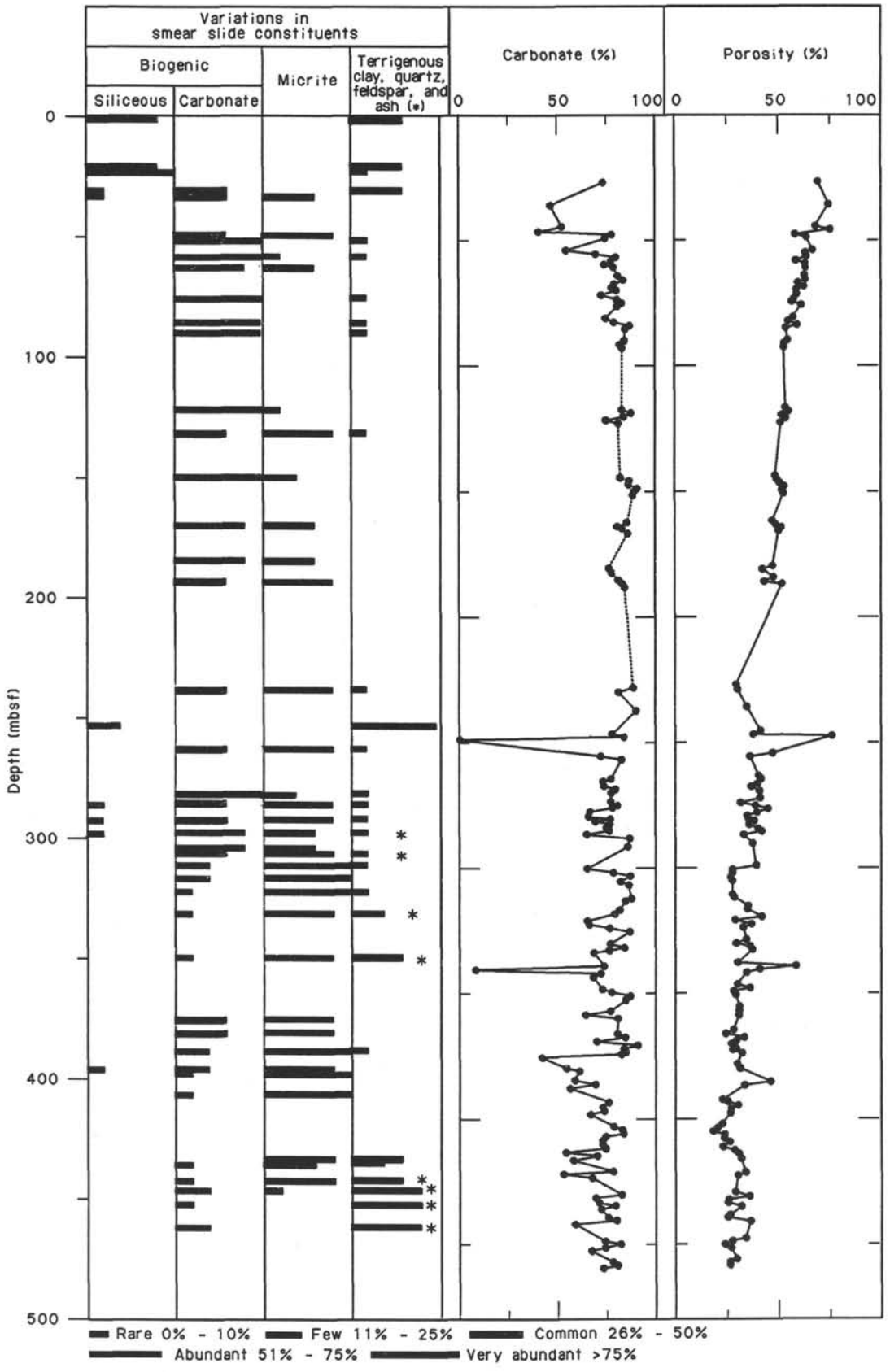

Figure 40 (continued).

tains ash-bearing zeolitic clay horizons. There is a gradual increase in the volcanic ash component downhole, and discrete ash layers are present in the deepest part. The subunit represents the Coniacian to Campanian.

A portion of Hole 700B, between 26.4 and 228.5 mbsf, repeats the lower to upper middle Eocene section recovered at Site 699. Duplication of this section provides better stratigraphic representation of an interval poorly recovered at both sites (55.2% at Site 699 and 40.2% at Site 700). A 256-m-thick Paleocene and Coniacian section provides a greatly expanded section for a ~30-m.y. interval that is only sparsely represented at Sites 698 and 699. Site 700 and companion Site 699 provide a Upper Cretaceous–Paleogene pelagic record spanning ~64 m.y. within a combined stratigraphic thickness of 887 m. These two sites provide the most continuous record of this period obtained from the Southern Ocean.

A clear succession of magnetic polarity zones was identified in the Upper Cretaceous to lower Paleocene chalks and limestones below 270 mbsf. Good recovery (69%) and relatively little core disturbance of this interval resulted in identification of latest Campanian to early Paleocene Chrons C33N to C26R. This section will allow the first calibration of high-latitude siliceous and calcareous microfossil assemblages to the GPTS, providing a temporal framework for interpretation of Southern Ocean Late Cretaceous–Paleocene oceanography.

Sedimentation rates were not more than 10 m/m.y. during the Coniacian-Santonian and were as high as 23 m/m.y. during the Maestrichtian, but decreased to 5 m/m.y. in the late Maestrichtian. Sedimentation rates averaged 15 m/m.y. during the Paleocene, decreasing to approximately 8 m/m.y. during the early middle Eocene. Recognized hiatuses include most of the Campanian, the Cretaceous/Tertiary boundary, and the upper middle Eocene to upper Pliocene.

Siliceous microfossils are abundant and well preserved in the Paleocene and upper Pliocene–Quaternary. Abundant and well-preserved radiolarians occur from the Maestrichtian through the Campanian. All calcareous microfossil groups are represented throughout the Upper Cretaceous and Paleogene, although there is evidence for secondary calcite overgrowths and recrystallization below the lowermost Eocene. As was the case with the previous sites, calcareous microfossil diversity is highest in sediments of early Eocene to Late Cretaceous age.

Conclusions

Seismic and Tectonic Interpretation

The seismic stratigraphy of the calcareous sequence at Site 700 shows a reflection pattern very similar to that of the deep section at Site 699 (Fig. 33). The seismic velocity of a carbonate rock is largely a function of its diagenetic state, but the lithification of a calcareous section is not a simple function of burial depth or time (Garrison, 1981; Schlanger and Douglas, 1974). The results from Sites 699 and 700 indicate that the degree of lithification must, at least in some cases, vary considerably along a depositional surface as well. This interpretation is borne out by the following observations:

1. The seismic response of the nannofossil chalk unit is characterized by numerous short, randomly distributed reflection segments and associated diffraction patterns, which results in a generally reflection-free appearance. Although variations of *P*-wave velocity with depth show stepwise changes of 0.3 km/s within this unit, similar lateral velocity variations must exist to generate an essentially random velocity distribution superimposed on the generally linear increase with depth.

2. Similarly, the acoustic image of the transition between the micritic nannofossil chalk and the indurated micritic nannofossil chalk is a semichaotic reflection pattern that is probably the most dramatic expression of the degree of lateral anisotropy of the diagenetic process. This reflection pattern could also be interpreted as a contorted upper surface of the underlying reflective unit for which there is no evidence in the recovered sequence.

Therefore, we infer that the velocity and the degree of lithification can, at least in some cases, show variation along a depositional surface as well as a complex variation with depth. The most continuous acoustic stratification is observed in the homogeneous micritic nannofossil-bearing limestone and the underlying subunit, in which alternating clay-bearing limestone intervals appear.

Sites 699 and 700 lie on the northeastern slope of Northeast Georgia Rise on crust that structurally must be considered part of the rise itself. The pore-water chemistry of the calcareous sediments at these sites shows an increase of Ca^{2+} and a decrease of Mg^{2+} with depth, which is indicative of reactions with a basaltic substratum (see "Geochemistry" section). Basement at Site 698, 150 km farther east on the rise, is Campanian (or older), iron-rich oceanic basalt that has been subjected to subaerial weathering. On the other hand, the occurrence of silica-rich crystalline and sedimentary rocks in a gravel bed at 233.5 mbsf at Site 699 raises the possibility of a continental fragment being part of the structure forming the Northeast Georgia Rise. The rise is considered to be oceanic crust deformed in a compressional regime generated by rotation of the Malvinas plate against the Falkland block during the Campanian to Eocene (LaBrecque and Hayes, 1979). The age of the crust is bracketed by the presence of anomaly 34 (Campanian) to the east of the rise and anomaly M0 (Aptian) to the west in the West Georgia Basin. Volcanic activity occurred in the vicinity of Site 700 during the Coniacian-Santonian, but waned by the early Campanian, and is manifested by the presence of discrete ash layers and thick zones of dispersed ash in the lower micritic clay-bearing limestone. The Campanian through Eocene depositional environment at Sites 698, 699, and 700 does not reflect any significant tectonic activity. Any incipient subduction to form a fossil island arc must be, therefore, of pre-early Campanian age.

Late Paleocene or younger tectonic events have significantly altered the environment of Site 700. The stratigraphic control and the seismic correlation between Sites 699 and 700 clearly demonstrate that corresponding stratigraphic levels have been vertically displaced along two major faults with a total throw of about 500 m (Fig. 33). This faulting involved basement. The older depositional units immediately east of Site 699 are conformable with the substratum up through the lower Oligocene, where onlap on a westward-tilting surface becomes apparent. Thus, post-early Oligocene block faulting exposed the elevated block at Site 700 to erosion until a change in the local current regime during the Quaternary allowed renewed deposition of siliceous ooze. A comparison of the variation of physical properties with depth for the two sites indicates that an estimated thickness of about 350 m of sediments has been removed from the top of the middle Eocene chalk at Site 700. This is reasonable in view of the observed 200 m thickness of upper middle Eocene to lower upper Oligocene sediments at Site 699. Post-late Paleogene tectonic events on the Northeast Georgia Rise must be related to the opening of the Scotia Sea (Barker and Hill, 1981) and interaction between the rise and the advancing South Georgia block.

Paleoenvironmental History

Late Cretaceous

During the Cretaceous, shallow portions of the Northeast Georgia Rise were above sea level and exposed to subaerial weathering. At Site 698 intense weathering in a "tropical" climate

produced a thick hematitic regolith that was later covered by a subaerial to shallow-water basalt flow. Subsidence of the Northeast Georgia Rise must have significantly preceded the deposition of the predominantly Campanian-Maestrichtian sequence above basement at Site 698, which contains benthic foraminifers indicative of water depths greater than 1000 m. The age of the possible subsidence of the rise is further constrained by the Upper Cretaceous sequence at Site 700. Benthic foraminifers of the Campanian-Maestrichtian of Site 700 are similar to equivalent-age faunas from the Falkland Plateau that were assigned a paleodepth of 1500–2500 m below sea level, significantly deeper than that of Site 698. Unlike the shallower Site 698, Site 700 received several influxes of shallow-water organisms in carbonate turbidity currents. The most conspicuous of these occurs in the middle upper Maestrichtian of Core 114-700B-40R, where the displaced fauna includes large nodosarids and agglutinated benthic foraminifers, bivalve fragments, echinoid spines, and heavily ornamented ostracodes. *Inoceramus* fragments were also found in Cores 114-700B-47R, 114-700B-50R, and 114-700B-54R. These occurrences together in Coniacian to lower Maestrichtian sediments suggest that parts of the Northeast Georgia Rise remained at, or near, shelf depth throughout most of the Late Cretaceous. Further shore-based analysis of pre-Campanian sediments from Site 698 and 699 may further constrain the subsidence history of the Northeast Georgia Rise. Preliminary results are consistent with the Northeast Georgia Rise having a Late Cretaceous subsidence history similar to that of to the Falkland Plateau, although portions of the Northeast Georgia Rise subsided to below shelf depth at a later time.

Sections 114-700B-50R, CC, through 114-700B-54R, CC, the basal recovery, were assigned a Coniacian-Santonian (88.5–84.0 Ma) to Turonian(?)–Coniacian(?) age based upon calcareous nannofossil flora and the planktonic foraminifer assemblage. In spite of the present uncertainty as to the age of the upper part of this interval, Sections 114-700B-52R, CC, through 114-700B-54R, CC, are undoubtedly of Coniacian age.

Surface-water productivity at this time included both calcareous and siliceous microfossil-producing organisms. Of the siliceous microfossil groups, only radiolarians are present. Radiolarians are confined to the upper part of the Santonian, where they are abundant, well preserved, and diverse. The disappearance of radiolarians in the lower part of the sequence coincides with an increase in clinoptilolite in basal Subunit VC, suggesting that radiolarians may have contributed to authigenic silicate formation, along with volcanic ash. Planktonic foraminifers and calcareous nannofossils were deposited below the lysocline, as dissolution-susceptible species are poorly represented. Planktonic foraminifer assemblages have a cooler water affinity than those of the lower latitudes; however, abundant globotruncanids attest to a warm, lower latitude influence by a more southerly subtropical gyre. Calcareous nannofossil preservation is generally too poor for comparisons with lower latitude assemblages to be meaningful.

At present, Coniacian to Santonian sedimentation rates are difficult to evaluate on the basis of existing biostratigraphic data. To the west of Site 700, on the Falkland Plateau, upper Turonian to Santonian sequences are very thin. Thicknesses for this interval at Falkland Plateau DSDP Sites 327 and 511 are ~15 and 57.5 m, respectively. The attenuated sections at Sites 327 and 511, and possibly at Site 700, may be the result of low rates of sedimentation as a consequence of low overall productivity. The Cenomanian through Turonian is poorly represented in drill sites throughout the Southern Hemisphere (Sliter, 1977), as well as in other parts of the world. This interval of the Late Cretaceous has previously been noted as a time of crisis or an "oligotaxic" episode in the world's oceans (Fisher and Arthur, 1977).

Santonian to Late Campanian/Early Maestrichtian Hiatus

A significant hiatus occurs between Sections 114-700B-49R, CC, and 114-700B-50R, CC. The combined magnetostratigraphic and biostratigraphic data bracketing this hiatus suggest that the missing interval includes all or nearly all of the Campanian and possibly some of the upper Santonian. The paleomagnetic polarity on either side of the hiatus is normal; however, a prominent reversed interval a short distance above the hiatus (Cores 114-700B-48R and 114-700B-47R) is almost certainly Chronozone C32R of the basal Maestrichtian (Fig. 27). Thus, the hiatus appears to occur within the long normal polarity sequence in Subunit VC in which the Santonian (C34N) is overlain by the upper Campanian to lowermost Maestrichtian (upper C33N) (see "Biostratigraphy" and "Paleomagnetics" sections for a more thorough discussion). If correct, the hiatus represents approximately 9–10 m.y. (~84–75 Ma).

On the Falkland Plateau the occurrence and thickness of Campanian sediments seems to be related to paleobathymetry. The thickest accumulation of Campanian sediments is at Site 511 (137 m), which is in a basin environment relative to the Maurice Ewing Bank, which is immediately to the northeast. This thickness of Campanian sediments contrasts sharply with that ~30 km away at Site 327 (present in only one core), which is upslope relative to Site 511 and on the flank of Maurice Ewing Bank. Perhaps the relatively elevated position of Sites 327, 698, and 700 made them more susceptible to erosional or winnowing processes. These sites also received a lower influx of terrigenous sediment than the deeper regions, where more than a kilometer of Upper Cretaceous sediments is present. Lower rates of terrigenous sedimentation and low surface-water productivity cannot sufficiently account for the near absence of Campanian sediments at Site 700. Site 511 occupied a similar paleolatitude to the west of Site 700, and foraminifer assemblages there exhibit maximum diversity within the Upper Cretaceous. Erosional processes were apparently responsible for eliminating any Campanian sediments, which probably did not accumulate to an appreciable thickness because of low rates of terrigenous sedimentation and possibly a shallow CCD.

Maestrichtian (74.5–66.5 Ma)

The Maestrichtian sections recovered at Sites 698 and 700 are the most complete and thickest accumulations of pelagic sediments of this age from the southern high latitudes. The high-quality paleomagnetic record obtained for this interval at Site 700 will provide age control for paleoenvironmental interpretation that can presently only be discussed in general terms on the basis of shipboard studies. Calibration of microfossil biostratigraphy to this paleomagnetic record will also allow a more thorough comparison with the less complete sections from the Falkland Plateau and a reinterpretation of those sequences.

Maestrichtian calcareous nannofossil assemblages are similar to those encountered in the Falkland Plateau holes and are dominated by typical high-latitude species. The planktonic foraminifer assemblage is more varied than assemblages encountered below the hiatus. Low-latitude globotruncanids decrease in abundance and are discontinuously present, with two peak occurrences, one within the lower Maestrichtian and another within the upper Maestrichtian. Between the peak occurrences of globotruncanids are faunas dominated by more dissolution-resistant species with cooler surface-water affinities (*Hedbergella, Heterohelix, Globigerinelloides*, etc.). It is possible that variations in the abundance of the globotruncanids are related

to dissolution because Site 700 appears to have remained below the lysocline throughout the Late Cretaceous. Dissolution alone may not account for the entire range of fluctuations in this warmer water genus. Similar variations were noted in the Campanian of Site 511, where dissolution was dismissed as a major contributing factor (Krasheninnikov and Basov, 1983). If the influence of dissolution of the assemblage can be determined by further study, this Maestrichtian section may provide a detailed record of relative surface-water temperature variations in the Southern Ocean during the latest Cretaceous.

Sites 700 and 698 are the first to recover Maestrichtian sediments from the subantarctic region. The presence of globotruncanids in the uppermost Maestrichtian of these sites is therefore later than the Campanian last occurrence of this genus on the Falkland Plateau. Their absence in the incomplete Maestrichtian sections of the Falkland Plateau had previously been interpreted as indicative of a major Maestrichtian cooling event (Krasheninnikov and Basov, 1983). Our findings indicate that Maestrichtian surface-water temperatures were perhaps more variable, but no long-term dramatic cooling preceded the Cretaceous/Tertiary boundary.

Cretaceous/Tertiary Hiatus

Calcareous nannofossil, planktonic foraminifer, and benthic foraminifer assemblages define the Cretaceous/Tertiary contact between Sections 114-700B-37R, CC, and 144-700B-36R, CC. More detailed sampling for calcareous nannofossils places the contact in a 1.6- to 0.3-m interval of no recovery between Section 114-700B-36R, CC, and Sample 114-700B-37R-1, 30 cm. Calcareous nannofossil Zone NP1, planktonic foraminifer Zone P1a, and possibly the upper *Nephrolithus frequens* Zone are missing, which is in agreement with the absence of the reversed polarity interval Chron C29R (see "Biostratigraphy" and "Paleomagnetics" for a more detailed discussion of the Cretaceous/Tertiary boundary). Combined biostratigraphic and magnetostratigraphic evidence support a missing interval of ~0.6 to 3.0 m.y., which may be accounted for by a brief hiatus or low sedimentation rate during deposition of the unrecovered interval.

Maurice Ewing Bank Site 327 represents the most complete Cretaceous/Tertiary boundary sequence on the Falkland Plateau. At this site, Maestrichtian foraminiferal nannofossil ooze is directly overlain by upper Paleocene zeolitic clay and nannofossil-bearing siliceous ooze. Elsewhere on the plateau an even broader hiatus occurs between the Cretaceous and Tertiary. Numerous seismic-reflection profiles across the Falkland Plateau reveal that a major scouring of the plateau occurred at or near the Cretaceous/Tertiary boundary, which truncated the southward-dipping sedimentary section of the plateau between the Falkland Islands and the Maurice Ewing Bank (Ludwig, 1983). The continuous or nearly continuous sedimentation across the Cretaceous/Tertiary boundary at Sites 698 and 700 contrasts significantly with the deep-cutting erosional episode on the Falkland Plateau and is difficult to explain at this time.

Paleocene (66.4–57.8 Ma)

Paleocene sediments differ little from those of the Maestrichtian. The carbonate content is high (65%–90%), and the section consists of chalks above the lowermost Paleocene chalk/limestone transition. In early Danian sediments, the diversity of planktonic foraminifers and calcareous nannofossils (e.g., *Thoracosphaera* spp.) is low, whereas benthic foraminifer assemblages are similar to those of the Upper Cretaceous. These findings are in keeping with observations elsewhere that the Cretaceous/Tertiary boundary crisis was found to have more seriously impacted the planktonic realm. Most of the Paleocene of Site 700 is characterized by a sparse to common occurrence of taxa with well-established lower latitude affinities. Paleocene planktonic foraminifers are assigned to a temperate province and warm-water acarininids appear after ~62 Ma, becoming common within the upper Paleocene, just prior to or during NP9 (~59 Ma). Coincident with the lower Paleocene increase in acarininids is the first occurrence of lower latitude calcareous nannofossil groups (sphenoliths and discoasters). An observed increase in the dissolution of planktonic foraminifers in upper Paleocene sediments suggests that the seafloor was below the lysocline. Increased dissolution at this time may have been related to further subsidence of Site 700 from a Late Cretaceous depth of 1500–2500 m to a depth ranging from 2000 to 2500 m, based upon benthic foraminifer assemblages.

Site 700 is the third consecutive Leg 114 site to have noted only sparse occurrences of siliceous microfossils within the Paleocene and Eocene. On the basis of the dissolved silica profiles, preservational status of siliceous microfossils, and the distribution of authigenic clinoptilolite and chert, it becomes increasingly clear that diagenesis of biogenic silica significantly influences the distribution of biogenic silica of early to middle Paleogene age. This observation points out the necessity of cautious observation before conclusions are drawn regarding the Paleogene productivity of silica-producing organisms. As at Site 699, Paleocene siliceous microfossils are primarily limited to the upper Paleocene (NP9–5) of Site 700, except for rare and poorly preserved occurrences in the lower Eocene.

Determination of the paleoenvironmental conditions across the Paleocene/Eocene boundary requires further study because of the present uncertainty of the boundary position, which differs slightly in its placement depending on whether it is based upon calcareous nannofossils or planktonic foraminifers. However, some changes appearing in the vicinity of the boundary are worth noting. Significant benthic foraminifer faunal changes take place across the boundary in Holes 699A and 700B. In Hole 698A, at the shallowest Leg 114 site, changes in the benthic foraminifer assemblages are apparently less abrupt. These differences may be indicative of a significant change in the characteristics of the deeper water mass rather than a consequence of subsidence alone. An alternative explanation for the abrupt change in Holes 699A and 700B may be the presence of an undetected hiatus that brings different assemblages into juxtaposition. A hiatus does appear to be present at the Paleocene/Eocene boundary of Hole 699A, although one may exist within the lower Paleocene. Assemblages of planktonic microfossils are less indicative of a substantial paleoenvironmental change. Planktonic foraminifers are indicative of some cooling across the boundary in Hole 700B, having a higher latitude affinity characterized by the lack of strongly keeled morozovellids.

Early Late Middle Eocene (~57.8–43.0 Ma)

An Eocene sedimentary record was obtained from Sites 698, 699, and 700. The early to middle Eocene paleoenvironmental record of Site 700 is similar to that reported for companion Site 699. Microfossils of the planktonic fauna and flora clearly delineate the early Eocene (57.8–52.0 Ma) as the period of maximum Cenozoic warmth. Planktonic foraminifers, including common to abundant warm-water acarininids (Fig. 19) and some strongly keeled morozovellids, attained their maximum diversity. Calcareous nannofossil floras were also diverse and include discoasters, sphenoliths, and common *Zygrhablithus bijugatus*.

The middle Eocene was a transitional period leading to cooler surface waters during the Oligocene. The diversity of nannofossil floras steadily declined but remained relatively high during the early middle Eocene. The nannofossil assemblages are transitional between the warmer water assemblages of the Paleocene–early Eocene and those of the the cooler water Oligocene. Planktonic foraminifer diversity also declined, with a much lower abundance of acarininids after ~50 Ma. The warm-water acarin-

inid group disappeared altogether by the middle middle Eocene (~45–46 Ma), as foraminifer assemblages became dominated by only cold water and dissolution-resistant forms.

Lower to middle Eocene sediments are remarkably homogeneous, consisting of nannofossil chalks and micritic nannofossil chalks, with carbonate percentages generally ranging from 70% to 90%. A significant decrease in carbonate content occurs in the upper middle Eocene, between ~46 and 43 Ma. Above this depth, middle Eocene sediments have a lower carbonate content (generally less than 50%) and contain clay-rich intervals. These changes were possibly caused by a rise of the lysocline and an increase in the transport and deposition of clays. The absence of siliceous microfossils is related to diagenesis of biogenic opal, as is the case in age-equivalent sediments from Site 699 ("Geochemistry" section).

Middle Eocene–Late Pliocene Hiatus (~42.6 Ma–Late Pliocene)

A striking difference exists in the post-middle Eocene sediment thickness of Holes 700B and 699A, which are only 21 km from one another (Fig. 1). The thickness of this interval in Hole 699A is ~360 m, whereas it is no more than 26.4 m in Hole 700B. Thicknesses of lower to middle Eocene sequences are comparable at both sites. This difference in post-middle Eocene sediment thickness can only be attributed to the post-early Oligocene block faulting in the area of these sites, as was discussed previously. This faulting left Site 700 as an isolated bathymetric high more exposed to the strong erosive forces of Circumpolar Deep Water (CPDW) and its precursor. Although the depth differential between the two sites was small (~500 m), the exposed position of Site 700 led to deep-cutting erosion that removed 350 to 550 m of overburden at Site 700 ("Physical Properties" section). The uplift of Site 700 occurred after diagenesis of the sediment and resulted in some rebound caused by relief of overburden pressure ("Physical Properties" section). A tectonic influence on the removal of the upper sedimentary sequence cannot be ruled out; however, no evidence was found in Hole 699A for mass transport (such as debris flows) of sediments triggered by the uplift.

Additional periods of nondeposition and erosion during the Neogene have reduced the accumulation of post-middle Eocene sediments to less than 26.4 m. The difference in Neogene sediment thickness between Sites 699 and 700 demonstrates the influence of CPDW upon restricting sedimentation on bathymetric highs, regardless of their relief. Previous studies have also demonstrated the effectiveness of CPDW in limiting late Neogene sediment accumulation on exposed regions of other rises this sector of the Southern Ocean (Ciesielski and Wise, 1977; Ciesielski et al., 1983; Ledbetter and Ciesielski, 1982).

Late Pliocene–Quaternary (~2.5–2.2 Ma to Holocene)

Little upper Pliocene–Quaternary sediment was recovered at Site 700. Only 40 cm of sediment of this age was recovered between the seafloor and 16.9 mbsf. Quaternary sediment, assigned to within the Brunhes Chron (0–0.62 Ma) on the basis of the diatom assemblage, was encountered in the upper 10 cm, whereas the upper Pliocene was represented between 0.1 and 9.6 mbsf. These upper Pliocene–Quaternary sediments (Unit I) are diatom ooze and muddy diatom ooze with a significant amount of ice-rafted detritus. The <1- to 34.6-m possible thickness of Pliocene to Quaternary sediment at Site 700 contrasts with 60 m of age-equivalent sediment at Site 699.

Paleocirculation

There is little evidence for major erosional events at Sites 699 and 700 that predate the Eocene opening of the Islas Orcadas Rise–Meteor Rise gateway. Present biostratigraphic data reveal two significant hiatuses, one encompassing most of the Campanian in Hole 700B and another spanning the upper middle to lower upper Eocene in Hole 699A. A tectonic influence on the formation of the Campanian hiatus cannot be ruled out. The Eocene hiatus in Hole 699A slightly postdates the opening of the Islas Orcadas Rise–Meteor Rise gateway. Although only a portion of this missing interval is present in Hole 700B, a significant reduction in the sedimentation rate is noted to precede the erosional/nondepositional episode at Site 699. An overall increase in bottom-current activity through the Georgia Basin, relative to the earlier Paleogene, is inferred from the records of Holes 699A and 700B. This increase occurred after formation of the Islas Orcadas Rise–Meteor Rise gateway, which might have been expected to have the opposite influence on benthic circulation through the Georgia Basin, unless it was accompanied by an overall increase in the strength of benthic circulation.

Prior to the late middle Eocene, Paleogene sedimentation in the vicinity of Sites 699 and 700 was remarkably continuous, even though the Georgia Basin should have been an avenue for deep-water exchange from the antarctic to the South Atlantic prior to formation of the Islas Orcadas Rise–Meteor Rise gateway. Therefore, if the East Georgia Basin served as an early Paleogene deep-water passage, thermohaline circulation was too weak to cause significant erosion. In contrast, the intensity of late Neogene benthic circulation in the basin exceeded that of the Paleogene, greatly attenuating Neogene to upper Paleogene sedimentary sequences.

REFERENCES

Archie, G. E., 1942. The electrical resistivity log as an aid in determining some reservoir characteristics. *Trans. Am. Inst. Min., Metall. Pet. Eng.*, 146:54–67.

Baker, P. A., 1986. Pore water chemistry of carbonate-rich sediments, Lord House Rise, Southwest Pacific Ocean. *In* Kennett, J. P., von der Borch, C. C., et al., *Init. Repts. DSDP*, 90: Washington (U.S. Govt. Printing Office), 1249–1256.

Barker, P. F., and Hill, I. A., 1981. Back-arc extension in the Scotia Sea. *Philos. Trans. R. Soc. London A*, 300:249–262.

Barker, P. F., Kennett, J. P., et al., 1988. *Proc. ODP, Init. Repts.*, 113: College Station, TX (Ocean Drilling Program).

Berggren, W. A., Kent, D. V., and Flynn, J. J., 1985. Paleogene geochronology and chronostratigraphy. *In* Snelling, N. J. (Ed.), *The Chronology of the Geological Record*: Geol. Soc. London Mem., 10:141–195.

Boersma, A., and Premoli Silva, I., 1983. Paleocene planktonic foraminiferal biogeography and the paleoceanography of the Atlantic Ocean. *Micropaleontology*, 29:355–381.

Bukry, D., 1976. Cenozoic silicoflagellate and coccolith stratigraphy, South Atlantic Ocean, Deep Sea Drilling Project Leg 36. *In* Hollister, C. D., Craddock, C., et al., *Init. Repts. DSDP*, 35: Washington (U.S. Govt. Printing Office), 885–917.

Busen, K. E., and Wise, S. W., Jr., 1977. Silicoflagellate stratigraphy. Leg 36. *In* Barker, P., Dalziel, I.W.D., et al., *Init. Repts. DSDP*, 36: Washington (U.S. Govt. Printing Office), 697–743.

Ciesielski, P. F., 1983. The Neogene and Quaternary diatom biostratigraphy of subantarctic sediments, Deep Sea Drilling Project Leg 71. *In* Ludwig, W. J., Krasheninnikov, V. A., et al., *Init. Repts. DSDP*, 71: Washington (U.S. Govt. Printing Office), 635–666.

Ciesielski, P. F., Ledbetter, M. T., and Ellwood, B. B., 1983. The development of Antarctic glaciation and the Neogene paleoenvironment of the Maurice Ewing Bank. *Mar. Geol.*, 46:1–51.

Ciesielski, P. F., and Wise, S. W., Jr., 1977. Geologic history of the Maurice Ewing Bank of the Falkland Plateau (Southwest Atlantic sector of the Southern Ocean) based upon piston and drill cores. *Mar. Geol.*, 25:175–207.

Crux, J. A., 1982. Upper Cretaceous (Cenomanian to Campanian) calcareous nannofossils. *In* Lord, A. R. (Ed.), *A Stratigraphical Index of Calcareous Nannofossils*: Chichester (Ellis Horwood), 81–135.

Dumitrica, P., 1973. Paleocene, late Oligocene and post-Oligocene silicoflagellates in southwestern Pacific sediments cored on DSDP Leg 21. *In* Burnes, R. E., Andrews, J. E., et al., *Init. Repts. DSDP*, 21: Washington (U.S. Govt. Printing Office), 837–883.

Fisher, A. G., and Arthur, M. A., 1977. Secular variations in the pelagic realm. *In* Cook, H. S., and Enos, P. (Eds.), *Basinal Carbonate Sediments*: Spec. Publ. Soc. Econ. Paleontol. Mineral., 25:19–50.

Garrison, R. E., 1981. Diagenesis of oceanic carbonate sediments: a review of the DSDP perspective. *In* Warme, J. E., Douglas, R. G., and Winterer, E. L. (Eds.), *The Deep Sea Drilling Project: A Decade of Progress:* Spec. Publ. Soc. Econ. Paleontol. Mineral., 32:181–207.

Gieskes, J. M., 1983. The chemistry of interstitial waters of deep-sea sediments: interpretation of deep-sea drilling data. *In* Riley, J. P., and Chester, R. (Eds.), *Chemical Oceanography* (Vol. 8): London (Academic Press), 221–269.

Gombos, A. M., Jr., 1977. Paleogene and Neogene diatoms from the Falkland Plateau and the Malvinas Outer Basin: Leg 36, Deep Sea Drilling Project. *In* Barker, P., Dalziel, I.W.D., et al., *Init. Repts. DSDP*, 36: Washington (U.S. Govt. Printing Office), 575–688.

———, 1984. Late Paleocene diatoms in the Cape Basin. *In* Hsü, K. J., LaBrecque, J. L., et al., *Init. Repts. DSDP*, 73: Washington (U.S. Govt. Printing Office), 495–511.

Hassan, M. L. 1976. Contribution a l'etude des comportements du thorium et du potassium dans las roches sedimentaires. *C. R. Acad. Sci. Ser. 2,* 280:533–535.

Jenkins, D. G., 1985. Southern mid-latitude Paleocene to Holocene planktic foraminifera. *In* Bolli, H. M., Saunders, J. B., and Perch-Nielsen, K. (Eds.), *Plankton Stratigraphy*: Cambridge (Cambridge Univ. Press), 263–282.

Kastner, M., 1981. Authigenic silicates in deep-sea sediments: formation and diagenesis. *In* Emiliani, C. (Ed.), *The Sea* (Vol. 7), *The Oceanic Lithosphere*: New York (Wiley), 915–980.

Kent, D. V., and Gradstein, F. M., 1985. A Cretaceous and Jurassic geochronology. *Geol. Soc. Am. Bull.*, 96:1419–1427.

Krasheninnikov, V. A., and Basov, I. A., 1983. Cenozoic planktonic foraminifers of the Falkland Plateau and Argentine Basin, Deep Sea Drilling Project Leg 71. *In* Ludwig, W. J., Krasheninnikov, V. A., et al., *Init. Repts. DSDP*, 71: Washington (U.S. Govt. Printing Office), 821–858.

LaBrecque, J. L., and Hayes, D. E., 1979. Seafloor spreading history of the Agulhas Basin. *Earth Planet. Sci. Lett.*, 45:411–428.

Ledbetter, M. T., and Ciesielski, P. F., 1982. Bottom-current erosion along a traverse in the South Atlantic sector of the Southern Ocean. *Mar. Geol.*, 46:329–341.

Ludwig, W. J., 1983. Geologic framework of the Falkland Plateau. *In* Ludwig, W. J., Krasheninnikov, V. A., et al., *Init. Repts. DSDP*, 71: Washington (U.S. Govt. Printing Office), 281–293.

Martini, E., 1971. Standard Tertiary and Quaternary calcareous nannoplankton zonation. *In* Farinacci, A. (Ed.), *Proc. Planktonic Conf. II Rome 1970*: Rome (Technoscienze), 2:739-785.

McCollum, D. W., 1975. Diatom stratigraphy of the Southern Ocean. *In* Hayes, D. E., Frakes, L. A., et al., *Init. Repts. DSDP*, 28: Washington (U.S. Govt. Printing Office), 515–572.

McGowran, B., 1986. Cainozoic oceanic and climatic events: the Indo-Pacific foraminiferal biostratigraphic records. *Palaeogeogr., Palaeoclimatol., Palaeoecol.*, 55:247–265.

Miller, K. G., and Katz, M. E., in press. Oligocene to Miocene benthic foraminiferal and abyssal circulation changes in the North Atlantic. *Micropaleontology*.

Morkhoven, F.P.C.M. van, Berggren, W. A., and Edwards, A. S., 1986. Cenozoic cosmopolitan deep-water benthic foraminifera. *Cent. Rech. Explor. Prod. Elf Aquitaine Mem.*, 11.

Perch-Nielsen, K., 1985. Cenozoic calcareous nannofossils. *In* Bolli, H. M., Saunders, J. B., and Perch-Nielsen, K. (Eds.), *Plankton Stratigraphy*: Cambridge (Cambridge Univ. Press), 427–554.

Pessagno, E. A., Jr., 1975. Upper Cretaceous radiolaria from DSDP Site 275. *In* Kennett, J. P., Houtz, R. E., et al., *Init. Repts. DSDP*, 29: Washington (U.S. Govt. Printing Office), 1011–1029.

Pujol, C., and Sigal, J., 1979. *Les Foraminiféres Planktoniques Paléogènes du Site 245 Bassin de Madagascar—Biostratigraphic (DSDP, Leg 25)*: Bordeaux (CNRS), 1–105.

Sanfilippo, A., and Riedel, W. R., 1985. Cretaceous radiolaria. *In* Bolli, H. M., Saunders, J. B., and Perch-Nielsen, K. (Eds.), *Plankton Stratigraphy*: Cambridge (Cambridge Univ. Press), 573–630.

Sanfilippo, A., Westberg-Smith, M. J., and Riedel, W. R., 1985. Cenozoic radiolaria. *In* Bolli, H. M., Saunders, J. B., and Perch-Nielsen, K. (Eds.), *Plankton Stratigraphy*: Cambridge (Cambridge Univ. Press), 631–712.

Schlanger, S. D., and Douglas, R. G., 1974. The pelagic-ooze-chalk-limestone transition and its implication for marine stratigraphy. *Spec. Publ. Int. Assoc. Sedimentol.*, 1:117–148.

Serra, O., 1984. *Fundamentals of Well Log Interpretation: Volume 1. The Acquisition of Logging Data*: Amsterdam (Elsevier).

Sissingh, W., 1977. Biostratigraphy of Cretaceous calcareous nannoplankton. *Geol. Mijnbouw*, 56:37–65.

Sliter, W. V., 1977. Cretaceous foraminifers from the southwestern Atlantic Ocean, Leg 36, Deep Sea Drilling Project. *In* Barker, P., Dalziel, I.W.D., et al., *Init. Repts. DSDP*, 36: Washington (U.S. Govt. Printing Office), 519–545.

Sliter, W. V., and Baker, R. A., 1972. Cretaceous bathymetric distribution of benthonic foraminifers. *J. Foraminiferal Res.*, 2:167–183.

Tjalsma, R. C., and Lohmann, G. P., 1983. Paleocene-Eocene bathyal and abyssal benthic foraminifera from the Atlantic Ocean. *Micropaleontol. Spec. Publ.*, 4.

Weaver, F. M., 1976. Antarctic Radiolaria from the Southeast Pacific Basin, Deep Sea Drilling Project, Leg 35. *In* Hollister, C. D., Craddock, C., et al., *Init. Repts. DSDP*, 35: Washington (U.S. Govt. Printing Office), 569–603.

Wise, S. W., Jr., and Weaver, F. M., 1974. Chertification of oceanic sediments. *In* Hsü, K. J., and Jenkyns, D. G. (Eds.), Pelagic Sediments: on Land and under the Sea. *Spec. Publ. Int. Assoc. Sedimentol.*, 1: 301–326.

Ms 114A-107

Summary log for Hole 700B.

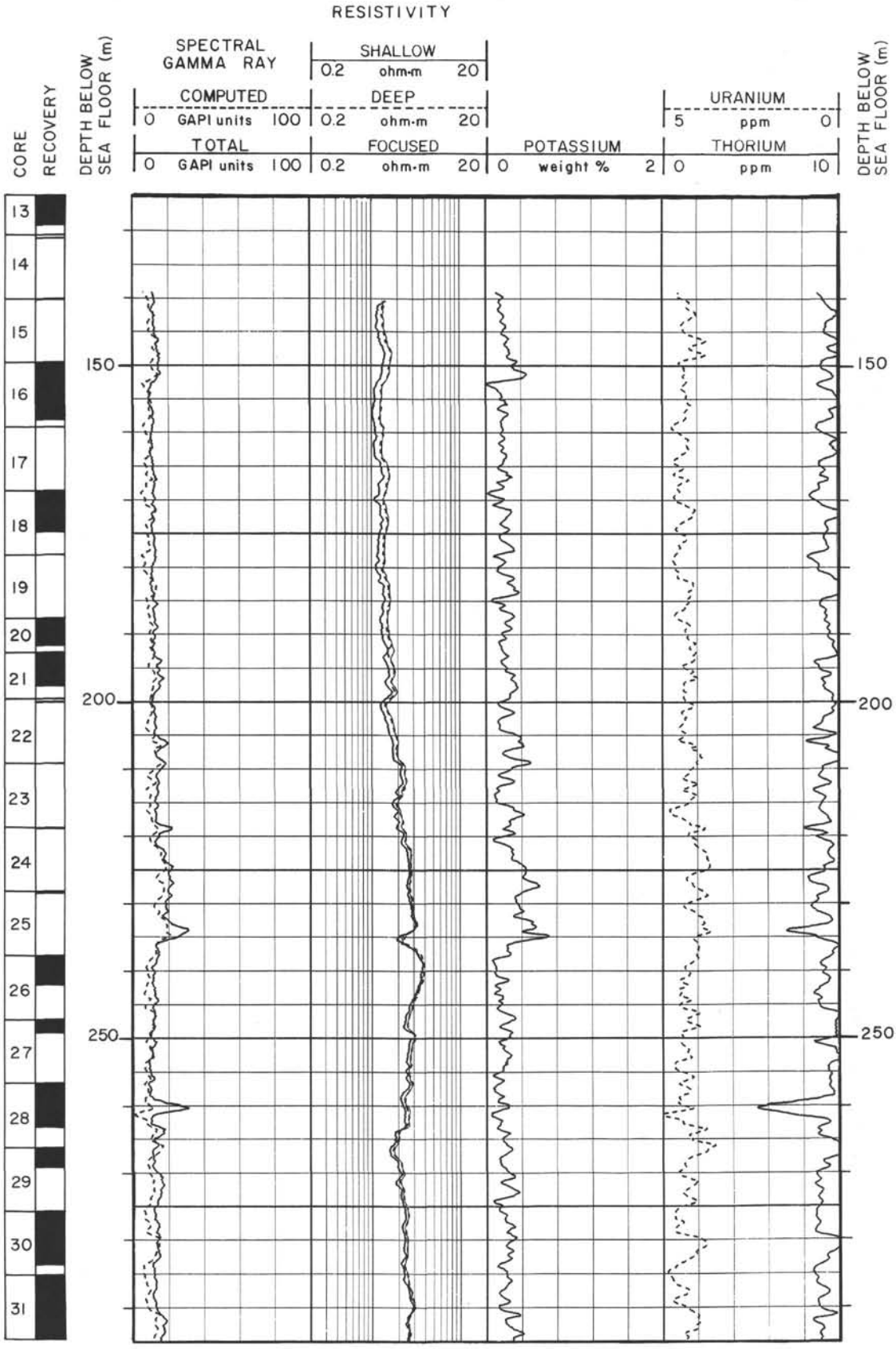

Summary log for Hole 700B (continued).

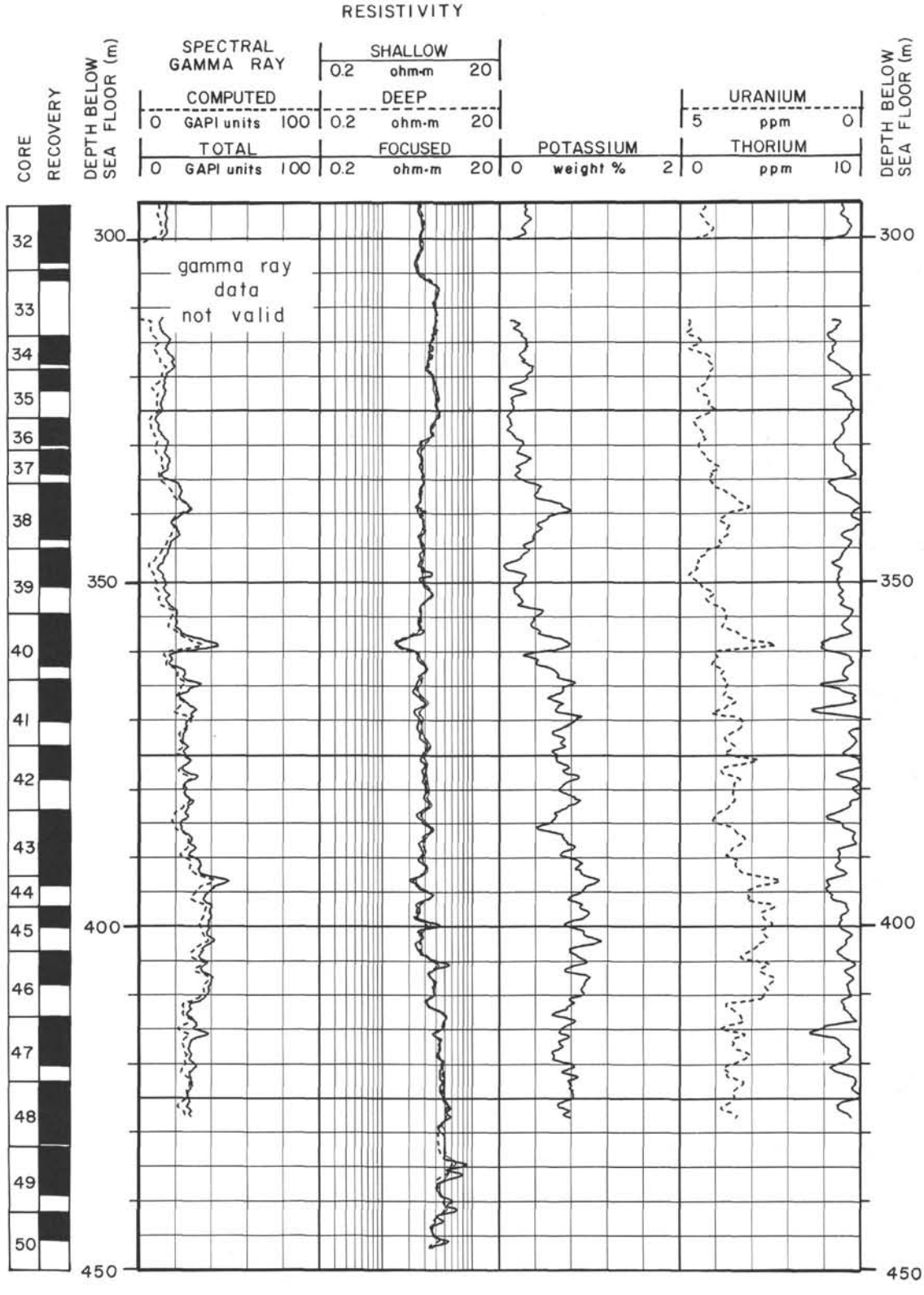

Summary log for Hole 700B (continued).

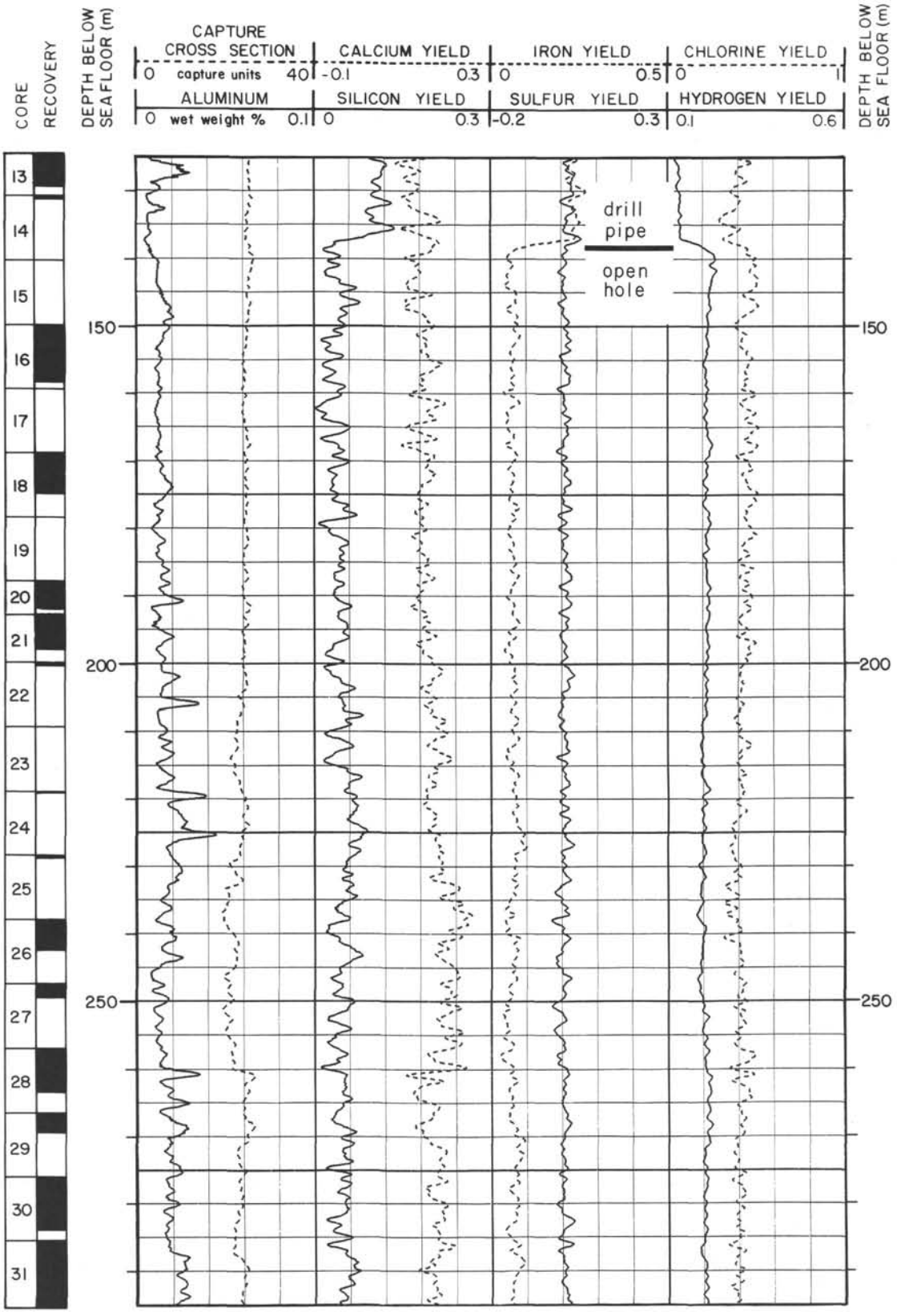

Summary log for Hole 700B (continued).

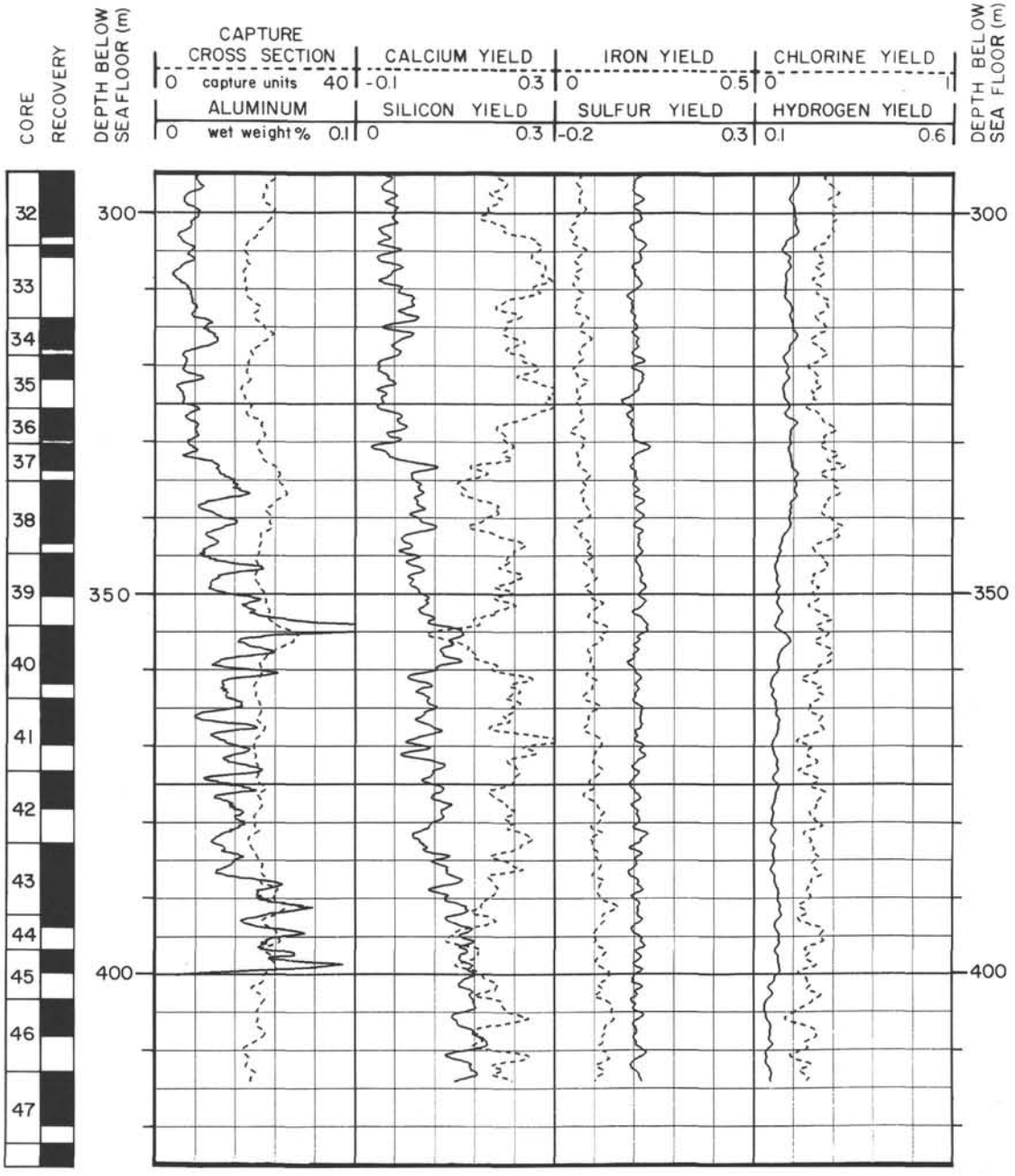

SITE 700 HOLE A CORE 1R CORED INTERVAL 3601.0-3601.1 mbsl; 0.0-0.1 mbsf

TIME-ROCK UNIT	BIOSTRAT. ZONE/ FOSSIL CHARACTER: FORAMINIFERS	NANNOFOSSILS	RADIOLARIANS	DIATOMS	SILICO-FLAGELLATES	PALEOMAGNETICS	PHYS. PROPERTIES	CHEMISTRY	SECTION	METERS	GRAPHIC LITHOLOGY	DRILLING DISTURB.	SED. STRUCTURES	SAMPLES	LITHOLOGIC DESCRIPTION
QUATERNARY		Barren	*Antarctissa denticulata*	*C. lentiginosus*					1						SURFACE GRAVEL Highly disturbed; very poor recovery. Recovery consists of surface gravel.

SITE 700 HOLE A CORE 2R CORED INTERVAL 3601.1-3610.7 mbsl; 0.1-9.6 mbsf

TIME-ROCK UNIT	BIOSTRAT. ZONE/ FOSSIL CHARACTER: FORAMINIFERS	NANNOFOSSILS	RADIOLARIANS	DIATOMS	SILICO-FLAGELLATES	PALEOMAGNETICS	PHYS. PROPERTIES	CHEMISTRY	SECTION	METERS	GRAPHIC LITHOLOGY	DRILLING DISTURB.	SED. STRUCTURES	SAMPLES	LITHOLOGIC DESCRIPTION
LOWER PLIOCENE			*Helothalus vema*	*C. vulnificus*	Unzoned				1			○		*	MUDDY DIATOM OOZE, with SURFACE GRAVEL Highly disturbed; very poor recovery. Recovery consists of diatom ooze, mixed with surface gravel. SMEAR SLIDE SUMMARY (%): 1, 10 D COMPOSITION: Quartz 3 Feldspar 2 Clay 10 Diatoms 80 Radiolarians 2 Silicoflagellates 3

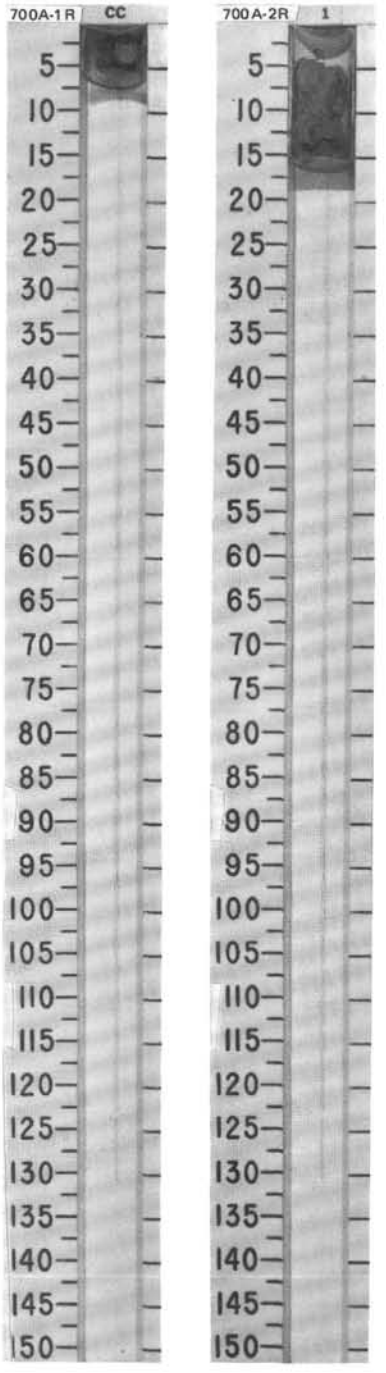

SITE 700 HOLE B CORE 1W CORED INTERVAL 3601.0-3617.9 mbsl; 0.0-16.9 mbsf

TIME-ROCK UNIT	BIOSTRAT. ZONE/ FOSSIL CHARACTER: FORAMINIFERS	NANNOFOSSILS	RADIOLARIANS	DIATOMS	SILICO-FLAGELLATES	PALEOMAGNETICS	PHYS. PROPERTIES	CHEMISTRY	SECTION	METERS	GRAPHIC LITHOLOGY	DRILLING DISTURB.	SED. STRUCTURES	SAMPLES	LITHOLOGIC DESCRIPTION
QUATERNARY	Barren		no sample examined	*C. lentiginosus*	no sample examined				1 CC					*	MUDDY DIATOM OOZE and PEBBLES

Highly disturbed.

Major lithology: Muddy diatom ooze, olive (5Y 5/4). Some pebbles, possibly ice-rafted dropstones(?).

SMEAR SLIDE SUMMARY (%):

	1, 4 D
COMPOSITION:	
Quartz	5
Feldspar	2
Clay	30
Diatoms	58
Radiolarians	3
Silicoflagellates	2

SITE 700 HOLE B CORE 2R CORED INTERVAL 3617.9-3627.4 mbsl; 16.9-26.4 mbsf

TIME-ROCK UNIT	BIOSTRAT. ZONE/ FOSSIL CHARACTER: FORAMINIFERS	NANNOFOSSILS	RADIOLARIANS	DIATOMS	SILICO-FLAGELLATES	PALEOMAGNETICS	PHYS. PROPERTIES	CHEMISTRY	SECTION	METERS	GRAPHIC LITHOLOGY	DRILLING DISTURB.	SED. STRUCTURES	SAMPLES	LITHOLOGIC DESCRIPTION
QUATERNARY			No sample examined	*C. elliptic us-A. ingens*	No sample examined				1						DIATOM OOZE

Highly disturbed.

Major lithology: Diatom ooze, olive (5Y 5/3).

SMEAR SLIDE SUMMARY (%):

	1, 15 D
COMPOSITION:	
Quartz/feldspar	4
Clay	40
Accessory minerals	3
Diatoms	50
Sponge spicules	1
Silicoflagellates	1
Pellets	1

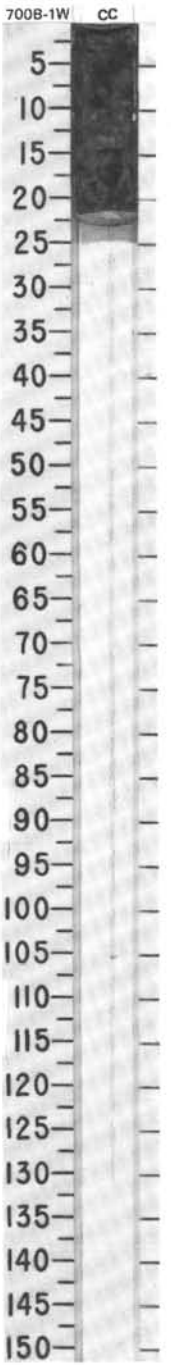

SITE 700 HOLE B CORE 3R CORED INTERVAL 3627.4-3636.9 mbsl; 26.4-35.9 mbsf

TIME-ROCK UNIT	BIOSTRAT. ZONE/ FOSSIL CHARACTER: FORAMINIFERS	NANNOFOSSILS	RADIOLARIANS	DIATOMS	SILICO-FLAGELLATES	PALEOMAGNETICS	PHYS. PROPERTIES	CHEMISTRY	SECTION	METERS	GRAPHIC LITHOLOGY	DRILLING DISTURB.	SED. STRUCTURES	SAMPLES
MIDDLE EOCENE	*Globigerinatheka index* Zone UPPER MIDDLE EOCENE P12 - P13	NP 16	Barren	Barren	Barren		ϕ=69.39 ρ_g=2.67		1, 2, CC	0.5, 1.0				* *

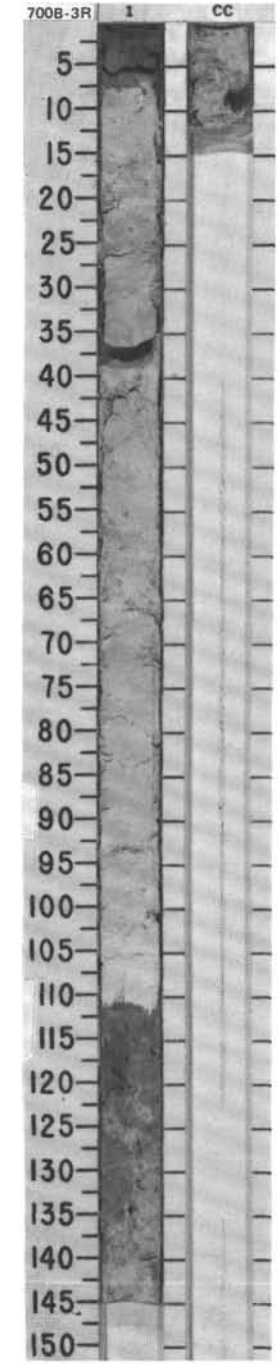

LITHOLOGIC DESCRIPTION

MICRITIC NANNOFOSSIL OOZE

Slightly disturbed, Section 1, 0–6 cm.

Major lithology: Micritic nannofossil ooze, white (5Y 8/1) to very pale brown (10YR 7/3).

Mottling (bioturbation?) throughout the core. *Zoophycos*, Section 1, 65 cm.

Minor lithologies:
a. Nannofossil mud, light yellowish brown (10YR 6/4), and gravel (Contamination in Section 1, 0-6 cm).
b. Clayey nannofossil ooze and clayey mud, Section 1, 110-150 cm.

SMEAR SLIDE SUMMARY (%):

	1, ? D
COMPOSITION:	
Quartz/feldspar	4
Clay	50
Volcanic glass	Tr
Accessory minerals	Tr
Diatoms	5

SITE 700 HOLE B CORE 4R CORED INTERVAL 3636.9-3646.4 mbsl; 35.9-45.4 mbsf

TIME-ROCK UNIT	BIOSTRAT. ZONE/ FOSSIL CHARACTER: FORAMINIFERS	NANNOFOSSILS	RADIOLARIANS	DIATOMS	SILICO-FLAGELLATES	PALEOMAGNETICS	PHYS. PROPERTIES	CHEMISTRY	SECTION	METERS	GRAPHIC LITHOLOGY	DRILLING DISTURB.	SED. STRUCTURES	SAMPLES
MIDDLE EOCENE	*Globigerinatheka index* Zone UPPER MIDDLE EOCENE P12 - P13	NP 16	Barren	Barren	Barren		ϕ=74.86 ρ_g=2.66		1, 2, CC	0.5, 1.0				*

LITHOLOGIC DESCRIPTION

MICRITIC NANNOFOSSIL OOZE

Major lithology: Micritic nannofossil ooze, white (10YR 8/3) to very pale brown (10YR 7/3). Progressive color variations appear down core.

Mottling due to bioturbation.

SMEAR SLIDE SUMMARY (%):

	1, 55 D
COMPOSITION:	
Calcite	70
Nannofossils	30
Pellets	Tr

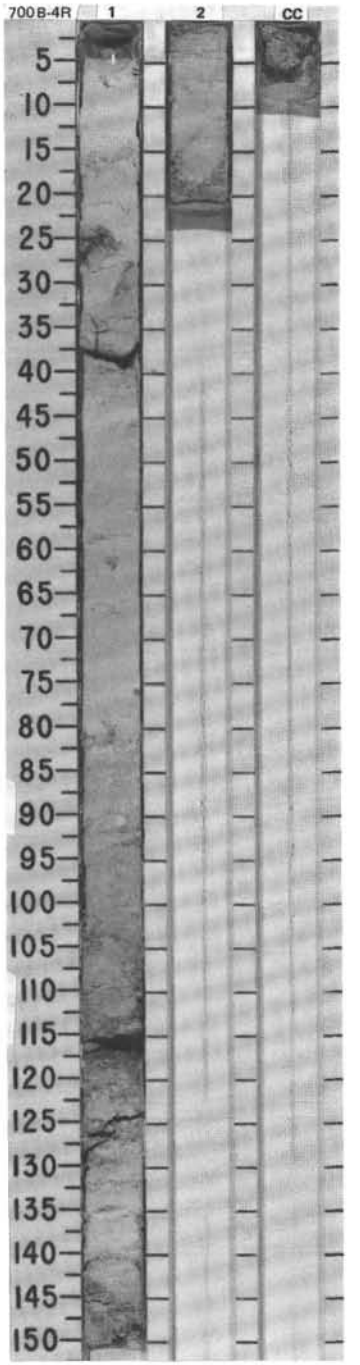

SITE 700 HOLE B CORE 5R CORED INTERVAL 3646.4-3655.9 mbsl; 45.4-54.9 mbsf

TIME-ROCK UNIT	BIOSTRAT. ZONE/ FOSSIL CHARACTER: FORAMINIFERS	NANNOFOSSILS	RADIOLARIANS	DIATOMS	SILICO-FLAGELLATES	PALEOMAGNETICS	PHYS. PROPERTIES	CHEMISTRY	SECTION	METERS	GRAPHIC LITHOLOGY	DRILLING DISTURB.	SED. STRUCTURES	SAMPLES
MIDDLE EOCENE	*Globigerinatheka index* Zone	UPPER MIDDLE EOCENE P12 - P13 NP 15-16 not examined	Barren	Barren	Barren	ϕ=63.99 ρ_g=2.88	ϕ=58.61 ρ_g=2.75 ϕ=75.37 ρ_g=2.97 ϕ=68.54 ρ_g=2.74		1 2 3 4 CC	0.5 1.0	Mr 2			* * *

LITHOLOGIC DESCRIPTION

NANNOFOSSIL CHALK

Major lithology: Nannofossil chalk, very pale brown (10YR 7/3, 8/3) and pinkish white (7.5YR 8/2); contacts are gradational and indistinct. Nannofossil ooze appears in softer intervals.

Mottling due to minor to moderate bioturbation.

Minor lithology: Manganese nodules, due to downhole contamination, and zeolitic clay, pale olive (5Y 6/3), containing manganese micronodules. Manganese micronodules appear at Section 2, 51 and 96 cm.

SMEAR SLIDE SUMMARY (%):

	1, 12 D	1, 72 D	4, 70 D
COMPOSITION:			
Quartz/feldspar	Tr	—	—
Clay	—	2	2
Calcite	65	—	—
Accessory minerals	Tr	—	Tr
Foraminifers	10	—	1
Nannofossils	20	98	97
Pellets (burrows?)	5	—	—

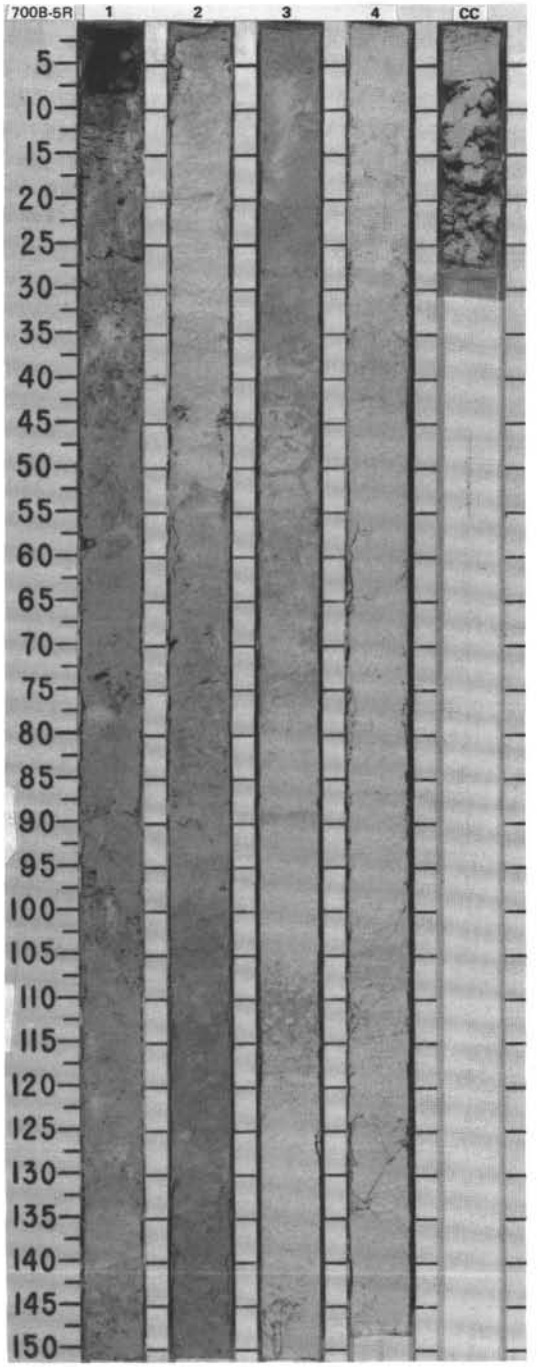

SITE 700 HOLE B CORE 6R CORED INTERVAL 3655.9-3665.4 mbsl; 54.9-64.4 mbsf

TIME-ROCK UNIT	BIOSTRAT. ZONE/ FOSSIL CHARACTER: FORAMINIFERS	NANNOFOSSILS	RADIOLARIANS	DIATOMS	SILICO. FLAGELLATES	PALEOMAGNETICS	PHYS. PROPERTIES	CHEMISTRY	SECTION	METERS	GRAPHIC LITHOLOGY	DRILLING DISTURB.	SED. STRUCTURES	SAMPLES
MIDDLE EOCENE	*Globigerinatheka index* Zone	LOWER MIDDLE EOCENE P12 - P13 NP 15-16	Barren	Barren	Barren	ϕ=64.14 ρ_g=2.62	ϕ=63.50 ρ_g=2.73 ϕ=59.24 ρ_g=2.72 ϕ=64.3 ρ_g=2.83 ϕ=63.77 ρ_g=2.77 ϕ=67.16 ρ_g=2.70		1 2 3 4 5 6 CC	0.5 1.0				* * *

LITHOLOGIC DESCRIPTION

NANNOFOSSIL CHALK

Moderately disturbed, Section 3, 60-150 cm; drilling slurry between hard "biscuits".

Major lithology: Nannofossil chalk, very pale brown (10YR 8/3) and pinkish white (7.5YR 8/2). Contact between colors is well defined at Section 2, 142 cm.

Moderately bioturbated, *Planolites* and *Thalassinoides*.

Minor lithology: Manganese nodules, Section 1, 24-30 cm.

SMEAR SLIDE SUMMARY (%):

COMPOSITION:	1, 82 D	3, 12 D	CC D
Quartz/feldspar	—	1	—
Feldspar	Tr	—	—
Mica	Tr	—	—
Clay	5	—	—
Calcite	9	5	41
Accessory minerals	Tr	Tr	1
Foraminifers	—	—	3
Nannofossils	86	89	50
Diatoms	—	Tr	—
Pellets	—	5	5

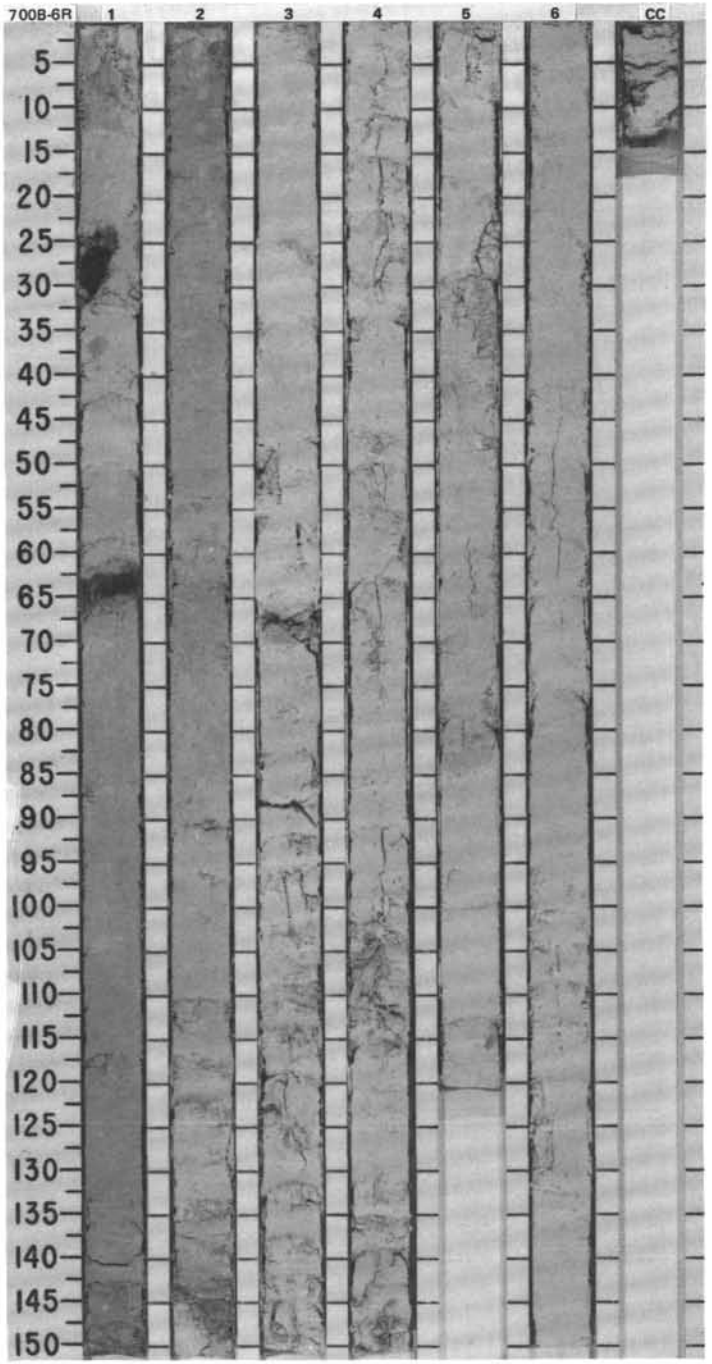

SITE 700 HOLE B CORE 7R CORED INTERVAL 3665.4-3674.9 mbsl; 64.4-73.9 mbsf

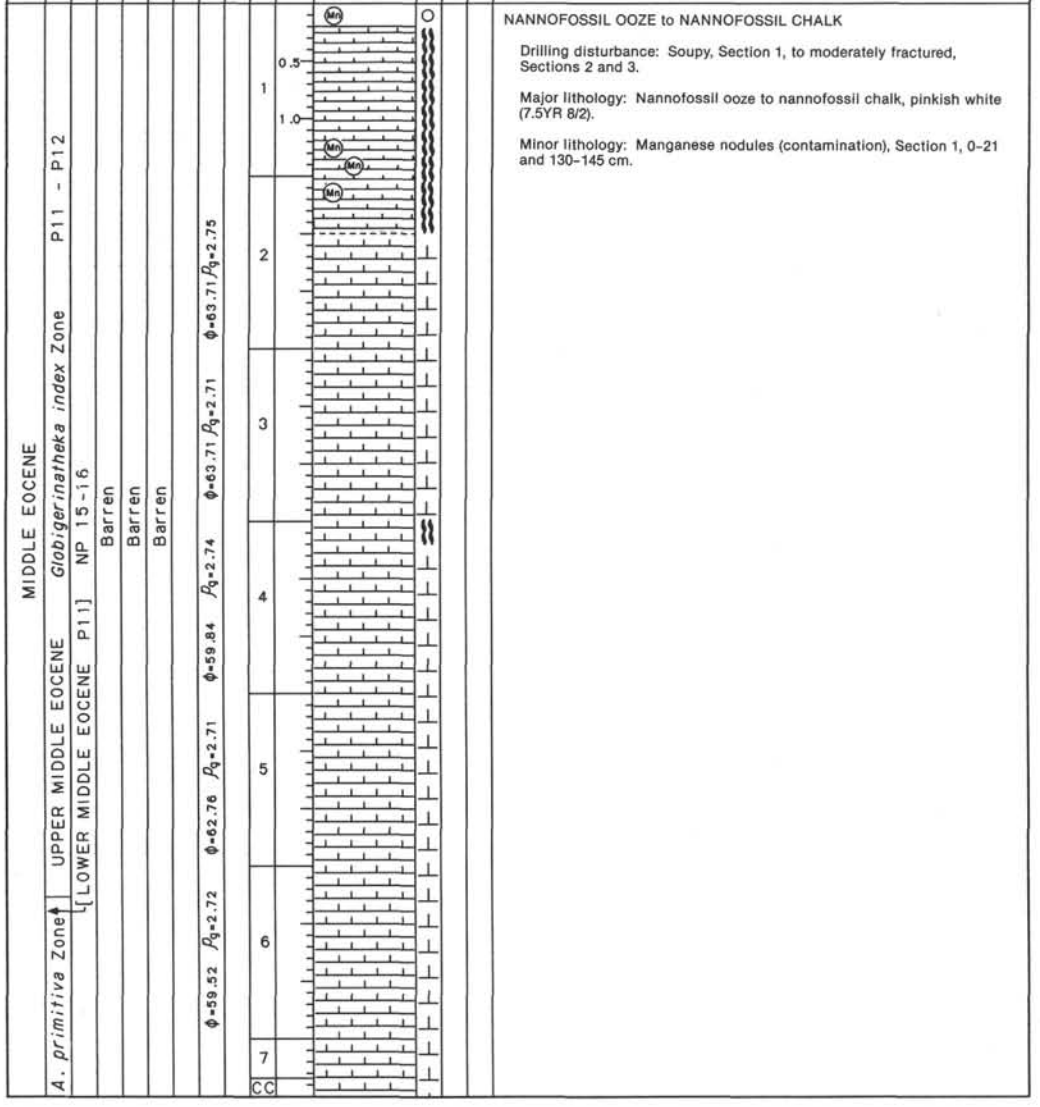

LITHOLOGIC DESCRIPTION

NANNOFOSSIL OOZE to NANNOFOSSIL CHALK

Drilling disturbance: Soupy, Section 1, to moderately fractured, Sections 2 and 3.

Major lithology: Nannofossil ooze to nannofossil chalk, pinkish white (7.5YR 8/2).

Minor lithology: Manganese nodules (contamination), Section 1, 0-21 and 130-145 cm.

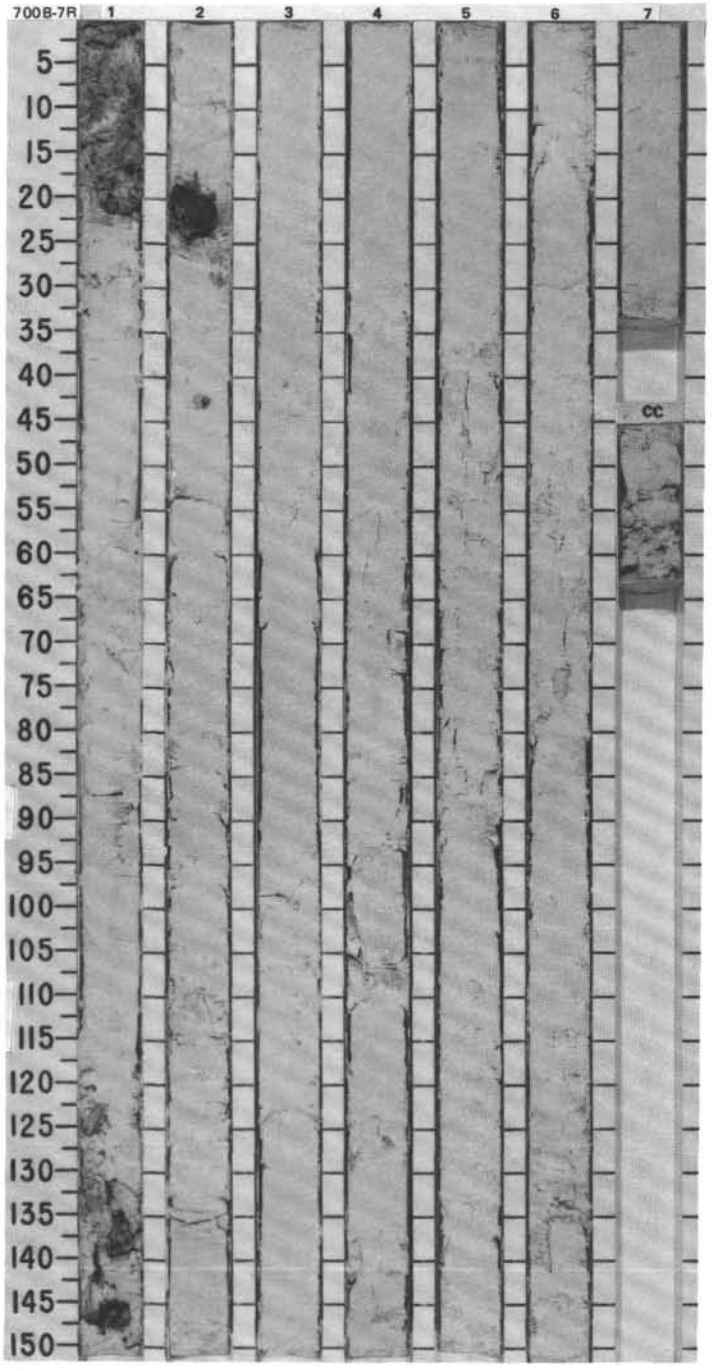

SITE 700 HOLE B CORE 8R CORED INTERVAL 3674.9-3684.4 mbsl; 73.9-83.4 mbsf

TIME-ROCK UNIT	BIOSTRAT. ZONE/ FOSSIL CHARACTER: FORAMINIFERS	NANNOFOSSILS	RADIOLARIANS	DIATOMS	SILICO. FLAGELLATES	PALEOMAGNETICS	PHYS. PROPERTIES	CHEMISTRY	SECTION	METERS	GRAPHIC LITHOLOGY	DRILLING DISTURB.	SED. STRUCTURES	SAMPLES
MIDDLE EOCENE	LOWER MIDDLE EOCENE (*Acarinina primitiva* Zone) P11	NP 15-16	Barren	Barren	Barren		ϕ=61.72 ρ_g=2.72; ϕ=56.93 ρ_g=2.73; ϕ=58.11 ρ_g=2.80; ϕ=59.4 ρ_g=2.73		1, 2, 3, 4, 5, CC	0.5, 1.0				*

LITHOLOGIC DESCRIPTION

NANNOFOSSIL CHALK

Major lithology: Nannofossil chalk, white (2.5Y 8/2 to 5Y 8/1). Faintly mottled to uniform structureless chalk.

SMEAR SLIDE SUMMARY (%):

	1, 83 D
COMPOSITION:	
Clay	1
Accessory minerals	Tr
Nannofossils	99

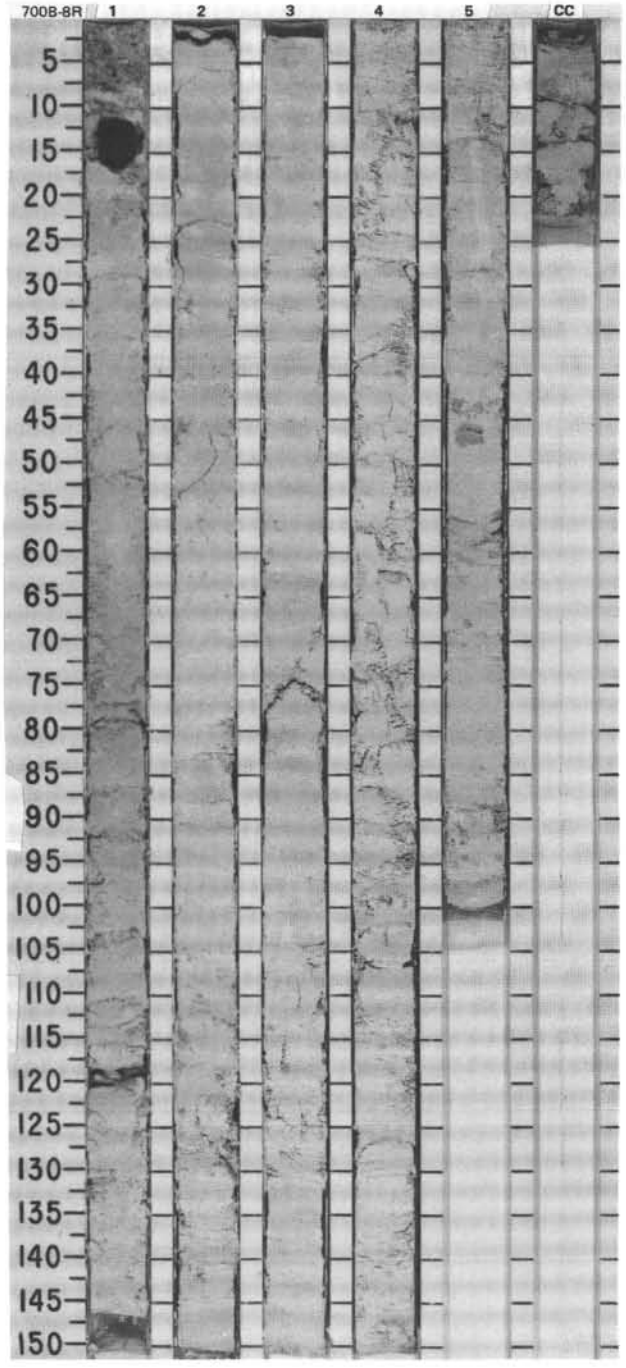

SITE 700 HOLE B CORE 9R CORED INTERVAL 3684.4-3693.9 mbsl; 83.4-92.9 mbsf

TIME-ROCK UNIT	BIOSTRAT. ZONE/ FOSSIL CHARACTER: FORAMINIFERS	NANNOFOSSILS	RADIOLARIANS	DIATOMS	SILICO-FLAGELLATES	PALEOMAGNETICS	PHYS. PROPERTIES	CHEMISTRY	SECTION	METERS	GRAPHIC LITHOLOGY	DRILLING DISTURB.	SED. STRUCTURES	SAMPLES	LITHOLOGIC DESCRIPTION
MIDDLE EOCENE	LOWER MIDDLE EOCENE (*Acarinina primitiva* Zone) P11	not examined	Barren	Barren	Barren	ϕ=54.28/ρ_g=2.66	ϕ=60.02 ρ_g=2.80	ϕ=55.51 ρ_g=2.75	ϕ=57.82 ρ_g=2.74						
				NP 14-15					1	0.5, 1.0	(Mn), VOID			*	
									2					*	
									3						
									4						
									5						
									6						
									CC						

NANNOFOSSIL CHALK

Major lithology: Nannofossil chalk, white (5Y 8/1) or absolute white (no hue on color chart).

Minor lithology: Mn nodules, basalt, Section 1, 0-10 cm.

SMEAR SLIDE SUMMARY (%):

	1, 70 D	2, 70 D
COMPOSITION:		
Clay	2	1
Accessory minerals	Tr	Tr
Foraminifers	Tr	—
Nannofossils	98	99

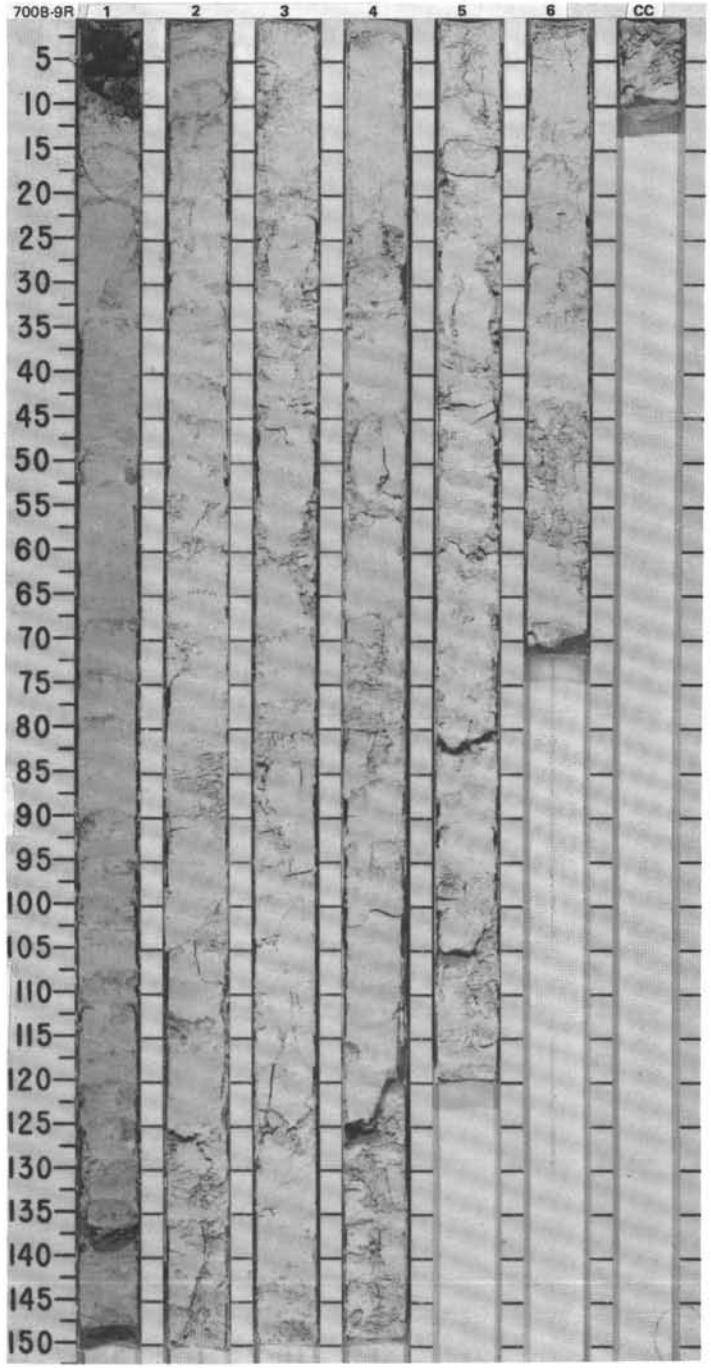

SITE 700 HOLE B CORE 10R CORED INTERVAL 3693.9-3703.4 mbsl; 92.9-102.4 mbsf

TIME-ROCK UNIT	BIOSTRAT. ZONE/ FOSSIL CHARACTER: FORAMINIFERS	NANNOFOSSILS	RADIOLARIANS	DIATOMS	SILICO-FLAGELLATES	PALEOMAGNETICS	PHYS. PROPERTIES	CHEMISTRY	SECTION	METERS	GRAPHIC LITHOLOGY	DRILLING DISTURB.	SED. STRUCTURES	SAMPLES	LITHOLOGIC DESCRIPTION
MIDDLE EOCENE	*A. primitiva* Zone P11 LOWER MIDDLE EOCENE	NP 14-15	Barren	Barren	Barren	ϕ=53.44 ρ_g=2.73	ϕ=53.49 ρ_g=2.74 ϕ=55.21 ρ_g=2.73		1 2 3	0.5 1.0					

NANNOFOSSIL CHALK

Drilling disturbance: Moderately fragmented.

Major lithology: Nannofossil chalk, white (no hue on color chart).

Bioturbation: *Zoophycos*, *Planolites*, and *Chondrites* in Section 1, 73-79 cm.

Minor lithologies:
a. Displaced manganese nodules, Section 1, 0-22 cm.
b. Manganese traces, Section 2, 106-112 cm.

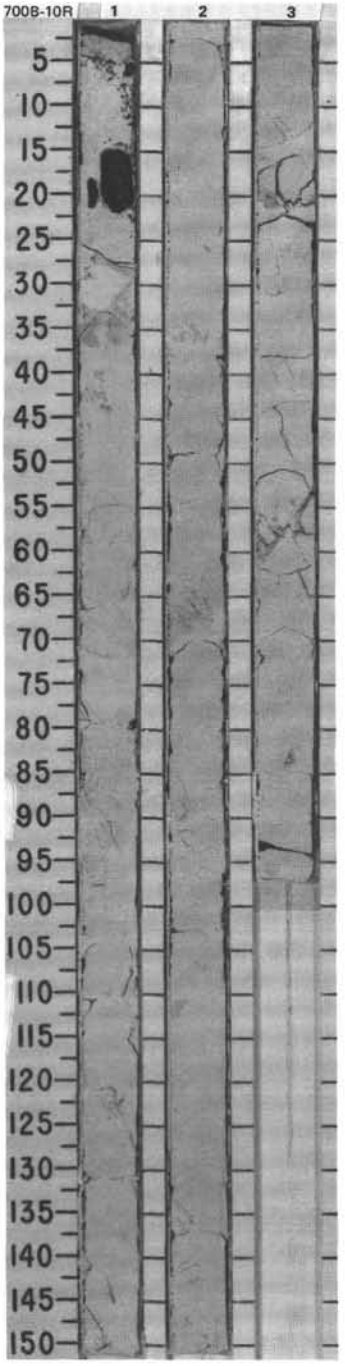

SITE 700 HOLE B CORE 11R CORED INTERVAL 3703.4-3712.9 mbsl; 102.4-111.9 mbsf

TIME-ROCK UNIT	BIOSTRAT. ZONE/ FOSSIL CHARACTER: FORAMINIFERS	NANNOFOSSILS	RADIOLARIANS	DIATOMS	SILICO-FLAGELLATES	PALEOMAGNETICS	PHYS. PROPERTIES	CHEMISTRY	SECTION	METERS	GRAPHIC LITHOLOGY	DRILLING DISTURB.	SED. STRUCTURES	SAMPLES	LITHOLOGIC DESCRIPTION
MIDDLE EOCENE	*A. primitiva* Zone	NP 14-15 [P10 - P11]	Barren	Barren	Barren				1		Mn Mn				NANNOFOSSIL CHALK Major lithology: Nannofossil chalk, white (no hue on the color chart). Minor lithology: Disseminated manganese fragments, Section 1, 29-35 cm.

SITE 700 HOLE B CORE 12R CORED INTERVAL 3712.9-3722.4 mbsl; 111.9-121.4 mbsf

TIME-ROCK UNIT	BIOSTRAT. ZONE/ FOSSIL CHARACTER: FORAMINIFERS	NANNOFOSSILS	RADIOLARIANS	DIATOMS	SILICO-FLAGELLATES	PALEOMAGNETICS	PHYS. PROPERTIES	CHEMISTRY	SECTION	METERS	GRAPHIC LITHOLOGY	DRILLING DISTURB.	SED. STRUCTURES	SAMPLES	LITHOLOGIC DESCRIPTION
MIDDLE EOCENE	*A. primitiva* Zone	NP 14-15 [P10 - P11]	Barren	Barren	Barren				CC		Mn				MANGANESE NODULES and PIECES OF BASALT (?) Only displaced large manganese nodules and pieces of basalt(?) appear in the CC.

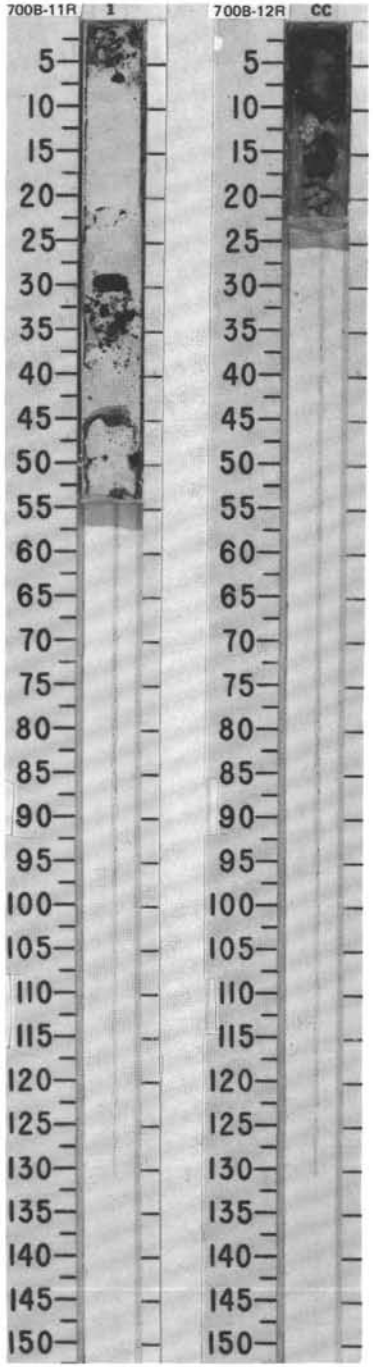

SITE 700 HOLE B CORE 13R CORED INTERVAL 3722.4-3731.9 mbsl; 121.4-130.9 mbsf

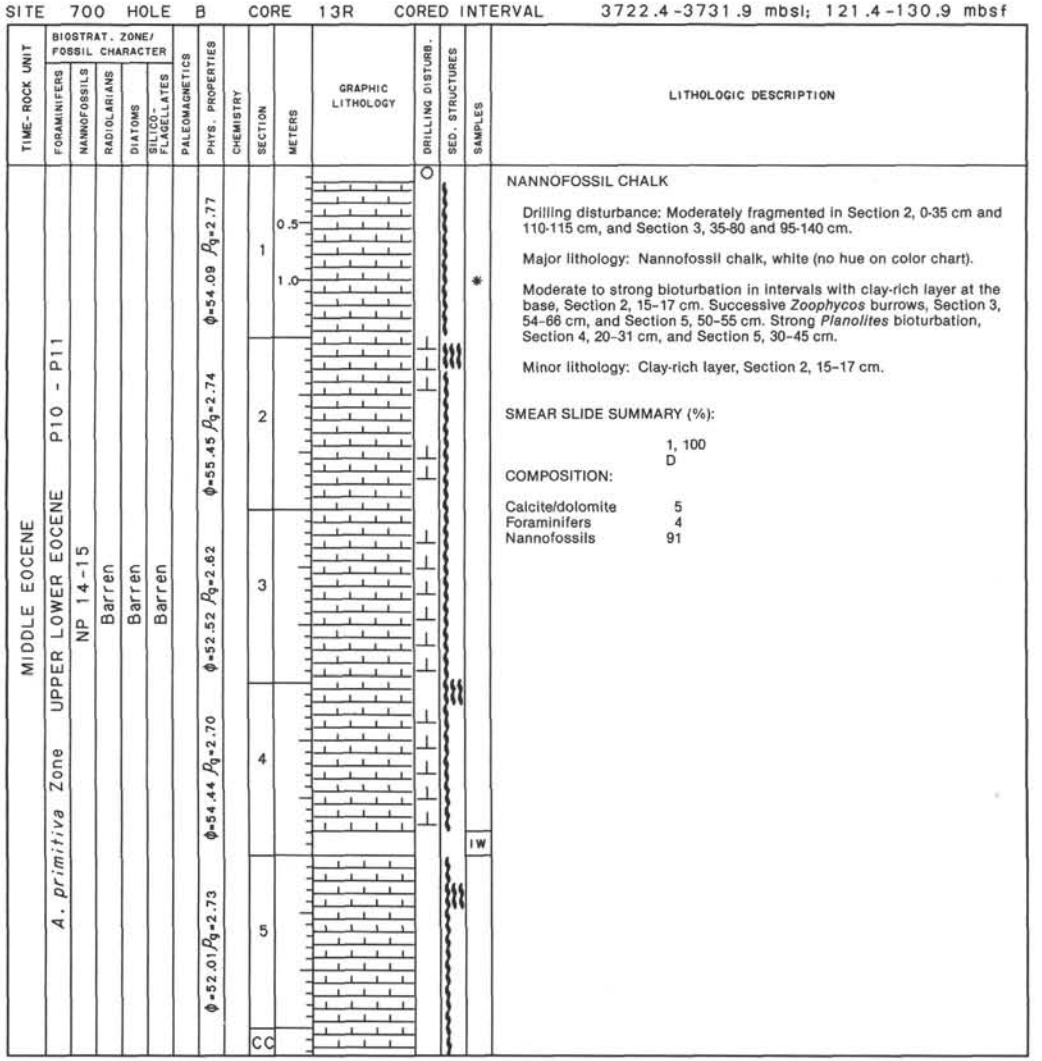

LITHOLOGIC DESCRIPTION

NANNOFOSSIL CHALK

Drilling disturbance: Moderately fragmented in Section 2, 0-35 cm and 110-115 cm, and Section 3, 35-80 and 95-140 cm.

Major lithology: Nannofossil chalk, white (no hue on color chart).

Moderate to strong bioturbation in intervals with clay-rich layer at the base, Section 2, 15-17 cm. Successive *Zoophycos* burrows, Section 3, 54-66 cm, and Section 5, 50-55 cm. Strong *Planolites* bioturbation, Section 4, 20-31 cm, and Section 5, 30-45 cm.

Minor lithology: Clay-rich layer, Section 2, 15-17 cm.

SMEAR SLIDE SUMMARY (%):

	1, 100
	D
COMPOSITION:	
Calcite/dolomite	5
Foraminifers	4
Nannofossils	91

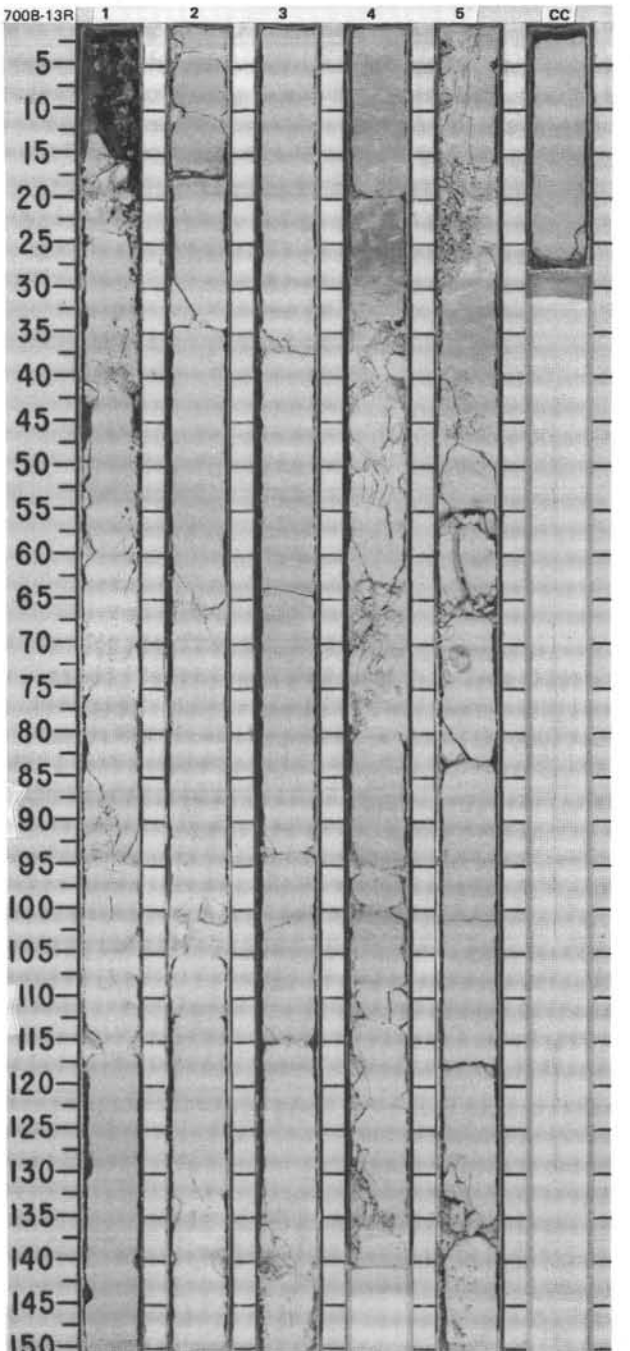

SITE 700 HOLE B CORE 14R CORED INTERVAL 3731.9-3741.4 mbsl; 130.9-140.4 mbsf

TIME-ROCK UNIT	BIOSTRAT. ZONE/ FOSSIL CHARACTER: FORAMINIFERS	NANNOFOSSILS	RADIOLARIANS	DIATOMS	SILICO-FLAGELLATES	PALEOMAGNETICS	PHYS. PROPERTIES	CHEMISTRY	SECTION	METERS	GRAPHIC LITHOLOGY	DRILLING DISTURB.	SED. STRUCTURES	SAMPLES	LITHOLOGIC DESCRIPTION
MIDDLE EOCENE	*A. primitiva* Zone LOWER MIDDLE EOCENE P10 - P11	NP 14-15	Barren	Barren	Barren				1		Mn			*	NANNOFOSSIL CHALK

Major lithology: Nannofossil chalk, white (no hue on the color chart).

Minor lithologies: Displaced manganese nodules and manganese-coated pumice pieces.

SMEAR SLIDE SUMMARY (%):

	1, 18 D
COMPOSITION:	
Clay	1
Accessory minerals:	
Zeolites	Tr
Micrite	60
Foraminifers	1
Nannofossils	38

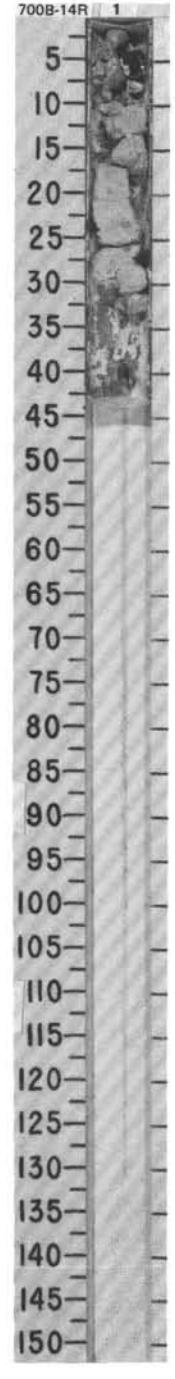

SITE 700 HOLE B CORE 15R CORED INTERVAL 3741.4-3750.9 mbsl; 140.4-149.9 mbsf

TIME-ROCK UNIT	BIOSTRAT. ZONE/ FOSSIL CHARACTER: FORAMINIFERS	NANNOFOSSILS	RADIOLARIANS	DIATOMS	SILICO-FLAGELLATES	PALEOMAGNETICS	PHYS. PROPERTIES	CHEMISTRY	SECTION	METERS	GRAPHIC LITHOLOGY	DRILLING DISTURB.	SED. STRUCTURES	SAMPLES	LITHOLOGIC DESCRIPTION
MIDDLE EOCENE	*A. primitiva* Zone LOWER MIDDLE EOCENE P10	NP 14	Barren	Barren	Barren				CC	1					PEBBLES Pebbles due to downhole contamination.

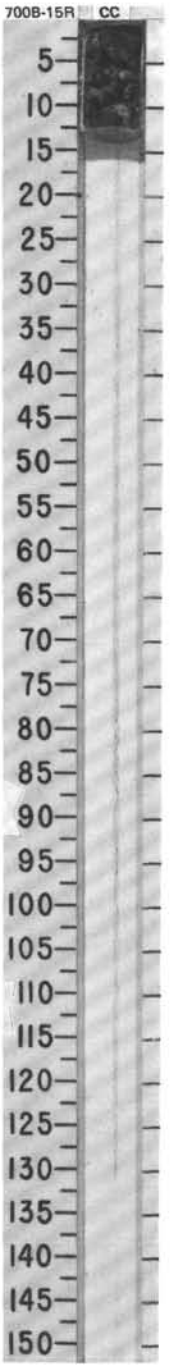

SITE 700 HOLE B CORE 16R CORED INTERVAL 3750.9-3760.4 mbsl; 149.9-159.4 mbsf

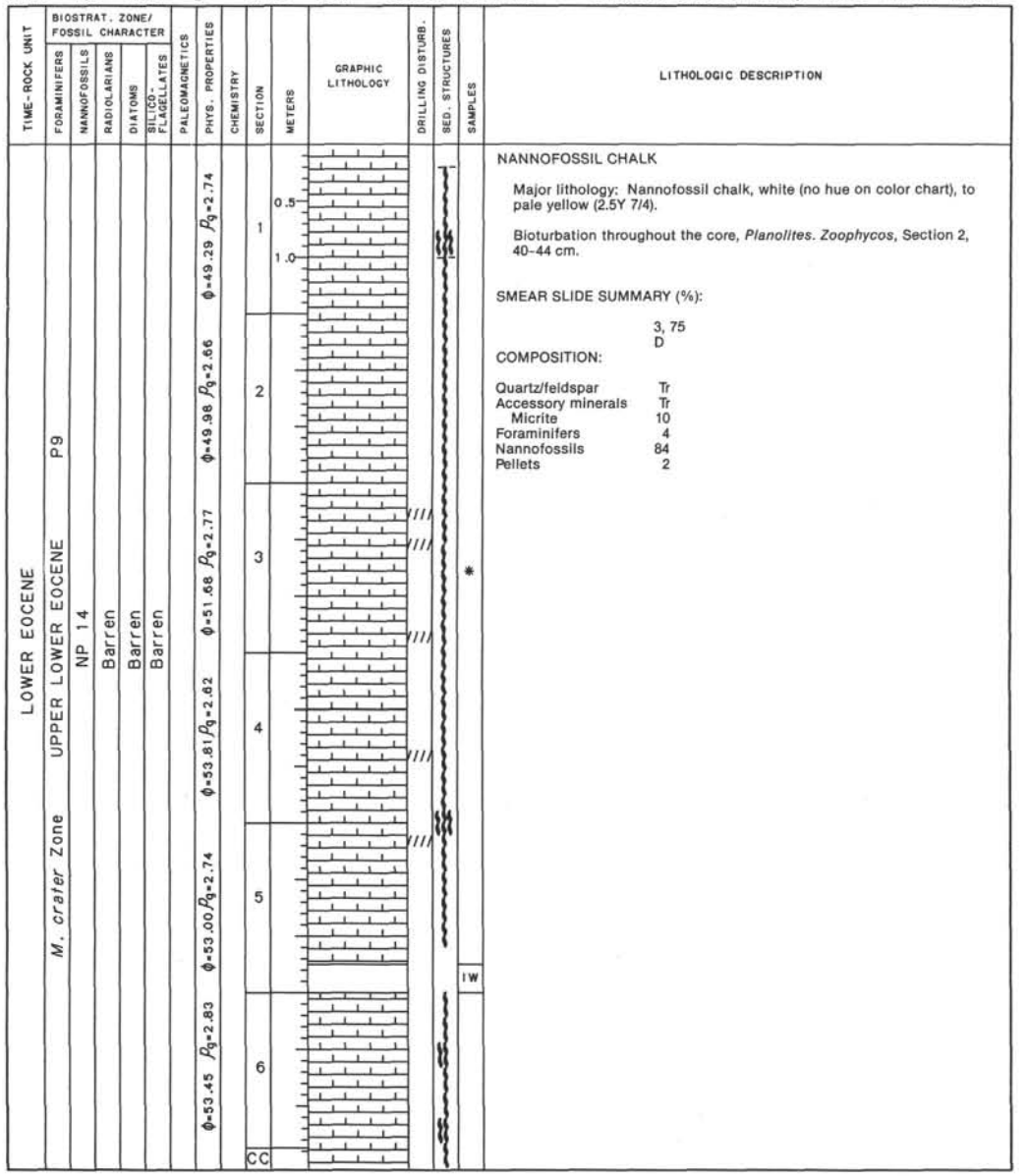

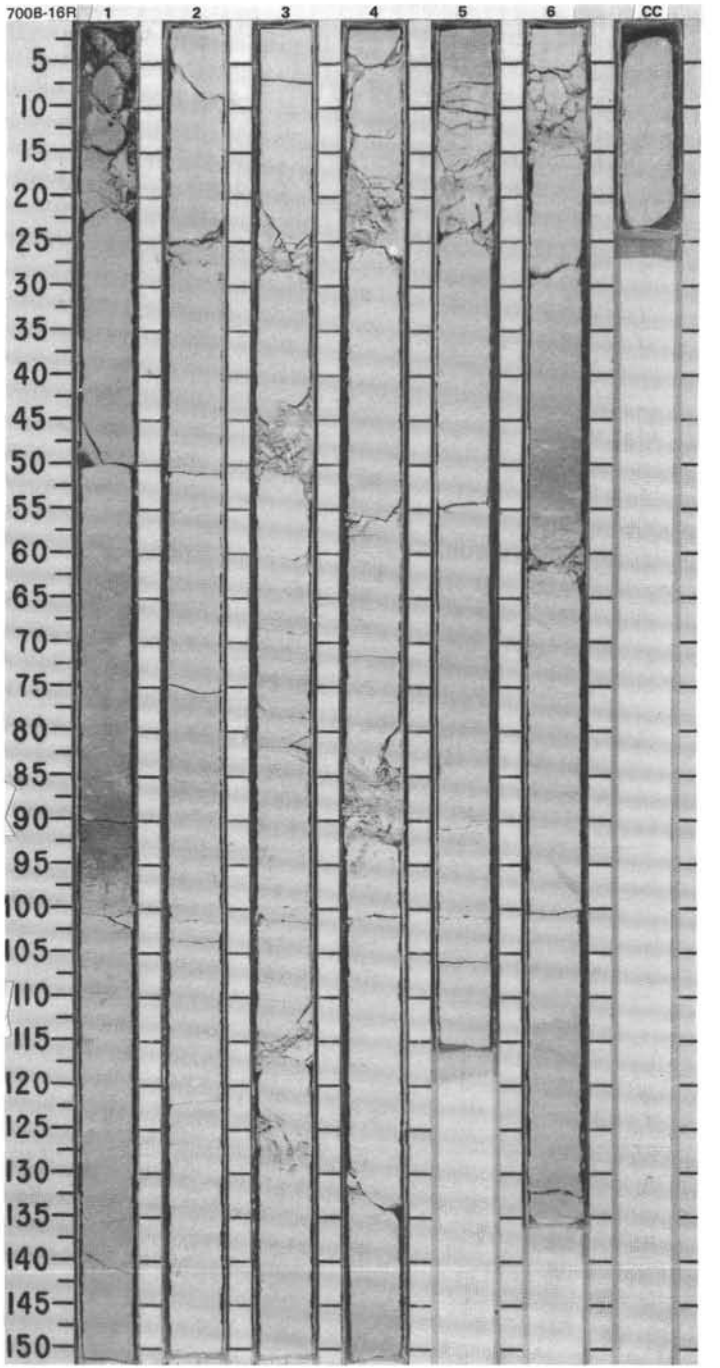

SITE 700 HOLE B CORE 17R CORED INTERVAL 3760.4-3769.9 mbsl; 159.4-168.9 mbsf

TIME-ROCK UNIT	BIOSTRAT. ZONE/ FOSSIL CHARACTER: FORAMINIFERS	NANNOFOSSILS	RADIOLARIANS	DIATOMS	SILICO-FLAGELLATES	PALEOMAGNETICS	PHYS. PROPERTIES	CHEMISTRY	SECTION	METERS	GRAPHIC LITHOLOGY	DRILLING DISTURB.	SED. STRUCTURES	SAMPLES	LITHOLOGIC DESCRIPTION
LOWER EOCENE			Barren	Barren	Barren				CC						GRAVEL Downhole contamination.

SITE 700 HOLE B CORE 18R CORED INTERVAL 3769.9-3779.4 mbsl; 168.9-178.4 mbsf

TIME-ROCK UNIT	BIOSTRAT. ZONE/ FOSSIL CHARACTER: FORAMINIFERS	NANNOFOSSILS	RADIOLARIANS	DIATOMS	SILICO-FLAGELLATES	PALEOMAGNETICS	PHYS. PROPERTIES	CHEMISTRY	SECTION	METERS	GRAPHIC LITHOLOGY	DRILLING DISTURB.	SED. STRUCTURES	SAMPLES	LITHOLOGIC DESCRIPTION
LOWER EOCENE	P9	not examined				ρ_g=2.76			1	0.5 1.0				*	NANNOFOSSIL CHALK Major lithology: Micritic nannofossil chalk, generally white (no hue on the color chart), locally very pale brown (10YR 7/3), Section 2, 73-80 cm; and white (10YR 8/2) to pale brown (10 YR 7/3) in Section 3, 25-75 cm. Minor bioturbation throughout the core with spots of strong bioturbation in Section 2, 73-80 cm, (with *Planolites*, *Chondrites*, and *Zoophycos*), and Section 3, (with *Planolites*, *Chondrites*, and *Zoophycos*(?)). SMEAR SLIDE SUMMARY (%): 1, 92 D COMPOSITION: Quartz/feldspar Tr Accessory minerals 1 Zeolites Tr Micrite 43 Foraminifers 5 Nannofossils 50 Pellets 1
	UPPER LOWER EOCENE	NP 13	Barren	Barren	Barren	ϕ=47.89	ρ_g=2.95		2						
						ϕ=49.70	ρ_g=2.74		3						
	M. crater Zone					ϕ=52.50	ρ_g=3.02		4						
						ϕ=51.24			CC						

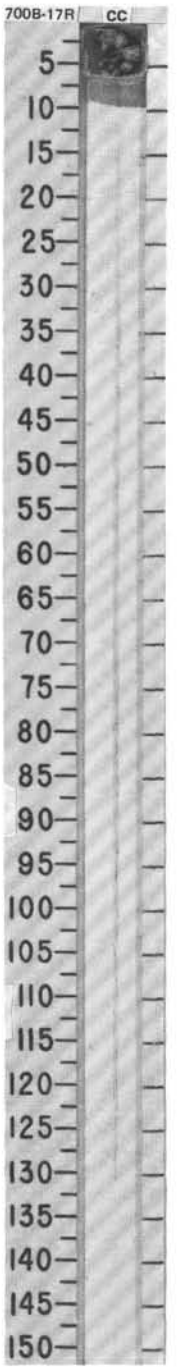

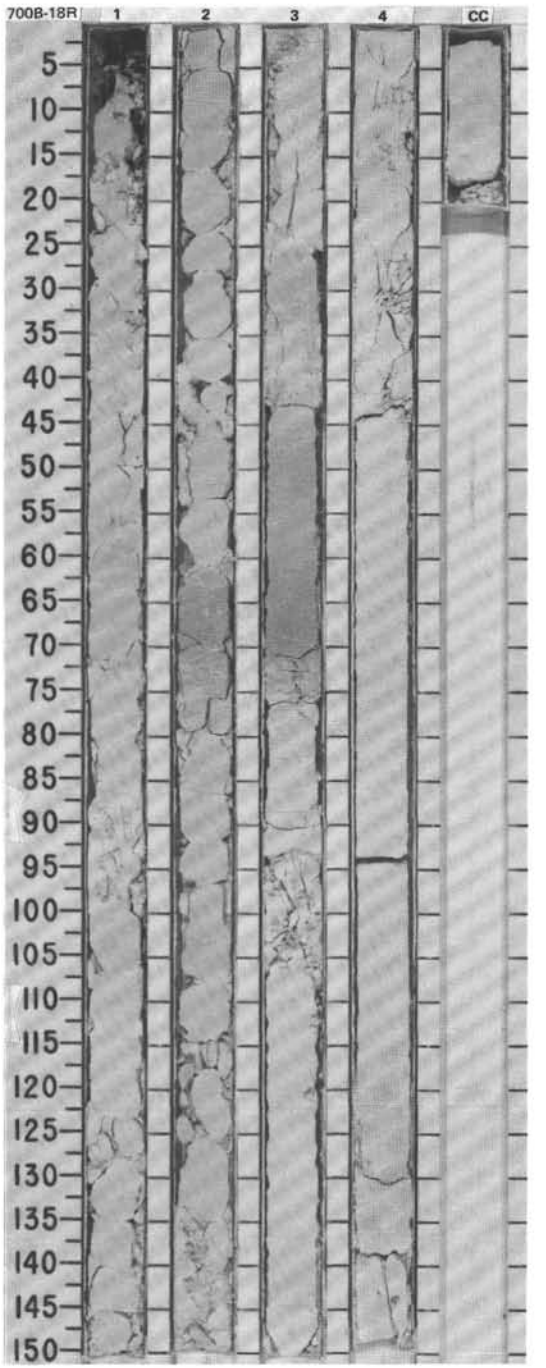

SITE 700 HOLE B CORE 19R CORED INTERVAL 3779.4-3788.9 mbsl; 178.4-187.9 mbsf

TIME-ROCK UNIT	BIOSTRAT. ZONE/ FOSSIL CHARACTER: FORAMINIFERS	NANNOFOSSILS	RADIOLARIANS	DIATOMS	SILICO-FLAGELLATES	PALEOMAGNETICS	PHYS. PROPERTIES	CHEMISTRY	SECTION	METERS	GRAPHIC LITHOLOGY	DRILLING DISTURB.	SED. STRUCTURES	SAMPLES	LITHOLOGIC DESCRIPTION
LOWER EOCENE		Barren	Barren	Barren	Barren							○			GRAVEL Pieces of gravel; downhole contamination.

SITE 700 HOLE B CORE 20R CORED INTERVAL 3788.9-3793.9 mbsl; 187.9-192.9 mbsf

TIME-ROCK UNIT	BIOSTRAT. ZONE/ FOSSIL CHARACTER: FORAMINIFERS	NANNOFOSSILS	RADIOLARIANS	DIATOMS	SILICO-FLAGELLATES	PALEOMAGNETICS	PHYS. PROPERTIES	CHEMISTRY	SECTION	METERS	GRAPHIC LITHOLOGY	DRILLING DISTURB.	SED. STRUCTURES	SAMPLES	LITHOLOGIC DESCRIPTION
LOWER EOCENE	P9	not examined	Barren	Barren	Barren		ϕ=48.30 ρ_g=2.74		1	0.5, 1.0				*	MICRITIC NANNOFOSSIL CHALK Major lithology: Micritic nannofossil chalk, white (10YR 8/2) to pale yellow (2.5Y 7/4), Section 2, 60-100 cm. Bioturbation throughout the core; abundant *Planolites*, Section 1, 90-96 cm. SMEAR SLIDE SUMMARY (%): 1, 70 D COMPOSITION: Accessory minerals: Zeolites Tr; Micrite 42; Foraminifers 5; Nannofossils 50; Pellets(?) 3
	UPPER LOWER EOCENE						ϕ=43.00 ρ_g=2.78		2					IW	
	M. crater Zone	NP 10-12							3						
									CC						

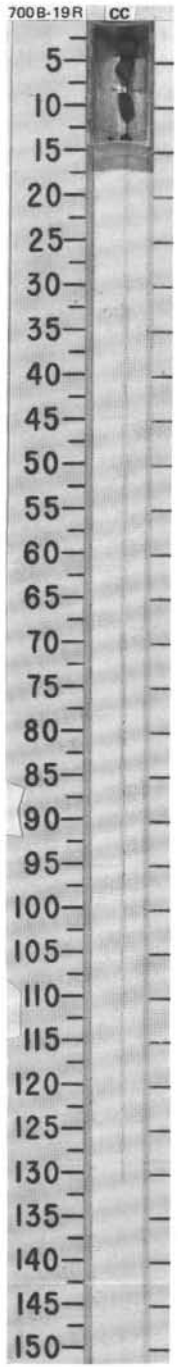

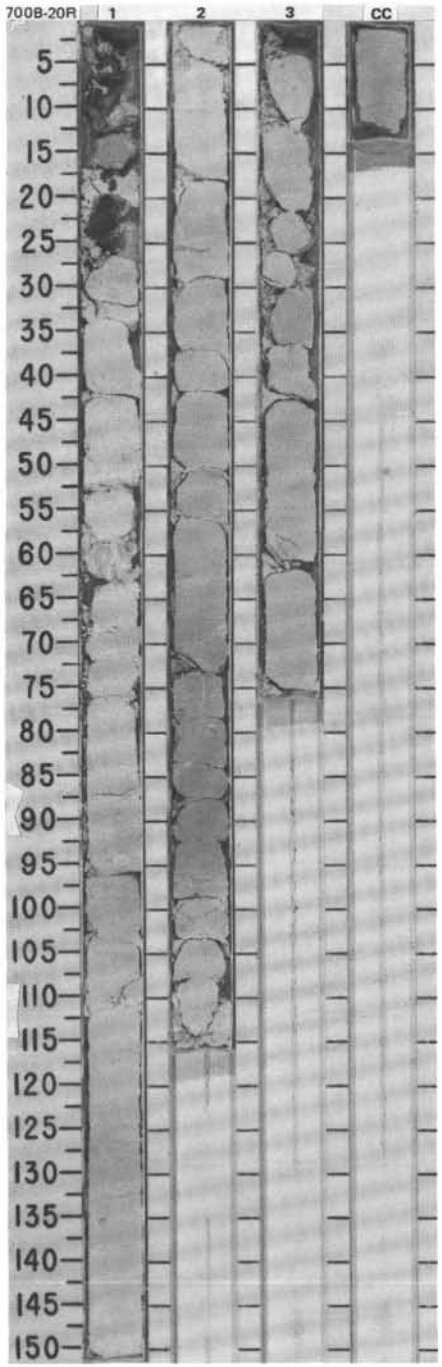

SITE 700 HOLE B CORE 21R CORED INTERVAL 3793.9-3801.0 mbsl; 192.9-200.0 mbsf

TIME-ROCK UNIT	BIOSTRAT. ZONE/ FOSSIL CHARACTER: FORAMINIFERS	NANNOFOSSILS	RADIOLARIANS	DIATOMS	SILICO-FLAGELLATES	PALEOMAGNETICS	PHYS. PROPERTIES	CHEMISTRY	SECTION	METERS	GRAPHIC LITHOLOGY	DRILLING DISTURB.	SED. STRUCTURES	SAMPLES
LOWER EOCENE	P8						ϕ=48.35 ρ_g=2.77		1	0.5, 1.0				*
LOWER EOCENE	NP 10-12		Barren	Barren	Barren		ϕ=44.06 ρ_g=2.73		2					
P. wilcoxensis Zone							ϕ=53.15 ρ_g=2.78		3					
									4					
									CC					

LITHOLOGIC DESCRIPTION

NANNOFOSSIL CHALK

Drilling disturbance: Downhole contamination in Section 1, 0-15 cm. Slight to moderate.

Major lithology: Micritic nannofossil chalk, very pale brown (10YR 8/3, 7/4). Slightly darker in Section 1, 64-81 cm. Again white (10YR 8/2) in Section 3; very pale brown (10YR 7/3) in Section 4.

Moderate to strong bioturbation throughout the core. *Planolites*, *Chondrites*, and *Zoophycos*, Section 2, 29-38 cm. *Planolites*, Section 3, 95 cm.

SMEAR SLIDE SUMMARY (%):

	1, 70
	D
COMPOSITION:	
Accessory minerals:	
Zeolites	Tr
Micrite	67
Foraminifers	5
Nannofossils	25
Pellets(?)	3

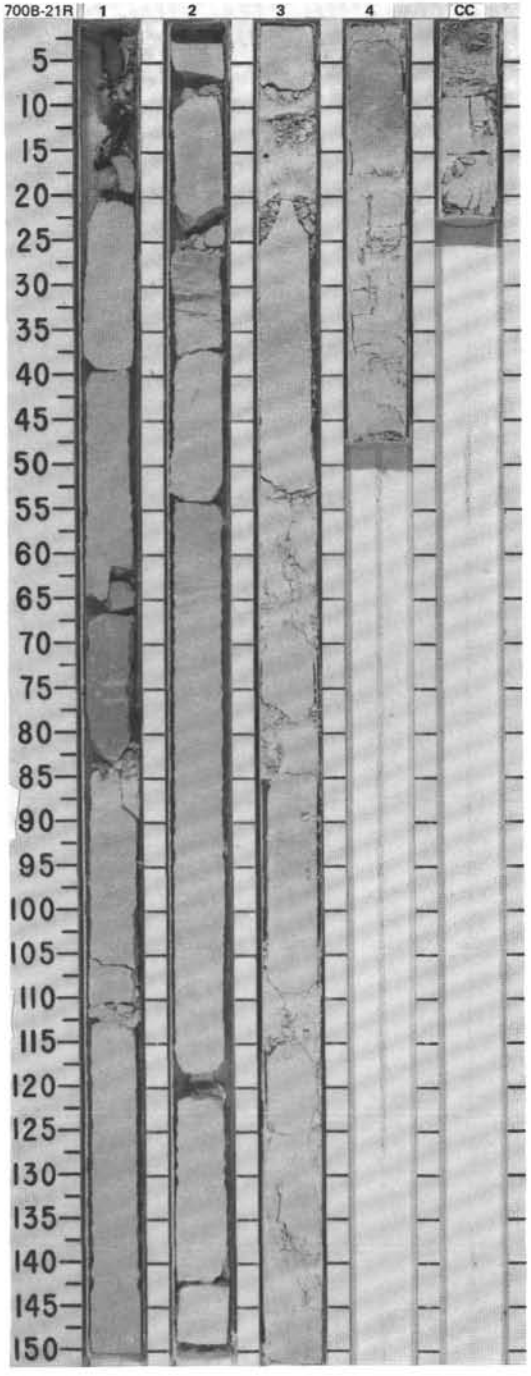

SITE 700 HOLE B CORE 22R CORED INTERVAL 3801.0-3810.5 mbsl; 200.0-209.5 mbsf

TIME-ROCK UNIT	BIOSTRAT. ZONE/ FOSSIL CHARACTER: FORAMINIFERS	NANNOFOSSILS	RADIOLARIANS	DIATOMS	SILICO-FLAGELLATES	PALEOMAGNETICS	PHYS. PROPERTIES	CHEMISTRY	SECTION	METERS	GRAPHIC LITHOLOGY	DRILLING DISTURB.	SED. STRUCTURES	SAMPLES	LITHOLOGIC DESCRIPTION
LOWER EOCENE	*P. wilcoxensis* Zone LOWER EOCENE	P7 NP 10-12	Barren	Barren	Barren				1 CC			X X X			GRAVEL and PIECES OF MICRITIC NANNOFOSSIL CHALK Drilling disturbance: Mixture of gravel and pieces of micritic nannofossil chalk, very pale brown (10YR 8/3).

700A-23R NO RECOVERY

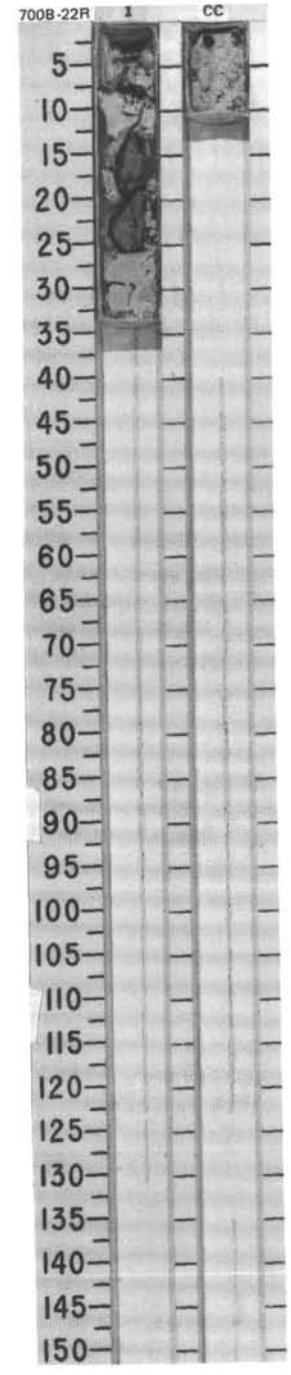

SITE 700 HOLE B CORE 24R CORED INTERVAL 3820.0-3829.5 mbsl; 219.0-228.5 mbsf

TIME-ROCK UNIT	BIOSTRAT. ZONE/ FOSSIL CHARACTER: FORAMINIFERS	NANNOFOSSILS	RADIOLARIANS	DIATOMS	SILICO-FLAGELLATES	PALEOMAGNETICS	PHYS. PROPERTIES	CHEMISTRY	SECTION	METERS	GRAPHIC LITHOLOGY	DRILLING DISTURB.	SED. STRUCTURES	SAMPLES	LITHOLOGIC DESCRIPTION
LOWER EOCENE	P6	NP 10?	Barren	Barren	Barren				1						GRAVEL and PIECES OF MICRITIC NANNOFOSSIL CHALK Drilling disturbance: Mixture of gravel and pieces of micritic nannofossil chalk, white (2.5Y 8/2).
	LOWER EOCENE														

SITE 700 HOLE B CORE 25R CORED INTERVAL 3829.5-3839.0 mbsl; 228.5-238.0 mbsf

TIME-ROCK UNIT	BIOSTRAT. ZONE/ FOSSIL CHARACTER: FORAMINIFERS	NANNOFOSSILS	RADIOLARIANS	DIATOMS	SILICO-FLAGELLATES	PALEOMAGNETICS	PHYS. PROPERTIES	CHEMISTRY	SECTION	METERS	GRAPHIC LITHOLOGY	DRILLING DISTURB.	SED. STRUCTURES	SAMPLES	LITHOLOGIC DESCRIPTION
			Barren		Barren				1						NANNOFOSSIL CHALK (INDURATED) Drilling disturbance: Downhole contamination, Section 1, 0-23 cm. Major lithology: Indurated nannofossil chalk, white (2.5Y 8/2). Moderate bioturbation: *Planolites*, *Chondrites*, and *Zoophycos*.

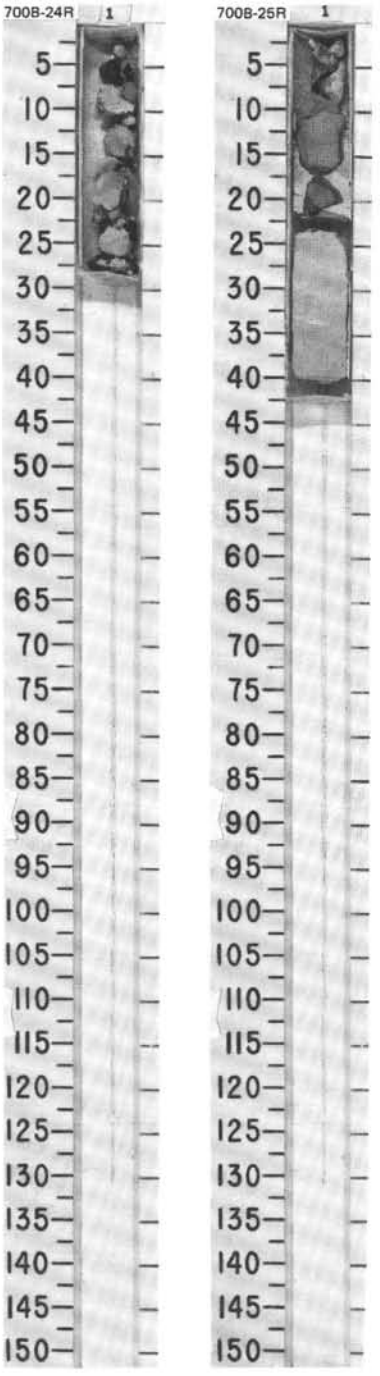

SITE 700 HOLE B CORE 26R CORED INTERVAL 3839.0-3848.5 mbsl; 238.0-247.5 mbsf

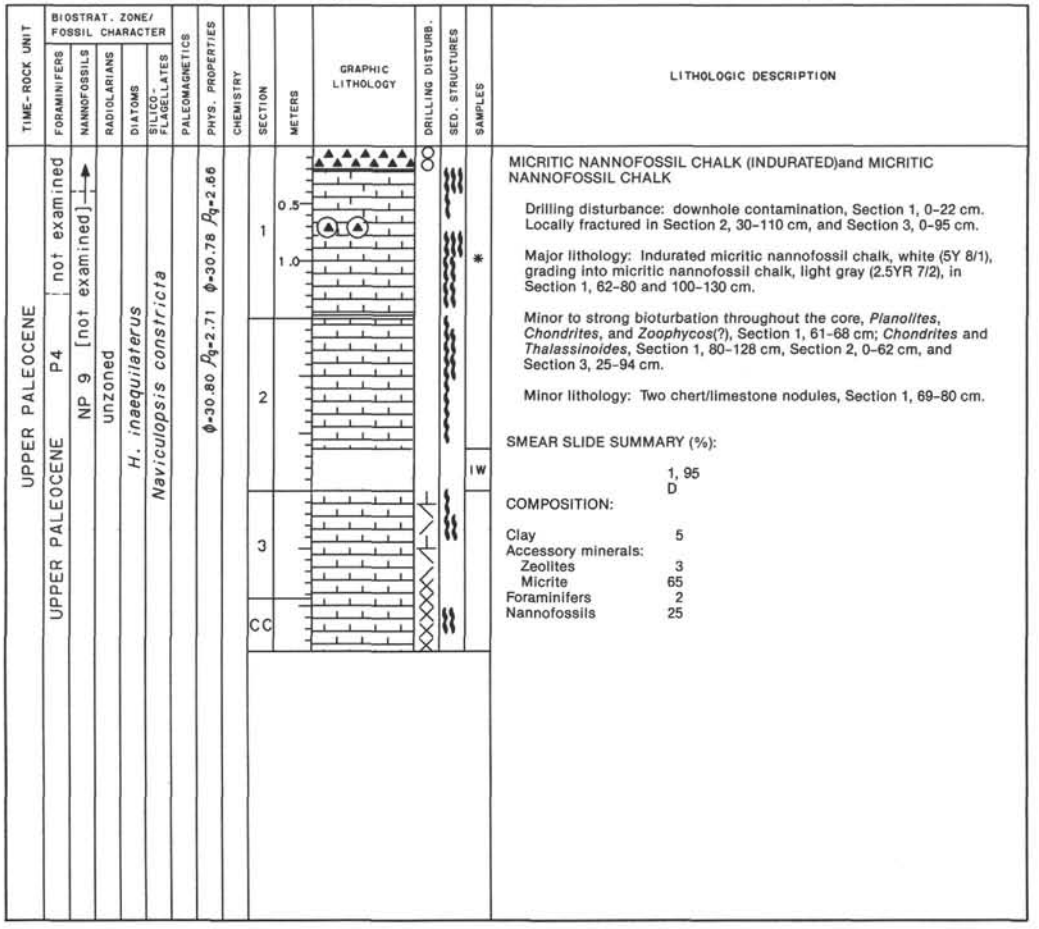

MICRITIC NANNOFOSSIL CHALK (INDURATED)and MICRITIC NANNOFOSSIL CHALK

Drilling disturbance: downhole contamination, Section 1, 0-22 cm. Locally fractured in Section 2, 30-110 cm, and Section 3, 0-95 cm.

Major lithology: Indurated micritic nannofossil chalk, white (5Y 8/1), grading into micritic nannofossil chalk, light gray (2.5YR 7/2), in Section 1, 62-80 and 100-130 cm.

Minor to strong bioturbation throughout the core, *Planolites*, *Chondrites*, and *Zoophycos*(?), Section 1, 61-68 cm; *Chondrites* and *Thalassinoides*, Section 1, 80-128 cm, Section 2, 0-62 cm, and Section 3, 25-94 cm.

Minor lithology: Two chert/limestone nodules, Section 1, 69-80 cm.

SMEAR SLIDE SUMMARY (%):

	1, 95 D
COMPOSITION:	
Clay	5
Accessory minerals:	
Zeolites	3
Micrite	65
Foraminifers	2
Nannofossils	25

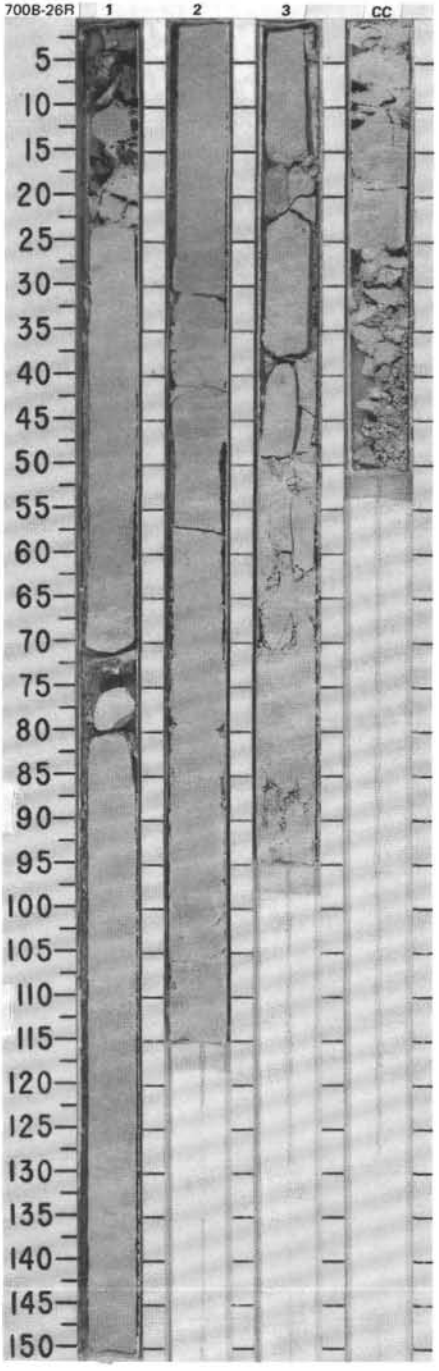

SITE 700 HOLE B CORE 27R CORED INTERVAL 3848.5-3858.0 mbsl; 247.5-257.0 mbsf

TIME-ROCK UNIT	BIOSTRAT. ZONE/ FOSSIL CHARACTER: FORAMINIFERS	NANNOFOSSILS	RADIOLARIANS	DIATOMS	SILICO-FLAGELLATES	PALEOMAGNETICS	PHYS. PROPERTIES	CHEMISTRY	SECTION	METERS	GRAPHIC LITHOLOGY	DRILLING DISTURB.	SED. STRUCTURES	SAMPLES	LITHOLOGIC DESCRIPTION
UPPER PALEOCENE	P4	not examined	unzoned	*H. inadequilaterus*	*Naviculopsis constricta*				1, 2, CC	0.5, 1.0					NANNOFOSSIL CHALK (INDURATED)
	UPPER PALEOCENE	NP 8													

NANNOFOSSIL CHALK (INDURATED)

Drilling disturbance: Slightly fractured, Section 1, 0-25 and 142-150 cm, and Section 2.

Major lithology: Indurated micritic nannofossil chalk, white (no hue on the color chart); light gray (2.5R 7/2), in Section 1.

Minor to moderate bioturbation throughout the core.

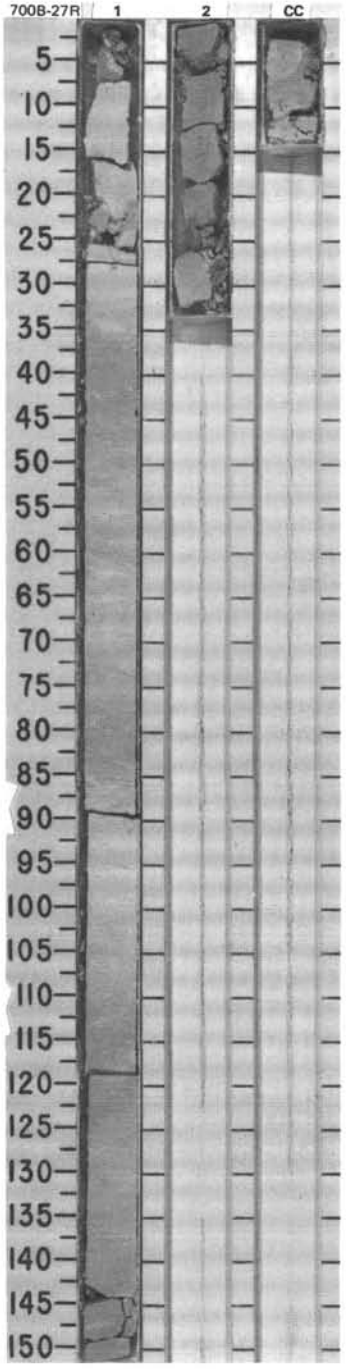

SITE 700 HOLE B CORE 28R CORED INTERVAL 3858.0-3867.5 mbsl; 257.0-266.5 mbst

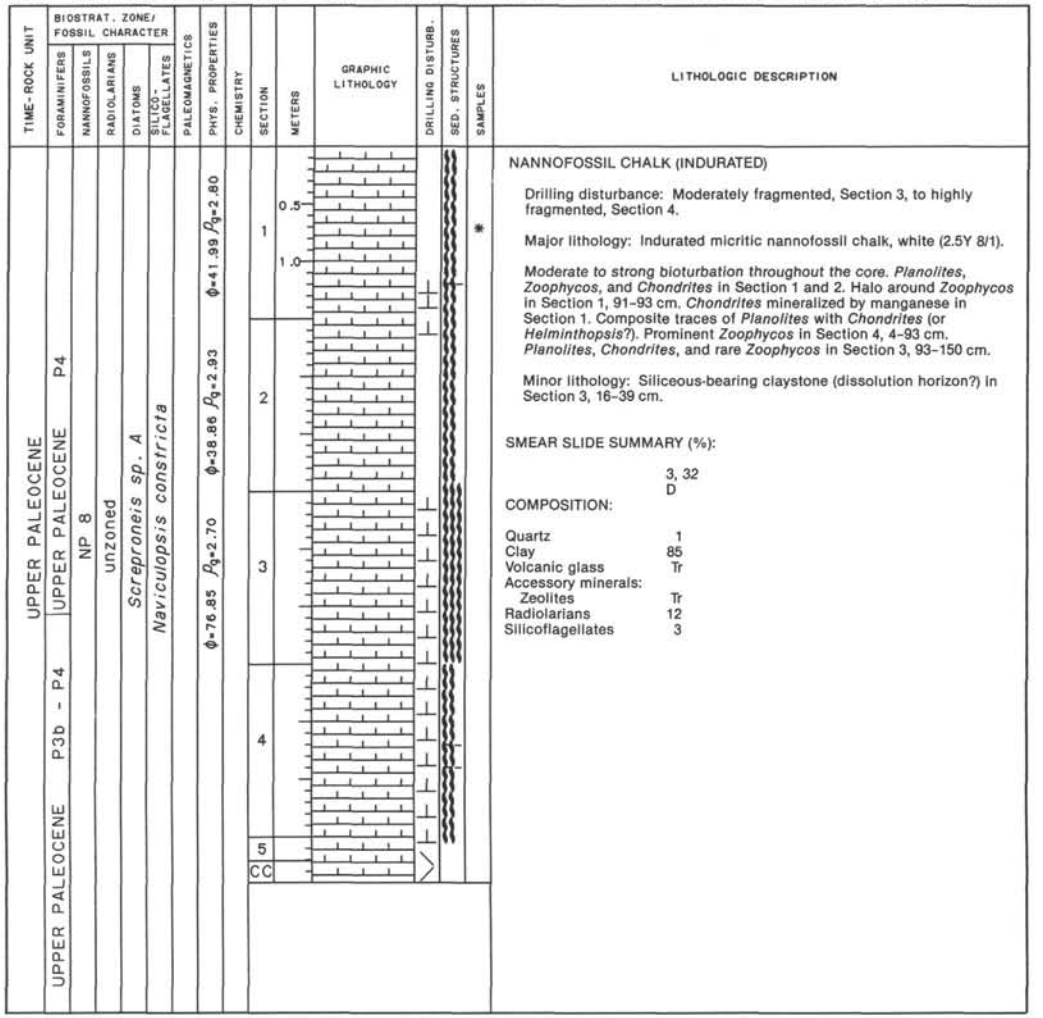

LITHOLOGIC DESCRIPTION

NANNOFOSSIL CHALK (INDURATED)

Drilling disturbance: Moderately fragmented, Section 3, to highly fragmented, Section 4.

Major lithology: Indurated micritic nannofossil chalk, white (2.5Y 8/1).

Moderate to strong bioturbation throughout the core. Planolites, Zoophycos, and *Chondrites* in Section 1 and 2. Halo around *Zoophycos* in Section 1, 91-93 cm. *Chondrites* mineralized by manganese in Section 1. Composite traces of *Planolites* with *Chondrites* (or *Helminthopsis*?). Prominent *Zoophycos* in Section 4, 4-93 cm. *Planolites, Chondrites,* and rare *Zoophycos* in Section 3, 93-150 cm.

Minor lithology: Siliceous-bearing claystone (dissolution horizon?) in Section 3, 16-39 cm.

SMEAR SLIDE SUMMARY (%):

	3, 32 D
COMPOSITION:	
Quartz	1
Clay	85
Volcanic glass	Tr
Accessory minerals:	
Zeolites	Tr
Radiolarians	12
Silicoflagellates	3

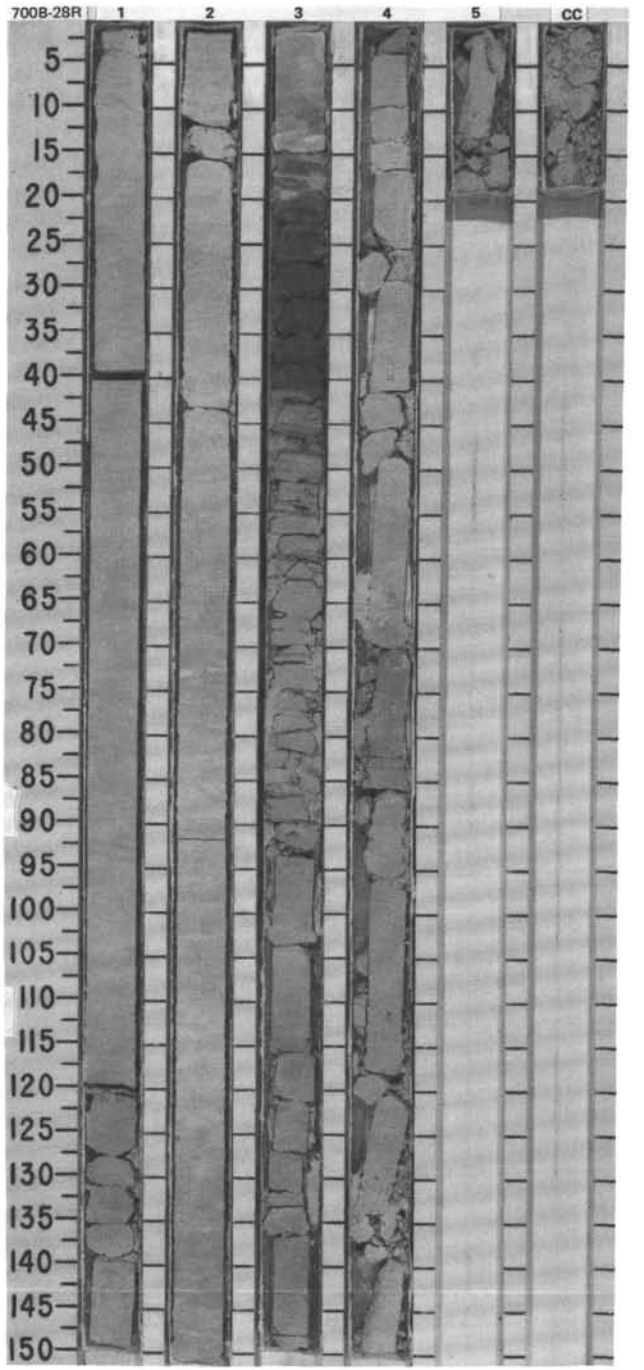

SITE 700 HOLE B CORE 29R CORED INTERVAL 3867.5-3877.0 mbsl; 266.5-276.0 mbsf

TIME-ROCK UNIT	BIOSTRAT. ZONE/ FOSSIL CHARACTER: FORAMINIFERS	NANNOFOSSILS	RADIOLARIANS	DIATOMS	SILICO-FLAGELLATES	PALEOMAGNETICS	PHYS. PROPERTIES	CHEMISTRY	SECTION	METERS	GRAPHIC LITHOLOGY	DRILLING DISTURB.	SED. STRUCTURES	SAMPLES
UPPER PALEOCENE	UPPER PALEOCENE P3b - P4	NP 8	unzoned	*Sceptroneis sp. A*	UPPER PALEOCENE	ϕ=37.08 ρ_g=2.67	ϕ=48.09 ρ_g=2.83		1, 2, CC	0.5, 1.0				*

LITHOLOGIC DESCRIPTION

NANNOFOSSIL CHALK (INDURATED)

Drilling disturbance: Moderately fragmented, Section 2, 0-60 cm.

Major lithology: Indurated micritic nannofossil chalk, light gray (5Y 7/1).

Minor bioturbation throughout the core; *Zoophycos* in Section 1, 115 and 120 cm, and Section 2, 105 and 120 cm.

SMEAR SLIDE SUMMARY (%):

	1, 100 D
COMPOSITION:	
Quartz	1
Accessory minerals:	
Micrite	59
Foraminifers	Tr
Nannofossils	40

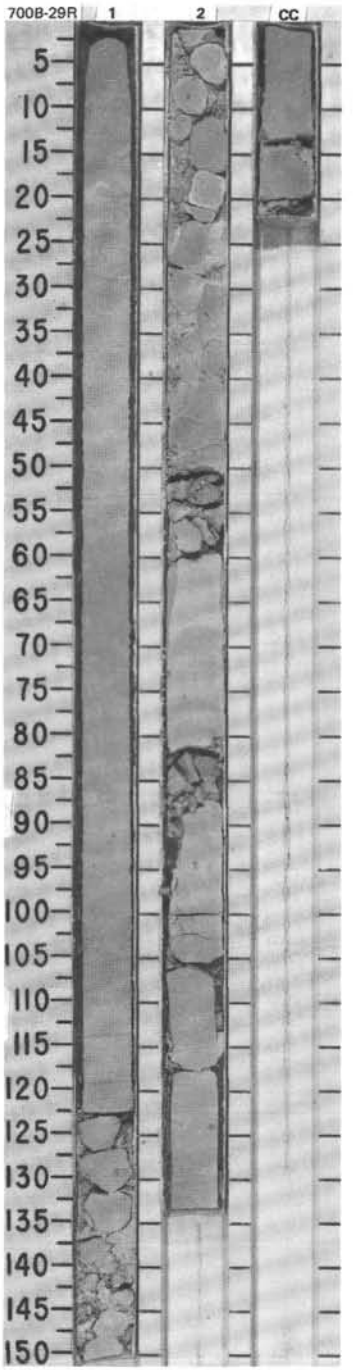

SITE 700 HOLE B CORE 30R CORED INTERVAL 3877.0-3886.5 mbsl; 276.0-285.5 mbsf

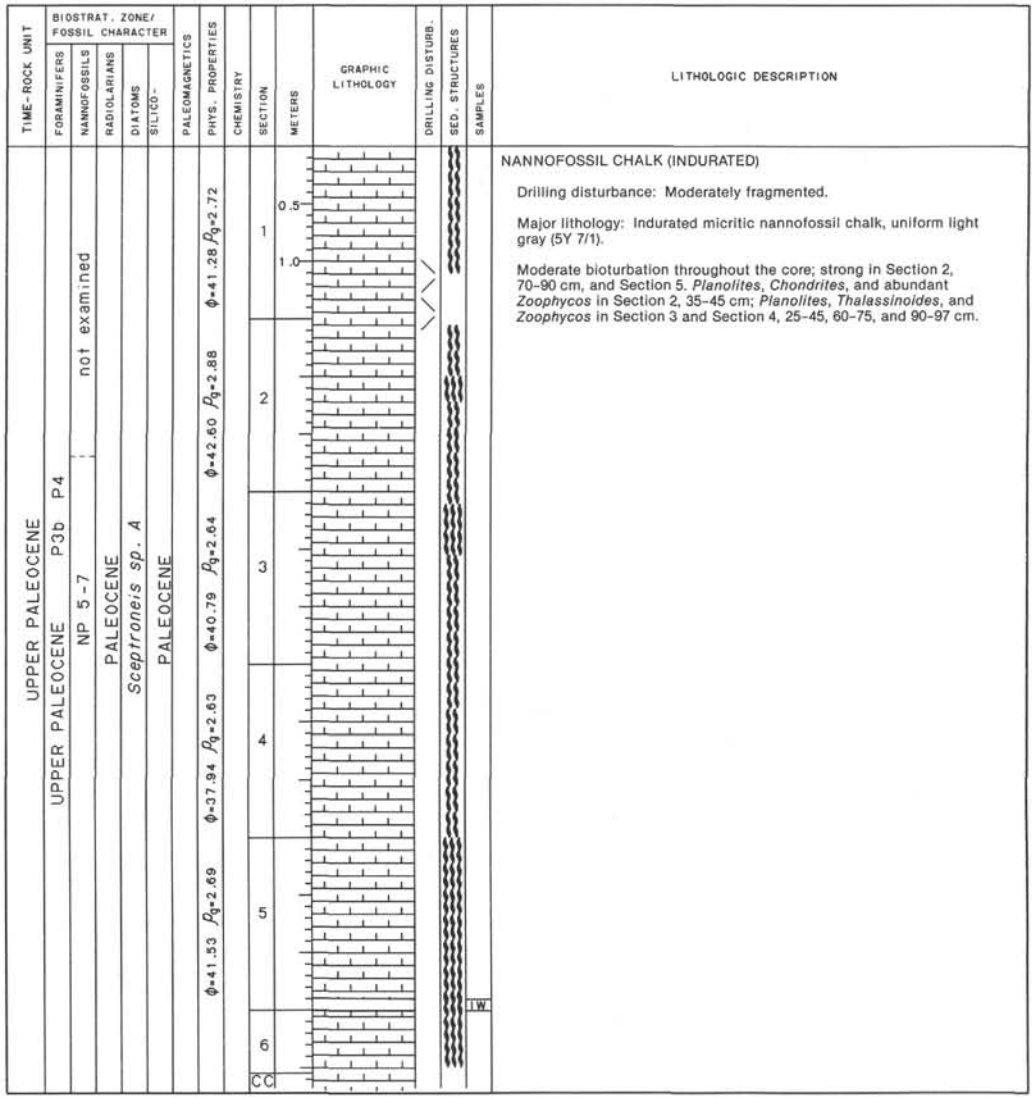

NANNOFOSSIL CHALK (INDURATED)

Drilling disturbance: Moderately fragmented.

Major lithology: Indurated micritic nannofossil chalk, uniform light gray (5Y 7/1).

Moderate bioturbation throughout the core; strong in Section 2, 70-90 cm, and Section 5. *Planolites*, *Chondrites*, and abundant *Zoophycos* in Section 2, 35-45 cm; *Planolites*, *Thalassinoides*, and *Zoophycos* in Section 3 and Section 4, 25-45, 60-75, and 90-97 cm.

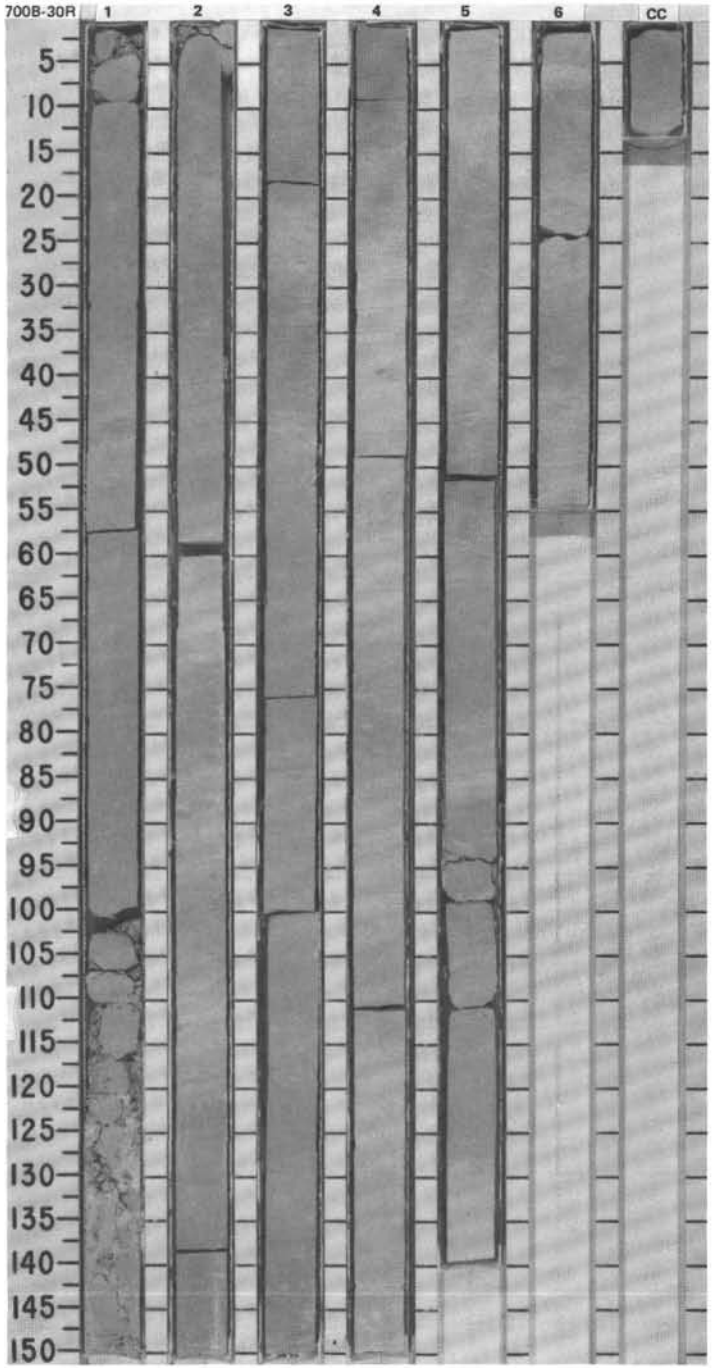

SITE 700 HOLE B CORE 31R CORED INTERVAL 3886.5-3896.0 mbsl; 285.5-295.0 mbsf

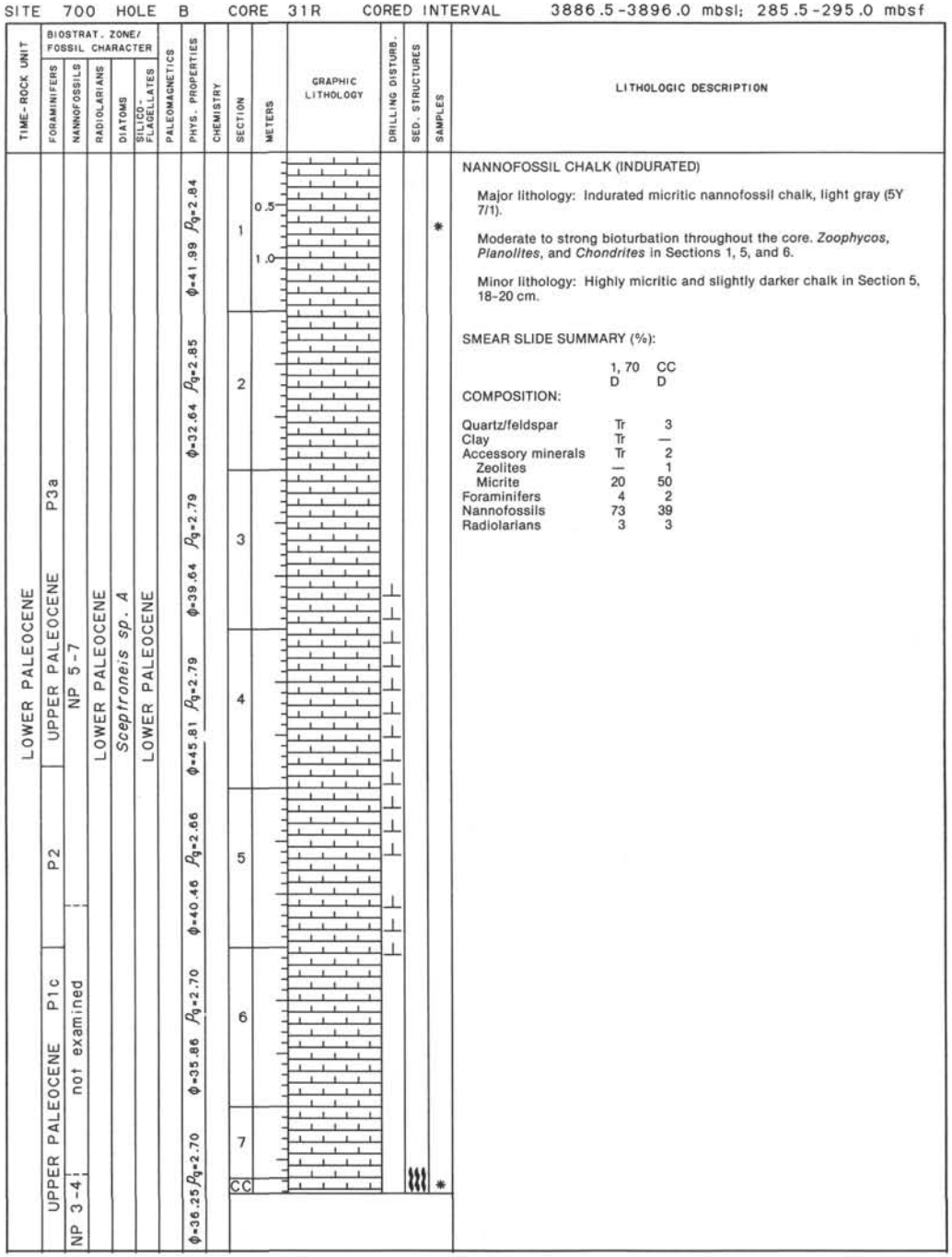

LITHOLOGIC DESCRIPTION

NANNOFOSSIL CHALK (INDURATED)

Major lithology: Indurated micritic nannofossil chalk, light gray (5Y 7/1).

Moderate to strong bioturbation throughout the core. *Zoophycos*, *Planolites*, and *Chondrites* in Sections 1, 5, and 6.

Minor lithology: Highly micritic and slightly darker chalk in Section 5, 18-20 cm.

SMEAR SLIDE SUMMARY (%):

COMPOSITION:	1, 70 D	CC D
Quartz/feldspar	Tr	3
Clay	Tr	—
Accessory minerals	Tr	2
Zeolites	—	1
Micrite	20	50
Foraminifers	4	2
Nannofossils	73	39
Radiolarians	3	3

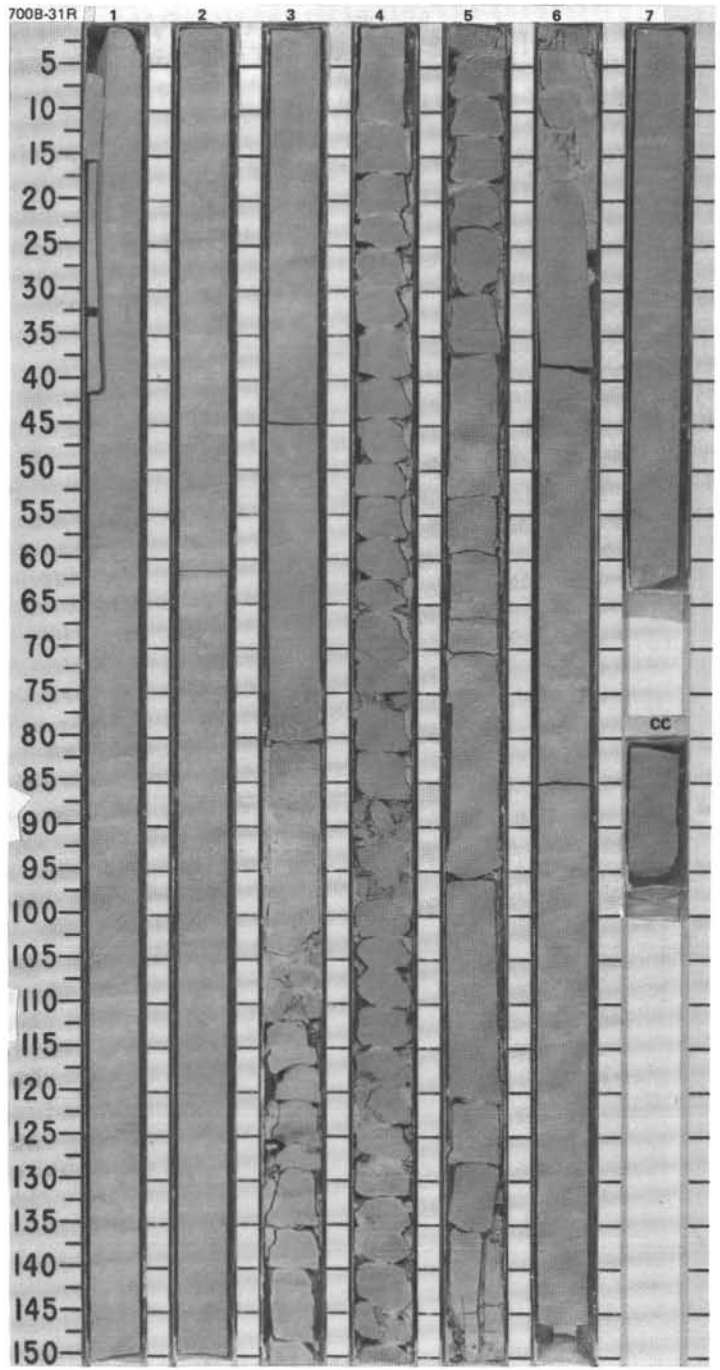

SITE 700 HOLE B CORE 32R CORED INTERVAL 3896.0-3905.5 mbsl; 295.0-304.5 mbsf

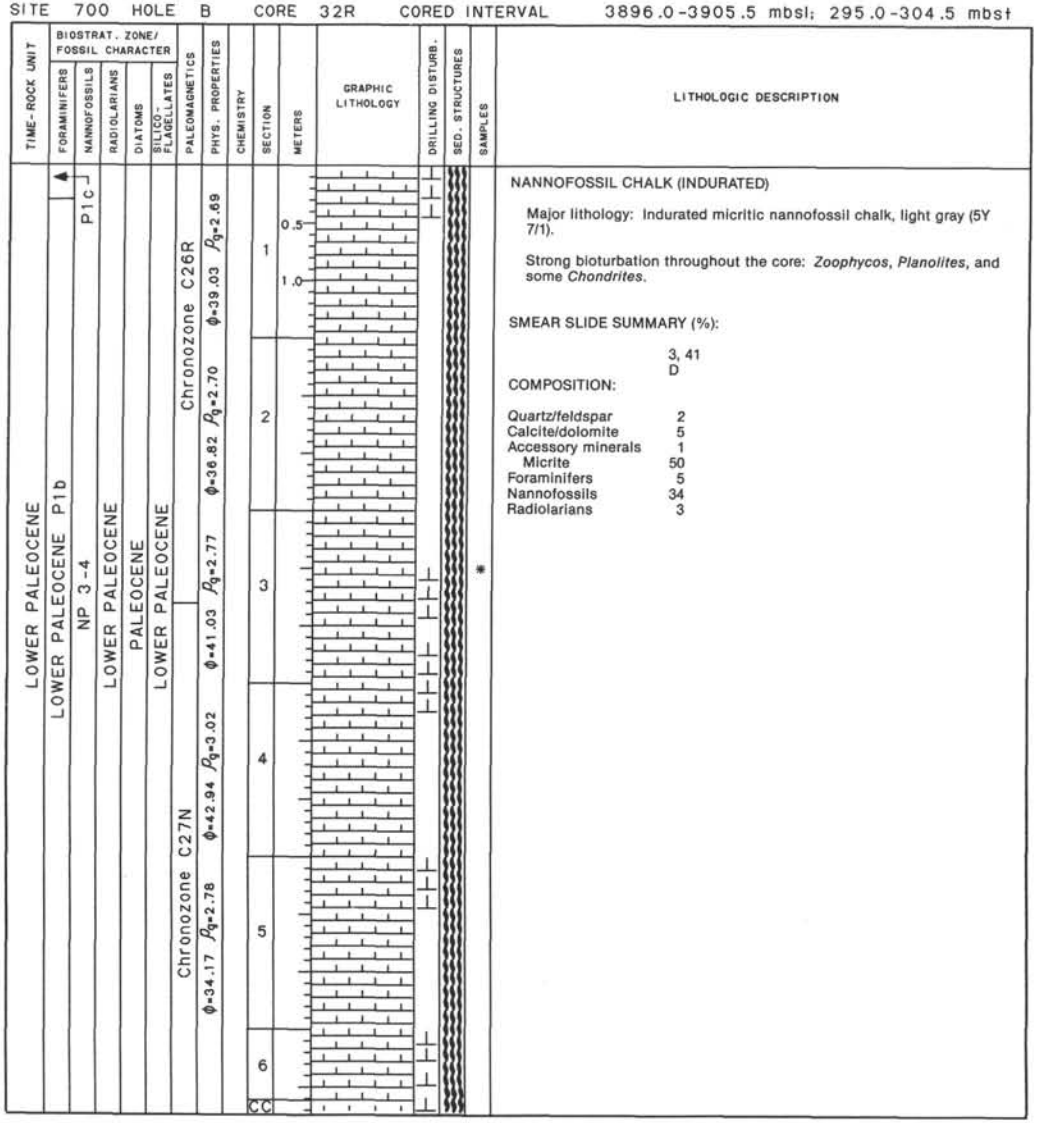

NANNOFOSSIL CHALK (INDURATED)

Major lithology: Indurated micritic nannofossil chalk, light gray (5Y 7/1).

Strong bioturbation throughout the core: *Zoophycos*, *Planolites*, and some *Chondrites*.

SMEAR SLIDE SUMMARY (%):

	3, 41
	D
COMPOSITION:	
Quartz/feldspar	2
Calcite/dolomite	5
Accessory minerals	1
Micrite	50
Foraminifers	5
Nannofossils	34
Radiolarians	3

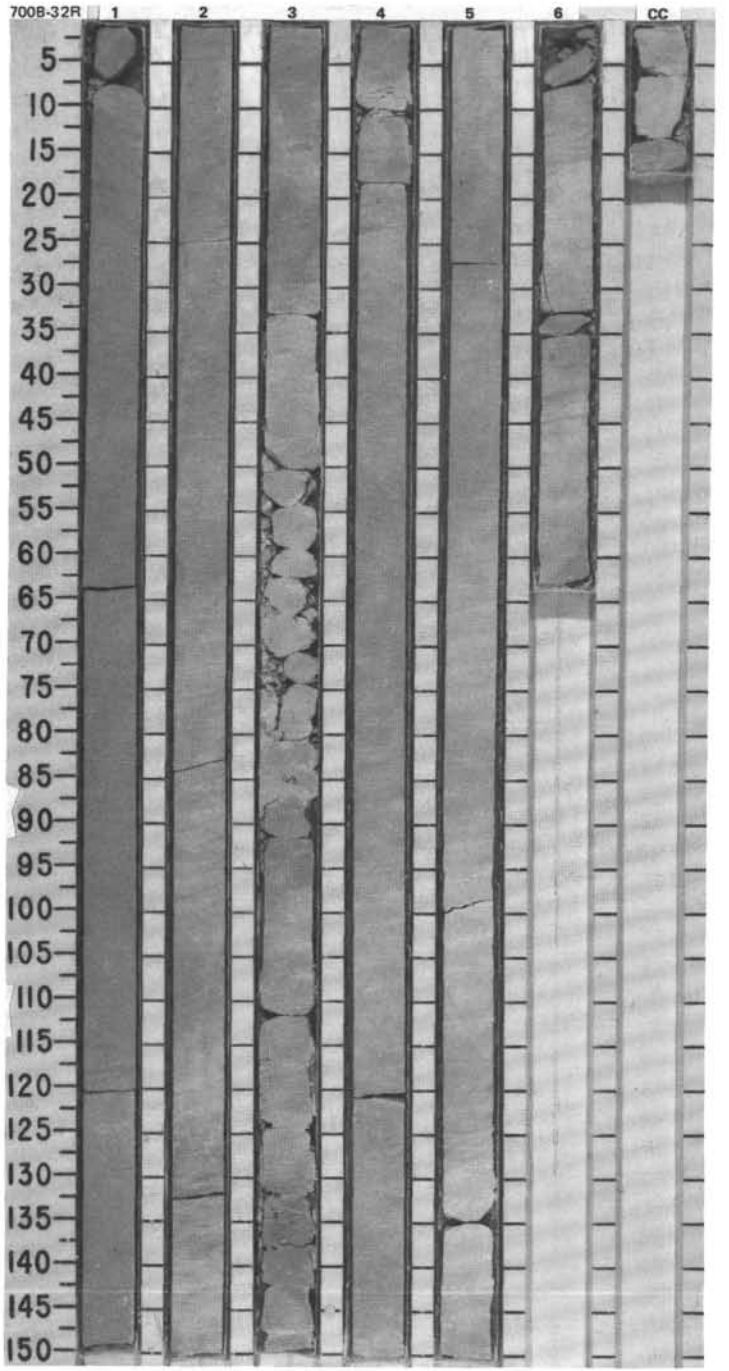

SITE 700 HOLE B CORE 33R CORED INTERVAL 3905.5-3915.0 mbsl; 304.5-314.0 mbsf

TIME-ROCK UNIT	BIOSTRAT. ZONE/ FOSSIL CHARACTER: FORAMINIFERS	NANNOFOSSILS	RADIOLARIANS	DIATOMS	SILICO-FLAGELLATES	PALEOMAGNETICS	PHYS. PROPERTIES	CHEMISTRY	SECTION	METERS	GRAPHIC LITHOLOGY	DRILLING DISTURB.	SED. STRUCTURES	SAMPLES
LOWER PALEOCENE	LOWER PALEOCENE P1b	NP 3-4	Barren	PALEOCENE	Barren		ϕ=38.29 ρ_g=2.84		1, CC	0.5, 1.0				*

LITHOLOGIC DESCRIPTION

NANNOFOSSIL CHALK (INDURATED)

Drilling disturbance: lithic fragments in Section 1, 0-40 cm.

Major lithology: Micritic nannofossil chalk, white (5Y 8/1).

Moderate bioturbation, Section 1.

Minor lithology: Chert fragments, Section 1, 76-78 cm (contamination?).

SMEAR SLIDE SUMMARY (%):

	1, 60 D
COMPOSITION:	
Quartz/feldspar	1
Volcanic glass	1
Calcite/dolomite	2
Accessory minerals:	
Micrite	45
Foraminifers	5
Nannofossils	45
Radiolarians	1

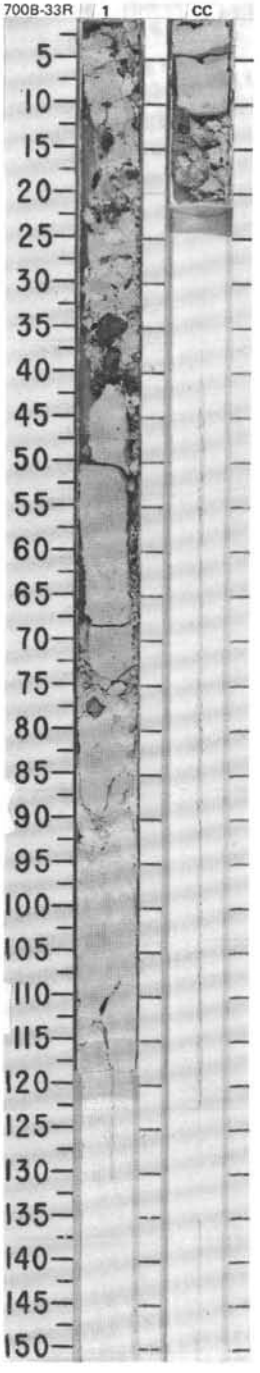

SITE 700 HOLE B CORE 34R CORED INTERVAL 3915.0-3920.0 mbsl; 314.0-319.0 mbsf

TIME-ROCK UNIT	BIOSTRAT. ZONE/ FOSSIL CHARACTER: FORAMINIFERS	NANNOFOSSILS	RADIOLARIANS	DIATOMS	SILICO-FLAGELLATES	PALEOMAGNETICS	PHYS. PROPERTIES	CHEMISTRY	SECTION	METERS	GRAPHIC LITHOLOGY	DRILLING DISTURB.	SED. STRUCTURES	SAMPLES
LOWER PALEOCENE	LOWER PALEOCENE P1b	NP 3-4	Barren	Barren	Barren	Chronozone C28N	ϕ=40.17 ρ_g=2.80 ϕ=28.65 ρ_g=2.78 ϕ=28.61 ρ_g=2.74		1 2 3 CC	0.5 1.0	VOID			TW

LITHOLOGIC DESCRIPTION

NANNOFOSSIL CHALK (INDURATED)

Drilling disturbance: Moderately fragmented in Section 1, Section 2, 0-25 cm, and most of Section 3.

Major lithology: Indurated micritic nannofossil chalk, light gray (5Y 7/1).

SMEAR SLIDE SUMMARY (%):

	1, 26 D
COMPOSITION:	
Quartz/feldspar	Tr
Volcanic glass(?)	1
Accessory minerals	1
Micrite	40
Foraminifers	8
Nannofossils	50

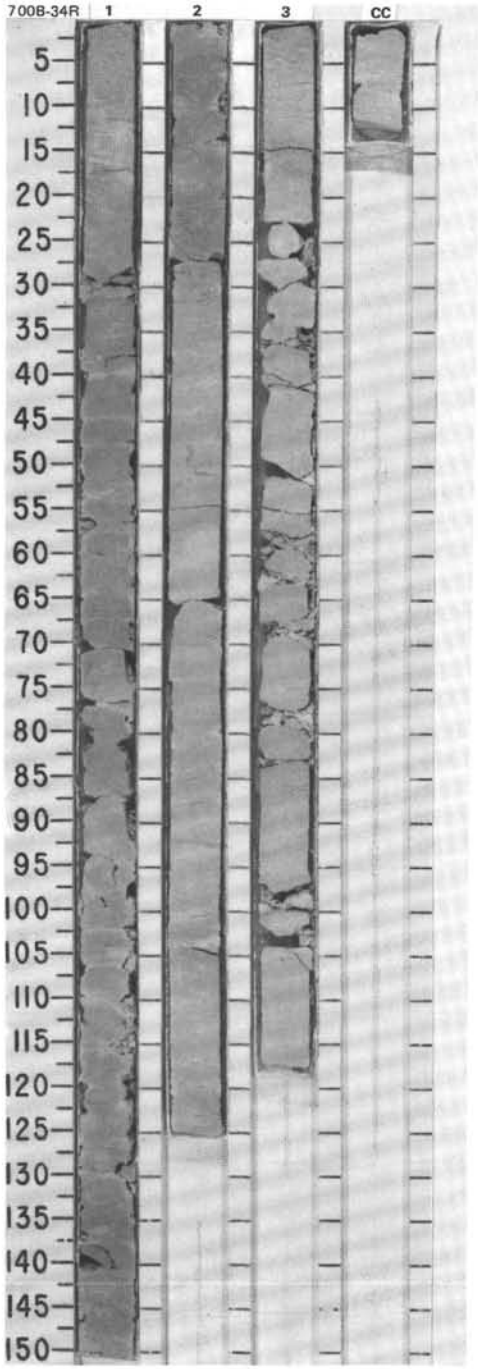

SITE 700 HOLE B CORE 35R CORED INTERVAL 3920.0-3927.0 mbsl; 319.0-326.0 mbsf

TIME-ROCK UNIT	BIOSTRAT. ZONE/ FOSSIL CHARACTER: FORAMINIFERS	NANNOFOSSILS	RADIOLARIANS	DIATOMS	SILICO-FLAGELLATES	PALEOMAGNETICS	PHYS. PROPERTIES	CHEMISTRY	SECTION	METERS	GRAPHIC LITHOLOGY	DRILLING DISTURB.	SED. STRUCTURES	SAMPLES	LITHOLOGIC DESCRIPTION
LOWER PALEOCENE	P1b					Chronozone 28N	ϕ=27.79 ρ_g=3.05		1	0.5, 1.0		X		*	NANNOFOSSIL-BEARING LIMESTONE
LOWER PALEOCENE		NP 3-4	Barren	Barren	Barren	Chronozone 28R	ϕ=28.34 ρ_g=2.77		2						
									CC						

Drilling disturbance: Moderate. Lithic fragments in Section 1, 0-12 cm.

Major lithology: Nannofossil-bearing limestone, light gray (5Y 7/1).

SMEAR SLIDE SUMMARY (%):

	1, 73
	D
COMPOSITION:	
Clay	5
Calcite	2
Accessory minerals:	
Zeolites	Tr
Micrite	82
Foraminifers	1
Nannofossils	10

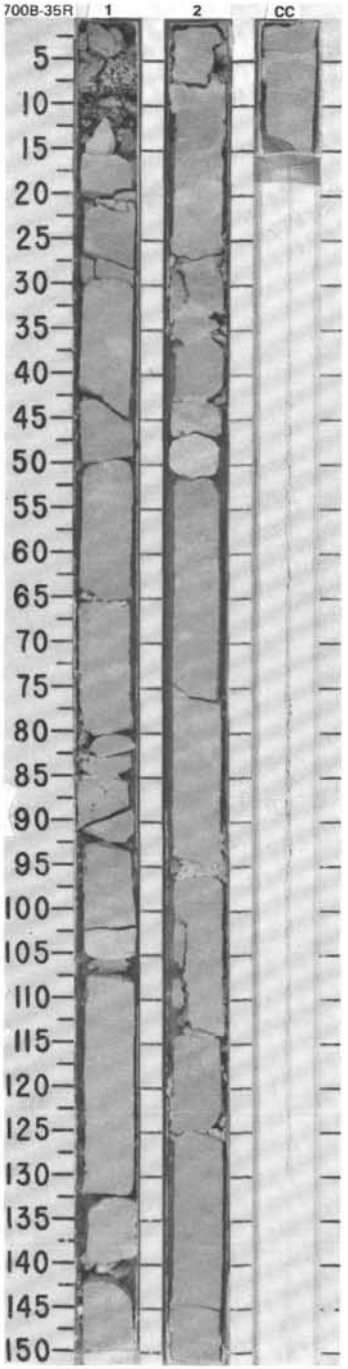

SITE 700 HOLE B CORE 36R CORED INTERVAL 3927.0-3931.7 mbsl; 326.0-330.7 mbsf

TIME-ROCK UNIT	BIOSTRAT. ZONE/ FOSSIL CHARACTER: FORAMINIFERS	NANNOFOSSILS	RADIOLARIANS	DIATOMS	SILICO-FLAGELLATES	PALEOMAGNETICS	PHYS. PROPERTIES	CHEMISTRY	SECTION	METERS	GRAPHIC LITHOLOGY	DRILLING DISTURB.	SED. STRUCTURES	SAMPLES
LOWER PALEOCENE	LOWER PALEOCENE (P1b)	NP 3-4	Barren	Barren	Barren	Chronozone C28R / Chronozone C29N	ϕ=28.49 ρ_g=2.69 / ϕ=29.40 ρ_g=2.87		1, 2, 3, CC	0.5, 1.0				* * IW

LITHOLOGIC DESCRIPTION

NANNOFOSSIL-BEARING MICRITIC LIMESTONE

Drilling disturbance: Slight.

Major lithology: Nannofossil-bearing micritic limestone, white (10YR 8/1), in Sections 1 and 2; and white (5Y 8/1), in Section 3.

Strong bioturbation in Sections 1 and 2, to minor or moderate in Section 3. *Planolites*, *Chondrites*, *Thalassinoides*, and rare *Zoophycos* in Section 1; *Planolites*, *Chondrites*, and *Zoophycos* in Section 2; and *Planolites* and *Chondrites* in Section 3.

Minor lithology: chert nodules in Section 1, 39–42 cm.

SMEAR SLIDE SUMMARY (%):

	1, 50 D	2, 8 D
COMPOSITION:		
Mica	—	Tr
Accessory minerals	Tr	1
Micrite	90	89
Foraminifers	—	Tr
Nannofossils	10	10

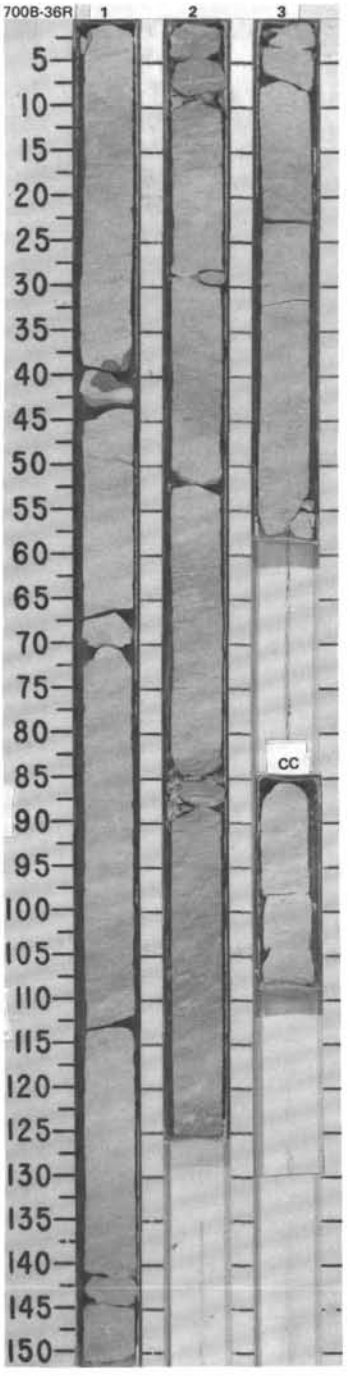

SITE 700 HOLE B CORE 37R CORED INTERVAL 3931.7-3936.5 mbsl; 330.7-335.5 mbsf

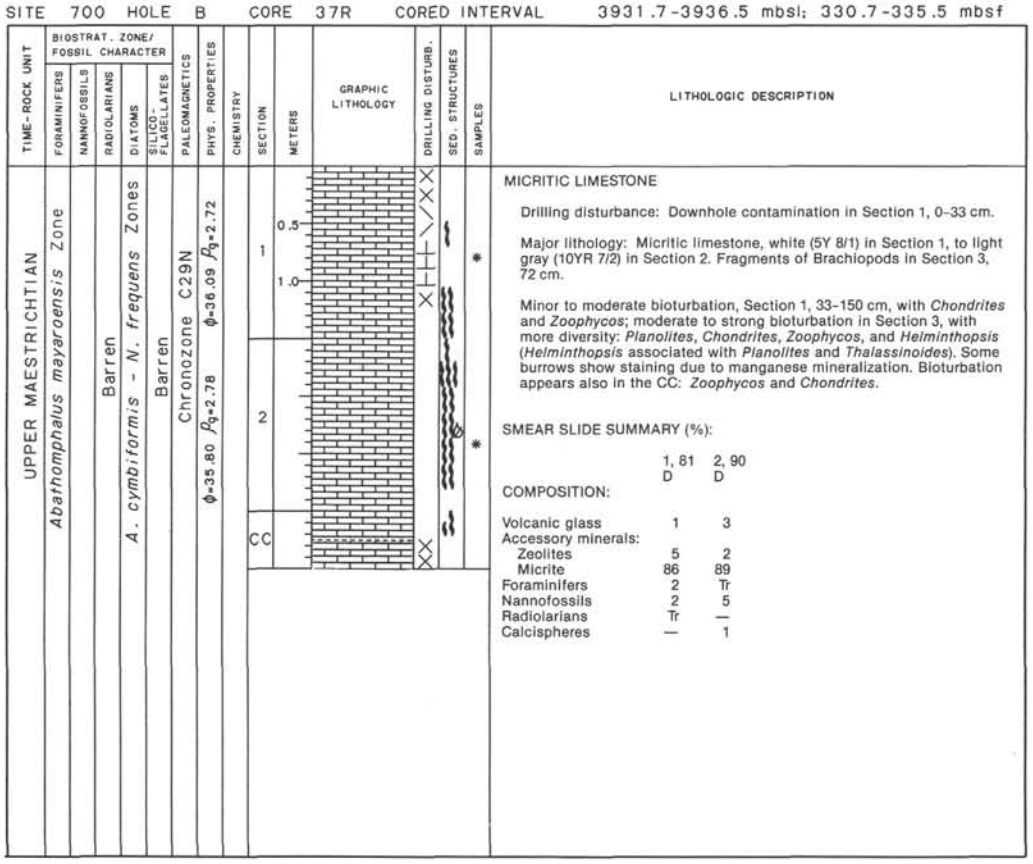

LITHOLOGIC DESCRIPTION

MICRITIC LIMESTONE

Drilling disturbance: Downhole contamination in Section 1, 0–33 cm.

Major lithology: Micritic limestone, white (5Y 8/1) in Section 1, to light gray (10YR 7/2) in Section 2. Fragments of Brachiopods in Section 3, 72 cm.

Minor to moderate bioturbation, Section 1, 33–150 cm, with *Chondrites* and *Zoophycos*; moderate to strong bioturbation in Section 3, with more diversity: *Planolites*, *Chondrites*, *Zoophycos*, and *Helminthopsis* (*Helminthopsis* associated with *Planolites* and *Thalassinoides*). Some burrows show staining due to manganese mineralization. Bioturbation appears also in the CC: *Zoophycos* and *Chondrites*.

SMEAR SLIDE SUMMARY (%):

	1, 81 D	2, 90 D
COMPOSITION:		
Volcanic glass	1	3
Accessory minerals:		
Zeolites	5	2
Micrite	86	89
Foraminifers	2	Tr
Nannofossils	2	5
Radiolarians	Tr	—
Calcispheres	—	1

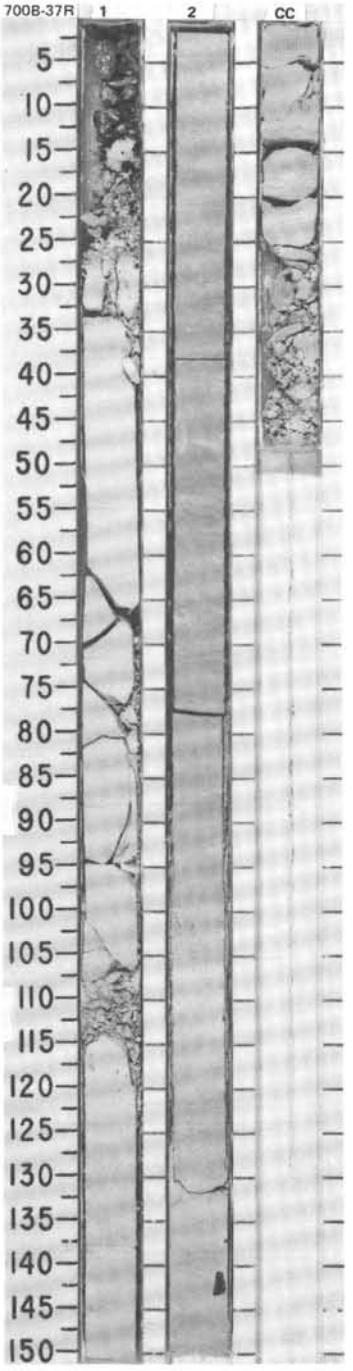

SITE 700 HOLE B CORE 38R CORED INTERVAL 3936.5-3946.0 mbsl; 335.5-345.0 mbsf

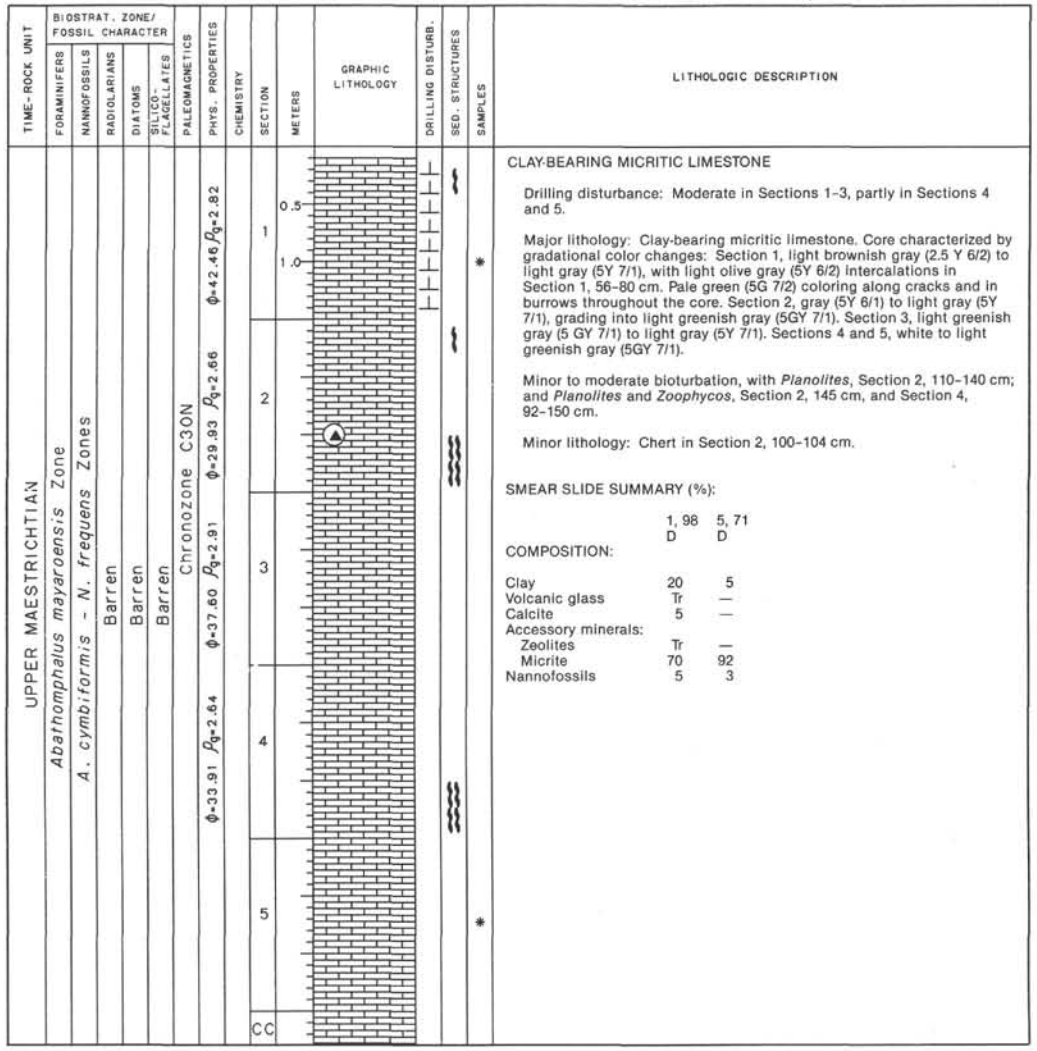

LITHOLOGIC DESCRIPTION

CLAY-BEARING MICRITIC LIMESTONE

Drilling disturbance: Moderate in Sections 1-3, partly in Sections 4 and 5.

Major lithology: Clay-bearing micritic limestone. Core characterized by gradational color changes: Section 1, light brownish gray (2.5 Y 6/2) to light gray (5Y 7/1), with light olive gray (5Y 6/2) intercalations in Section 1, 56-80 cm. Pale green (5G 7/2) coloring along cracks and in burrows throughout the core. Section 2, gray (5Y 6/1) to light gray (5Y 7/1), grading into light greenish gray (5GY 7/1). Section 3, light greenish gray (5 GY 7/1) to light gray (5Y 7/1). Sections 4 and 5, white to light greenish gray (5GY 7/1).

Minor to moderate bioturbation, with *Planolites*, Section 2, 110-140 cm; and *Planolites* and *Zoophycos*, Section 2, 145 cm, and Section 4, 92-150 cm.

Minor lithology: Chert in Section 2, 100-104 cm.

SMEAR SLIDE SUMMARY (%):

	1, 98 D	5, 71 D
COMPOSITION:		
Clay	20	5
Volcanic glass	Tr	—
Calcite	5	—
Accessory minerals:		
Zeolites	Tr	—
Micrite	70	92
Nannofossils	5	3

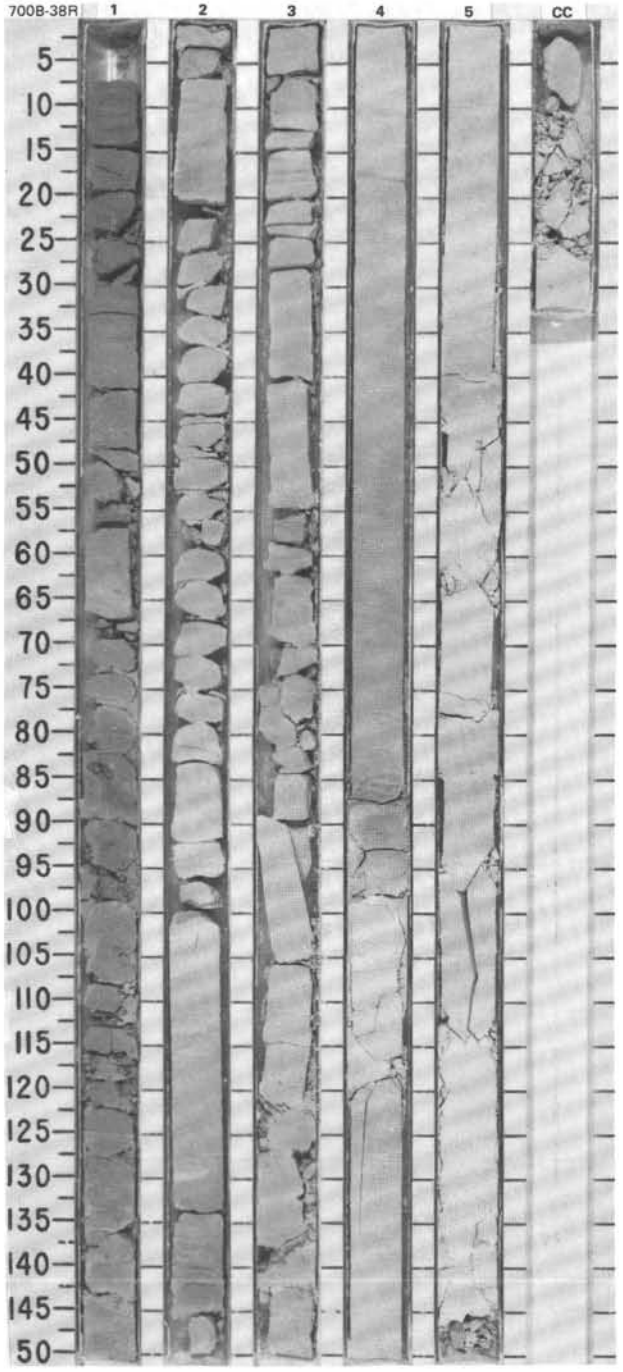

SITE 700 HOLE B CORE 39R CORED INTERVAL 3946.0-3955.5 mbsl; 345.0-354.5 mbsf

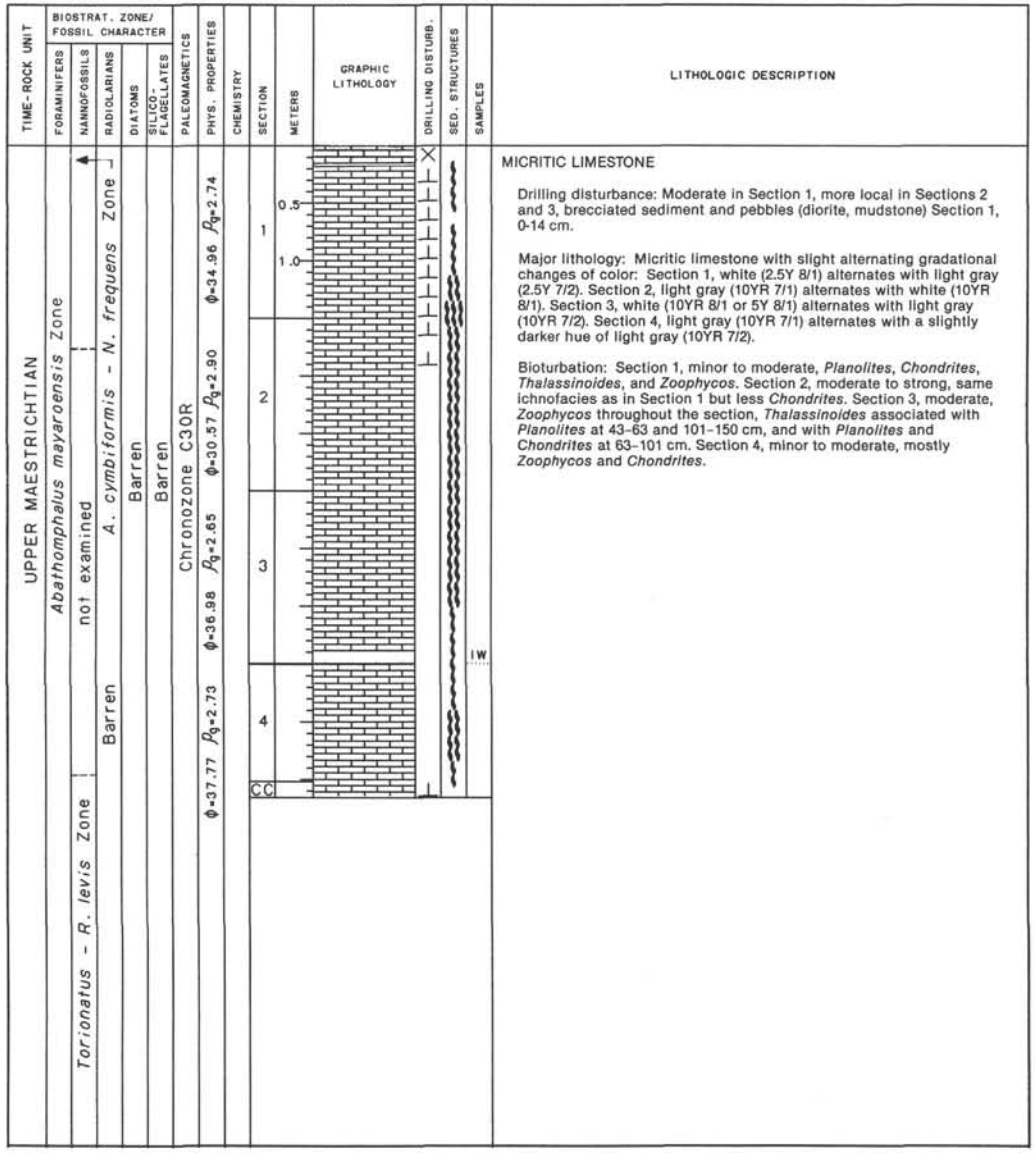

LITHOLOGIC DESCRIPTION

MICRITIC LIMESTONE

Drilling disturbance: Moderate in Section 1, more local in Sections 2 and 3, brecciated sediment and pebbles (diorite, mudstone) Section 1, 0-14 cm.

Major lithology: Micritic limestone with slight alternating gradational changes of color: Section 1, white (2.5Y 8/1) alternates with light gray (2.5Y 7/2). Section 2, light gray (10YR 7/1) alternates with white (10YR 8/1). Section 3, white (10YR 8/1 or 5Y 8/1) alternates with light gray (10YR 7/2). Section 4, light gray (10YR 7/1) alternates with a slightly darker hue of light gray (10YR 7/2).

Bioturbation: Section 1, minor to moderate, *Planolites*, *Chondrites*, *Thalassinoides*, and *Zoophycos*. Section 2, moderate to strong, same ichnofacies as in Section 1 but less *Chondrites*. Section 3, moderate, *Zoophycos* throughout the section, *Thalassinoides* associated with *Planolites* at 43-63 and 101-150 cm, and with *Planolites* and *Chondrites* at 63-101 cm. Section 4, minor to moderate, mostly *Zoophycos* and *Chondrites*.

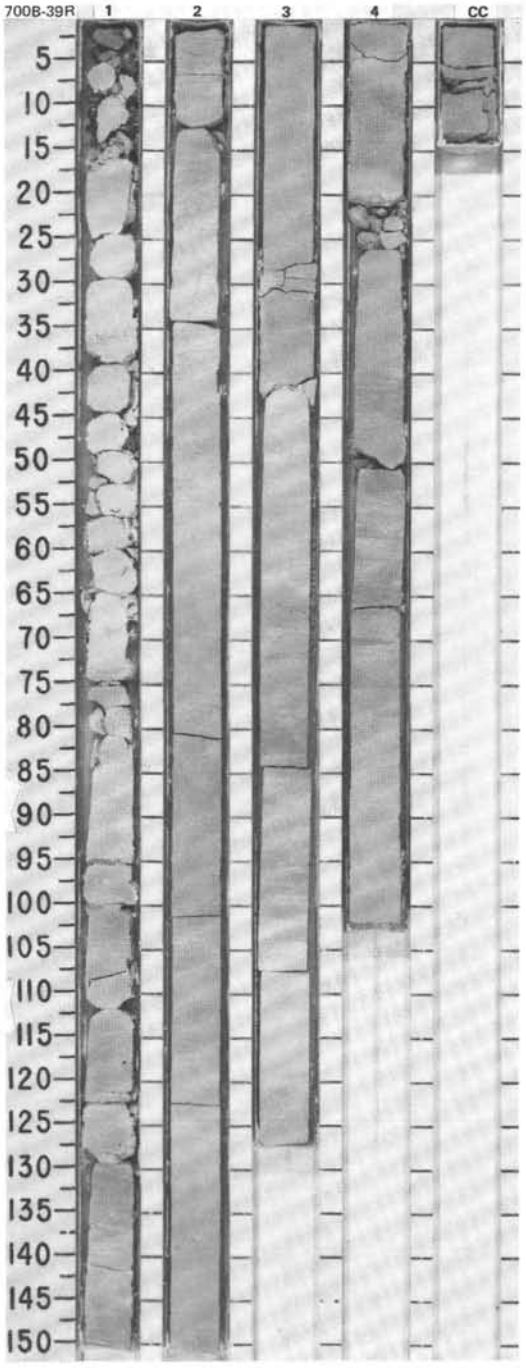

SITE 700 HOLE B CORE 40R CORED INTERVAL 3955.5-3965.0 mbsl; 354.5-364.0 mbsf

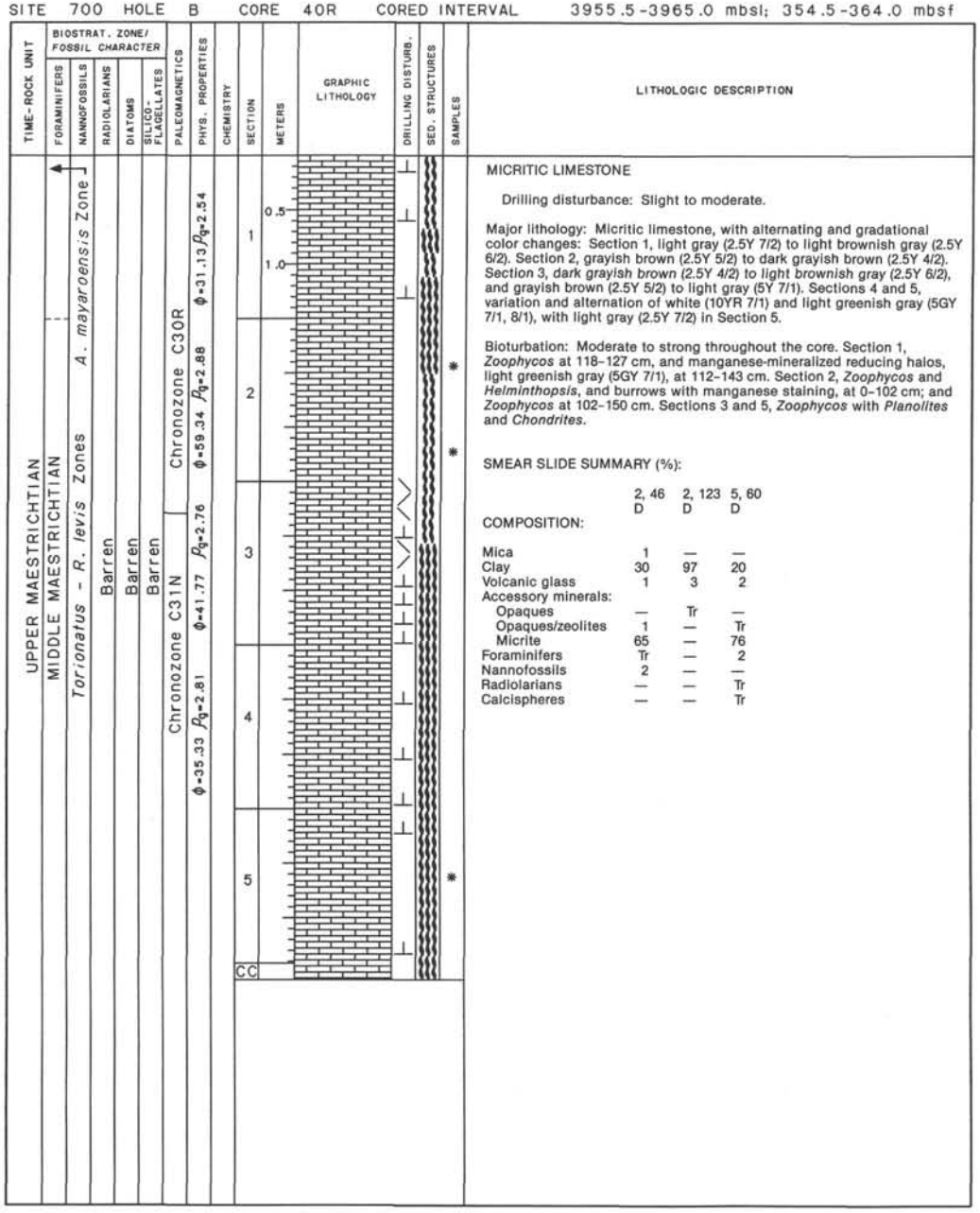

LITHOLOGIC DESCRIPTION

MICRITIC LIMESTONE

Drilling disturbance: Slight to moderate.

Major lithology: Micritic limestone, with alternating and gradational color changes: Section 1, light gray (2.5Y 7/2) to light brownish gray (2.5Y 6/2). Section 2, grayish brown (2.5Y 5/2) to dark grayish brown (2.5Y 4/2). Section 3, dark grayish brown (2.5Y 4/2) to light brownish gray (2.5Y 6/2), and grayish brown (2.5Y 5/2) to light gray (5Y 7/1). Sections 4 and 5, variation and alternation of white (10YR 7/1) and light greenish gray (5GY 7/1, 8/1), with light gray (2.5Y 7/2) in Section 5.

Bioturbation: Moderate to strong throughout the core. Section 1, *Zoophycos* at 118-127 cm, and manganese-mineralized reducing halos, light greenish gray (5GY 7/1), at 112-143 cm. Section 2, *Zoophycos* and *Helminthopsis*, and burrows with manganese staining, at 0-102 cm; and *Zoophycos* at 102-150 cm. Sections 3 and 5, *Zoophycos* with *Planolites* and *Chondrites*.

SMEAR SLIDE SUMMARY (%):

	2, 46 D	2, 123 D	5, 60 D
COMPOSITION:			
Mica	1	—	—
Clay	30	97	20
Volcanic glass	1	3	2
Accessory minerals:			
Opaques	—	Tr	—
Opaques/zeolites	1	—	Tr
Micrite	65	—	76
Foraminifers	Tr	—	2
Nannofossils	2	—	—
Radiolarians	—	—	Tr
Calcispheres	—	—	Tr

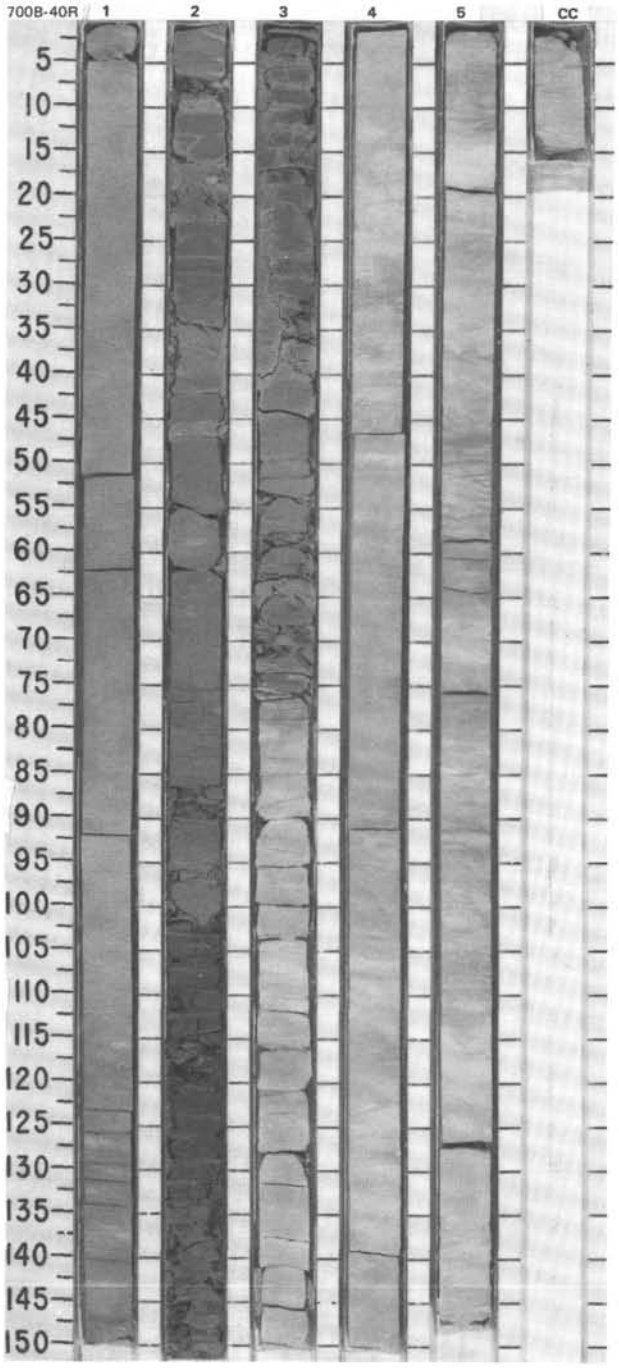

SITE 700 HOLE B CORE 41R CORED INTERVAL 3965.0-3974.5 mbsl; 364.0-373.5 mbsf

TIME-ROCK UNIT	BIOSTRAT. ZONE/ FOSSIL CHARACTER: FORAMINIFERS	NANNOFOSSILS	RADIOLARIANS	DIATOMS	SILICO-FLAGELLATES	PALEOMAGNETICS	PHYS. PROPERTIES	CHEMISTRY	SECTION	METERS	GRAPHIC LITHOLOGY	DRILLING DISTURB.	SED. STRUCTURES	SAMPLES
LOWER MAESTRICHTIAN	LOWER - MIDDLE MAESTRICHTIAN	*Torionatus - R. levis* Zones	Barren	Barren	Barren	Chronozone C31N	ϕ=30.03 ρ_g=2.69; ϕ=29.20 ρ_g=2.80; ϕ=36.73 ρ_g=2.62; ϕ=30.88 ρ_g=2.62		1, 2, 3, 4	0.5, 1.0				

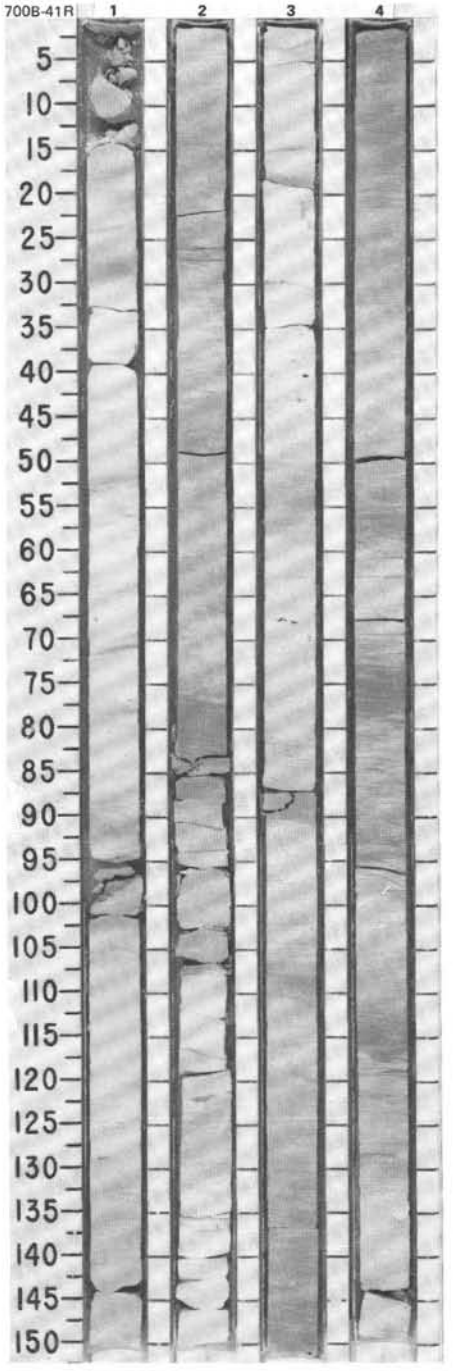

LITHOLOGIC DESCRIPTION

CLAY-BEARING MICRITIC LIMESTONE, alternating with CLAYEY MICRITIC LIMESTONE and MICRITIC LIMESTONE

Major lithology: Clay-bearing micritic limestone, alternating with clayey micritic limestone and micritic limestone. Alternation is clearly visible by gradational changes of color throughout the core. Clay-bearing micritic limestone occurs in Section 1, white (no hue on color chart), to light greenish gray (5Y 7/1); and in Section 2, light gray (5Y 7/1) to light greenish gray (5G 7/2), sometimes finely laminated. Clayey micritic limestone occurs in Section 2, light greenish gray (5G 7/1), in Section 3, greenish gray (5GY 6/1), and in Section 5, light greenish gray (5GY 7/1). Alternation to micritic limestone occurs in Section 3, white (no hue on color chart), and in Sections 4 and 5, light gray (5Y 7/1).

Minor to moderate bioturbation, mainly *Zoophycos* in Section 3, with *Planolites* in Section 4.

Minor lithology: Chert nodules in Section 2, 120-123 cm.

SITE 700 HOLE B CORE 42R CORED INTERVAL 3974.5-3984.0 mbsl; 373.5-383.0 mbsf

TIME-ROCK UNIT	BIOSTRAT. ZONE/ FOSSIL CHARACTER: FORAMINIFERS	NANNOFOSSILS	RADIOLARIANS	DIATOMS	SILICO-FLAGELLATES	PALEOMAGNETICS	PHYS. PROPERTIES	CHEMISTRY	SECTION	METERS	GRAPHIC LITHOLOGY	DRILLING DISTURB.	SED. STRUCTURES	SAMPLES
LOWER MAESTRICHTIAN	LOWER - MIDDLE MAESTRICHTIAN	*Torionatus* - *R. levis* Zones	Barren	Barren	Barren	Chronozone C31N / Chronozone C31R	ϕ=31.87 ρ_g=2.73 / ϕ=31.87 ρ_g=2.73 / ϕ=31.81 ρ_g=2.68		1 / 2 / 3 / 4 / CC	0.5 / 1.0				OG

LITHOLOGIC DESCRIPTION

MICRITIC LIMESTONE, alternating with CLAY-BEARING MICRITIC LIMESTONE TO CLAYEY MICRITIC LIMESTONE

Drilling disturbance: Slight.

Major lithology: Micritic limestone, light gray (5Y 7/1), alternating with gradational contacts of gray (5Y 6/1) or light greenish gray (5GY 7/1) clay-bearing to clayey micritic limestone.

Wavy structures caused by compaction and diagenesis.

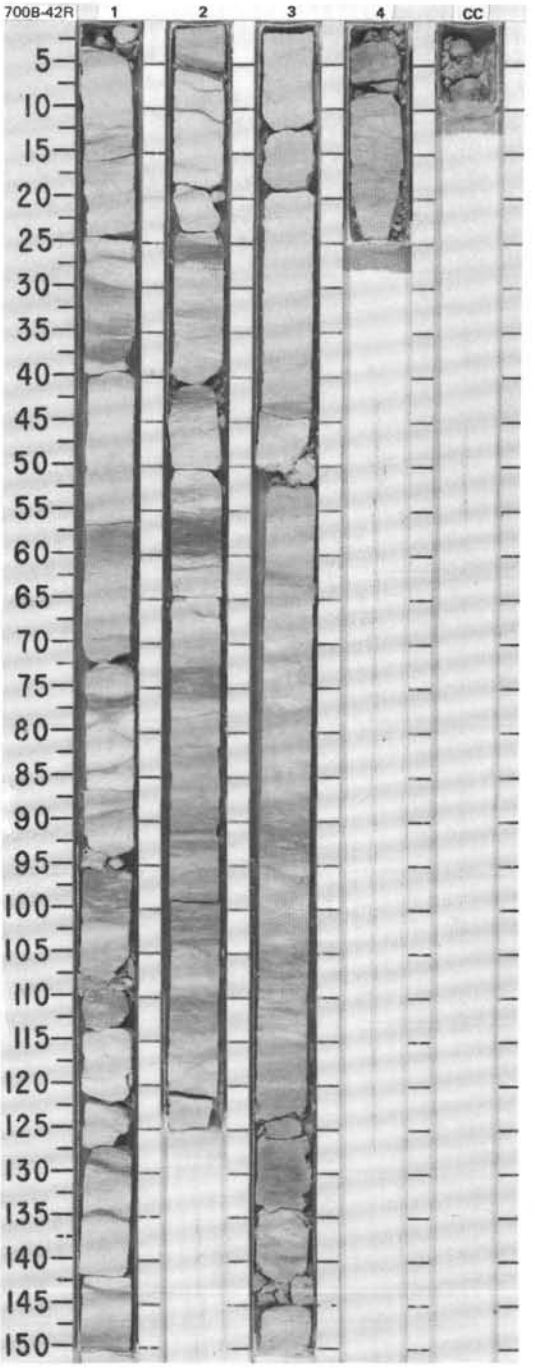

SITE 700 HOLE B CORE 43R CORED INTERVAL 3984.0-3993.5 mbsl; 383.0-392.5 mbsf

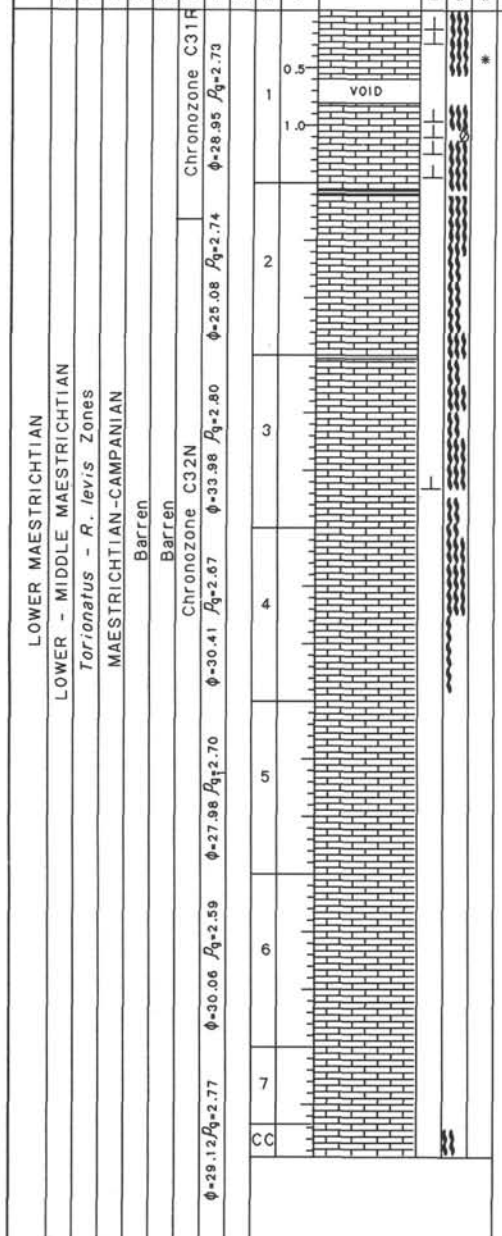

LITHOLOGIC DESCRIPTION

MICRITIC LIMESTONE

Major lithology: Micritic limestone in Sections 1-4, white (5Y 8/1) alternating with darker gray (5Y 6/1) horizons; and in Section 5, white (2.5Y 8/2) alternating with light brownish gray (2.5Y 6/2). Possible *Inoceramus* shell fragments, Section 1, 124-126 cm, epigenized by transparent silica.

Moderate to strong bioturbation with two generations of Ichnofauna occurring locally in Section 3, 55-65 cm, and Section 5, 80-90 cm. *Planolites* and *Zoophycos* appear clearly in Sections 5 and 6. Wavy structures caused by compaction and diagenesis.

SMEAR SLIDE SUMMARY (%):

	1, 48 D
COMPOSITION:	
Quartz/feldspar(?)	Tr
Accessory minerals(?)	Tr
Micrite	70
Foraminifers	3
Nannofossils	26
Radiolarians	1

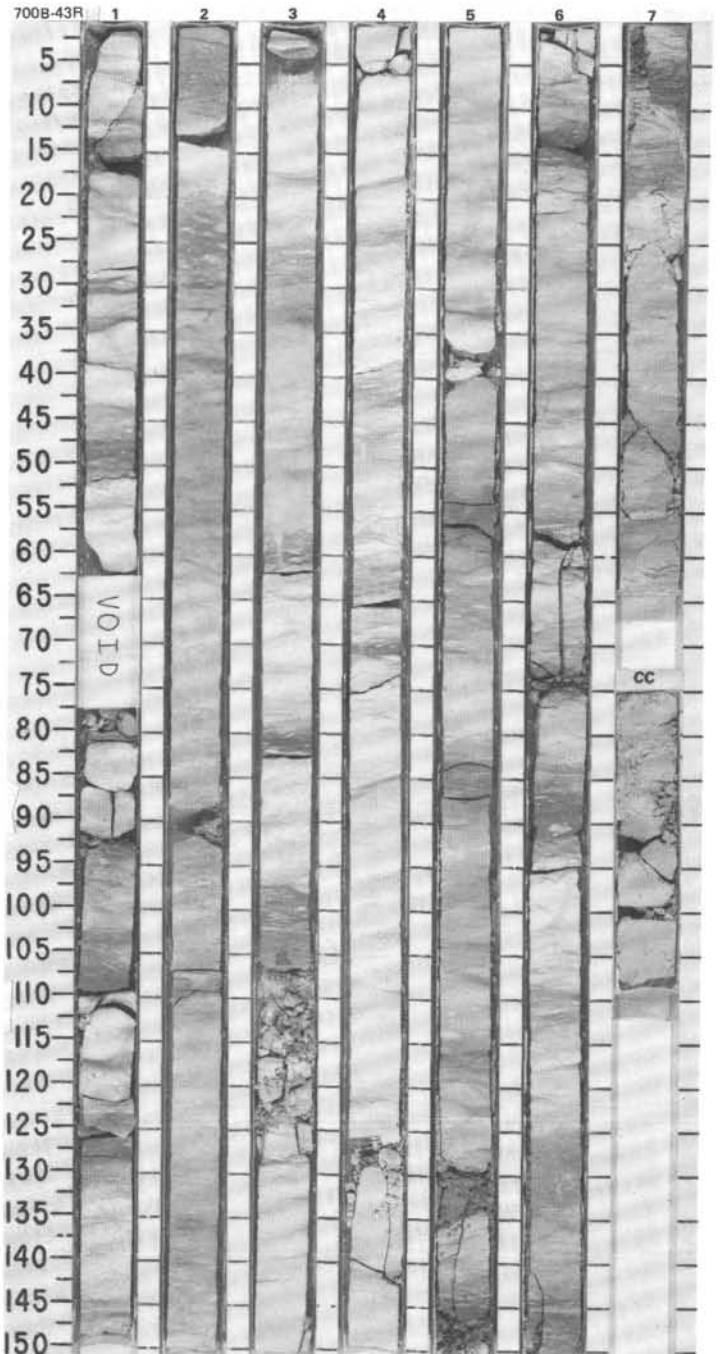

SITE 700 HOLE B CORE 44R CORED INTERVAL 3993.5-3998.0 mbsl; 392.5-397.0 mbsf

TIME-ROCK UNIT	BIOSTRAT. ZONE/ FOSSIL CHARACTER: FORAMINIFERS	NANNOFOSSILS	RADIOLARIANS	DIATOMS	SILICO-FLAGELLATES	PALEOMAGNETICS	PHYS. PROPERTIES	CHEMISTRY	SECTION	METERS	GRAPHIC LITHOLOGY	DRILLING DISTURB.	SED. STRUCTURES	SAMPLES	LITHOLOGIC DESCRIPTION
LOWER MAESTRICHTIAN	LOWER - MIDDLE MAESTRICHTIAN	*T. orionatus - R. levis* Zones	MAESTRICHTIAN-CAMPANIAN	Barren	Barren	Chronozone C32N	ϕ=33.44 ρ_g=2.70		1	0.5 1.0					MICRITIC LIMESTONE Drilling disturbance: Moderate to high. Major lithology: Micritic limestone, brown (10YR 5/3). SMEAR SLIDE SUMMARY (%): CC D COMPOSITION: Quartz/feldspar Tr Volcanic glass(?) Tr Accessory minerals: Micrite 54 Foraminifers 1 Nannofossils 43 Radiolarians(?) 2
									CC					*	

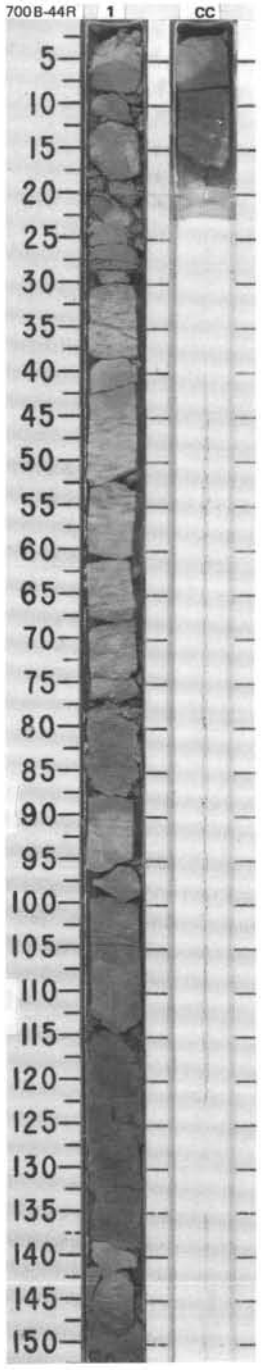

SITE 700 HOLE B CORE 45R CORED INTERVAL 3998.0-4004.5 mbsl; 397.0-403.5 mbsf

TIME-ROCK UNIT	BIOSTRAT. ZONE/ FOSSIL CHARACTER: FORAMINIFERS	NANNOFOSSILS	RADIOLARIANS	DIATOMS	SILICO-FLAGELLATES	PALEOMAGNETICS	PHYS. PROPERTIES	CHEMISTRY	SECTION	METERS	GRAPHIC LITHOLOGY	DRILLING DISTURB.	SED. STRUCTURES	SAMPLES
LOWER MAESTRICHTIAN	LOWER - MIDDLE MAESTRICHTIAN	*T. orionatus* - *R. levis* Zones	MAESTRICHTIAN-CAMPANIAN	Barren	Barren	Chronozone C32N	ϕ=32.13 ρ_g=2.75 ϕ=30.44 ρ_g=2.60		1, 2, CC	0.5, 1.0				*

LITHOLOGIC DESCRIPTION

MICRITIC LIMESTONE

Drilling disturbance: Slight.

Major lithology: Micritic limestone, white (7.5Y 8/) to pale brown (10YR 6/3) in Sections 1 and 2, to light gray (10YR 7/2) in the CC.

Minor bioturbation.

Minor lithologies:
a. Lithic fragments (contamination), Section 1, 38-42 cm.
b. Thin chert layers and small clasts, Section 2, 51 cm.

SMEAR SLIDE SUMMARY (%):

	1, 75 D
COMPOSITION:	
Quartz/feldspar	1
Volcanic glass(?)	Tr
Accessory minerals	Tr
Micrite	89
Nannofossils	10

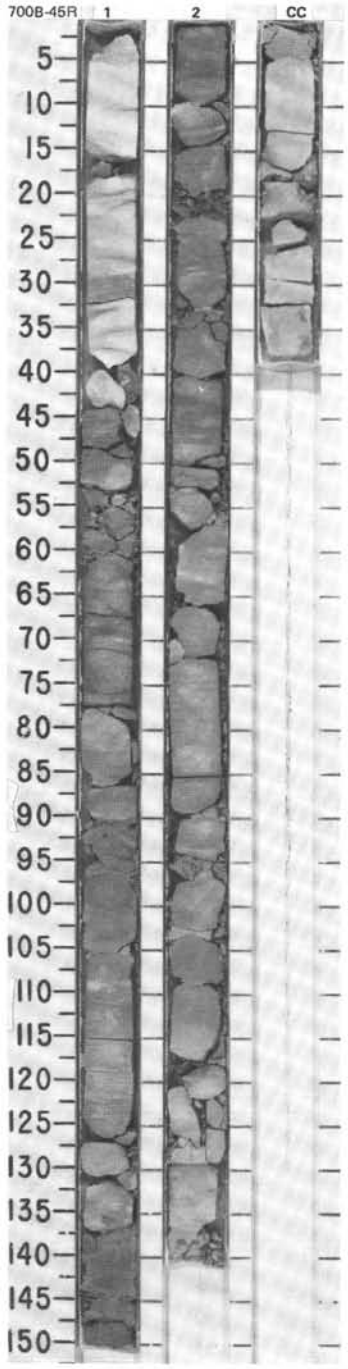

SITE 700 HOLE B CORE 46R CORED INTERVAL 4004.5-4014.0 mbsl; 403.5-413.0 mbsf

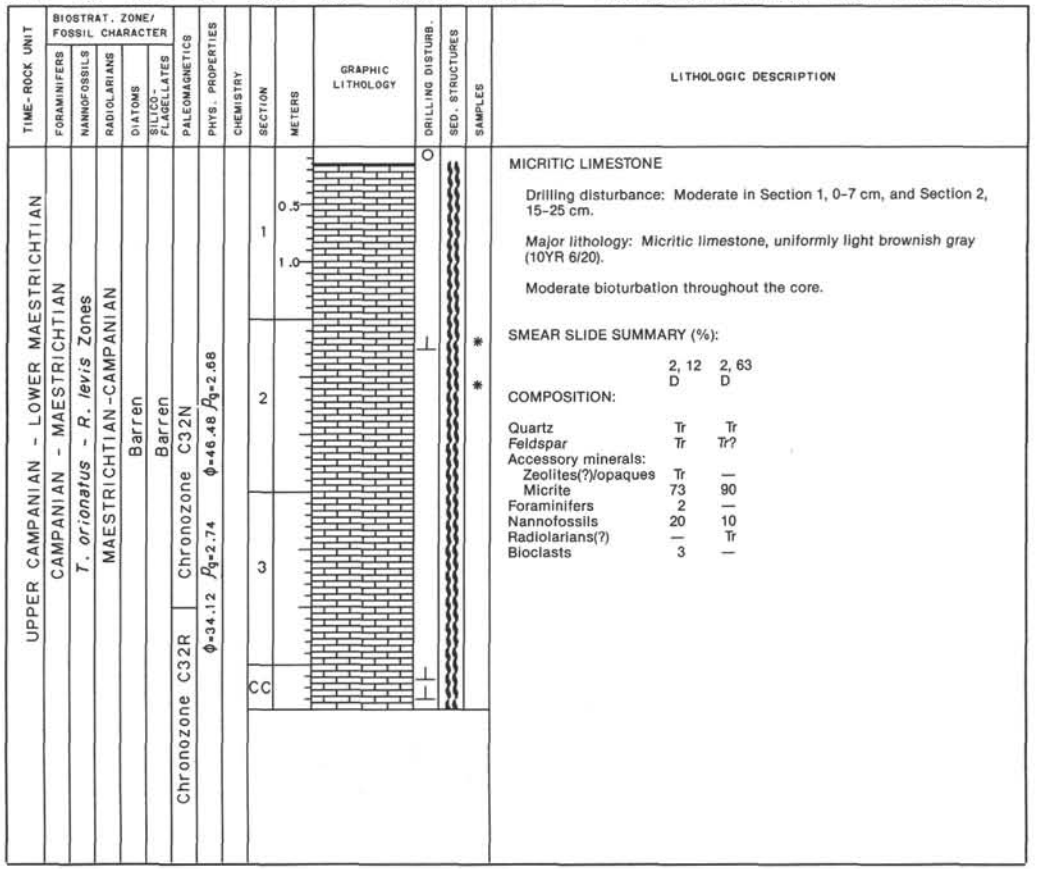

LITHOLOGIC DESCRIPTION

MICRITIC LIMESTONE

Drilling disturbance: Moderate in Section 1, 0-7 cm, and Section 2, 15-25 cm.

Major lithology: Micritic limestone, uniformly light brownish gray (10YR 6/20).

Moderate bioturbation throughout the core.

SMEAR SLIDE SUMMARY (%):

	2, 12 D	2, 63 D
COMPOSITION:		
Quartz	Tr	Tr
Feldspar	Tr	Tr?
Accessory minerals:		
Zeolites(?)/opaques	Tr	—
Micrite	73	90
Foraminifers	2	—
Nannofossils	20	10
Radiolarians(?)	—	Tr
Bioclasts	3	—

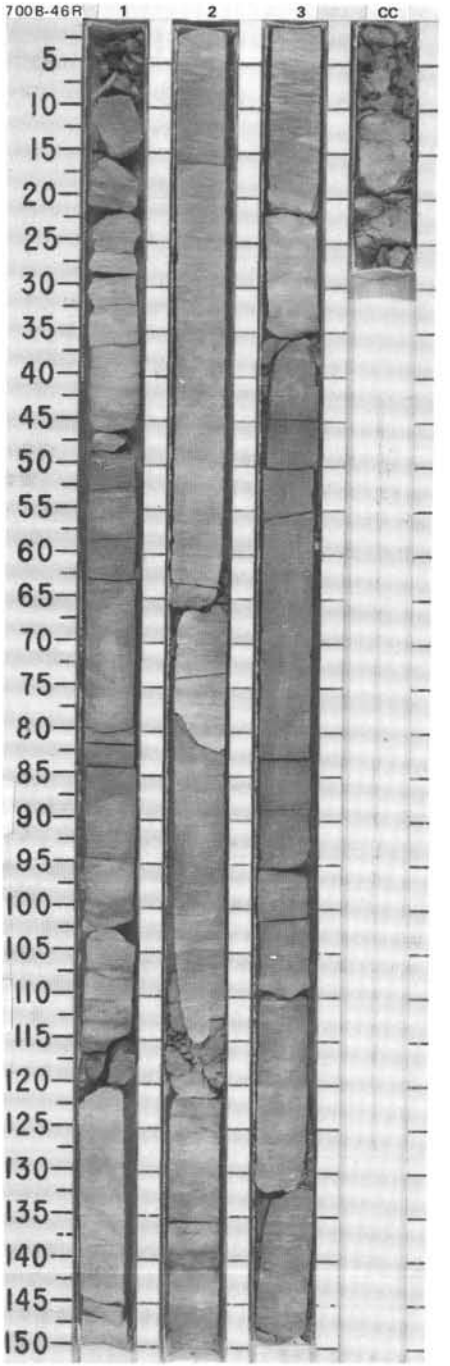

SITE 700 HOLE B CORE 47R CORED INTERVAL 4014.0-4023.5 mbsl; 413.0-422.5 mbsf

TIME-ROCK UNIT	BIOSTRAT. ZONE/ FOSSIL CHARACTER: FORAMINIFERS	NANNOFOSSILS	RADIOLARIANS	DIATOMS	SILICO-FLAGELLATES	PALEOMAGNETICS	PHYS. PROPERTIES	CHEMISTRY	SECTION	METERS	GRAPHIC LITHOLOGY	DRILLING DISTURB.	SED. STRUCTURES	SAMPLES
UPPER CAMPANIAN - LOWER MAESTRICHTIAN	CAMPANIAN - MAESTRICHTIAN	*T. orionatus* - *R. levis* Zones	MAESTRICHTIAN-CAMPANIAN	Barren	Barren	Chronozone C32R	ϕ=27.30 ρ_g=2.90 ϕ=27.76 ρ_g=2.91 ϕ=30.97 ρ_g=2.80 ϕ=23.28 ρ_g=2.79		1 2 3 4 5 CC	0.5 1.0				* *

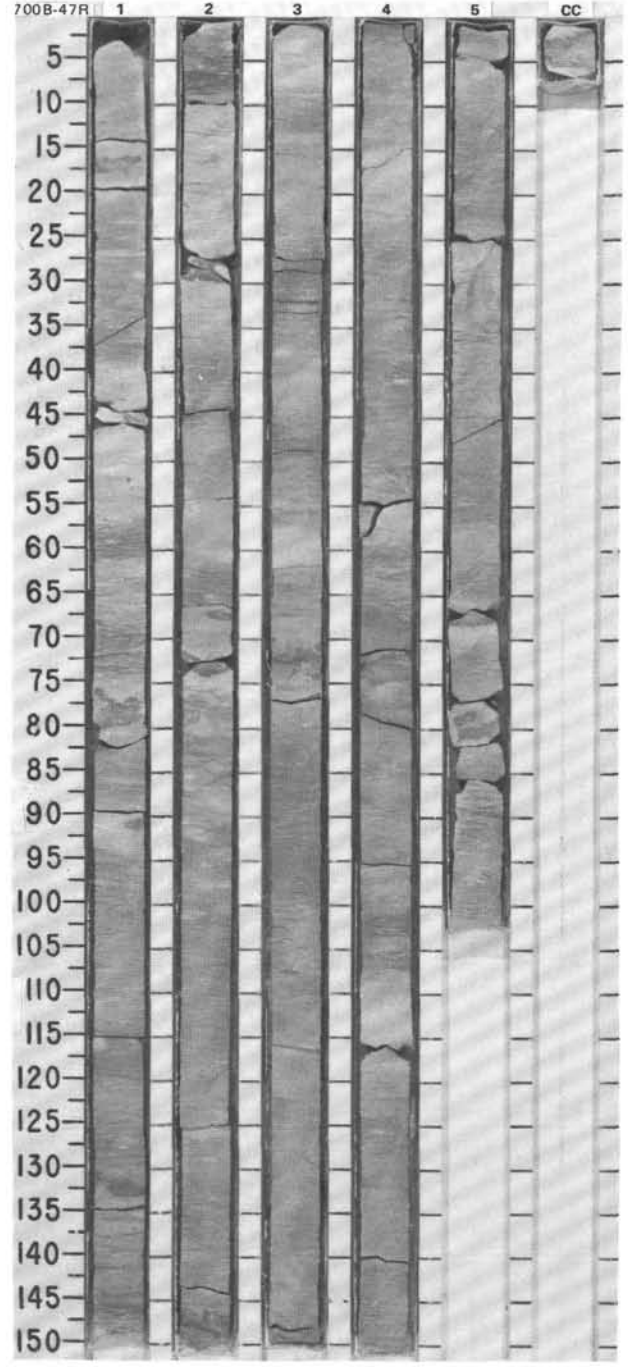

LITHOLOGIC DESCRIPTION

LIMESTONE

Major lithology: Limestone, greenish gray (5GY 7/1) to light brownish gray (10YR 6/2) in Section 1; more uniform pale brown (10YR 6/3) in the rest of the core.

Minor lithologies:
a. Chert horizons in Section 2, 27-29, 65-72, and 143-150 cm; Section 3, 69-75 cm; and Section 4, 70-75 cm; and small patches of chert in Section 5, 65-67 and 79-81 cm.
b. *Inoceramus* shell fragments, epigenized by silica.
c. Chert, brown (10YR 5/3), in CC.

SMEAR SLIDE SUMMARY (%):

	1, 16 D	1, 77 D
COMPOSITION:		
Quartz/feldspar(?)	1	Tr
Accessory minerals	—	Tr
Micrite	90	90
Nannofossils	9	10

SITE 700 HOLE B CORE 48R CORED INTERVAL 4023.5-4033.0 mbsl; 422.5-432.0 mbsf

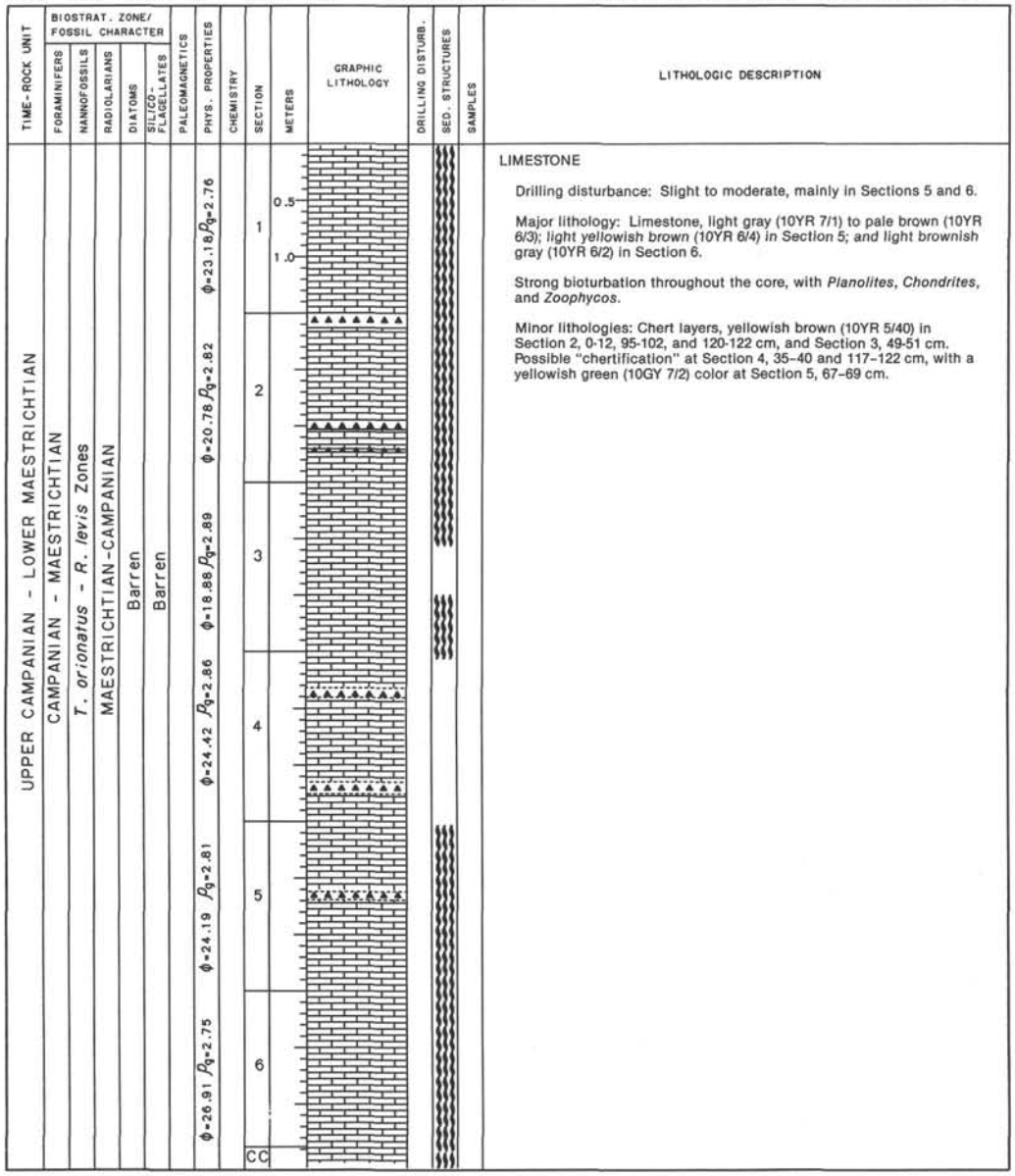

LITHOLOGIC DESCRIPTION

LIMESTONE

Drilling disturbance: Slight to moderate, mainly in Sections 5 and 6.

Major lithology: Limestone, light gray (10YR 7/1) to pale brown (10YR 6/3); *light yellowish brown (10YR 6/4) in Section 5; and light brownish* gray (10YR 6/2) in Section 6.

Strong bioturbation throughout the core, with *Planolites*, *Chondrites*, and *Zoophycos*.

Minor lithologies: Chert layers, yellowish brown (10YR 5/40) in Section 2, 0-12, 95-102, and 120-122 cm, and Section 3, 49-51 cm. Possible "chertification" at Section 4, 35-40 and 117-122 cm, with a yellowish green (10GY 7/2) color at Section 5, 67-69 cm.

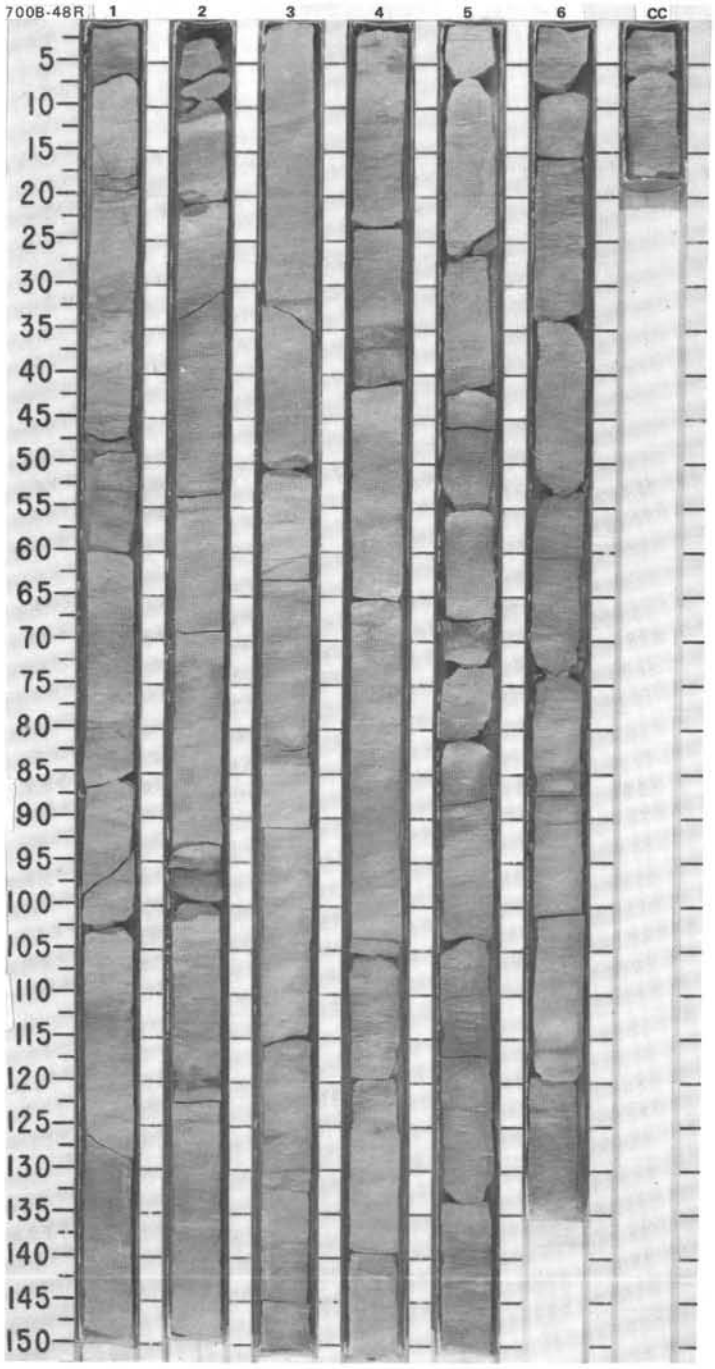

SITE 700 HOLE B CORE 49R CORED INTERVAL 4033.0-4042.5 mbsl; 432.0-441.5 mbsf

TIME-ROCK UNIT	BIOSTRAT. ZONE/ FOSSIL CHARACTER: FORAMINIFERS	NANNOFOSSILS	RADIOLARIANS	DIATOMS	SILICO-FLAGELLATES	PALEOMAGNETICS	PHYS. PROPERTIES	CHEMISTRY	SECTION	METERS	GRAPHIC LITHOLOGY	DRILLING DISTURB.	SED. STRUCTURES	SAMPLES	LITHOLOGIC DESCRIPTION
CAMPANIAN - LOWER MAESTRICHTIAN	CAMPANIAN - MAESTRICHTIAN; LOWER CAMPANIAN	*T. orionatus* - *R. levis* Zones	MAESTRICHTIAN-CAMPANIAN	Barren	Barren	Chronozone C33N	ϕ=23.64 ρ_g=2.72; ϕ=29.23 ρ_g=2.83; ϕ=31.11 ρ_g=2.83; ϕ=32.25 ρ_g=3.17		1, 2, 3, 4, 5, CC	0.5, 1.0				IW	MICRITIC LIMESTONE Drilling disturbance: Moderate. Major lithology: Micritic limestone, pale brown (10YR 6/3) in Section 1, to gray (10YR 6/1) in Sections 3 and 5, interbedded with horizons of limestone, light greenish gray (5GY 7/1) in Section 2, 63 and 90-106 cm; some with clay-rich layers, grayish brown (10YR 5/2), in Section 3, 57-58, 72-73, and 111-112 cm; or clay-bearing layers, greenish gray (5G 6/1) or (5GY 6/1), in Section 4. Minor lithology: Chert, light gray (10YR 7/2), Section 5, 15-18, 32-35, 50-59, and 73-77 cm.

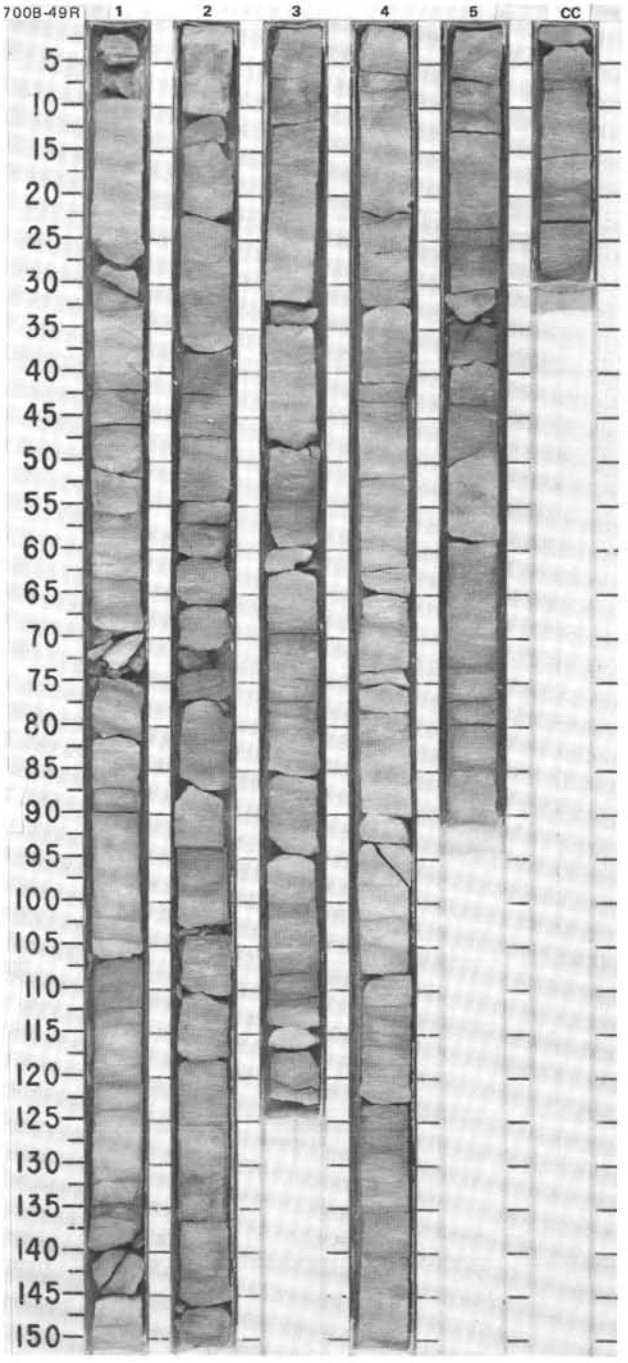

SITE 700 HOLE B CORE 50R CORED INTERVAL 4042.5-4052.0 mbsl; 441.5-451.0 mbsf

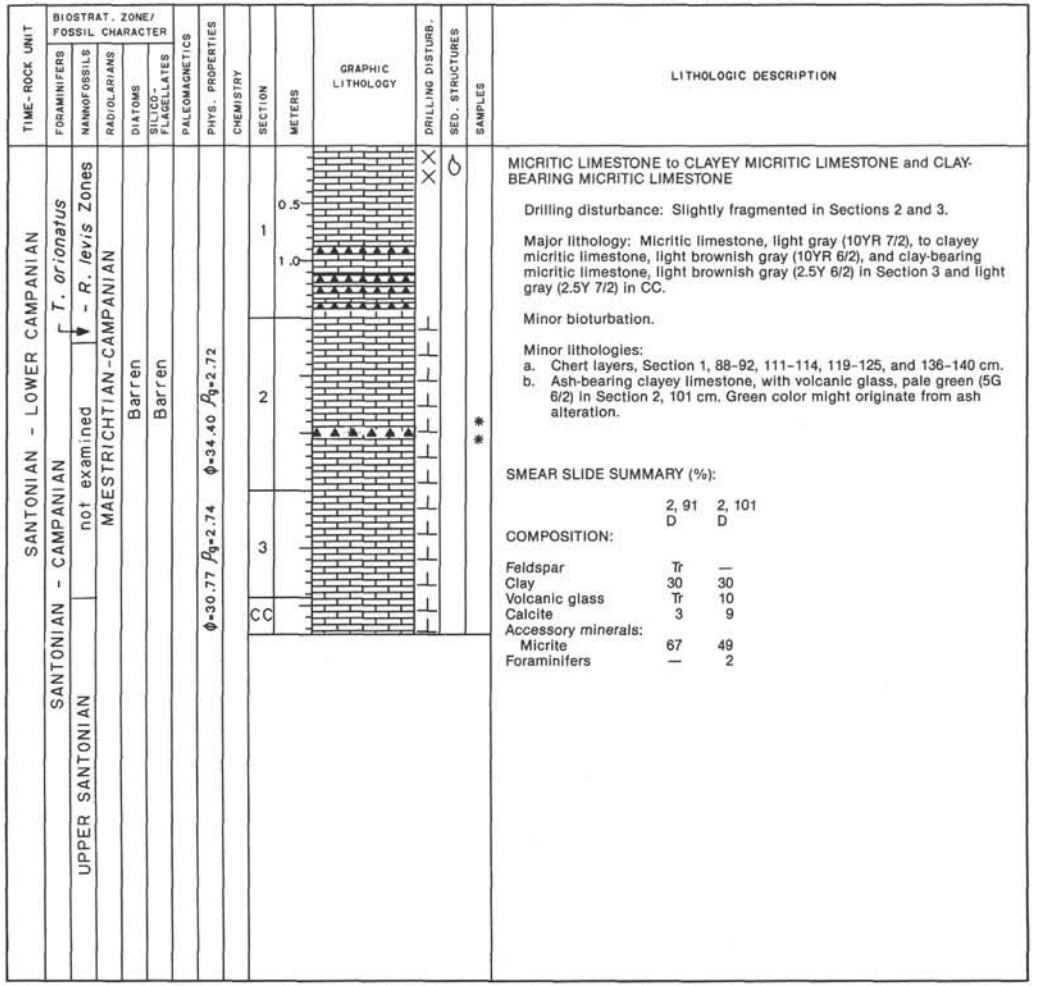

LITHOLOGIC DESCRIPTION

MICRITIC LIMESTONE to CLAYEY MICRITIC LIMESTONE and CLAY-BEARING MICRITIC LIMESTONE

Drilling disturbance: Slightly fragmented in Sections 2 and 3.

Major lithology: Micritic limestone, light gray (10YR 7/2), to clayey micritic limestone, light brownish gray (10YR 6/2), and clay-bearing micritic limestone, light brownish gray (2.5Y 6/2) in Section 3 and light gray (2.5Y 7/2) in CC.

Minor bioturbation.

Minor lithologies:
a. Chert layers, Section 1, 88-92, 111-114, 119-125, and 136-140 cm.
b. Ash-bearing clayey limestone, with volcanic glass, pale green (5G 6/2) in Section 2, 101 cm. Green color might originate from ash alteration.

SMEAR SLIDE SUMMARY (%):

	2, 91 D	2, 101 D
COMPOSITION:		
Feldspar	Tr	—
Clay	30	30
Volcanic glass	Tr	10
Calcite	3	9
Accessory minerals:		
Micrite	67	49
Foraminifers	—	2

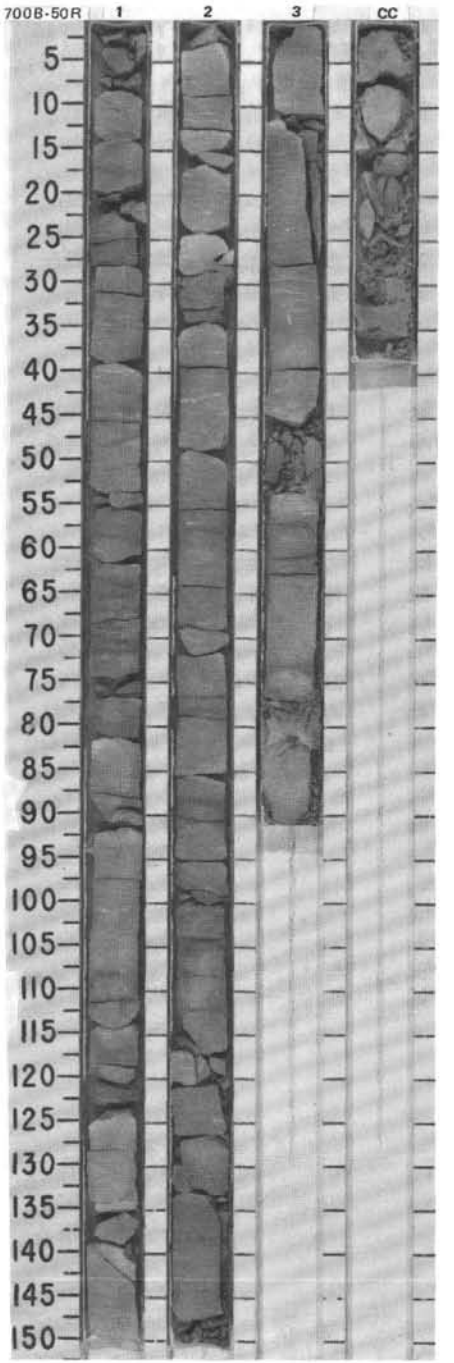

SITE 700 HOLE B CORE 51R CORED INTERVAL 4052.0-4061.5 mbsl; 451.0-460.5 mbsf

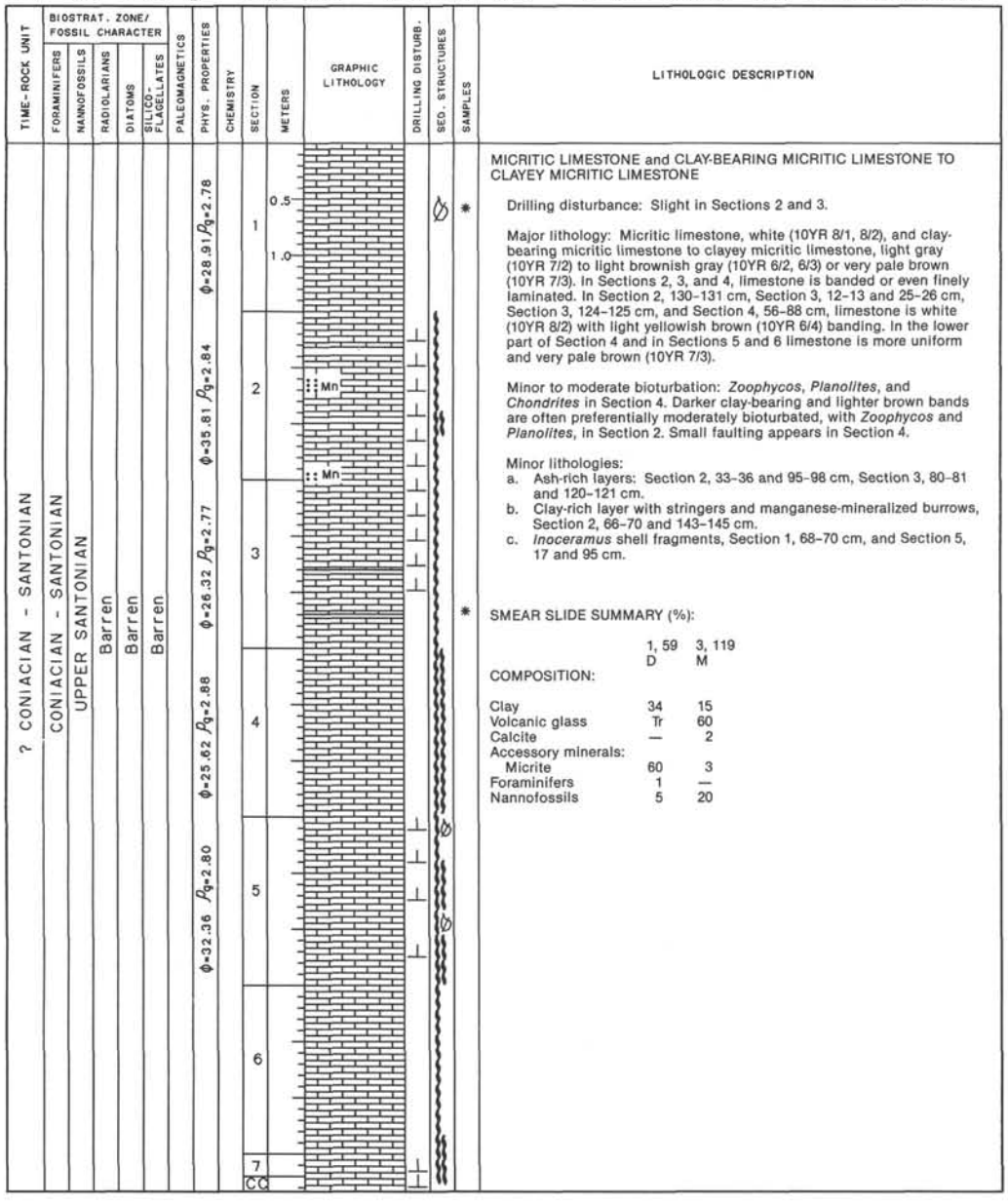

LITHOLOGIC DESCRIPTION

MICRITIC LIMESTONE and CLAY-BEARING MICRITIC LIMESTONE TO CLAYEY MICRITIC LIMESTONE

Drilling disturbance: Slight in Sections 2 and 3.

Major lithology: Micritic limestone, white (10YR 8/1, 8/2), and clay-bearing micritic limestone to clayey micritic limestone, light gray (10YR 7/2) to light brownish gray (10YR 6/2, 6/3) or very pale brown (10YR 7/3). In Sections 2, 3, and 4, limestone is banded or even finely laminated. In Section 2, 130-131 cm, Section 3, 12-13 and 25-26 cm, Section 3, 124-125 cm, and Section 4, 56-88 cm, limestone is white (10YR 8/2) with light yellowish brown (10YR 6/4) banding. In the lower part of Section 4 and in Sections 5 and 6 limestone is more uniform and very pale brown (10YR 7/3).

Minor to moderate bioturbation: *Zoophycos*, *Planolites*, and *Chondrites* in Section 4. Darker clay-bearing and lighter brown bands are often preferentially moderately bioturbated, with *Zoophycos* and *Planolites*, in Section 2. Small faulting appears in Section 4.

Minor lithologies:
a. Ash-rich layers: Section 2, 33-36 and 95-98 cm, Section 3, 80-81 and 120-121 cm.
b. Clay-rich layer with stringers and manganese-mineralized burrows, Section 2, 66-70 and 143-145 cm.
c. *Inoceramus* shell fragments, Section 1, 68-70 cm, and Section 5, 17 and 95 cm.

SMEAR SLIDE SUMMARY (%):

	1, 59 D	3, 119 M
COMPOSITION:		
Clay	34	15
Volcanic glass	Tr	60
Calcite	—	2
Accessory minerals:		
Micrite	60	3
Foraminifers	1	—
Nannofossils	5	20

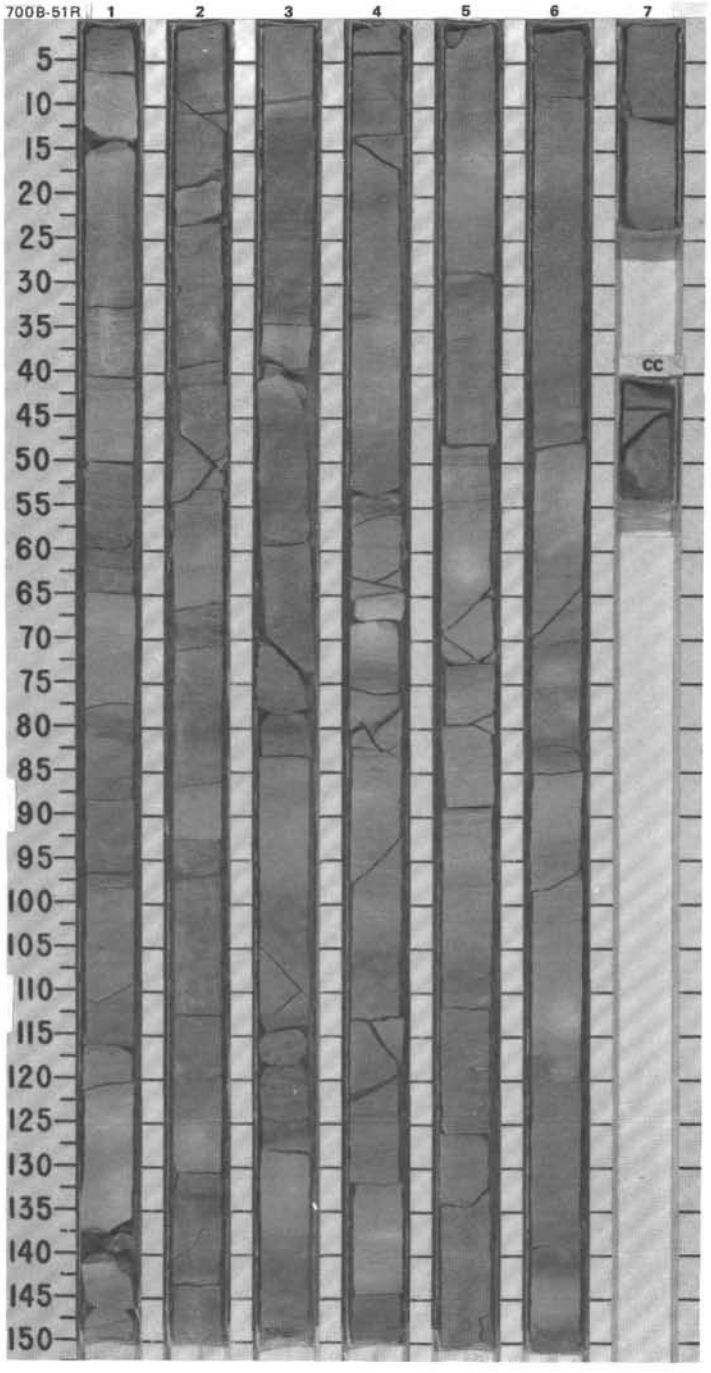

SITE 700 HOLE B CORE 52R CORED INTERVAL 4061.5-4071.0 mbsl; 460.5-470.0 mbsf

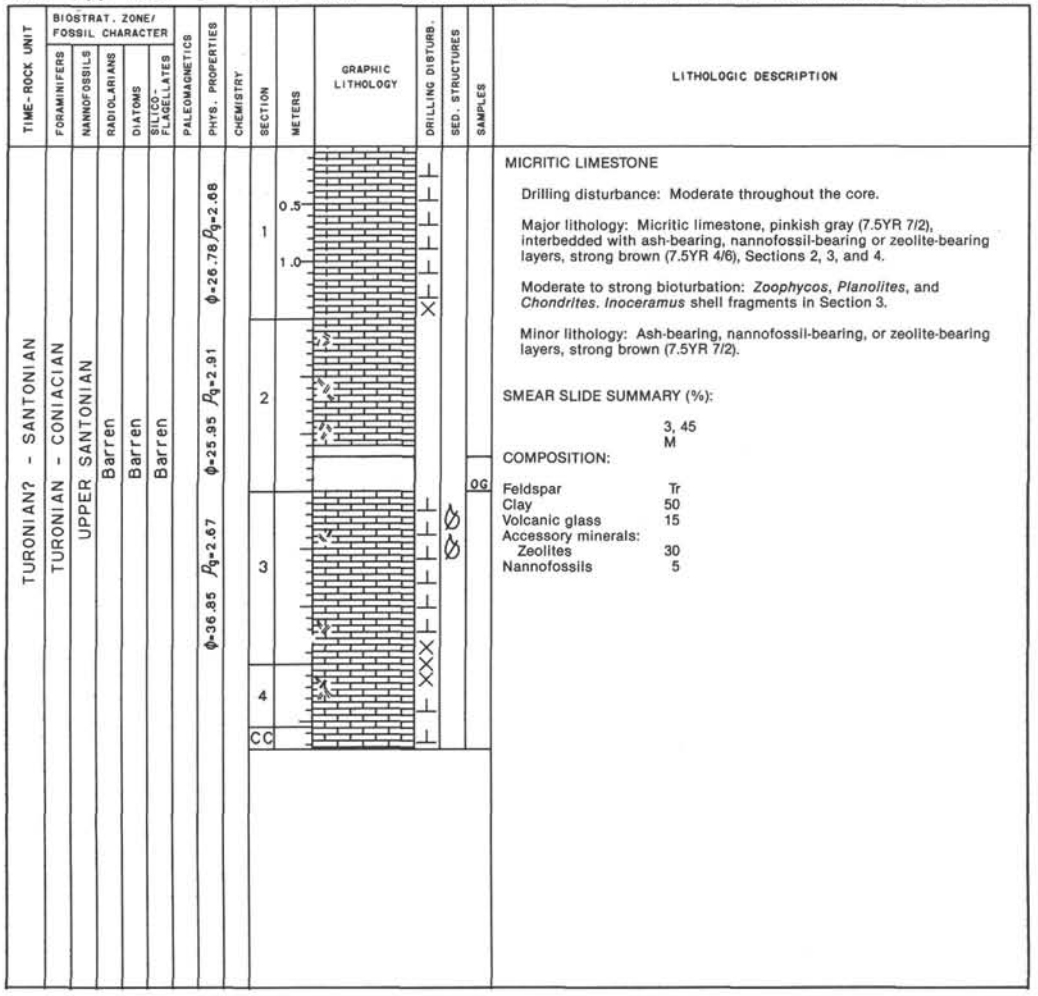

LITHOLOGIC DESCRIPTION

MICRITIC LIMESTONE

Drilling disturbance: Moderate throughout the core.

Major lithology: Micritic limestone, pinkish gray (7.5YR 7/2), interbedded with ash-bearing, nannofossil-bearing or zeolite-bearing layers, strong brown (7.5YR 4/6), Sections 2, 3, and 4.

Moderate to strong bioturbation: *Zoophycos*, *Planolites*, and *Chondrites*. *Inoceramus* shell fragments in Section 3.

Minor lithology: Ash-bearing, nannofossil-bearing, or zeolite-bearing layers, strong brown (7.5YR 7/2).

SMEAR SLIDE SUMMARY (%):

	3, 45
	M
COMPOSITION:	
Feldspar	Tr
Clay	50
Volcanic glass	15
Accessory minerals:	
Zeolites	30
Nannofossils	5

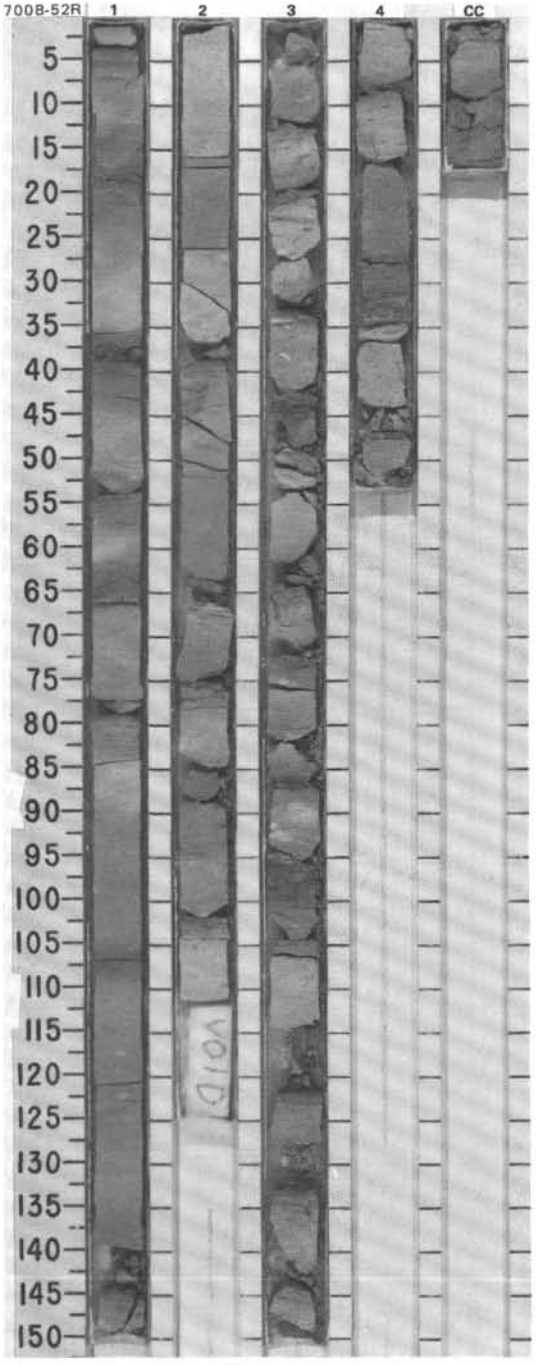

SITE 700 HOLE B CORE 53R CORED INTERVAL 4071.0-4080.5 mbsl; 470.0-479.5 mbsf

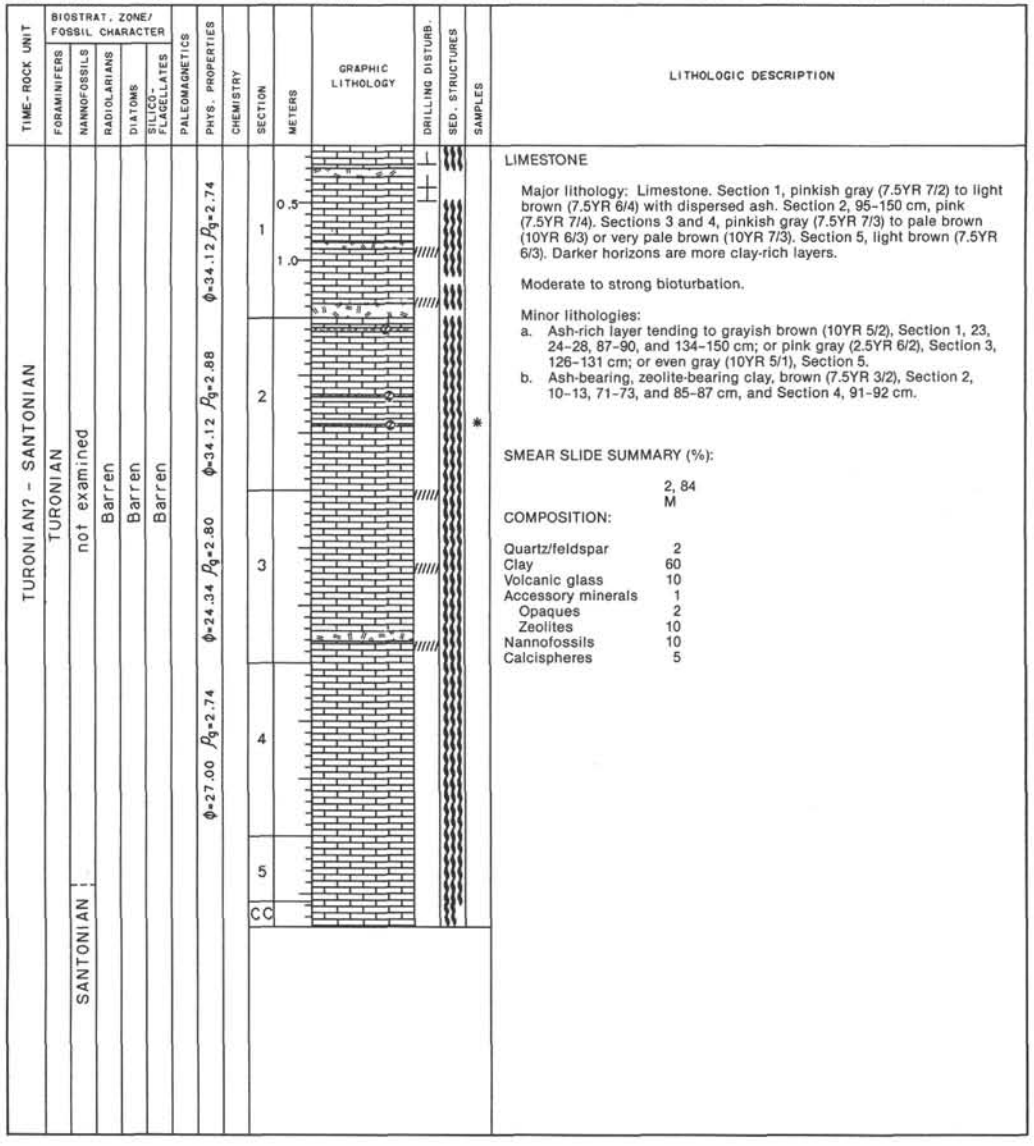

LITHOLOGIC DESCRIPTION

LIMESTONE

Major lithology: Limestone. Section 1, pinkish gray (7.5YR 7/2) to light brown (7.5YR 6/4) with dispersed ash. Section 2, 95-150 cm, pink (7.5YR 7/4). Sections 3 and 4, pinkish gray (7.5YR 7/3) to pale brown (10YR 6/3) or very pale brown (10YR 7/3). Section 5, light brown (7.5YR 6/3). Darker horizons are more clay-rich layers.

Moderate to strong bioturbation.

Minor lithologies:

a. Ash-rich layer tending to grayish brown (10YR 5/2), Section 1, 23, 24-28, 87-90, and 134-150 cm; or pink gray (2.5YR 6/2), Section 3, 126-131 cm; or even gray (10YR 5/1), Section 5.

b. Ash-bearing, zeolite-bearing clay, brown (7.5YR 3/2), Section 2, 10-13, 71-73, and 85-87 cm, and Section 4, 91-92 cm.

SMEAR SLIDE SUMMARY (%):

	2, 84 M
COMPOSITION:	
Quartz/feldspar	2
Clay	60
Volcanic glass	10
Accessory minerals	1
Opaques	2
Zeolites	10
Nannofossils	10
Calcispheres	5

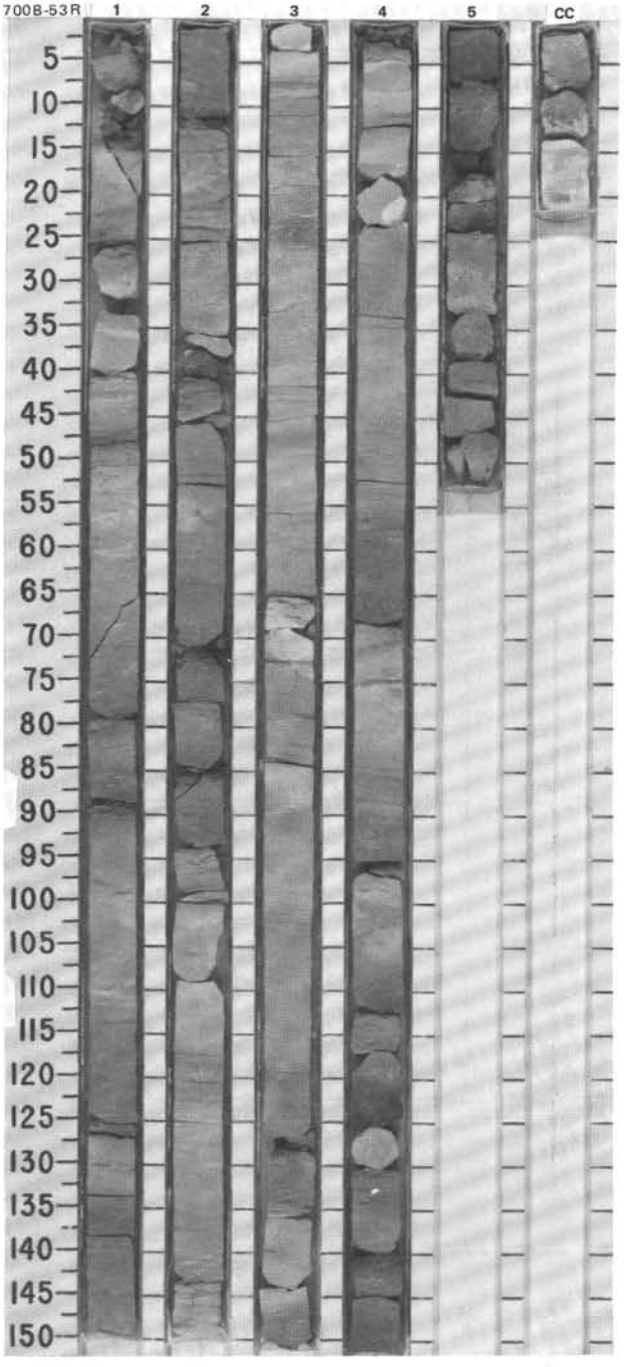

SITE 700 HOLE B CORE 54R CORED INTERVAL 4080.5-4090.0 mbsl; 479.5-489.0 mbsf

TIME-ROCK UNIT	BIOSTRAT. ZONE/ FOSSIL CHARACTER: FORAMINIFERS	NANNOFOSSILS	RADIOLARIANS	DIATOMS	SILICO-FLAGELLATES	PALEOMAGNETICS	PHYS. PROPERTIES	CHEMISTRY	SECTION	METERS	GRAPHIC LITHOLOGY	DRILLING DISTURB.	SED. STRUCTURES	SAMPLES	LITHOLOGIC DESCRIPTION
TURONIAN? - SANTONIAN	TURONIAN	SANTONIAN	Barren	Barren	Barren	ϕ-26.63 ρ_g=2.75	ϕ-26.74 ρ_g=2.74 ϕ-29.78 ρ_g=2.83		1 2 3 CC	0.5 1.0					LIMESTONE

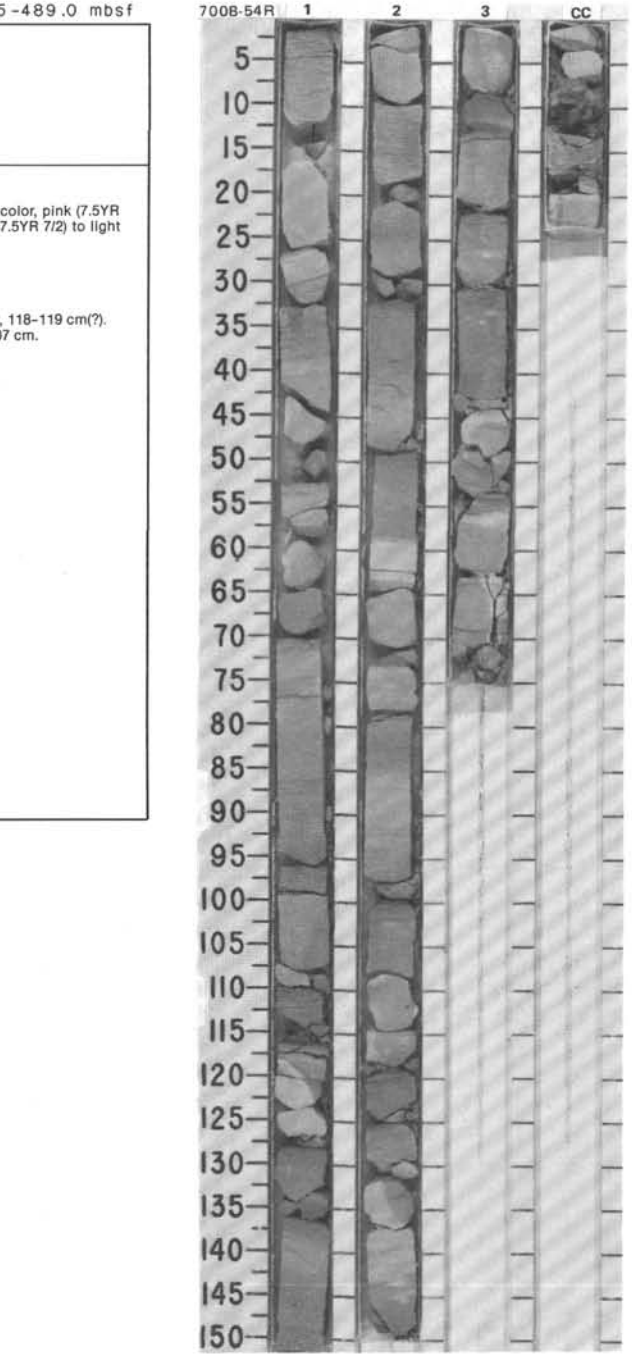

LIMESTONE

Major lithology: Limestone, showing alternation of color, pink (7.5YR 7/4) to light brown (7.5YR 6/4), or even pinkish gray (7.5YR 7/2) to light greenish gray (5GY 7/1).

Moderate to strong bioturbation.

Minor lithologies:
a. Ash layers, Section 2, 99-100 cm, and Section 2, 118-119 cm(?).
b. Clay layers, brown (7.5YR 4/4), Section 1, 105-107 cm.